Particle Detectors (*)

CMS Experiment at LHC, CERN
Data recorded: Mon May 28 01:16:20 2012 CEST
Run/Event: 195099 / 35438125
Lumi section: 65
Orbit/Crossing: 16992111 / 2295

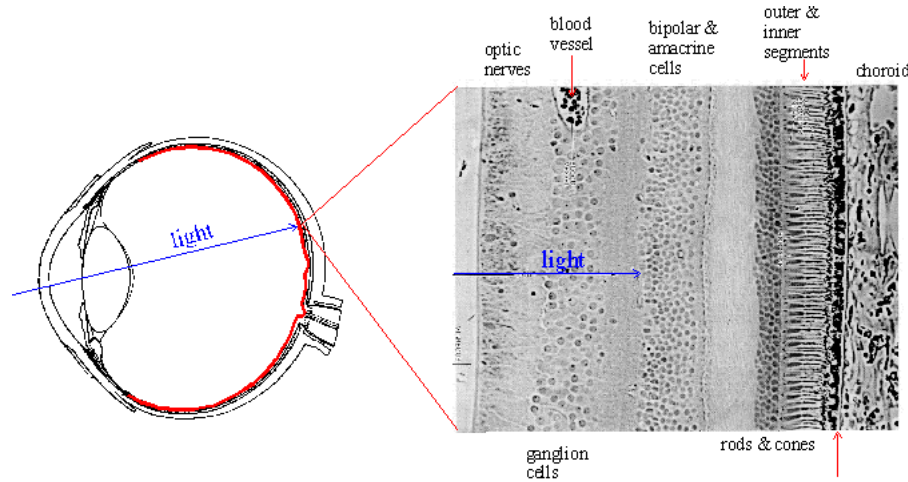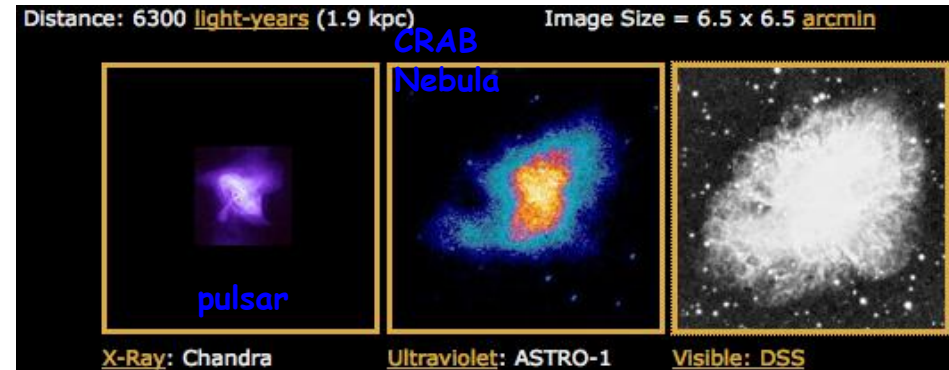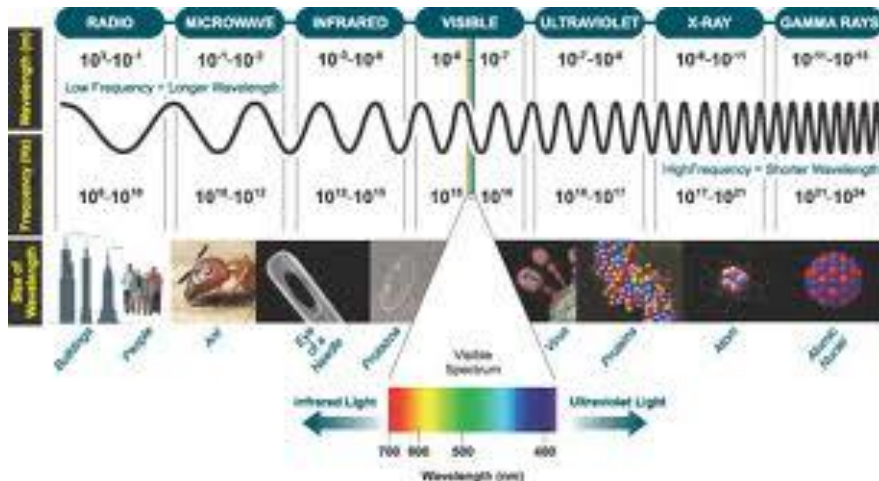**Rino Castaldi**

Sezione INFN di Pisa

(rino.castaldi@pi.infn.it)

(*) Mission impossible in 1h$^{15'}$: add several backup slides
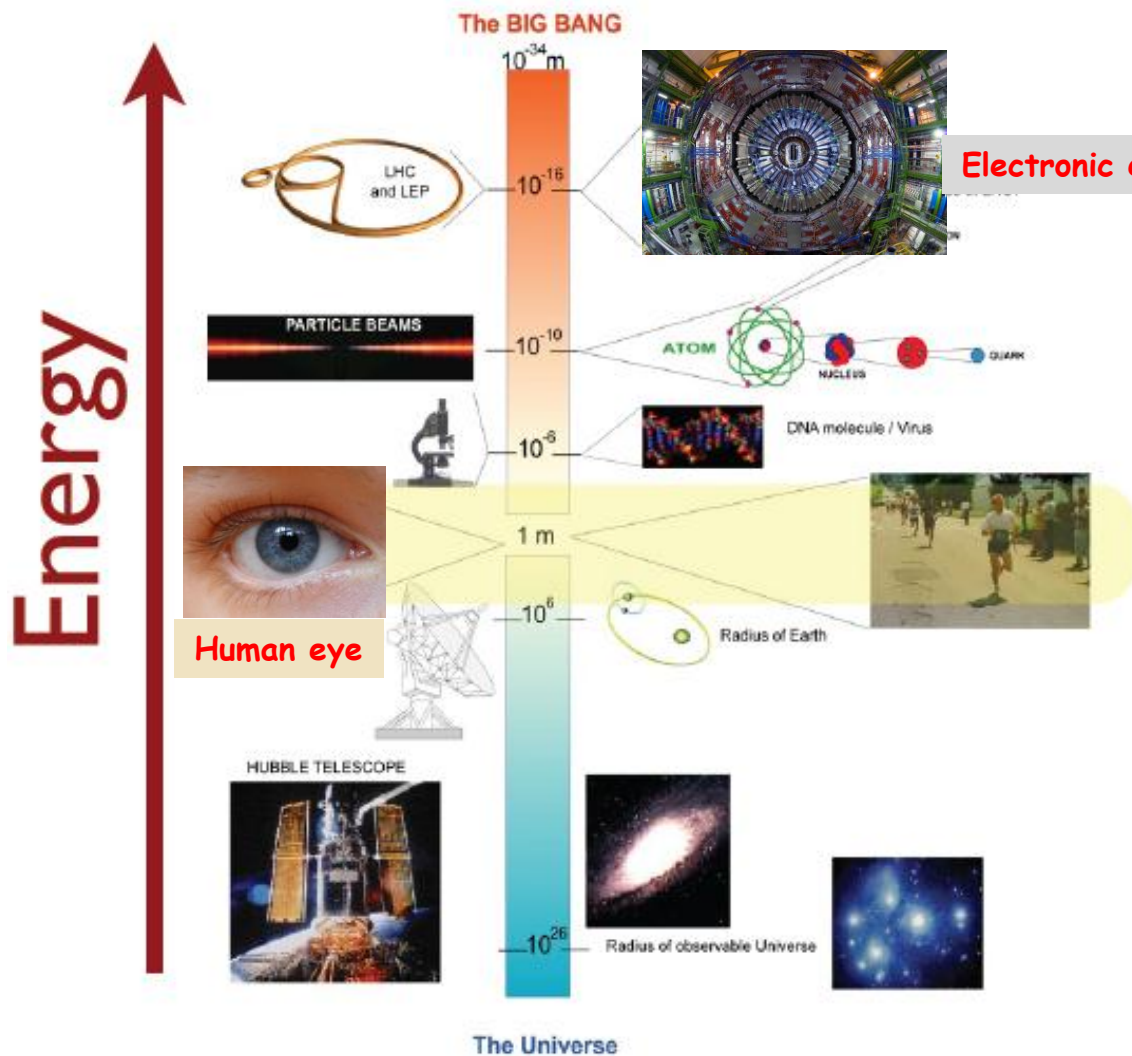
"The oldest particle (photon) detector"

- ✓ Good spatial resolution
- ✓ Very large dynamic range (1:10^6 + automatic threshold adaptation)
- ✓ Energy (wavelength λ) discrimination (λ 400÷700 nm)
- ✓ Modest sensitivity: 500 to 900 photons must arrive at the eye every second for our brain to register a conscious signal
- ✓ Modest speed: data taking rate ~ 10Hz (incl. processing)

Distance: 6300 light-years (1.9 kpc)   Image Size = 6.5 x 6.5 arcmin

CRAB Nebula

pulsar

X-Ray: Chandra   Ultraviolet: ASTRO-1   Visible: DSS

The right instrument for a given dimension

The BIG BANG

10^{-34} m

LHC and LEP

10^{-16}

PARTICLE BEAMS

10^{-10}

ATOM

NUCLEUS

QUARK

10^{-6}

DNA molecule / Virus

1 m

Radius of Earth

10^{6}

HUBBLE TELESCOPE

10^{26}

Radius of observable Universe

The Universe

Electronic eyes

Human eye

Wavelength of probe radiation should be smaller than the object to be resolved

$$\lambda \;\ll\; \frac{h}{p} \;=\; \frac{hc}{E}$$

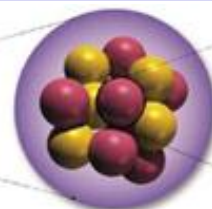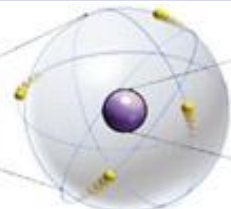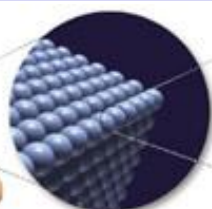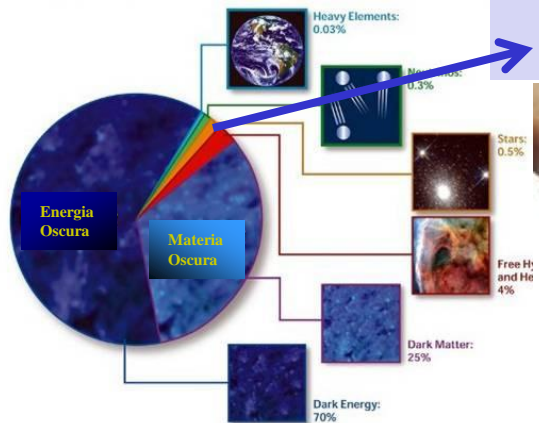| Object	Size	Energy of Radiation
Atom	10^{-10} m	0.00001 GeV (electrons)
Nucleus	10^{-14} m	0.01 GeV (alphas)
Nucleon	10^{-15} m	0.1 GeV (electrons)
Quarks	?	> 1 GeV (electrons)

Radioactive sources give energies in the range of MeV

Need accelerators for higher energies.
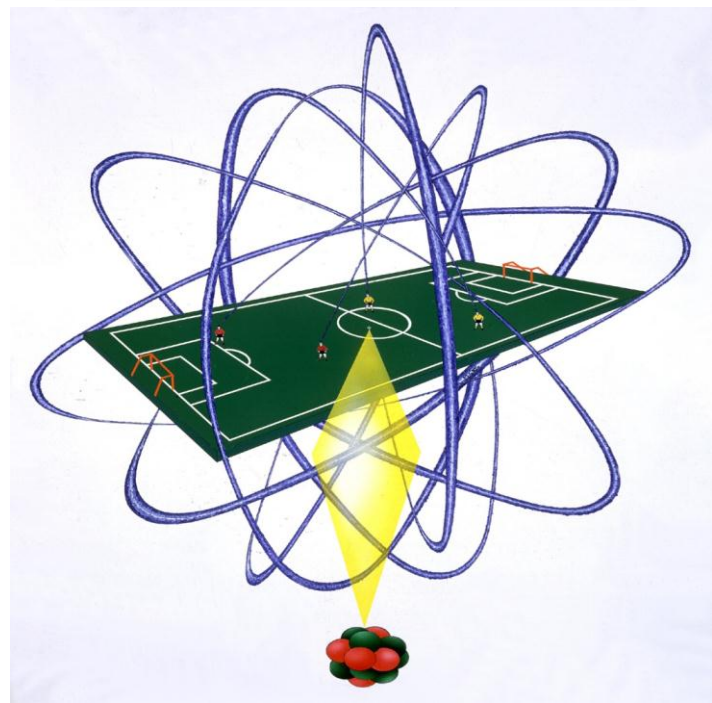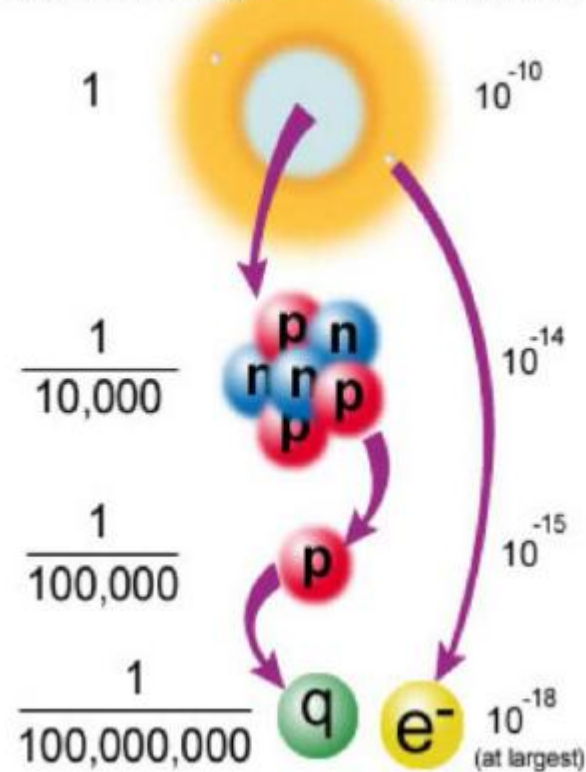
"electronic eyes"

La materia ordinaria (~5%)

Energia Oscura
Materia Oscura

Heavy Elements: 0.03%
Stars: 0.5%
Free Hydrogen and Helium: 4%
Dark Matter: 25%
Dark Energy: 70%

Sostanza   Atomo   Nucleo   Protone

u d u Quark
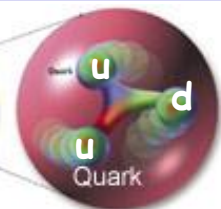
Atomo
(ingrandito mille milliardi di volte)

A questa scala, il Nucleo è ~ 1 cm

size in atoms   and in meters

1   10^{-10}

$\dfrac{1}{10,000}$ p n n n p p 10^{-14}

$\dfrac{1}{100,000}$ p 10^{-15}

$\dfrac{1}{100,000,000}$ q e⁻ 10^{-18} (at largest)

La materia ordinaria

Sostanza   **Atomo**   **Nucleo**   **Protone**
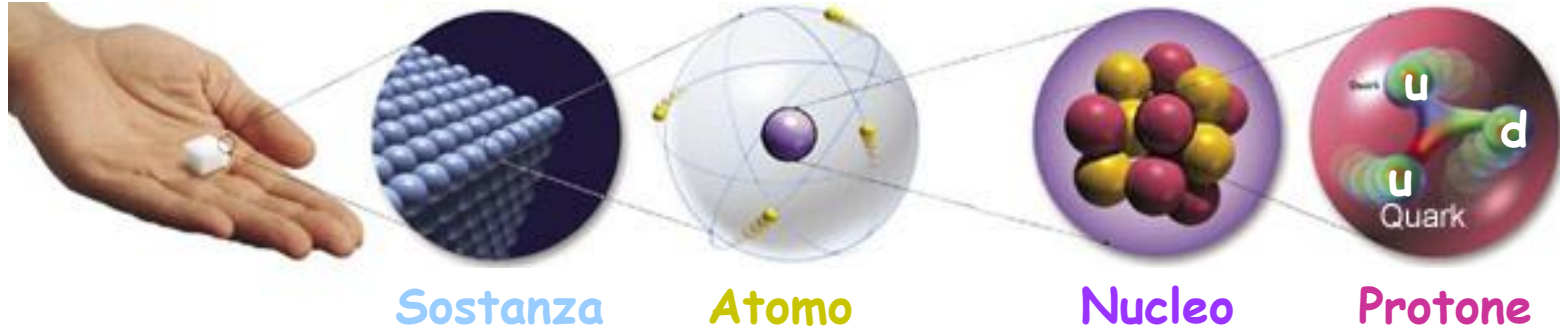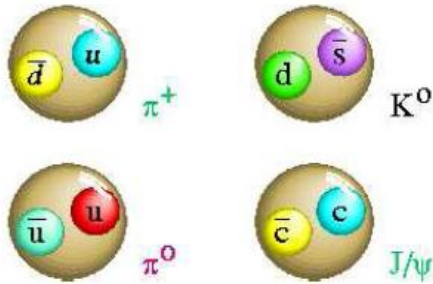
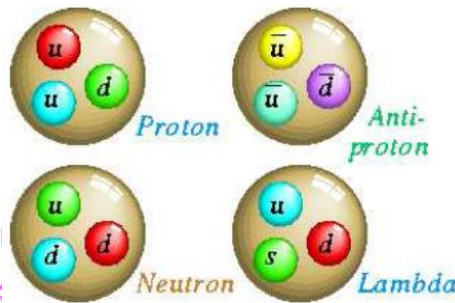## Acceleratori di particelle

$$E = mc^2$$
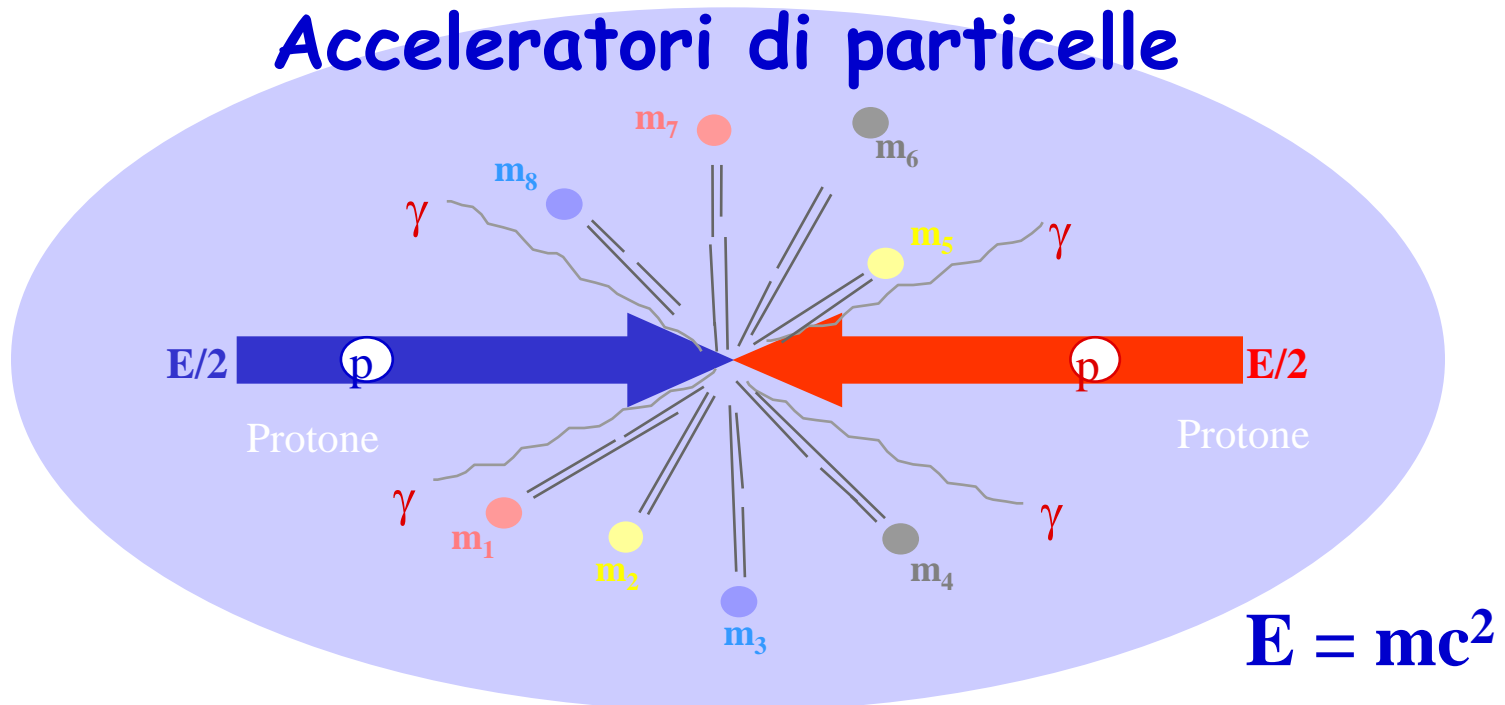
**Nella collisione vengono prodotte molte particelle
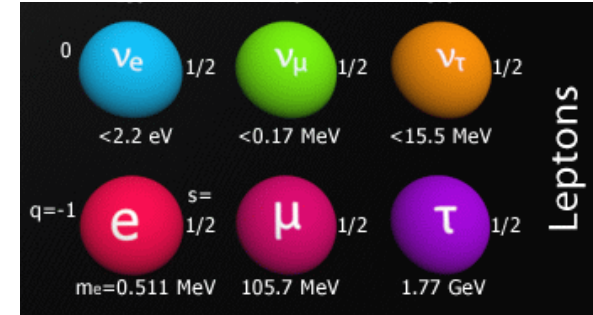sia di materia che di antimateria**

Lo zoo delle particelle

Mesoni $(q_1 q_2^{bar})$

Barioni $(q_1 q_2 q_3)$

Proton
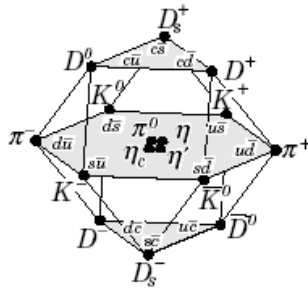Anti-proton
Neutron
Lambda

Leptoni

SU(4): u, d, s, c $(L=0)$

SU(4): u, d, s, c $(L=0)$

$J=0$

$J=1$

$J=\frac{1}{2}$
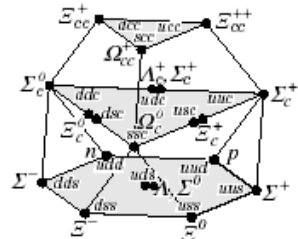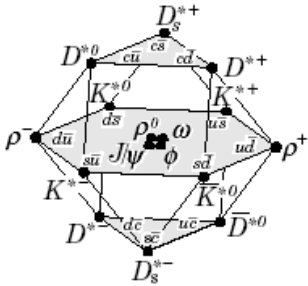
$J=\frac{3}{2}$
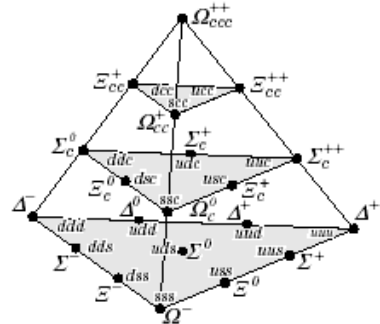
Si conoscono più di 200 particelle, la stragrande maggioranza sono instabili e decadono in tempi brevissimi, altre vivono abbastanza a lungo da poter essere rivelate direttamente.

Il Modello Standard
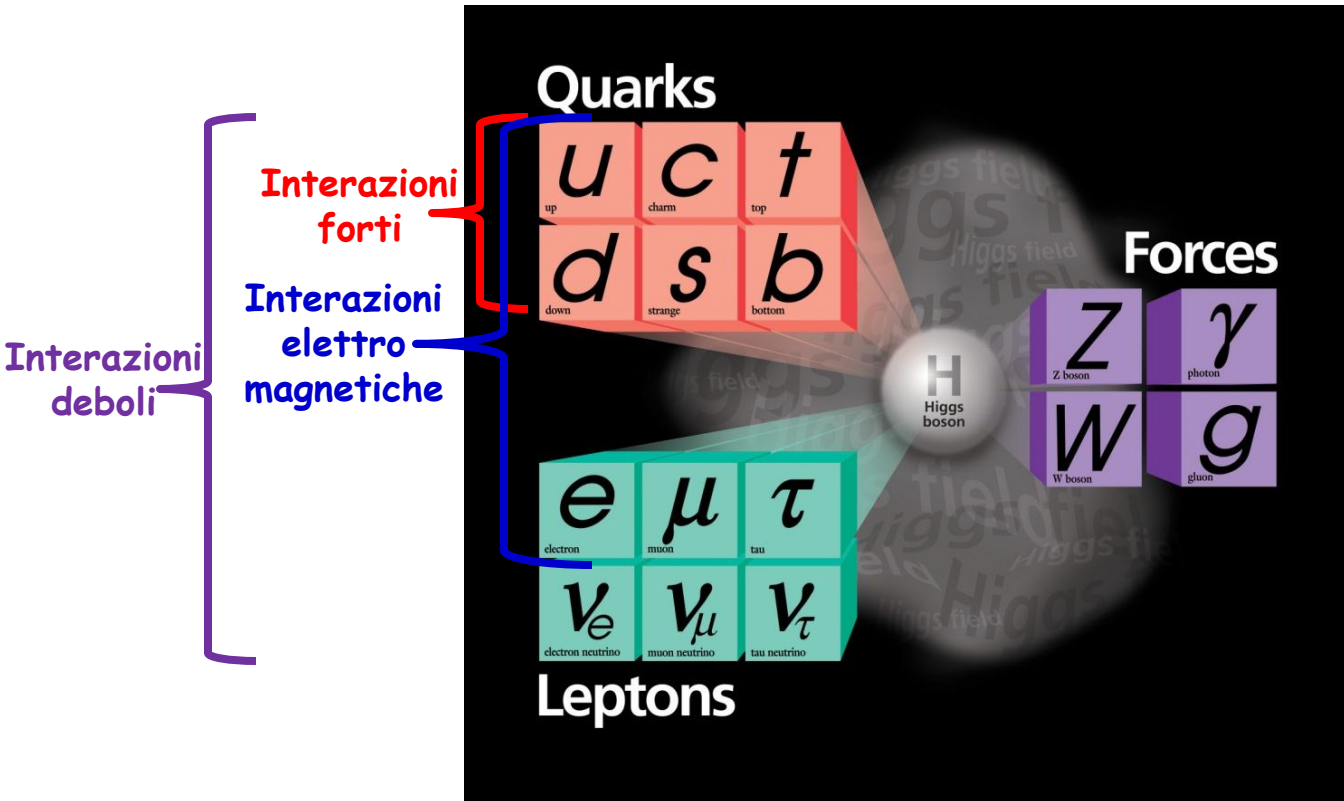
La validità del Modello Standard è dimostrata da moltissime misure sperimentali di alta precisione fatte ai recenti acceleratori (LEP, SLC,Tevatron, B-factories, e LHC)
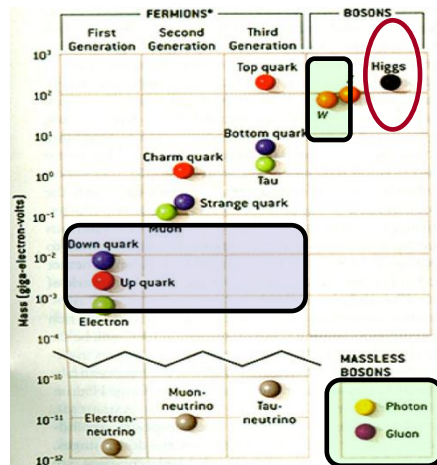
Le masse delle particelle di materia variano da quasi 0 a circa 170 GeV.

Le masse delle particelle delle forze variano da 0 a circa 90 GeV....

e finalmente m_H ~ 125 GeV !!

Collide

Colliding-Beam Experiments

$$E_{CM} = 2E_{beam}$$

Detector elements

$$\vec{p}_1 = -\vec{p}_2$$

1 → ← 2

Fixed-Target Experiments
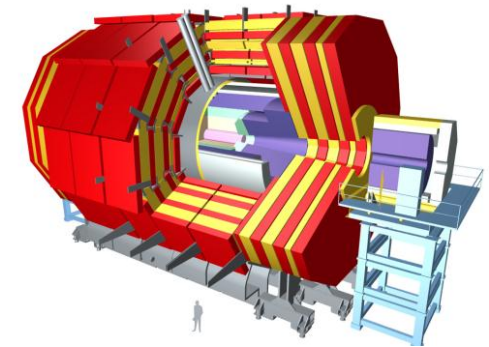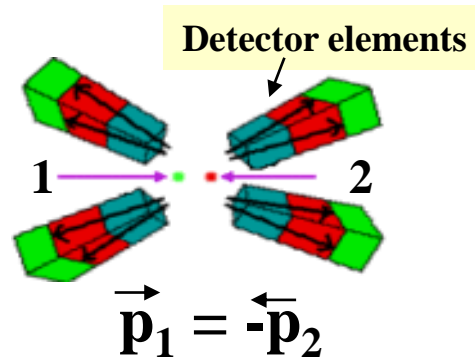
$$E_{CM} = \sqrt{2E_{beam}m_{target}}$$

1 → 2 $$\vec{p}_2 = 0$$
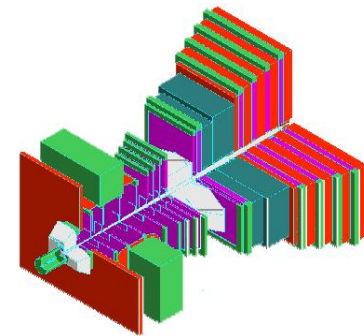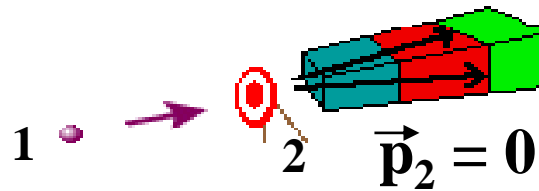
Goal : measure as many as possible of the resulting particles from the interaction.

⇒ put detector "around" the interaction point

Particles (stable or with long livetime)[(*)] to be detected

- ➢ **Charged particles**
  e^-, e^+, p (protons), $\pi^{\pm}$, $K^{\pm}$ (mesons), $\mu^{\pm}$ (muons)

- ➢ **Neutral particles**
  γ (photons), n (neutrons), K^0 (mesons),
  ν (neutrinos, **very difficult**)

- ✧ **Different particle types interact differently with matter and these interactions can be used to detect and identify the various types of particle**

  - ➢ **need different types of detectors to measure different types of particles**

(*)
Pioni, $\tau = 2.6 \times 10^{-8}$ sec, E=20 GeV, γ = E/m = 20/0.140 = 142.86, $\gamma\tau$ =0.0037 msec, distanza media percorsa = c γ τ= 1.1 km
Muoni, $\tau = 2.2 \times 10^{-6}$ sec, E=20 GeV, m = 0.1 GeV/c^2 $\Rightarrow$ $\gamma\tau$ =0.44 msec, distanza media percorsa= **132 km!**
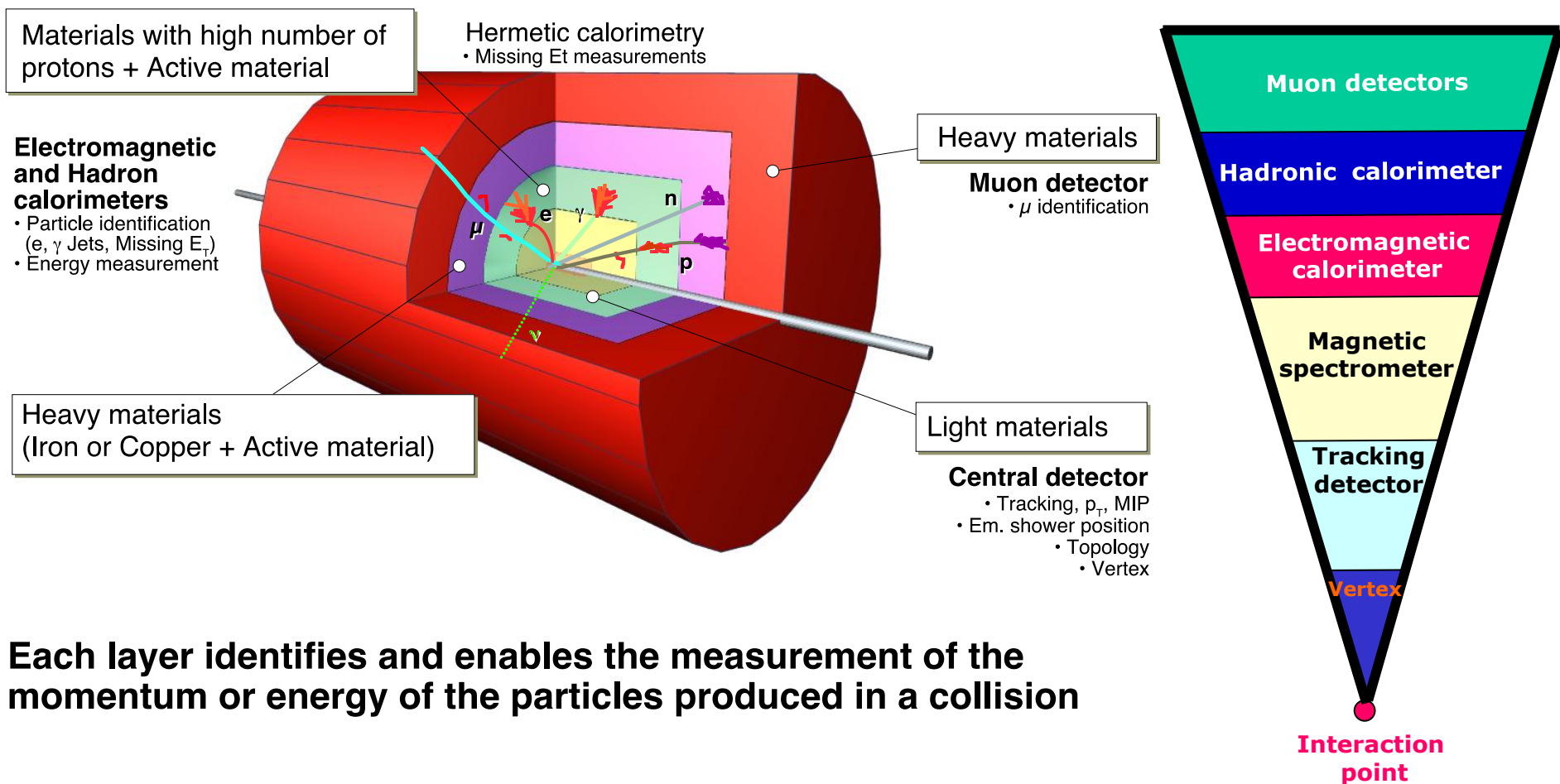
Detectors at LHC

Combine different detector types/technologies into one large detector system

Materials with high number of protons + Active material

Hermetic calorimetry
• Missing Et measurements

Heavy materials

Muon detector
• μ identification

Electromagnetic and Hadron calorimeters
• Particle identification (e, γ Jets, Missing E_T)
• Energy measurement

Heavy materials
(Iron or Copper + Active material)

Light materials

Central detector
• Tracking, p_T, MIP
• Em. shower position
• Topology
• Vertex

Muon detectors

Hadronic calorimeter

Electromagnetic calorimeter

Magnetic spectrometer
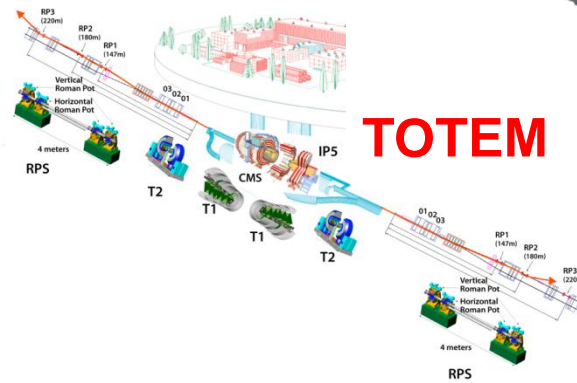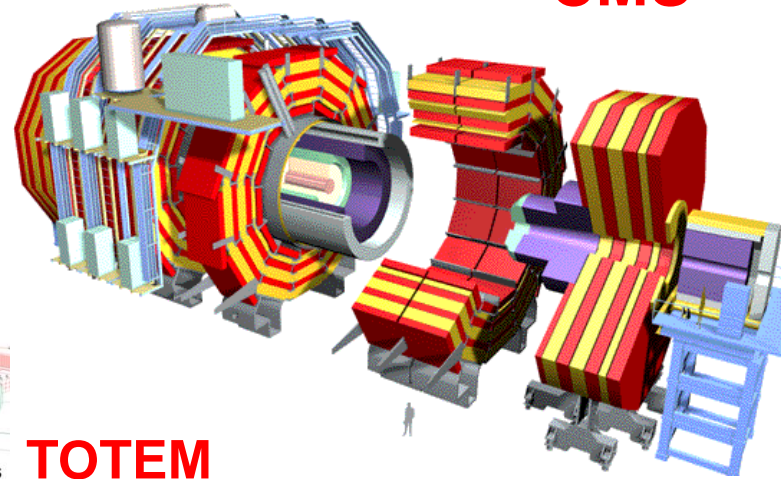
Tracking detector

Vertex

Interaction point

Each layer identifies and enables the measurement of the momentum or energy of the particles produced in a collision

The LHC Detectors

ATLAS
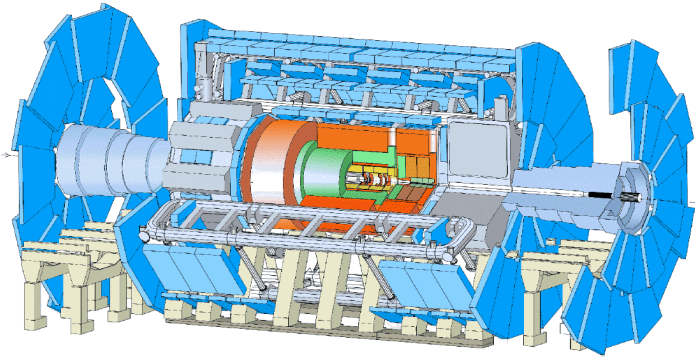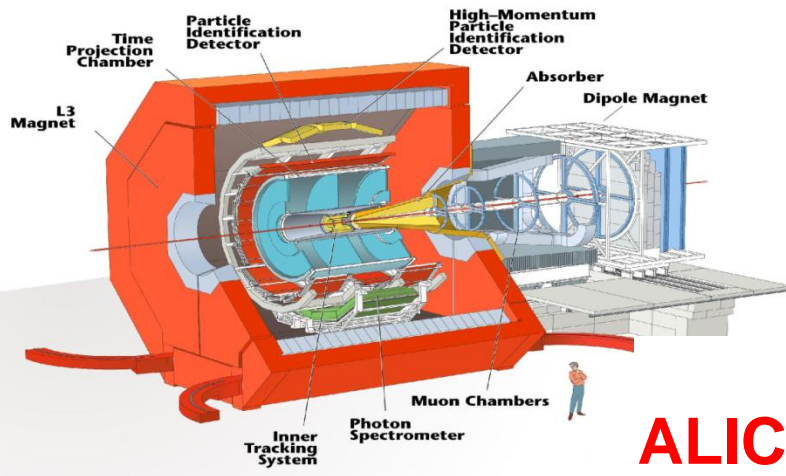
CMS

TOTEM

ALICE
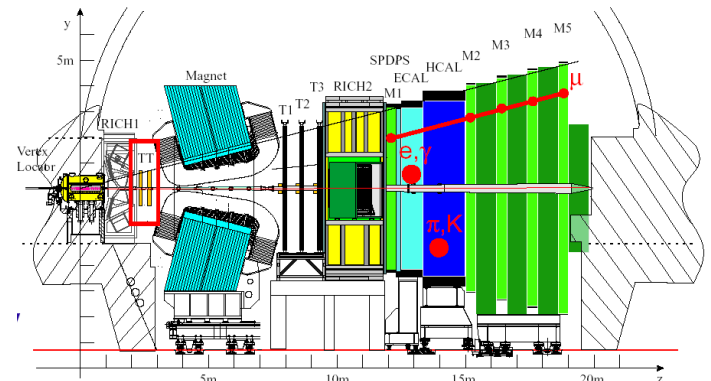
LHCb

What to measure, why?

- *"Ideal detector"* measures
  - all produced particles
  - their energy, momentum
  - type (mass, charge, life time, spin, decays)

- The passage
  of a particle (--> type)

Particle Detectors
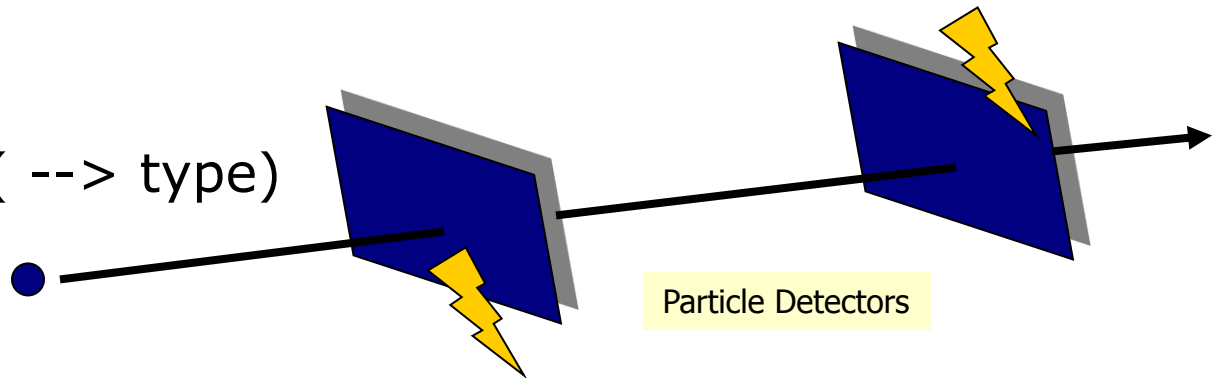
- Its four-momentum

$$\vec{p} = \begin{pmatrix} p_x \\ p_y \\ p_z \end{pmatrix}$$

$$\begin{pmatrix} \text{Energy} \\ \text{momentum in x-dir} \\ \text{momentum in y-dir} \\ \text{momentum in z-dir} \end{pmatrix} = \begin{pmatrix} E \\ \vec{p} \end{pmatrix}$$

- Its velocity $\beta = v/c$

Derived properties
Mass

❑ **Particle stable or with long livetime:**

if E and **p** measured: $E^2 = \mathbf{m^2} c^4 + \mathbf{p^2}c^2$

if v and **p** measured: $\mathbf{p} = \mathbf{m}\ v / \sqrt{(1 - \beta^2)}$
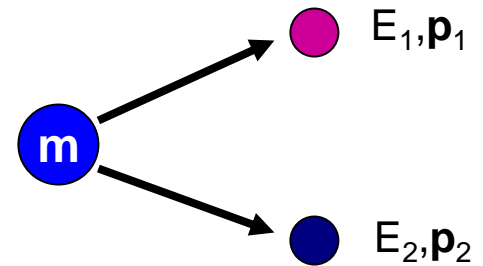
❑ **Particle unstable with short livetime:**

▪ from E and **p** of decay products:

▪ $\mathbf{m^2} c^4 = (E_1 + E_2)^2 - (c\mathbf{p_1} + c\mathbf{p_2})^2$

$E_1, \mathbf{p_1}$

m

$E_2, \mathbf{p_2}$

Further measurable properties...

- **The charge (at least the sign...)**
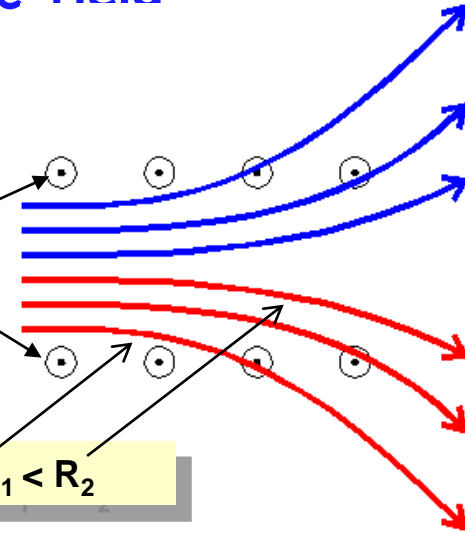 - from curvature in a magnetic field

$$\vec{F} = \frac{d\vec{p}}{dt} = q\vec{E} + q\left(\vec{v} \times \vec{B}\right)$$

Magnetic field, pointing out of the plane

Negative charge

Positive charge

$P_T(GeV) = 0.3\ B(T)\ R(m)$ $p_1 < p_2 \Leftrightarrow R_1 < R_2$

- **The lifetime t**
  - from flight path before decay

jet

Secondary vtx

displaced track

Primary vtx d_0
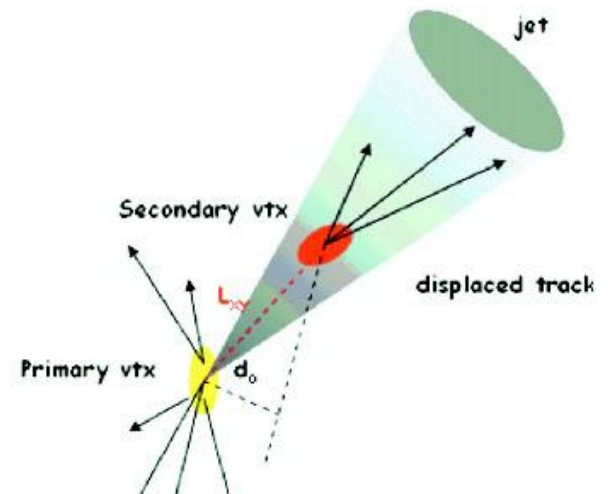
Interactions of Charged Particles with Matter

> The fact that charged particles interact with matter allows us to measure their properties

> Dominant interaction is due to the electromagnetic force.
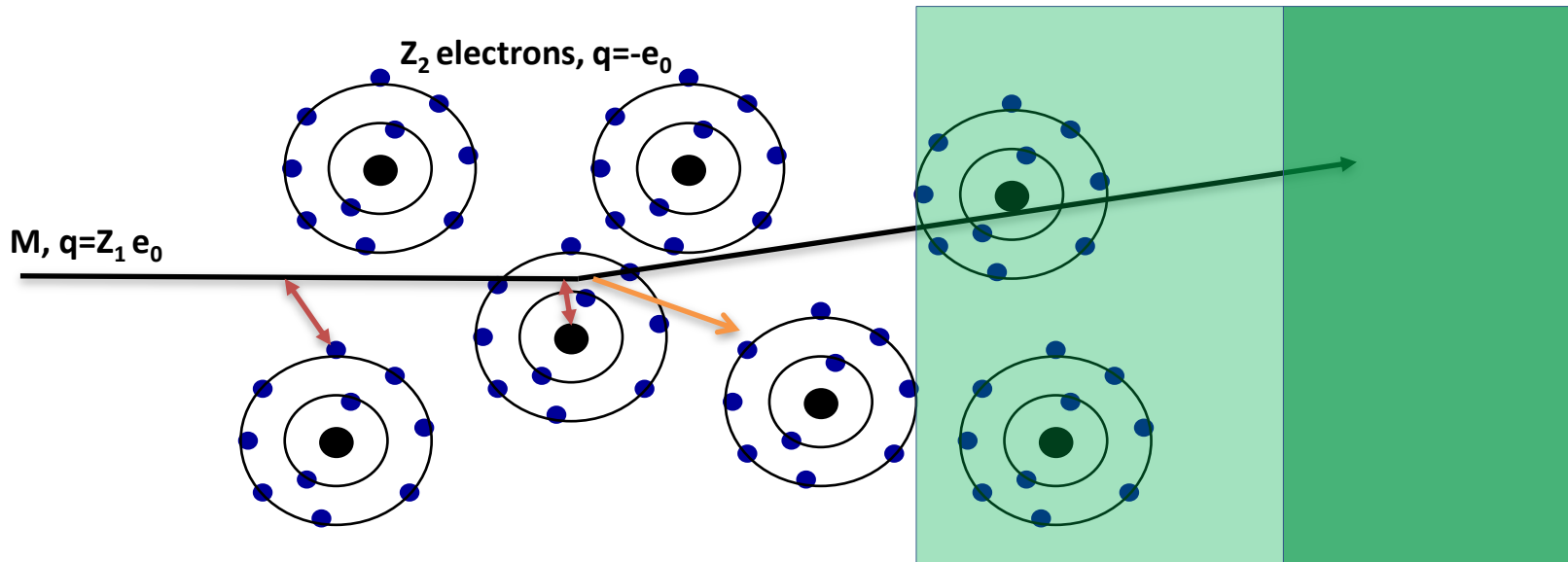
Z$_2$ electrons, q=-e$_0$

M, q=Z$_1$ e$_0$

Interaction with the atomic electrons. The incoming particle loses energy and the atoms are excited or ionized.

Interaction with the atomic nucleus. The particle is deflected (scattered) causing multiple scattering of the particle in the material. During this scattering a Bremsstrahlung photon can be emitted. This process is particularly important for electrons.

In case the particle's velocity is larger than the velocity of light in the medium, the resulting EM shockwave manifests itself as Cherenkov Radiation. When the particle crosses the boundary between two media, there is a probability of the order of 1% to produce and X ray photon, called Transition radiation.

Principles of measurement
(ionization and exitation)

measureable signals occur via the interaction of charged particles with the detector material.

Dominant interaction is due to the coulomb interactions with the atomic *electrons* of the detector.
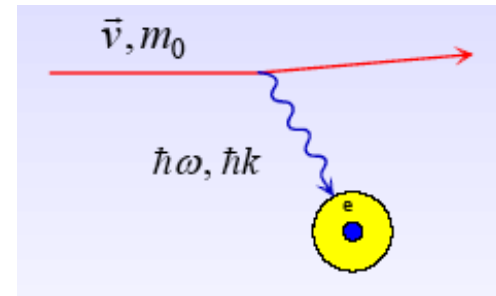
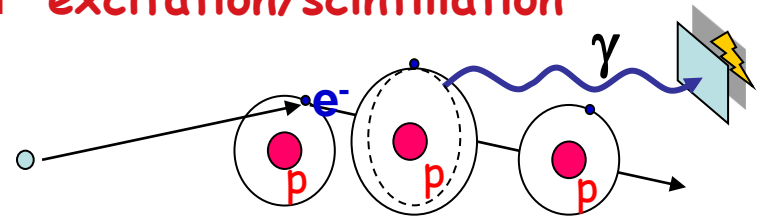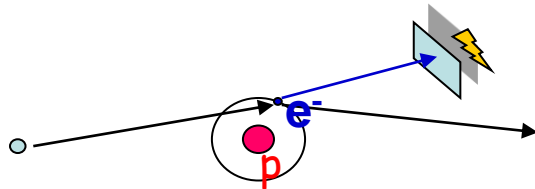Depending on the $\hbar\omega$ value we may have:

❑ **ionization**   or   ❑ **excitation/scintillation**

Ionization and excitation of atomic electrons in matter are the most common processes and allow to build precise tracking detectors .

Ionization: the Bethe-Bloch formula

$$\left\langle \frac{dE}{dx} \right\rangle = -4\pi N_A r_e^2 m_e c^2 z^2 \frac{Z}{A} \frac{1}{\beta^2} \left[\tfrac{1}{2} \ln \frac{2 m_e c^2 \gamma^2 \beta^2}{I^2} T^{\max} - \beta^2 - \frac{\delta}{2} \right]$$
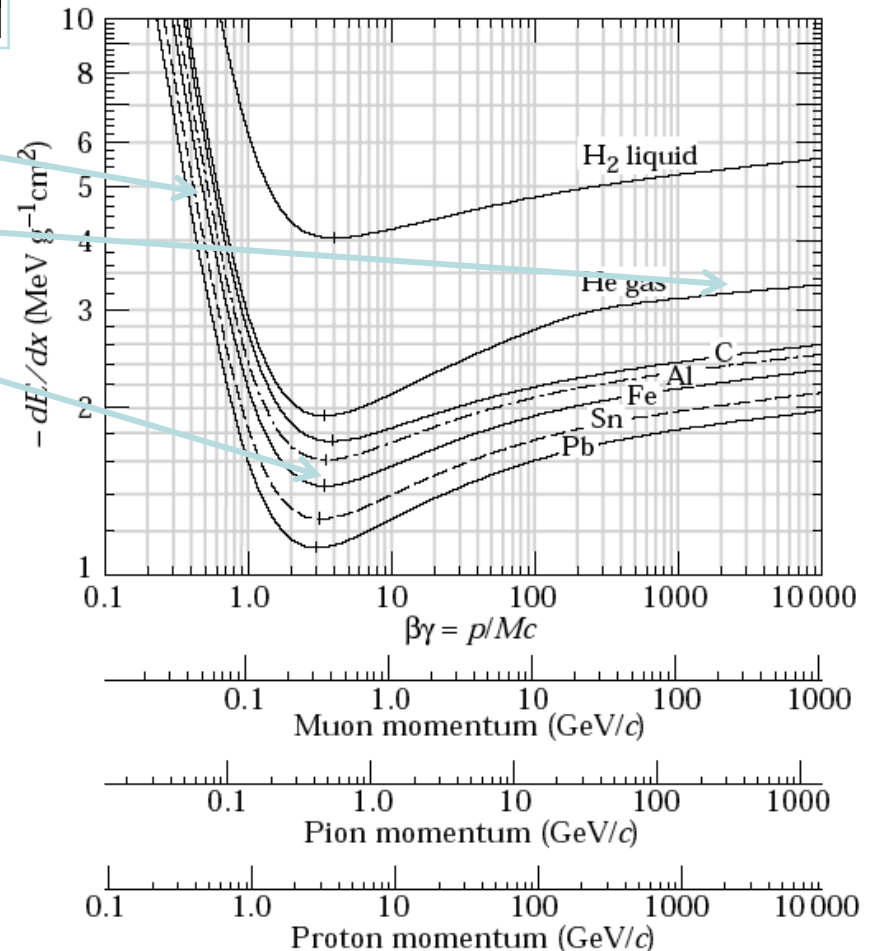
$$T_{\max} \approx 2 m_e c^2 \beta^2 \gamma^2 \qquad -\frac{dE}{dx} \approx K q^2 \frac{Z}{A\beta^2} \left[\ln \frac{2 m_e c^2 \beta^2 \gamma^2}{I^2} - \beta^2 \right]$$

Charaterized by:
- **a fall off at low energy ~1/β²**
- **a relativistic rise ~ ln βγ**
- **a minimum at βγ ≈ 3**
- **depends only on βγ not on m**

High energy charged particles lose
energy **slowly** in material
due to ionization leaving tracks
as they pass **(For Z≈0.5A at ßγ≈3**
**1/ρ dE/dx ≈ 1.4 MeV cm²/g)**

➡ **many kinds of tracking**
detectors can be done !

Particle Identification by Energy Loss

Energy loss depends on the $\beta\gamma$ of the particle and is ≈ independent from the mass of the particle. As a function of particle momentum $p = Mc\beta\gamma$ the energy loss depends on the mass of the particle.

By measuring the energy loss and the momentum of the particle, the mass of the particle can be measured: → Particle Identification !
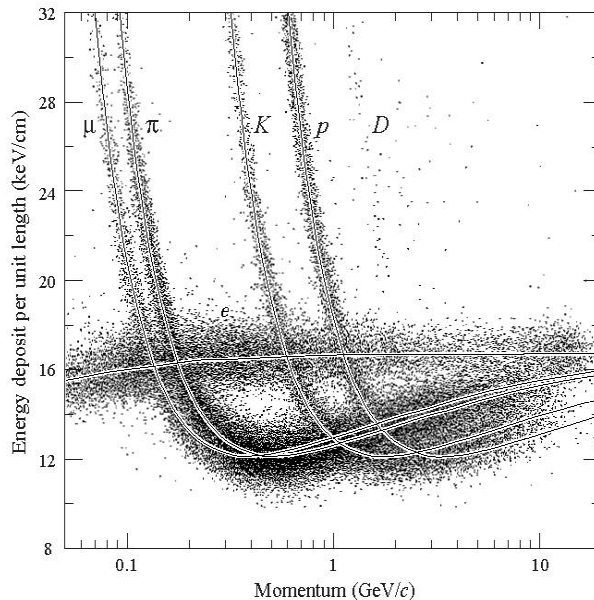
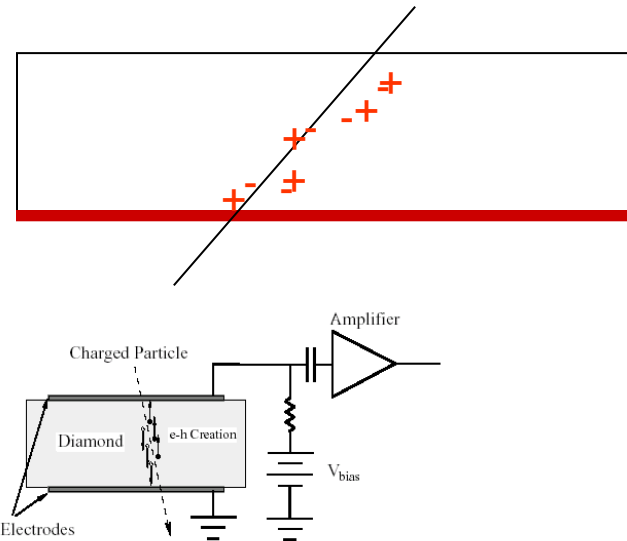**TPC in magnetic field**
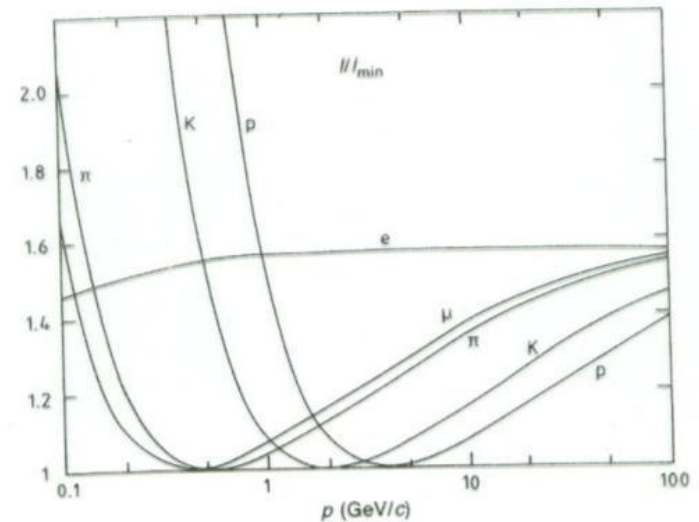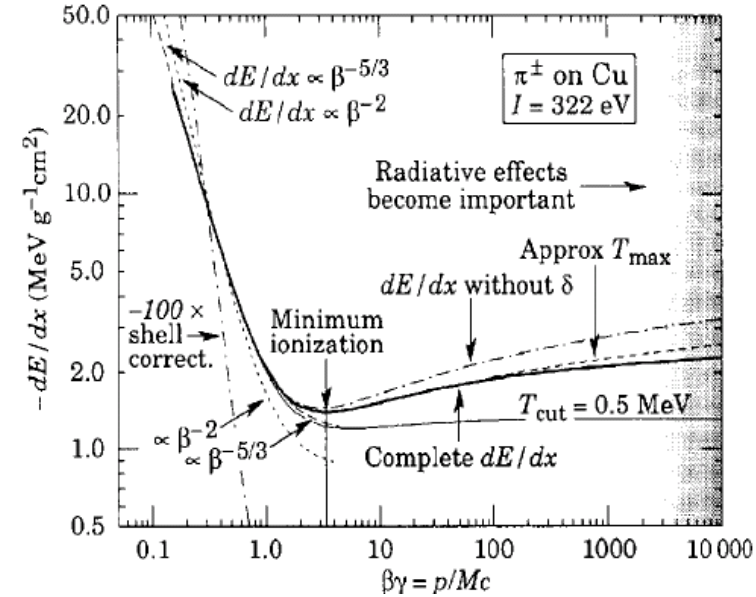
$$\frac{1}{\rho}\frac{dE}{dx} = -4\pi r_e^2 \, m_e c^2 \, Z_1^2 \frac{p^2 + M^2 c^2}{p^2} N_A \frac{Z}{A} \left[\ln \frac{2m_e c^2 F}{I} \frac{p^2}{M^2 c^2} - \frac{p^2}{p^2 + M^2 c^2} \right]$$

Tracking Detectors

Charged particles crossing a material loose energy by ionizing (and exciting) atoms and thus leaving along their path a trace of electron-ion pairs in gases and liquids and electron-hole pairs in solids.

Measurable electronics signals can be induced by the charges produced in this way and can be read by dedicated electronics

❑ In solid state detectors the charges produced by the ionization due to the incoming particle are sufficient to provide a measurable signal.

- Mean (most probable) energy loss:
  116 (78) keV for 300μm Si thickness
- 3.6 eV to create an e-h pair
  ⇒ 72 e-h/μm (most probable)
  ⇒ 108 e-h/μm (mean)
- Most probable charge (300μm Si)
  ≈ 21600 e   ≈ 3.5 fC

❑ In gas detectors the charges produced by the primary ionization due to the incoming particle need amplification in order to provide a measurable signal.
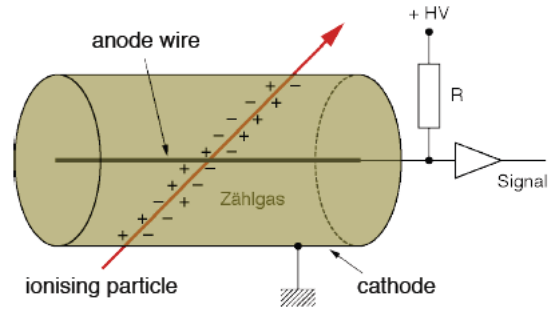
| GAS)	Helium	Argon	Xenon	CH$_4$	DME
dE/ dx (keV/ cm)	0.32	2.4	6.7	1.5	3.9
<n> (ion-pair/ cm)	5.9	29	44	16	55

Wire Chamber: Electron Avalanche

❑ **Basic design:** ionization chamber with HV sense wire

Typically a gas detector will have ~20 primary ions per cm created by a track: amplification needed in order to provide a measurable signal.

Consider a thin wire with radius a (10-25μm) at voltage V=0 in a tube of outer radius b (1-3cm) voltage V_0. The electric field inside the tube is given by:
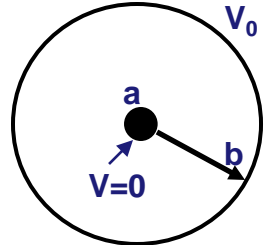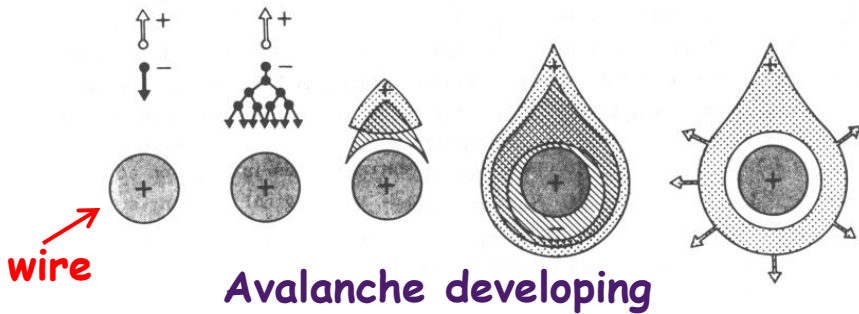
$$E = 2\lambda/r, \quad V_0 = 2\lambda\ln(b/a), \quad V(r) = V_0\frac{\ln(r/a)}{\ln(b/a)}, \quad E(r) = \frac{V_0}{r\ln(b/a)}$$

Example: V_0=1000V, a=10μm, b=10mm,
E(a)=150kV/cm

Electric field is sufficient to accelerate electrons to energies which are sufficient to produce secondary ionization → electron avalanche → signal.
(tipical amplification: 10^3-10^5)

wire

Avalanche developing
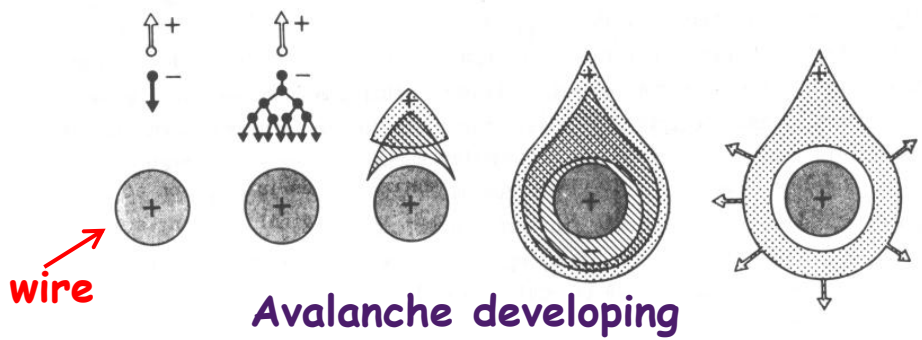
Wire Chamber: Signals from Electron Avalanches

wire

Avalanche developing

The electron avalanche happens very close to the wire. First multiplication only around R =2x wire radius. Electrons are moving to the wire surface very quickly (<<1ns). Ions are drifting slowly towards the tube wall (typically several 100μs).

The signal is characterized by a very fast 'spike' from the electrons and a long ion tail.

The total charge induced by the electrons amounts to 1-2% of the total induced charge.

Signal due to ions dominates, as they travel all the way to the cathode.

The signal is characterized by a very fast peak from the electrons and a long ion tail.
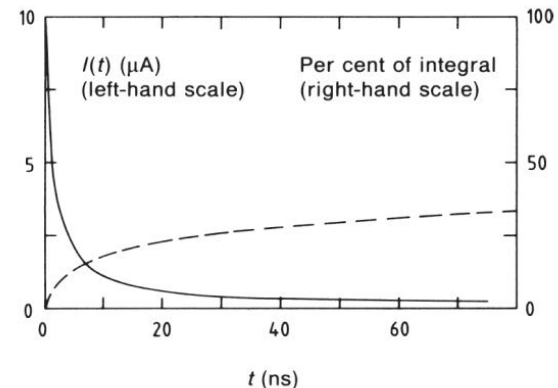
Amplification vs applied voltage

❖ Average energy lost in creating ion pair ~ 10-20 eV.
❖ Primary ionization: number of ionizing collisions per unit length for the incident particle. (Poisson distribution)
❖ Secondary ionization: the electric field is sufficient to accelerate electrons to energies which are sufficient to produce secondary ionization

For intermediate value of the electric field the number of electrons produced in the avalanche is proportional to the primary ionization (amplification $A \approx 10^3 - 10^4$; Landau distribution)

Increasing the electric field the amplification increases but the detector is not working anymore in a proportional regime:

$A \approx 10^4 - 10^5$ Semi proportional region due to space charge screening around the anode
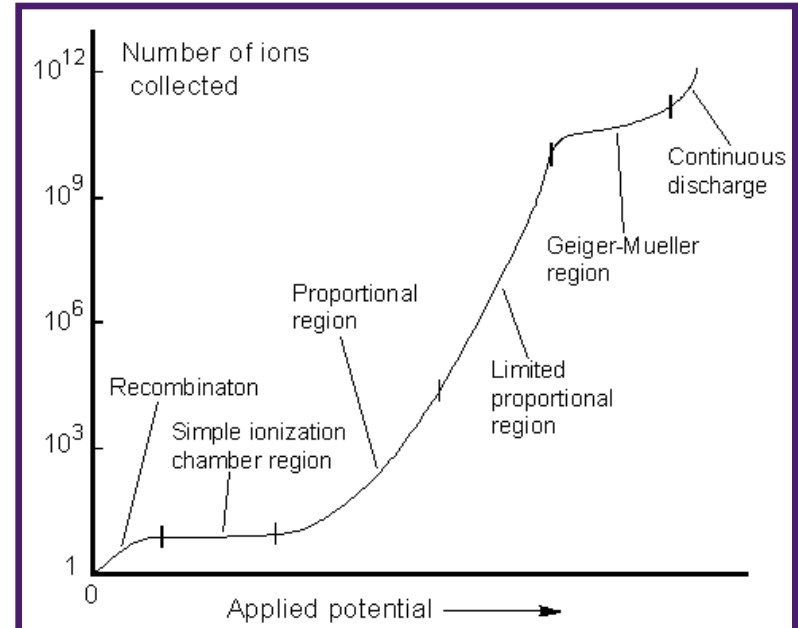
$A > 10^6$ Saturation region: the number of ions collected are independent from the number of primary electrons.

$A > 10^7$ Streamer region: the avalanche develops along the particle track.

$A > 10^8$ Limited Geiger region: the avalanche is propagated by UV photons.

$A \approx 10^9$ Geiger region: the avalanche is produced along the entire wire.
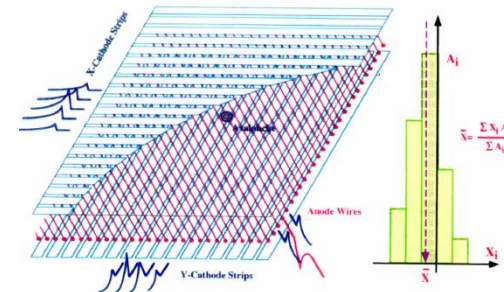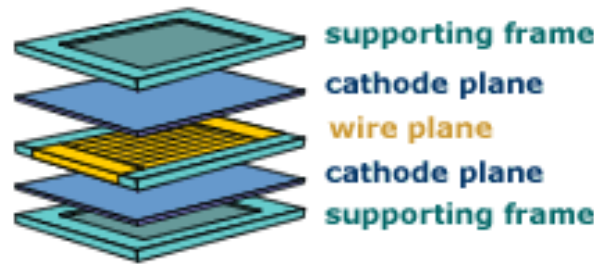
• • • • Continuous discharge !
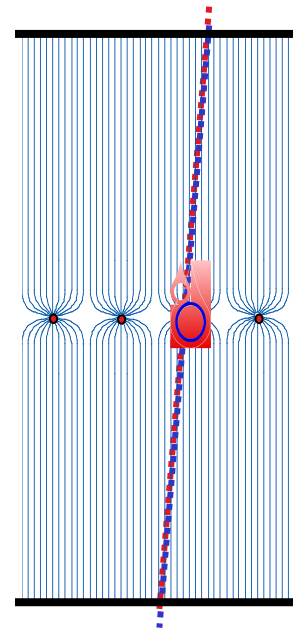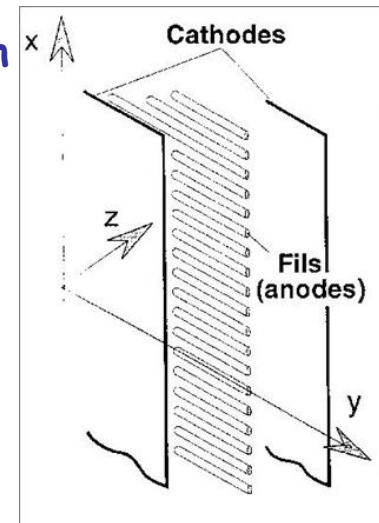
Multiwire Proportional Chambers

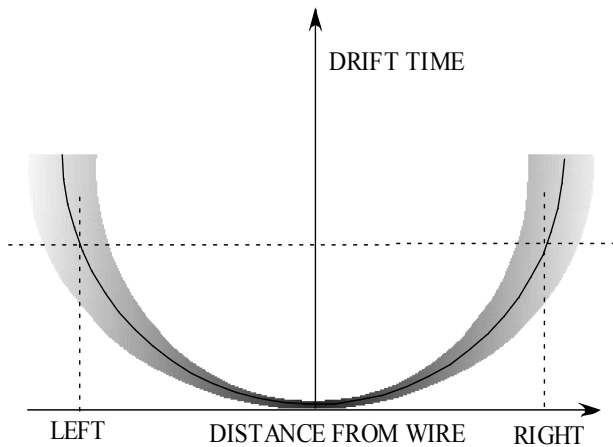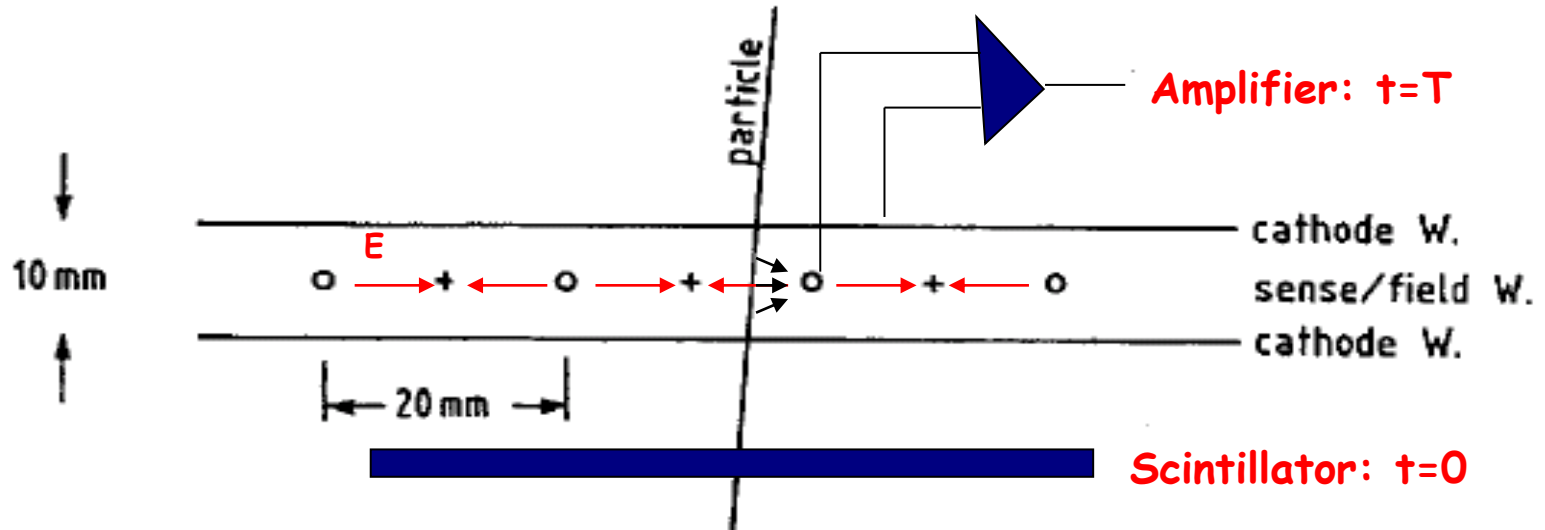The MWPC was invented by Charpak at CERN   1992 **NOBEL** Prize

Principle of proportional counter is extended to large areas. One plane of thin sense wires is placed between two parallel plates. Typical dimensions: wire distance 2-5mm, distance between cathode planes ~10mm. Electrons (v≈5cm/μs) are collected within ≈ 100ns. The movement of the charges induces a signal on the wire AND on the cathode. By segmentation of the cathode plane and charge interpolation, resolutions of 50μm can be achieved.
Stack several wire planes up in different direction to get position location.

supporting frame
cathode plane
wire plane
cathode plane
supporting frame

$$\bar{x} = \frac{\sum x_i A_i}{\sum A_i}$$

Drift Chamber (1971: H. Walenta)

Amplifier: t=T

10 mm

E

cathode W.
sense/field W.
cathode W.

particle

← 20 mm →

Scintillator: t=0

DRIFT TIME

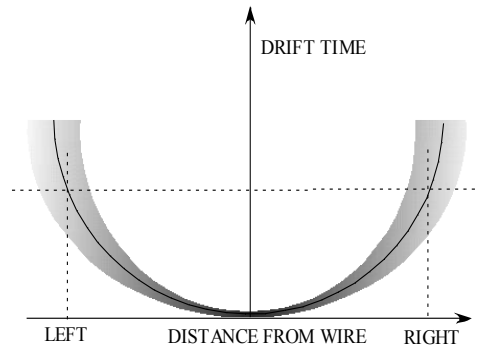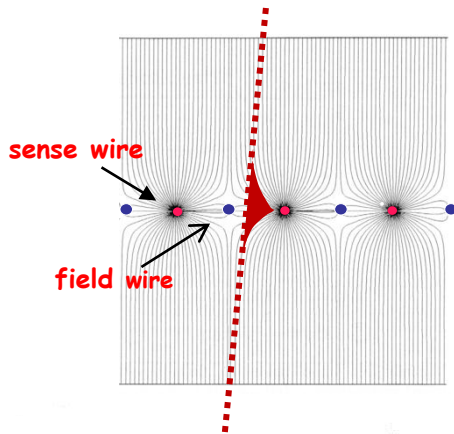LEFT   DISTANCE FROM WIRE   RIGHT

The electric field in an alternating sequence of sense and field wires at different potentials cause the electrons to drift toward the sense wire. The measurement of the drift time T between the passage of the particle and the arrival of the electrons at the sense wire is a measurement of the position of the particle (precision ~100μm)
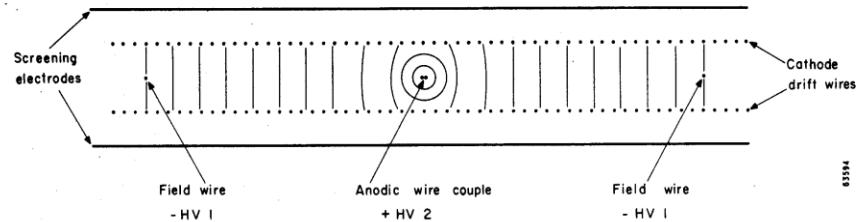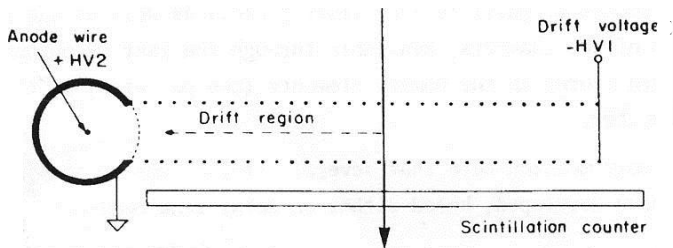The wire distance can be increased up to several centimeters (drift time ~μs; v≈5cm/μs) saving a lot of electronics channels with respect to the MWPC.
however:
❑ Left-Right ambiguity
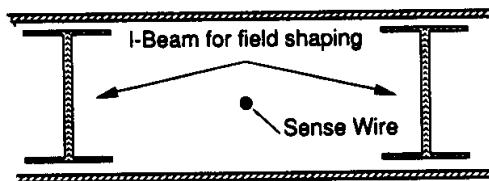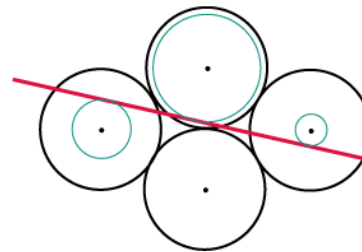❑ Not a linear relation between drift time and distance from the wire

Drift Chambers

sense wire

field wire

DRIFT TIME

LEFT   DISTANCE FROM WIRE   RIGHT

improved drift cell geometry with constant field

Anode wire
+ HV2

Drift region

Drift voltage
-H V I

Scintillation counter

Screening
electrodes

Cathode
drift wires

Field wire
- HV I

Anodic wire couple
+ HV 2

Field wire
- HV I

simplified drift geometry for construction of very large area chambers
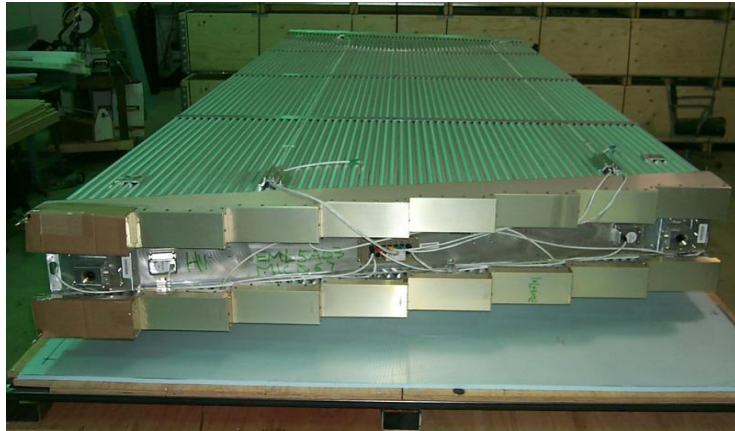

I-Beam for field shaping

Sense Wire

**DT CMS
(muon chambers)**

**MDT ATLAS
(muon chambers)**

ATLAS Drift Tube Chambers

Cross plate
Multilayer
In-plane alignment
Longitudinal beam
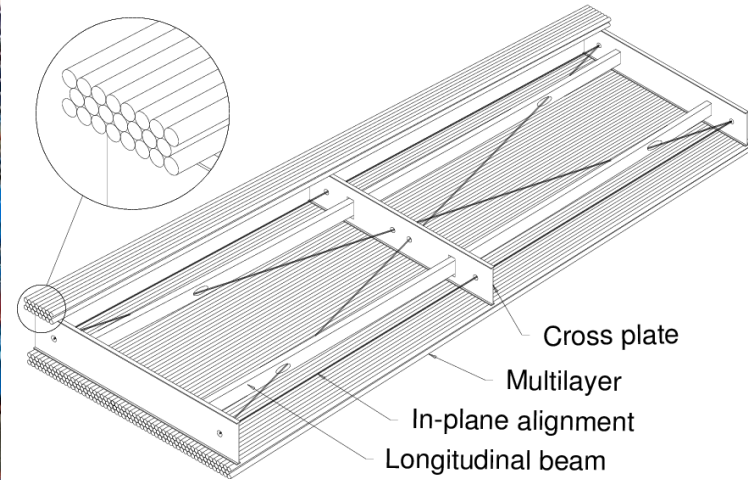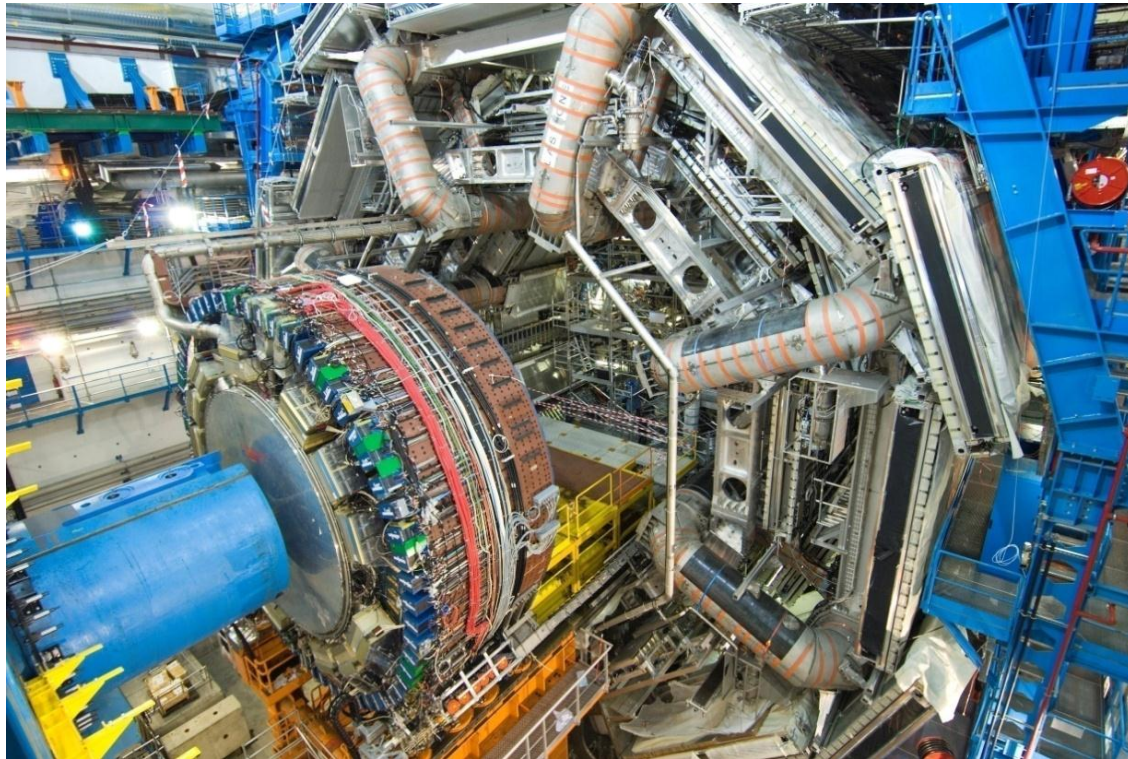
- 6 / 8 drift tube layers, arranged in 2 multilayers glued to a spacer frame
- length: 1 – 6 m, width: 1 – 2 m
- optical system to monitor chamber deformations
- gas: $Ar:CO_2$ (93:7) to prevent aging, 3 bar

- chamber resolution: 50 μm
  - ➡ single tube resolution: 100 μm
  - ➡ required wire position accuracy: 20 μm

CMS Drift Tube Chambers

42mm

13 mm

Electrode Strip

Mylar

Cathode Al Strips
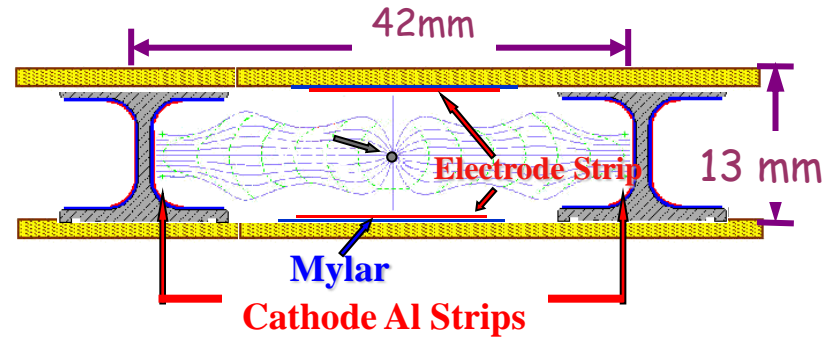
GAS	Ar/CO$_2$ (85/15)	
HV:	Wires	3600 V
	Strips	1800 V
	I-beams	-1200 V

250 Chambers
172200 Anode Channels

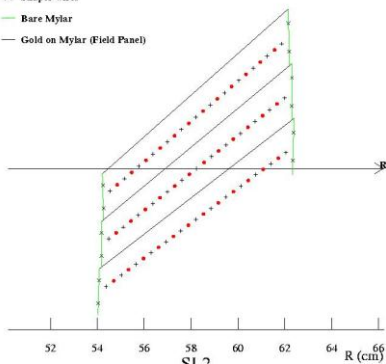|		
Tmax:	< 400 ns	
Drift Velocity :	~ 55μm/ns	
Single Wire Resolution :	< 300 μm	
	100 μm	Φ
	150 μm	Θ

Drift Chambers
CDF Central Tracking Chamber
660 drift cells tilted 45⁰ with respect to the particle track to take into account ExB drift!
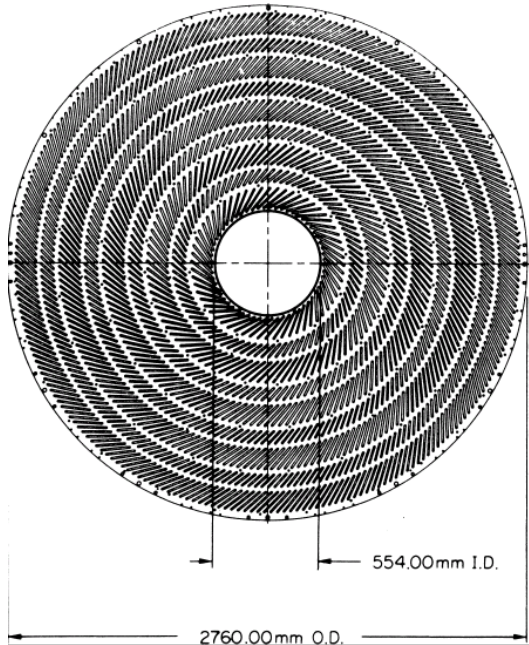
Time Projection Chamber (TPC)
1976: D. Nygren (LBL)
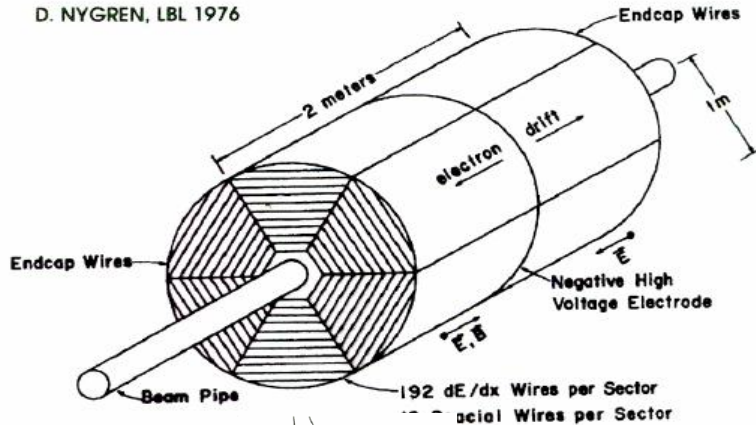
- E~100-300 V/cm. Drift times 10-100 μs
- B for momentum measurement
  (limit electron diffusion up to a factor 5)
- Wire chamber to detect projected tracks. Timing gives z measurement
- Long drift distances up to 2.5 m

gas volume

wire chamber to detect projected track

drift

B

E

charged track

B=0   B>0

The ALEPH TPC

ALEPH DALI

Run=15768   Evt=5906

CHARGE MAX 60KG

COIL
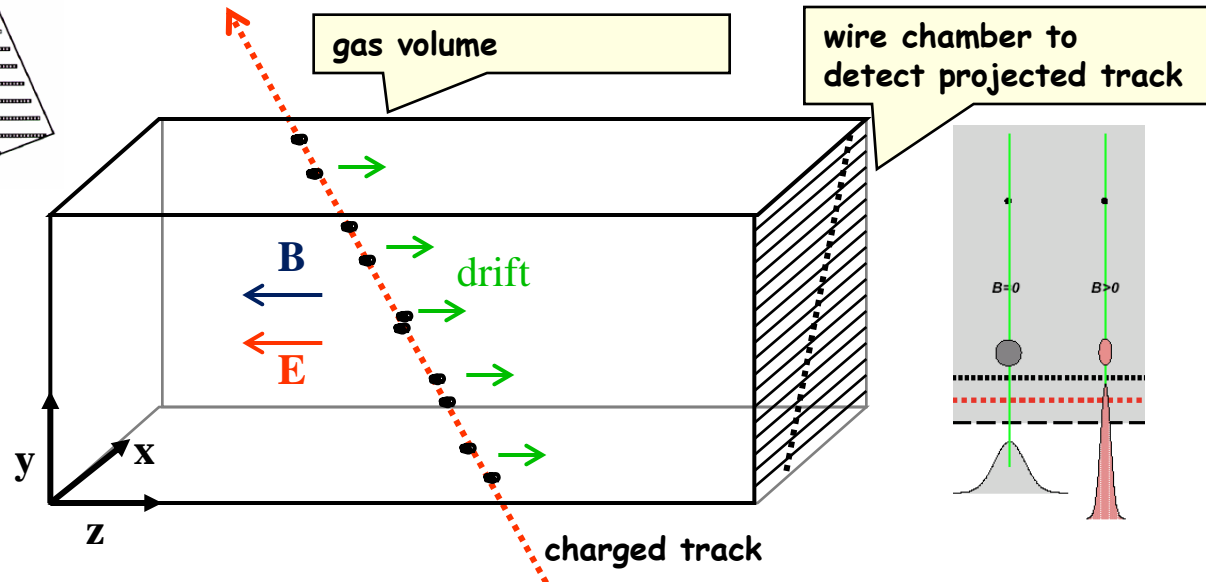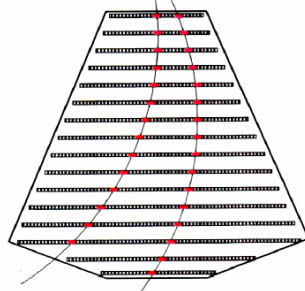WIRE CHAMBERS
INNER FIELD CAGE
OUTER FIELD CAGE
HV MEMBRANE
WIRE CHAMBER SUPPORT
Ø 3600
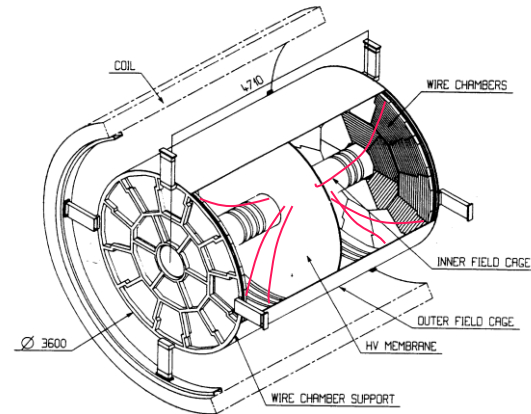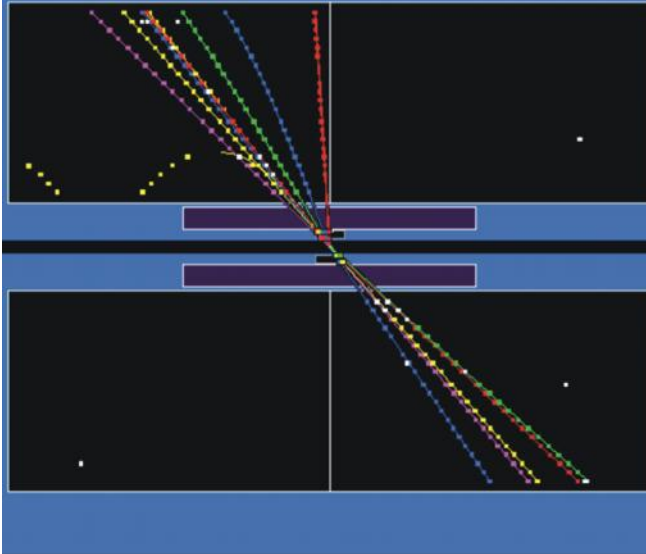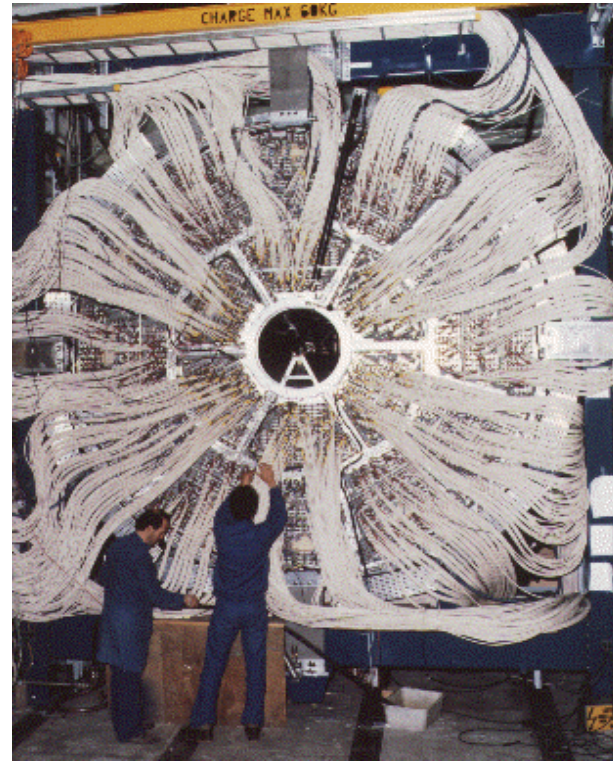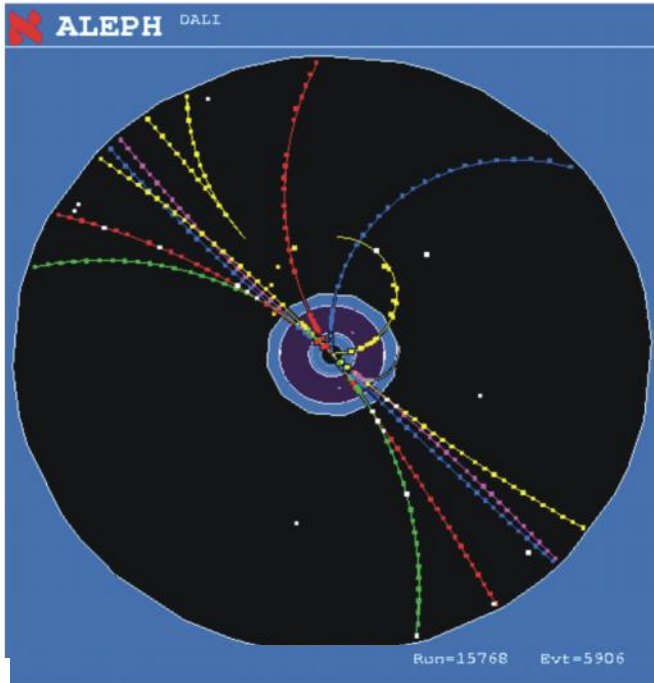
$\sigma_{R\phi} = 170\ \mu m$
$\sigma_z = 740\ \mu m$

very low multiple scattering in the gas volume of the detector
→ very good momentum resolution down to low momenta !

ALICE TPC

- **General features:**
  - Diameter $\times$ Length : 5 m $\times$ 5 m
  - Pseudo-rapidity interval: $|\eta| < 0.9$
  - Readout chambers: 72
  - Drift field: 400 V/cm
  - Maximum drift time: 92 μs
  - Central electrode HV: 100kV
- **Gas:**
  - Active volume: 90 m^3
  - Ne-CO$_2$-N$_2$: 85.7% - 9.5% - 4.8%
  - Cold gas - low diffusion
  - Non-saturated drift velocity
    - $\Rightarrow$ temperature stability and
    - $\Rightarrow$ homogeneity ≤ 0.1 K

HV electrode (100 kV)

field cage

readout chamber

5 m

5 m

TPC

ITS
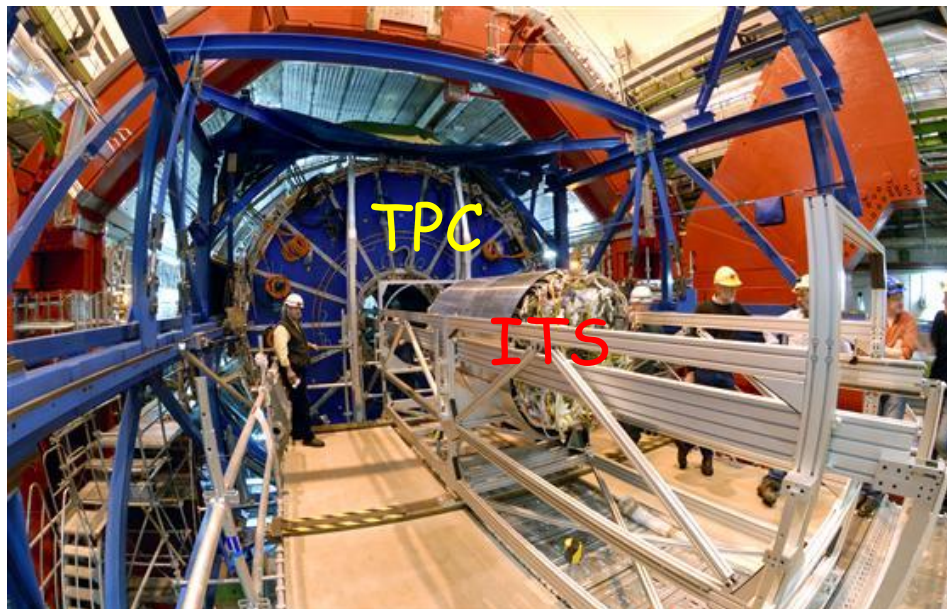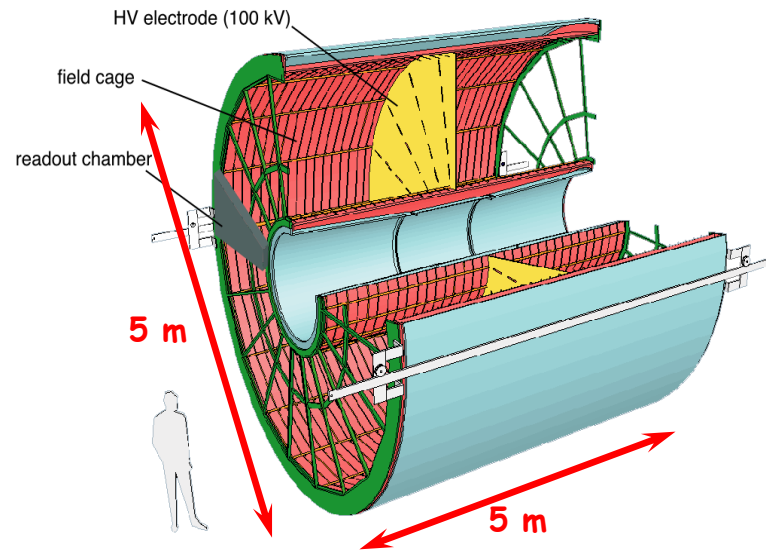
The family of gas detectors
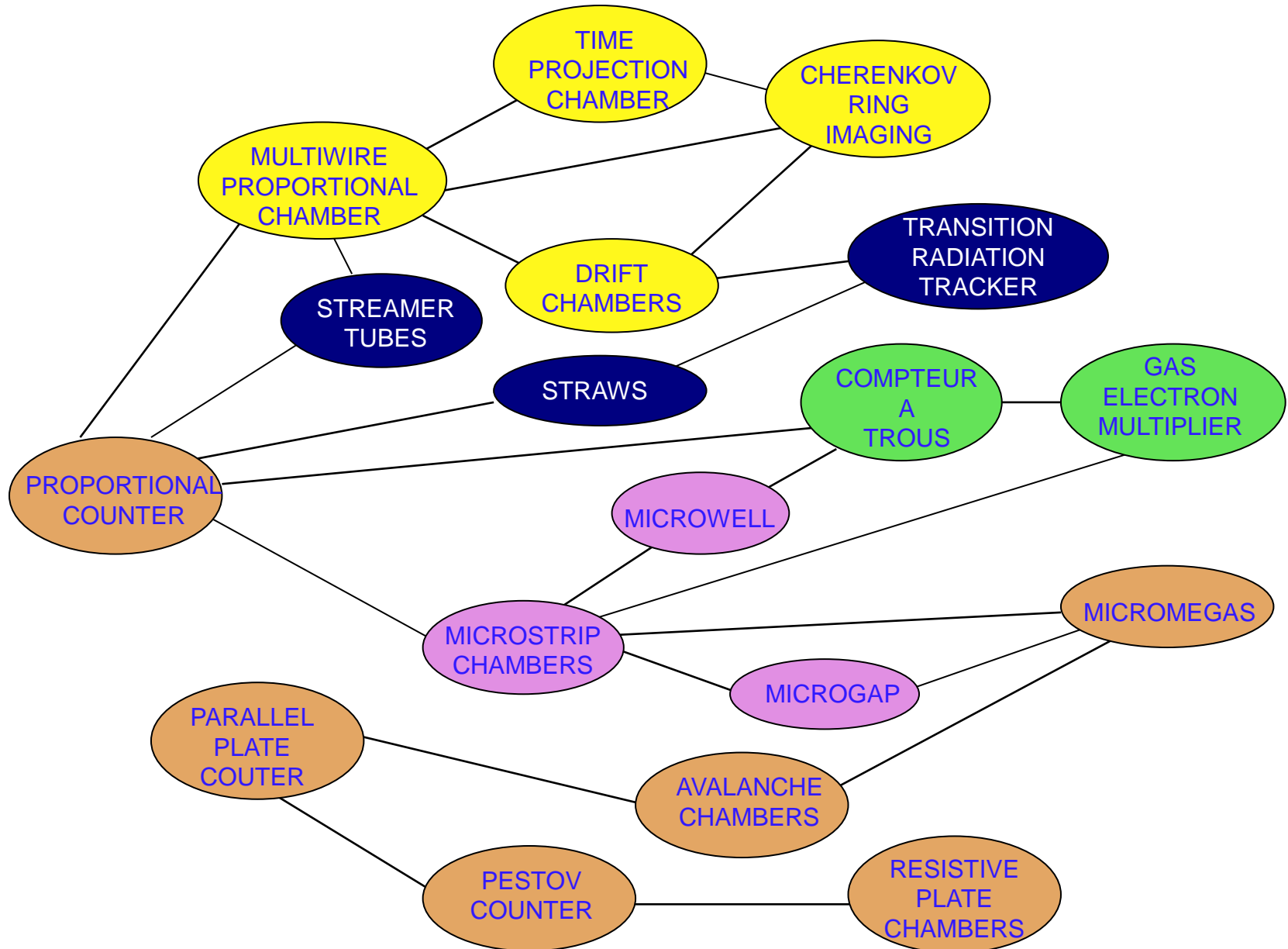
Gas Electron Multiplier (GEM)

Thin Kapton foil (50 μm) double side metal-coated (Cu 5 μm) 70 μm holes at 200 μm pitch

Ions

$-V_D$

3 mm DRIFT   CONVERSION AND DRIFT

$-V_2$

V_{GEM}

$-V_1$

1 mm transfer gap   INDUCTION

GEM

PC BOARD

Electrons

200 μm

I+

e⁻

transfer gap

e⁻

S1   S2   S3   S4

Driftcathode

DRIFT

GEM 1

TRANSFER 1

GEM 2

TRANSFER 2

GEM 3

COLLECTION

Readout PCB

Triple GEM

Standard *GEM*

55 μm

70 μm

F. Sauli, Nucl. Instr. and Methods A386(1997)531
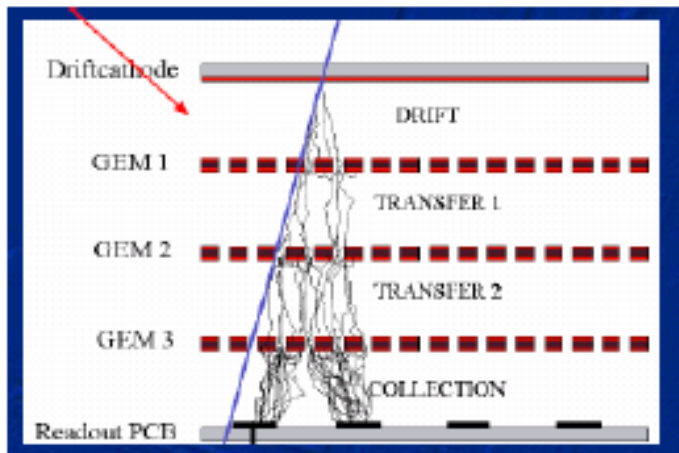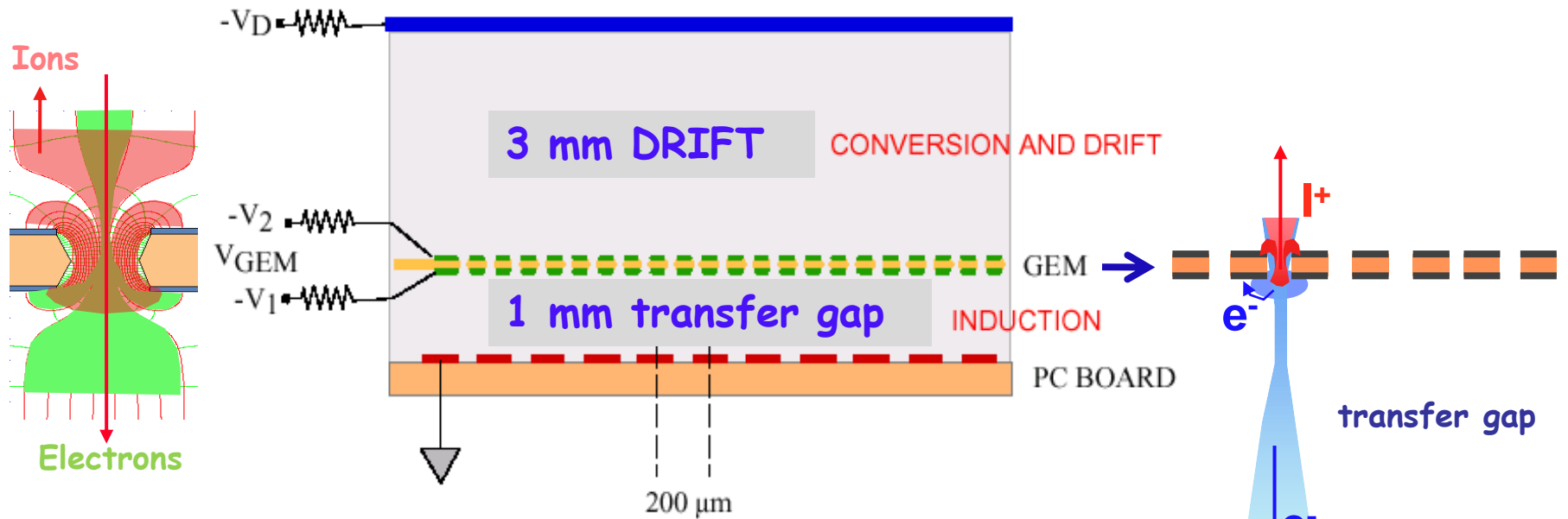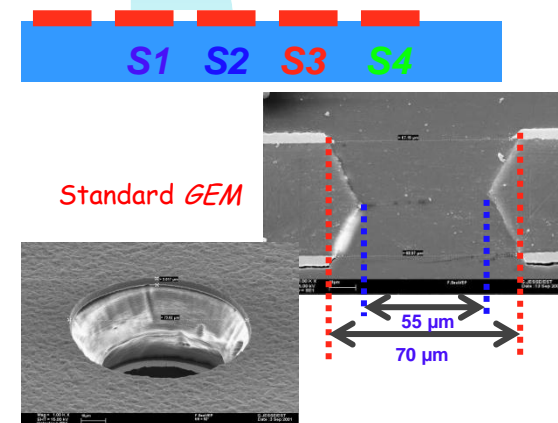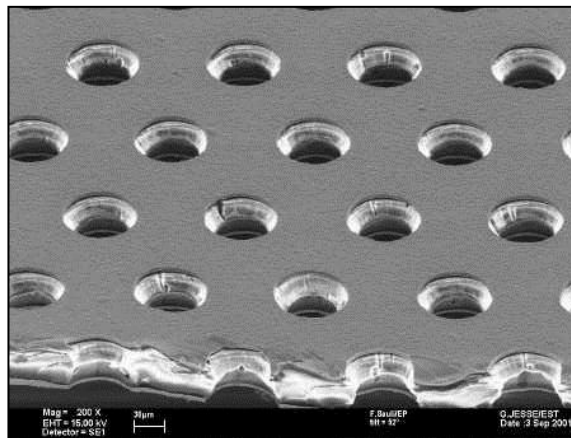
T2 Telescope

◆ **Gas Electron Multiplier (GEM)**

◆ **$5.3 < |\eta| < 6.5$**

◆ **10 half-planes @ 13.5 m from IP5**

◆ **Half-plane:**

- 512 strips (width 80 μm, pitch of 400 μm), radial coordinate
- 65*24=1560 pads (2x2 mm^2 -> 7x7 mm^2), radial and azimuth coord.
- Resolution: $\sigma(R)$ ~ 100 μm, $\sigma(\varphi)$ ~ 1°

◆ **Primary vertex reconstruction (beam-gas interaction removal)**

◆ **Trigger using (super) pads**
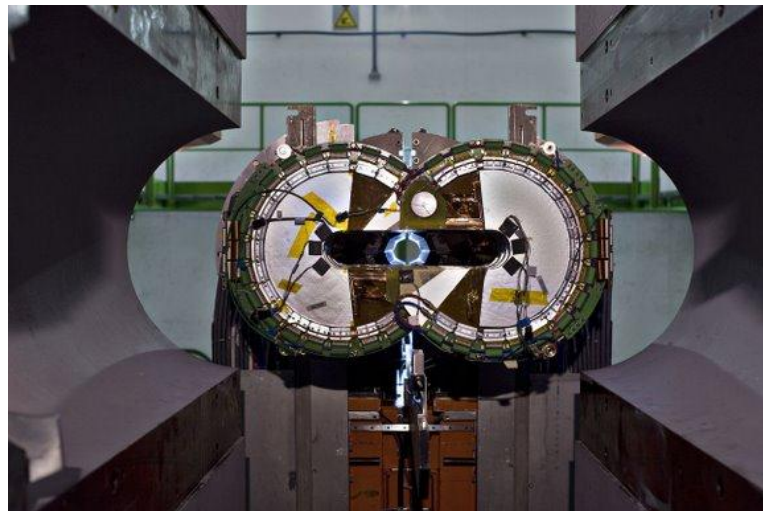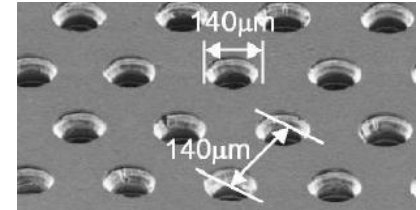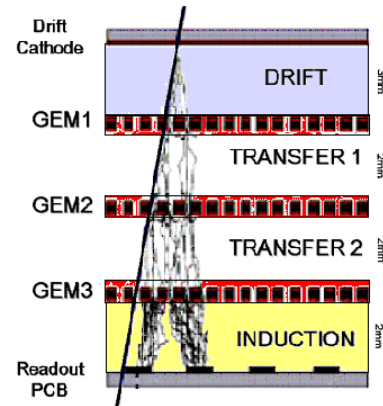
Solid State Detectors

In solid state detectors the charges produced by the ionization due to the incoming particle are sufficient to provide a measurable signal.

❑ **Solid state detectors have a high density**
   ➔ **large energy loss in a short distance:**
   116 (78) keV = mean (most probable) energy loss
   for 300μm Silicon thickness

❑ **Low ionisation energy (few eV per e-hole pair) compared to gas detectors (20-40 eV per e-ion pair)**
   3.6 eV for silicon to create an e-hole pair
   $\Rightarrow$ **72 e-h/μm (most probable); 108 e-h/μm (mean)**
   $\Rightarrow$ **most probable charge 300μm Silicon thickness:**
   $\approx$ **21600 e $\approx$ 3.5 fC**

❑ **Drift velocity much faster than in gas detectors:**
   ➔ **Very fast signals of only a few ns length !**

❑ **Diffusion effect is smaller than in gas detectors:**
   ➔ **achievable position resolution of less than 10 μm**

Si-Diode as Si-Detector

By applying an external voltage V, the depletion zone can be extended to the entire diode.

An incoming particle can then produce by ionization free charge carriers in the diode. The charges carriers drift in the electric field and induce an electrical signal on the electrodes.
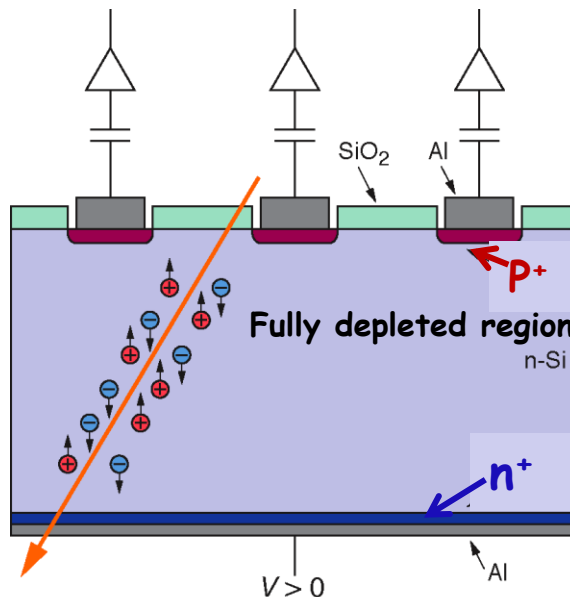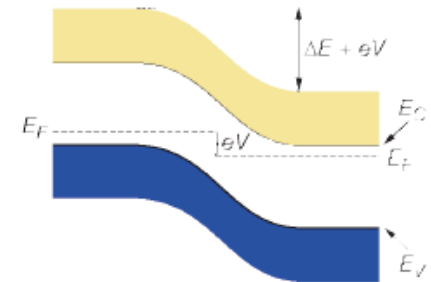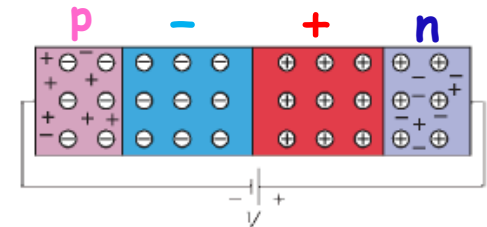
➔ **That is the way a Silicon detector can work !**

Detector Structures

Top view of a strip detector with polysilicon resistors:

- bias line
- polisilicon resistors
- guard ring
- readout strip
- bond pads
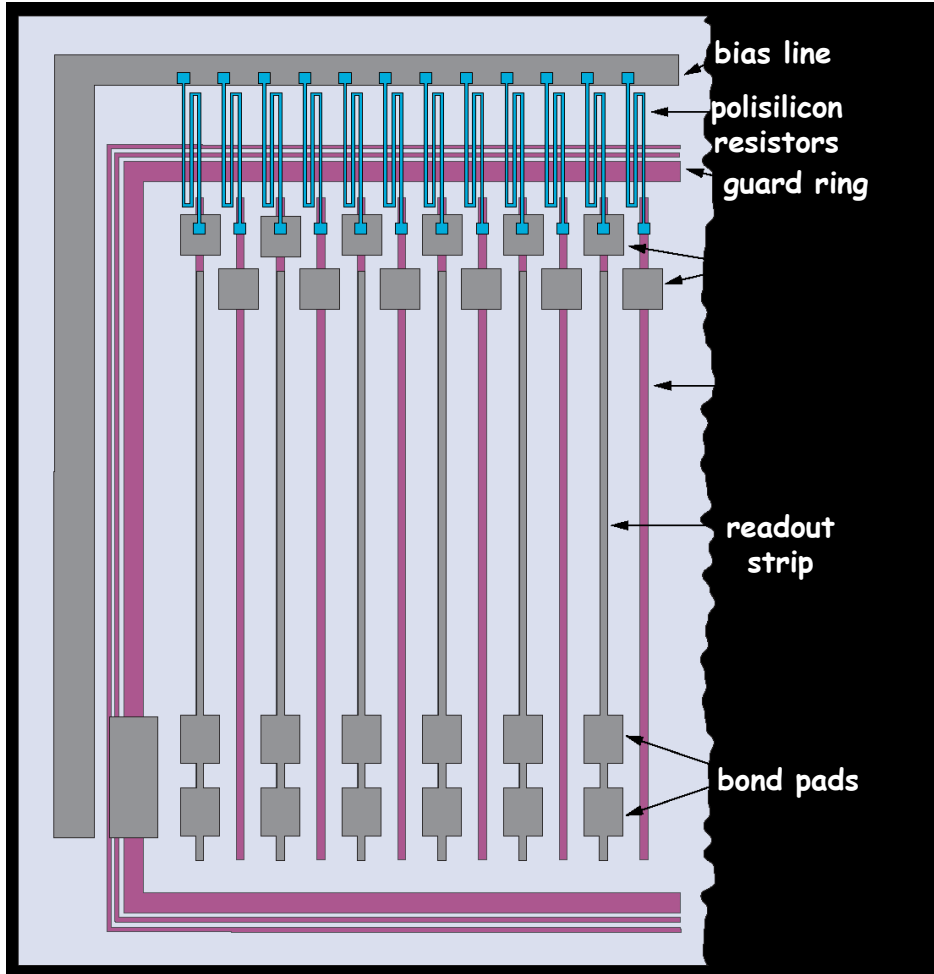
CMS-Microstrip-Detector: Close view of area with polysilicon resistors, probe pads, strip ends.

polysilicon resistor — Al (bias line)

Al (readout strip)

Al (probe pad)

SiO₂

SiO₂

SiO₂

V

p⁺-Si (readout strip)

p⁺-Si (guard rings)

n-Si

n⁺-Si

Al
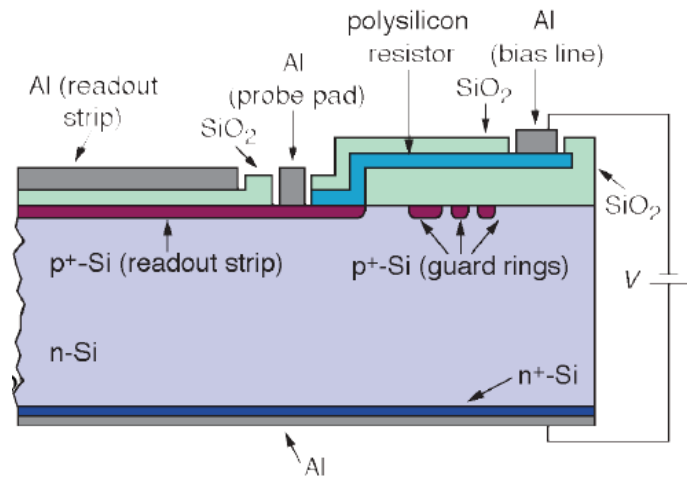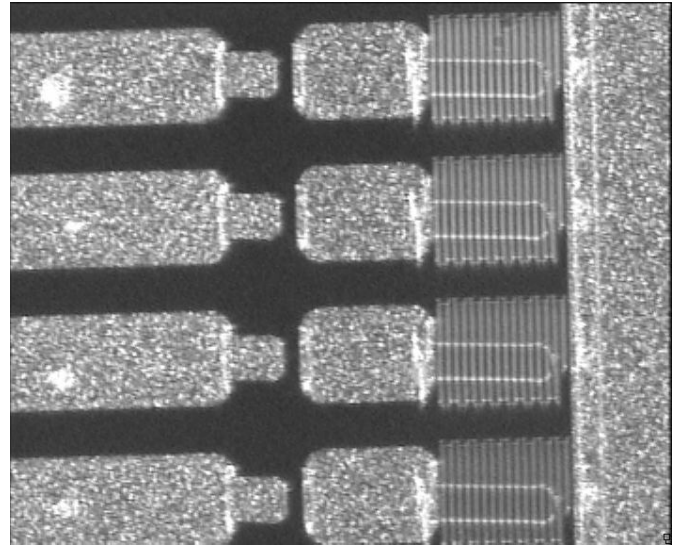
Polysilicon pieces

Single crystal

Wafers in a package box

Silicon wafers with different diameter

Electronic parts

A CMS silicon strip detector built with a 6" wafer
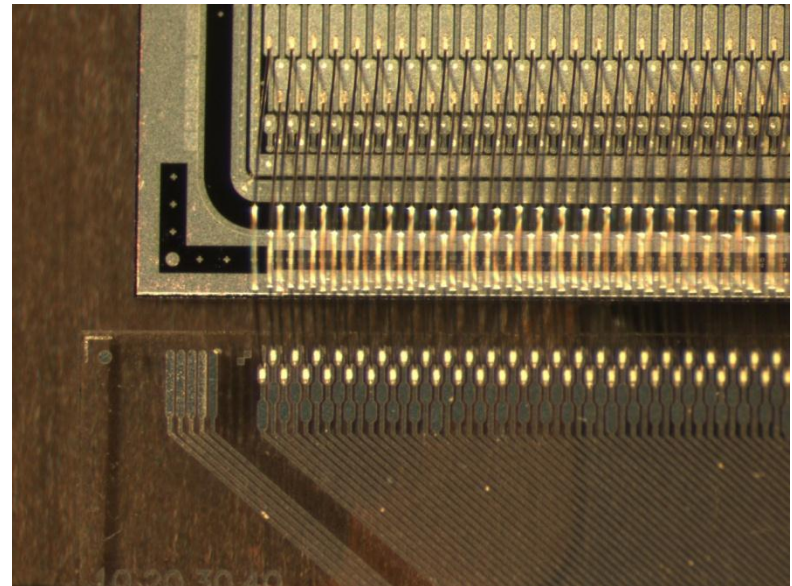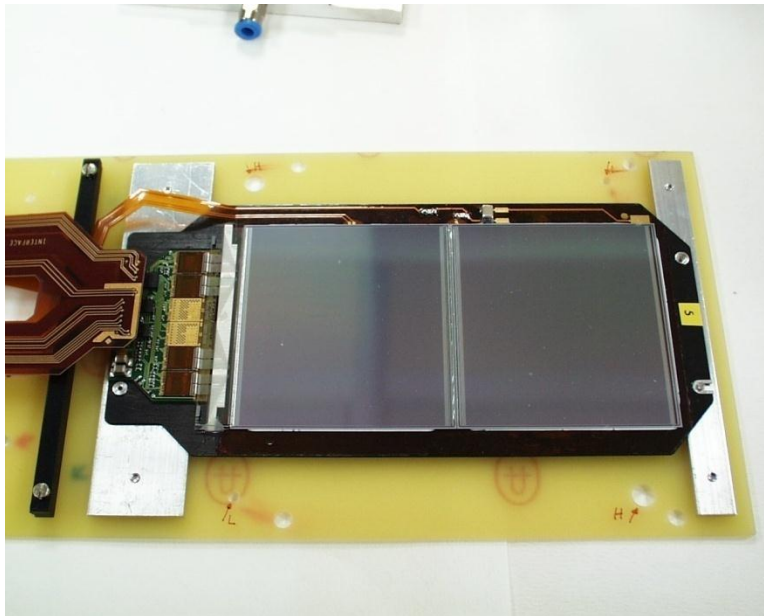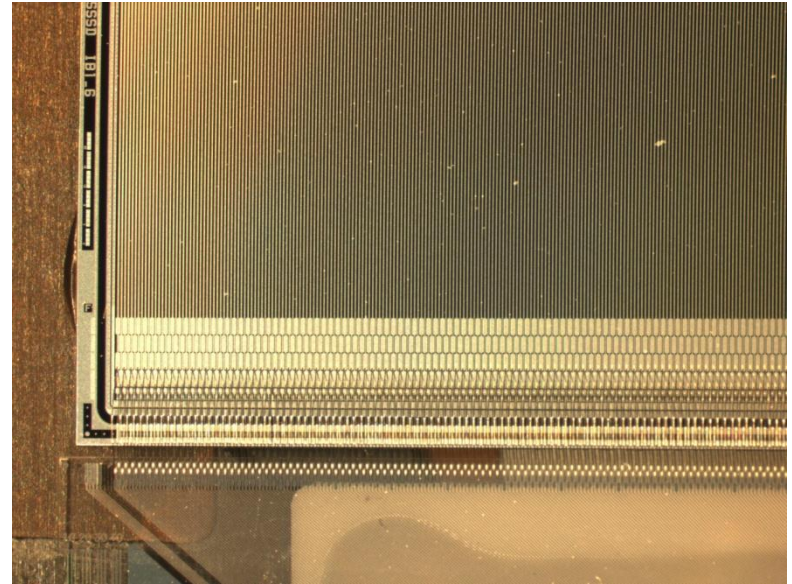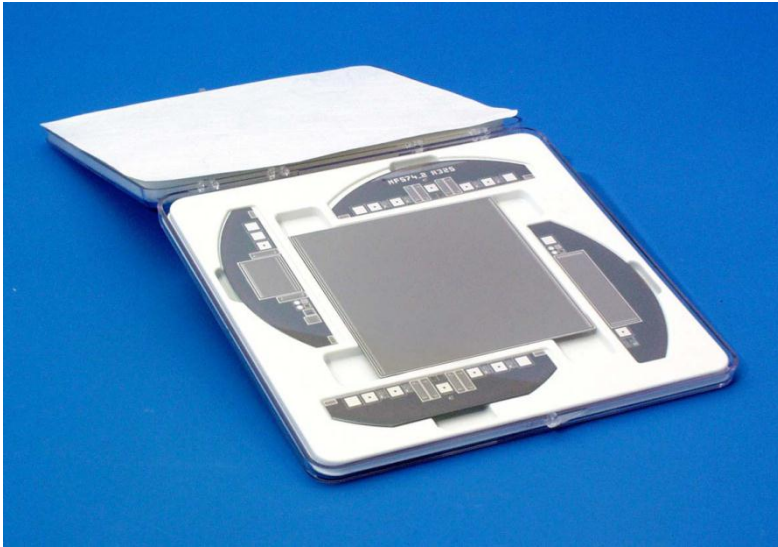
CMS modules of Silicon Strip Tracker

hybrid conn.

readout hybrid
- 4 or 6 APV à 128 channel
- 192x25ns analog pipel.
- 0,25 µm CMOS technol.
- capton flex circuit
- ceramic stabiliser

pitch adapter

kapton bias

TEC petal
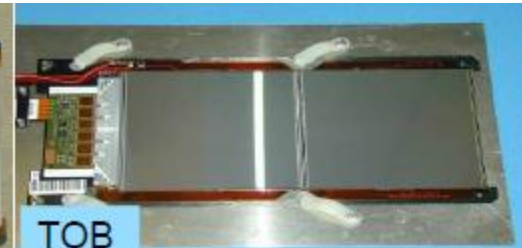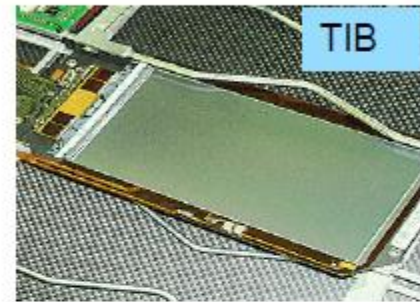
Carbon fibre or graphite frame

TEC

TOB

TIB

- **sensor**
- 6" wafer size
- p^+ on n
- 80..205 µm pitch
- 512 or 768 strips
- STM / HPK

Analog optical signal
transmitted O(100)m
digitized by FED

76 000 APVs
36 000 fibres
440 FED
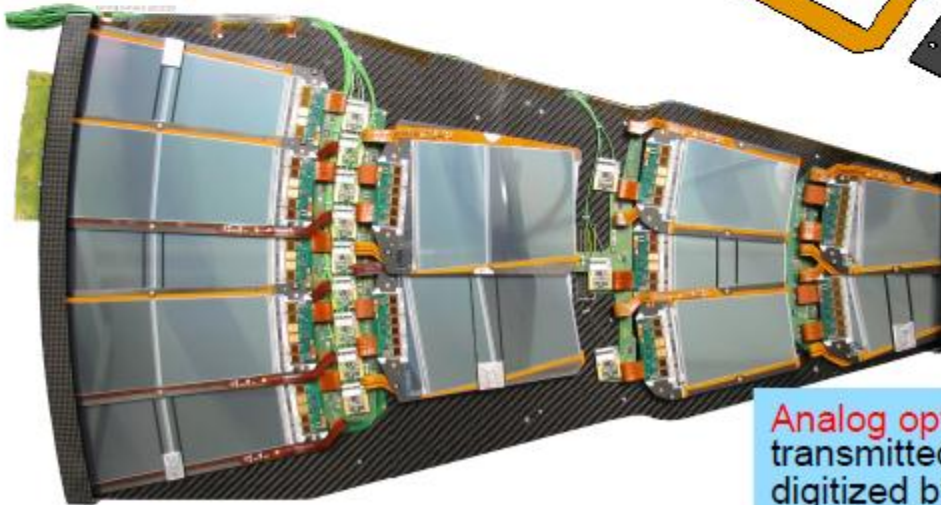
CMS has chosen an all-silicon configuration

Outer Barrel –TOB–

Pixel

End cap –TEC–

Inner Barrel –TIB–

Inner Disks –TID–

2.4 m

5.4 m

volume 24.4 m^3
running temperature – 10 ^{0}C

Cables and services
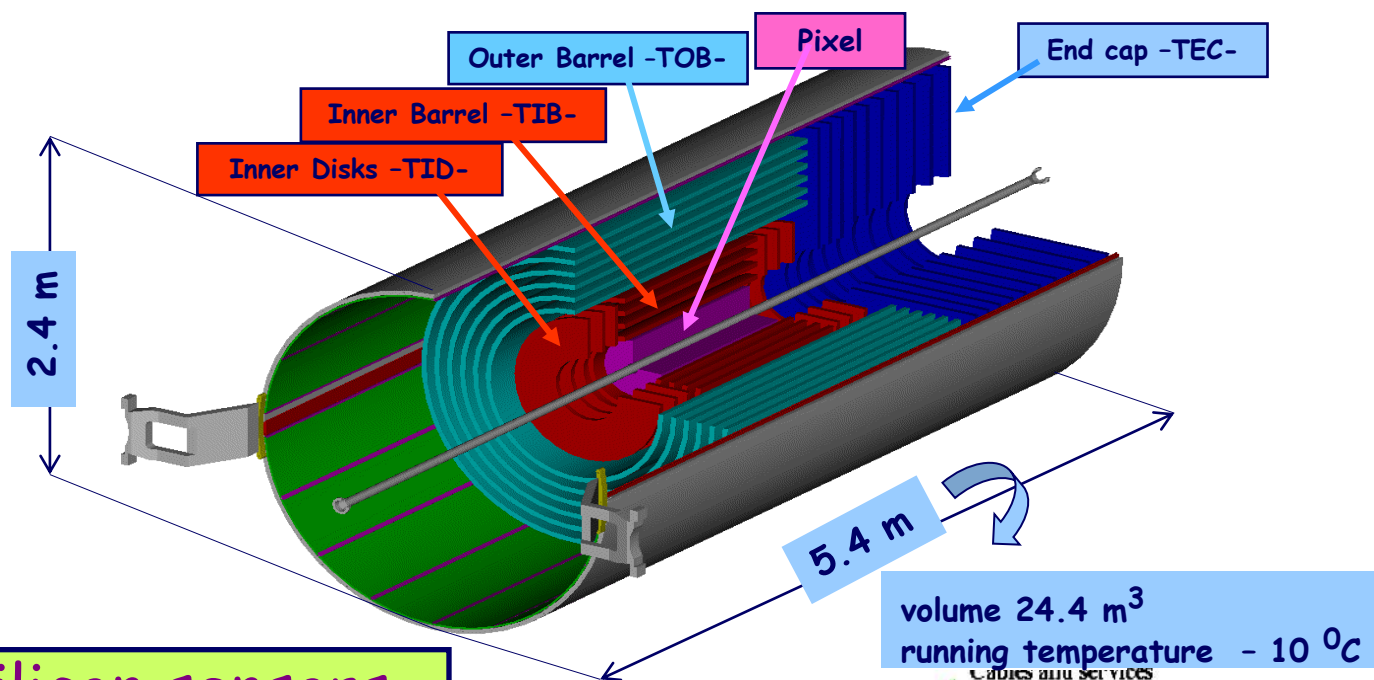
207m^2 of silicon sensors
10.6 million silicon strips
65.9 million pixels ~ 1.1m^2

Strips:
  Pitch: 80 µm to 180µm
  Hit Resolution: 20 µm to 50µm

Pixels:
  100 µm x 150µm
  rφ and z resolution: ~15 µm

TOB 6 Layers

TEC
9 Disks

TIB 4 Layers
TID
3 Disks

Pixels 3 Layers and 2 Disks
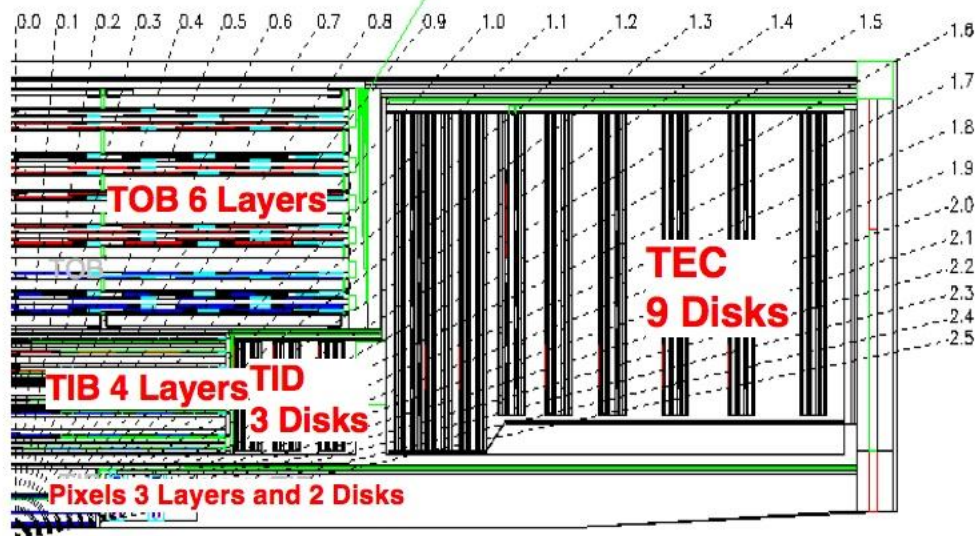
The CMS Silicon Strip Tracker

Cables and services

0.0 0.1 0.2 0.3 0.4 0.5 0.6 0.7 0.8 0.9 1.0 1.1 1.2 1.3 1.4 1.5 1.6 1.7 1.8 1.9 2.0 2.1 2.2 2.3 2.4 2.5

TOB 6 Layers

TEC 9 Disks

TIB 4 Layers **TID 3 Disks**

Pixels 3 Layers and 2 Disks

TIB

TOB

TEC
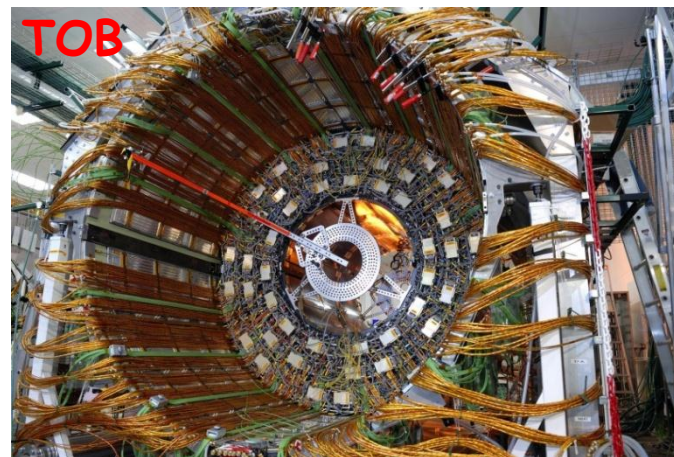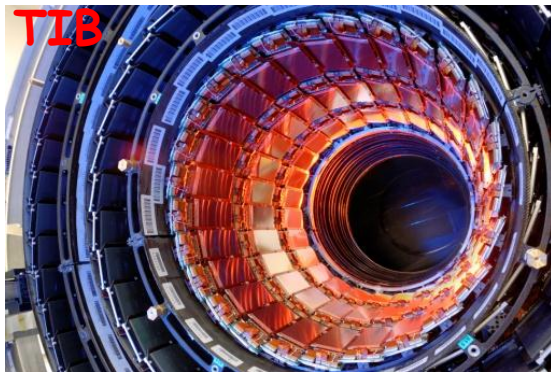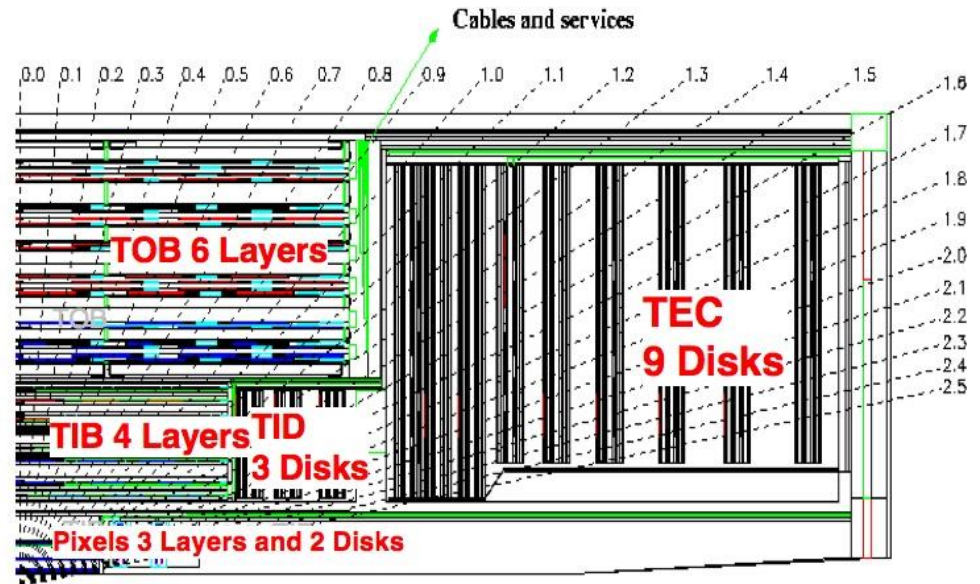
ATLAS Inner Detector

- **Transition Radiation Tracker (TRT)**
  - **4 mm diameter straw tubes**
  - **351 k channels**
  - **resolution 130 μm**
  - **polypropylene/polyethylene as transition radiation material: electron id 0.5 GeV<E<150 GeV**

- **SemiConductor Tracker (SCT)**
  - **4088 modules**
  - **80 μm strips (40 mrad stereo)**
  - **6 M channels**
  - **resolution 17 μm × 580 μm**

- **Pixel**
  - **1744 modules of 46080 pixels**
  - **mostly 50 μm × 400 μm**
  - **80 M channels**
  - **resolution 10 μm × 110 μm**
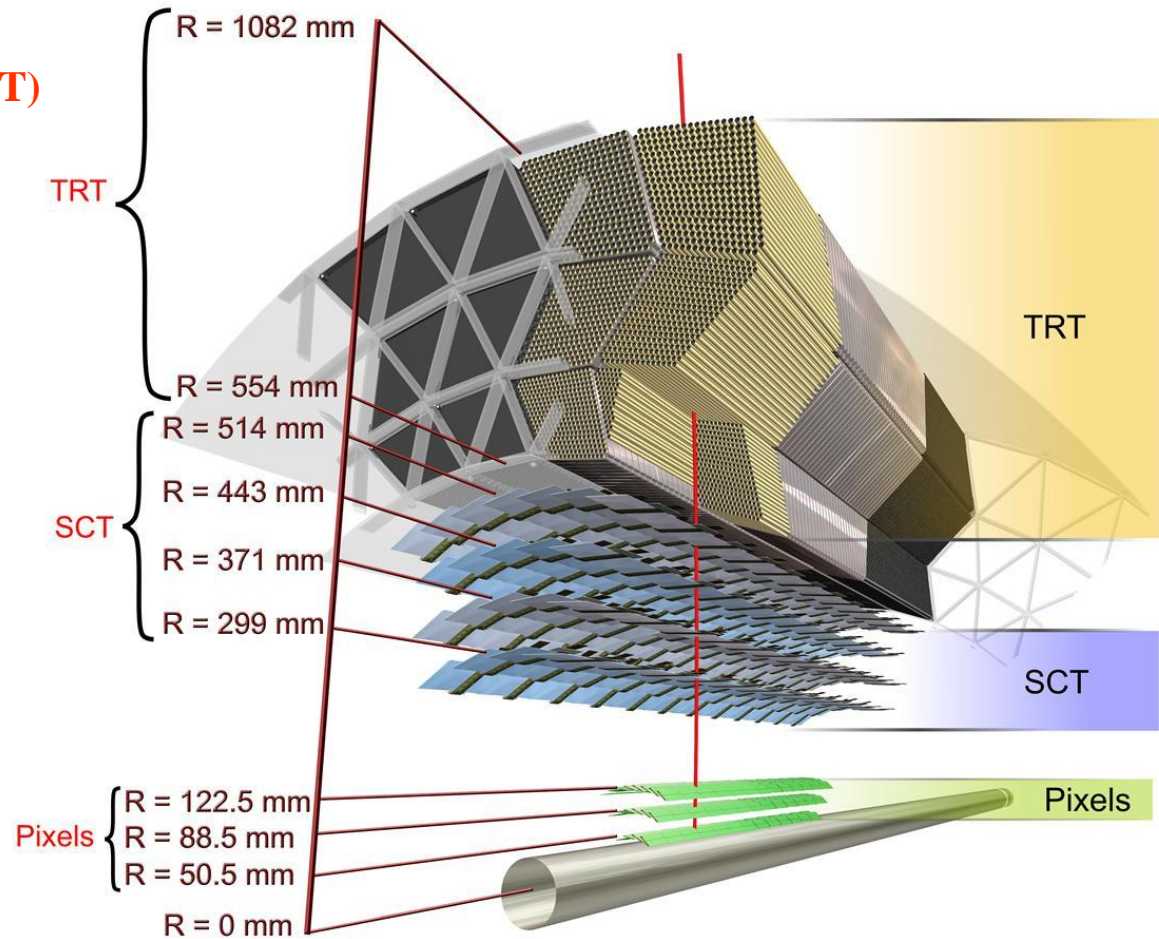
- **7-points silicon (pixels + strips) tracker (|η|<2.5)**
- **straw tubes quasi-continuous tracker (36 points +electron id) (TRT) (|η|<2).**
- **2 T solenoidal magnetic field**

- Momentum resolution:
  $$\sigma(p_t)/p_t = 0.05\% \, p_t \,(GeV/c) \oplus 1\%$$
- IP resolution:
  $$\sigma(d_0) = 10 \, \mu m \oplus 140 \, \mu m / p_t \,(GeV/c)$$

The ATLAS Semiconductor Tracker (SCT)

Forward SCT

Barrel SCT

Pixel Detectors

TRT
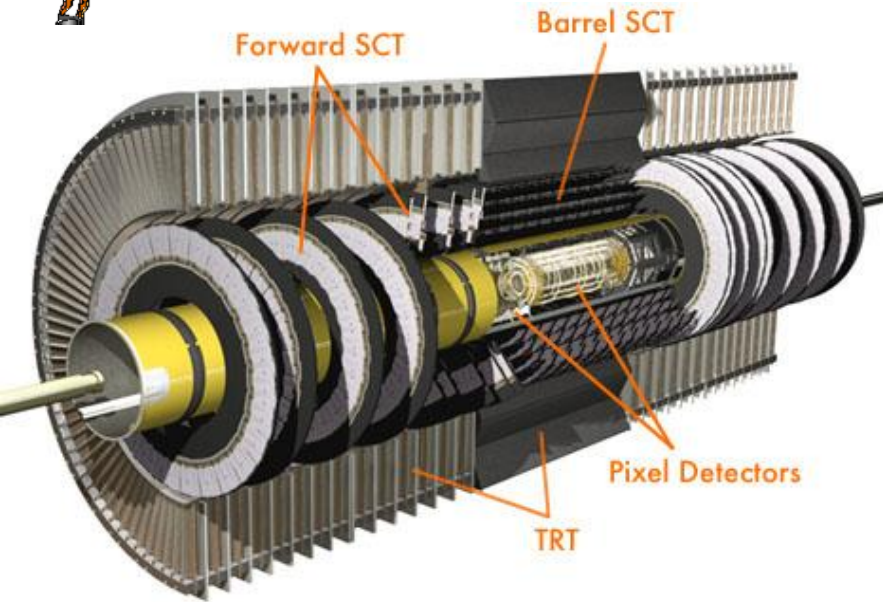
The SemiConductor Tracker (SCT) is a silicon strip detector. It's organized in 4 layers barrel, built with 2112 modules and two 9 disks end-caps, made of 1976 modules. The total number of strips is $6.3 \cdot 10^6$.

Physics requirements

- Resolution (x* y): **17 µm * 580 µm**
- Alignment tolerances (x*y): **12 µm * 50 µm**
- Noise occupancy: **$< 5 * 10^{-4}$**
- Efficiency: **> 99%**
- Radiation : **~ $2 * 10^{14}$ Neq cm^{-2} over 10 years**

The barrel module consists of four single sided p-on-n strip detectors:

- Pitch 80 mm
- Strip length 120 mm
- Stereo angle 40 mrad

40 mrad

~12 cm

~6 cm

SCT barrel module

The end-caps are built with three different modules:

- Pitch 57-95 mm
- Strip length 55-120 mm
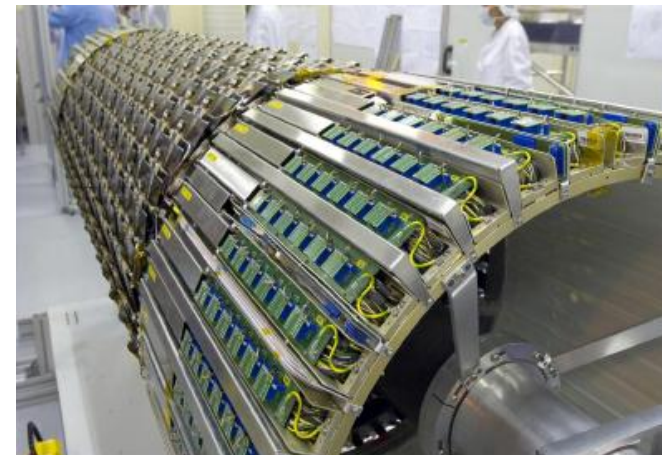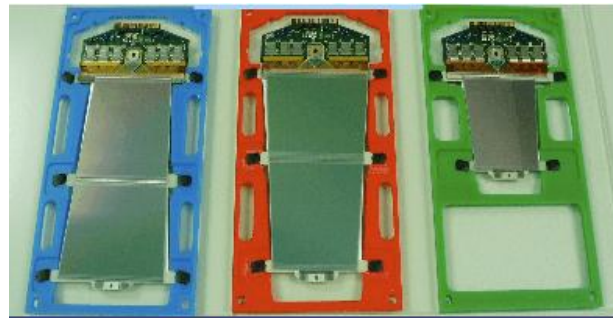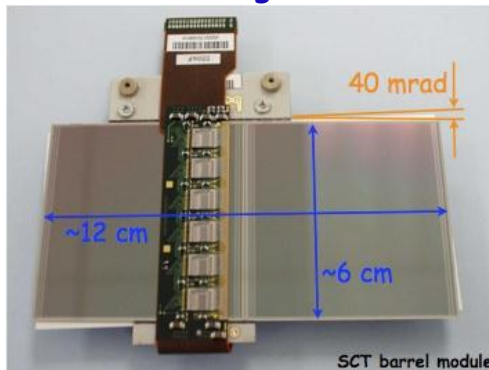
Double Sided Strip Detectors
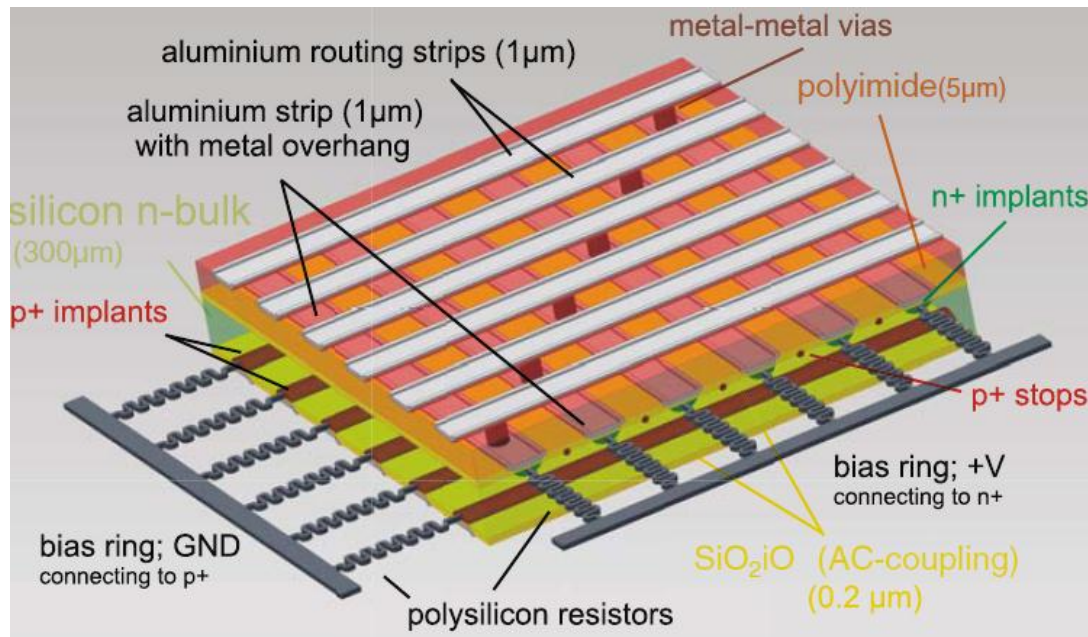
❖ **Single sided strip detector measures only one coordinate.**
   To measure second coordinate requires second detector layer.
❖ **Double sided strip detector minimizes material measuring two**
   coordinates in one detector layer.
❖ **In n-type detector the n+ backside becomes segmented**
   e.g. strips orthogonal to p+ strips.
❖ **Drawback: Production, handling, tests are more complicated and**
   hence double sided detector are expensive.

Double Sided Strip Detectors

charged particle A

charged particle B
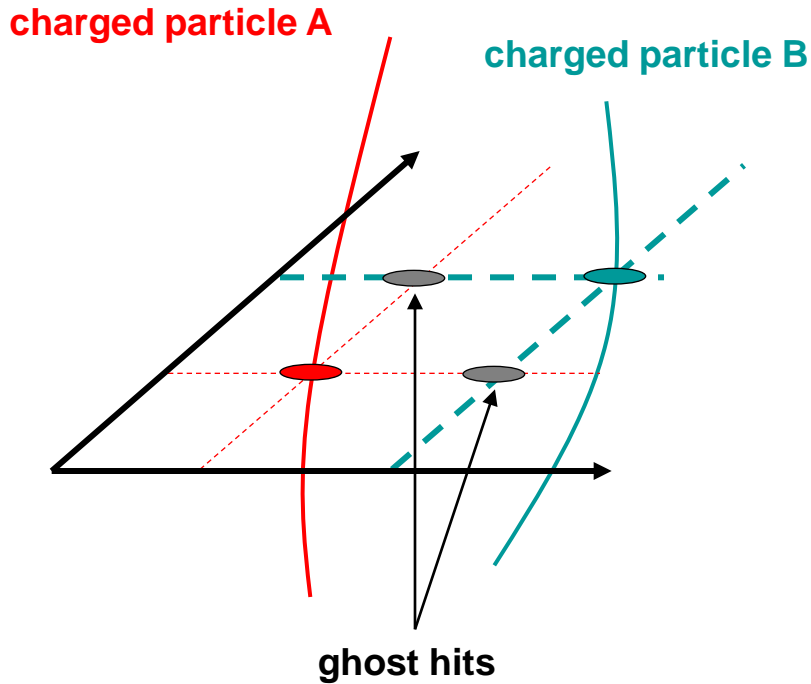
Double sided strip sensors measure the 2 dimensional position of a particle track. However, if more than one particle hits the strip detector the measured position is no longer unambiguous. "Ghost"-hits appear!

ghost hits

Pixel detectors produce 2-dimensional position measurements without ambiguity also in case of two particles crossing the detector!

150 μm

100 μm

chip pixel unit cell

solder bump

sensor pixel

silicon sensor

readout chip

data buffers

readout control

data
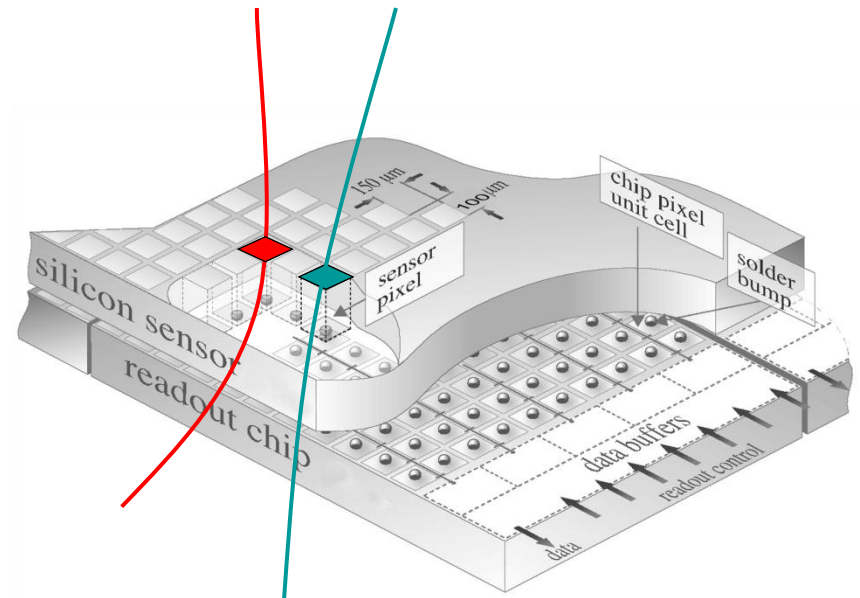
Pixel Detectors

❑ **Typical pixel size 50 x 200 µm^2; 100 x 100 µm^2:**
  ➢ **Small pixel area ➔ low detector capacitance (≈1 fF/Pixel)**
     ➔ large signal-to-noise ratio (e.g. 150:1).
  ➢ **Small pixel volume ➔ low leakage current (≈1 pA/Pixel)**
❑ **Large number of readout channels:**
  ➢ **Large number of electrical connections**
  ➢ **Large power consumption of electronics**

Problem:
  Coupling of readout electronics to the detector
Solution:
  Bump bonding
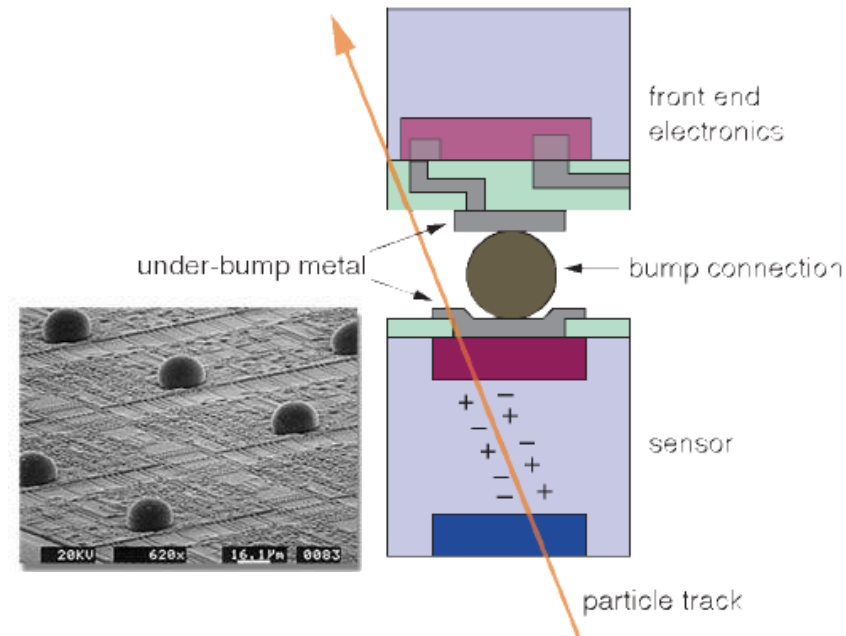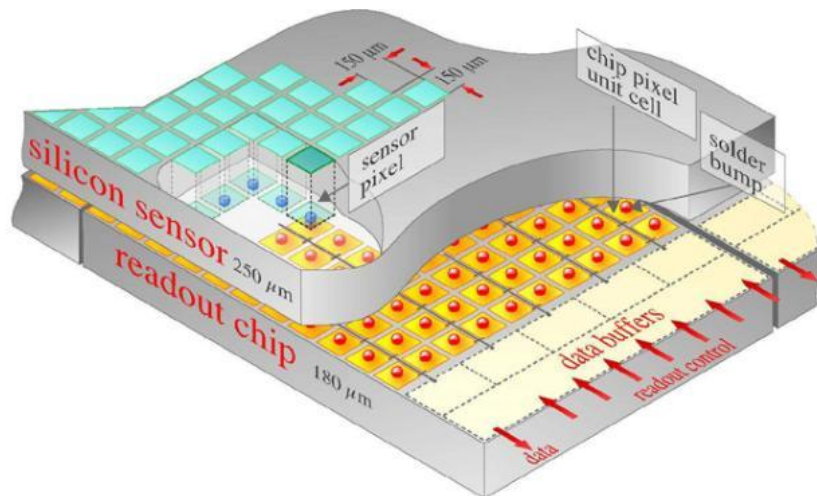
The ATLAS Pixel Detector

- **Requirements:**
  - **Position resolution in $r\Phi$-direction < 15µm**
  - **3 track points for $|\eta| < 2.5$**
  - **Time resolution < 25 ns**
  - **Hit detection efficiency > 97%**
- **3 barrel layers**
  - **r = 5.05 cm, 8.85 cm, 12.25 cm**
- **3 pairs of Forward/Backward disks**
  - **z = 49.5 cm, 58.0 cm, 65.0 cm**
- **Pixel size:**
  - **50 µm x 400 µm & 50 µm x 600 µm**
- **~ 2.0 m² of sensitive area with 8×10^7 ch**

- **Modules are the basic building elements**
  - **1456 in the barrel + 288 in the endcaps**
  - **Active area 16.4 mm x 60.8 mm**
  - **Radiation tolerance 500 kGy / 10^{15} 1 MeVn$_{eq}$cm^{-2}**

The same module is used in the barrel and in the disks:

- **staves (13 modules along the beam axis) for the barrel.**
- **sectors (6 modules on a two-sided octant) for the disks.**
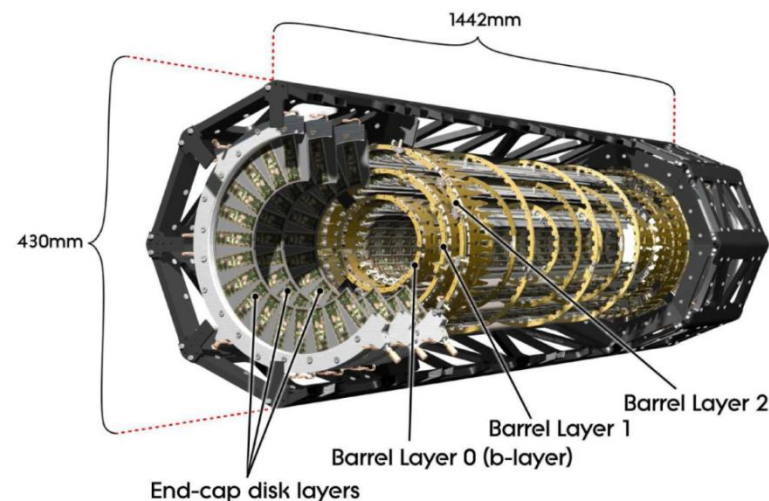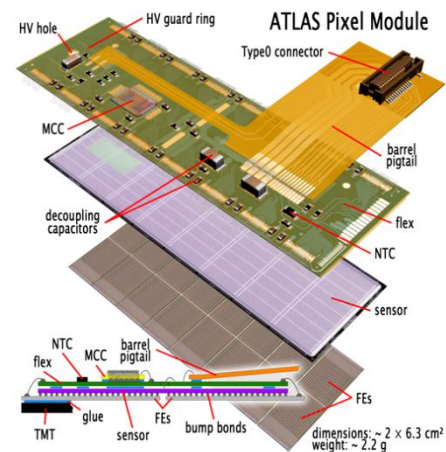
The CMS Pixel Detector

- **3 Barrel layers at 4.3, 7.2, 11.0 cm**
- **2 Forward Disks**
- **3-hit coverage for tracks |η|<2.5**

Total Area: 0.78+0.28 m^2
66 Million Pixels

Sensors: n on n Silicon 265 – 270 μm
150 x 100 μm pixels $\sigma(z) \sim \sigma(r\varphi) \sim$ 15μm
Bump-bonded to PSI 46 Read Out Chips (analog readout)
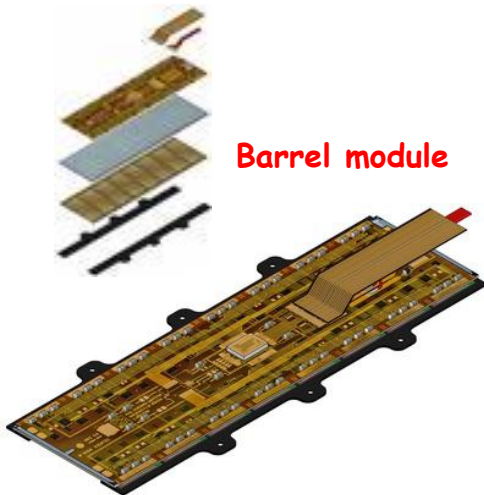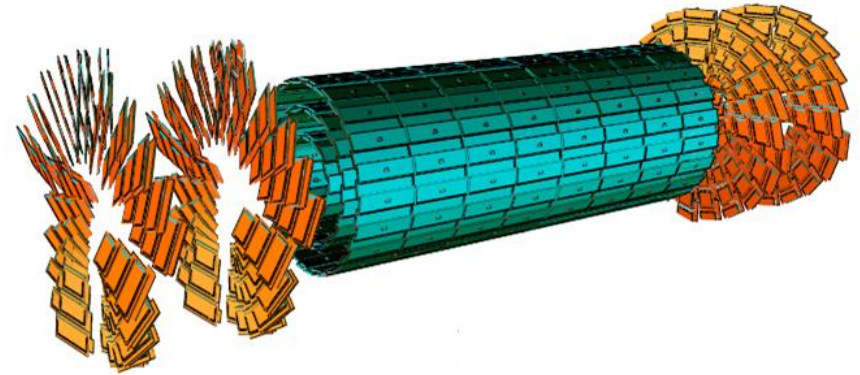
Barrel module
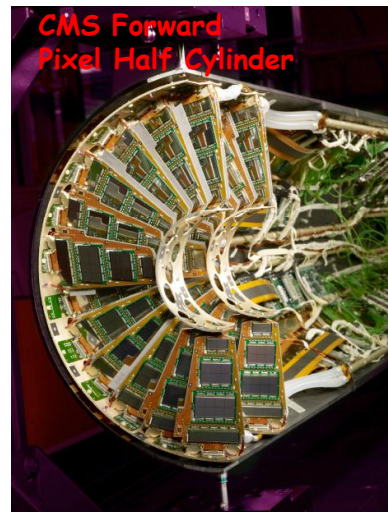
CMS Forward
Pixel Half Cylinder
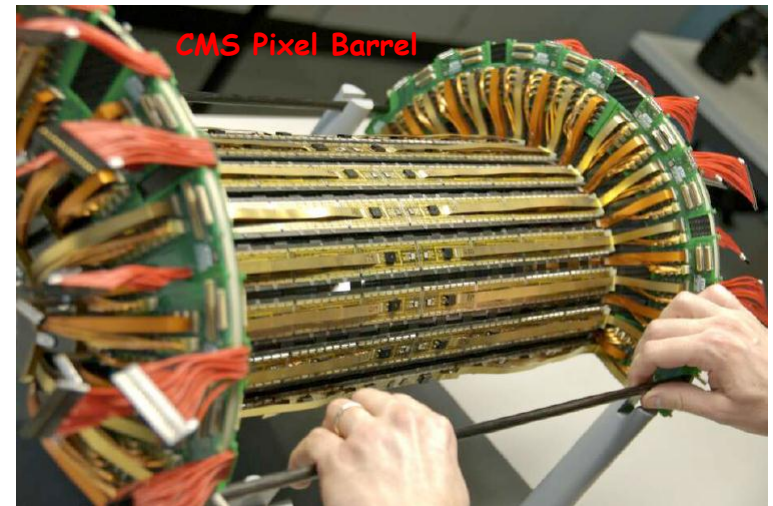
CMS Pixel Barrel

Silicon Drift Detector (like gas TPC !)
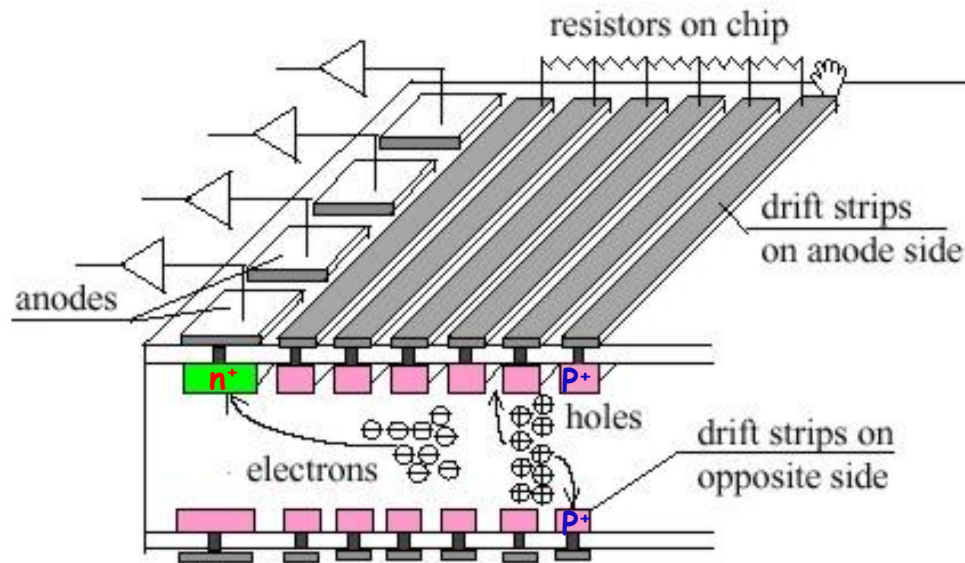
In silicon drift detectors the p+ strips and the backplane p+ implantation are used to fully deplete the bulk.

A drift field transports the generated electrodes to the readout electrodes (n+).

One coordinate is measured by signals on strips, the second by the drift time.

ALICE: Inner Tracking System
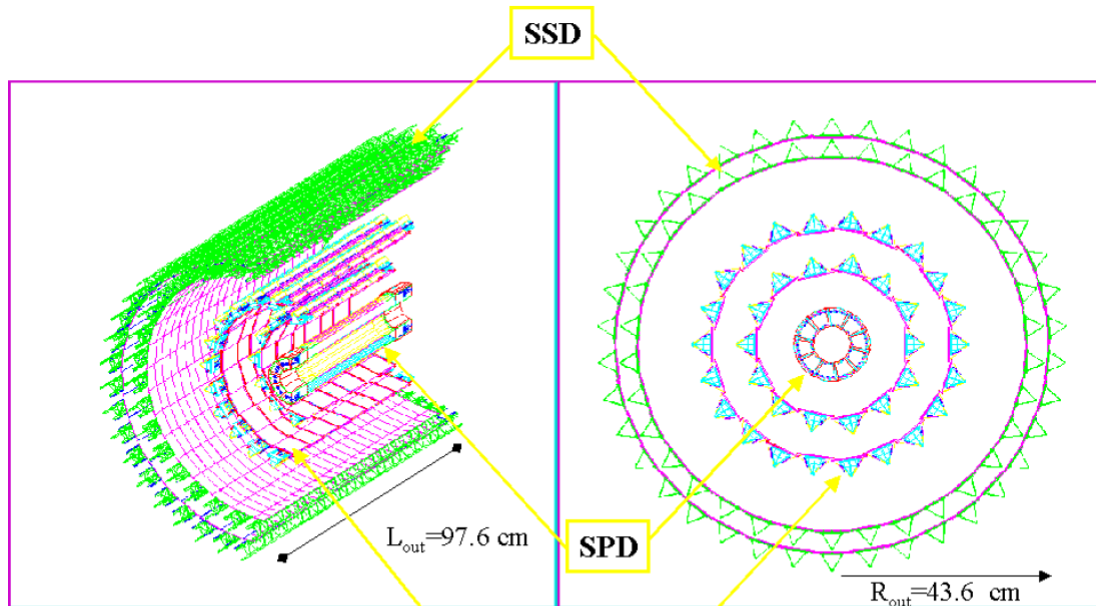
Silicon Pixel Detector (SPD):
- ~10M channels
- 240 sensitive vol. (60 ladders)

Silicon Drift Detector (SDD):
- ~133k channels
- 260 sensitive vol. (36 ladders)

Silicon Strip Detector (SSD):
- ~2.6M channels
- 1698 sensitive vol. (72 ladders)

L_{out}=97.6 cm

R_{out}=43.6 cm

SSD

SPD

SDD
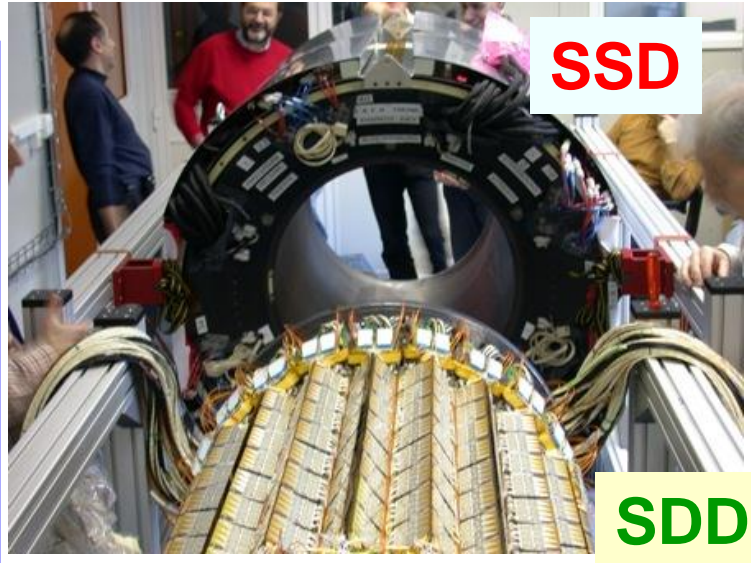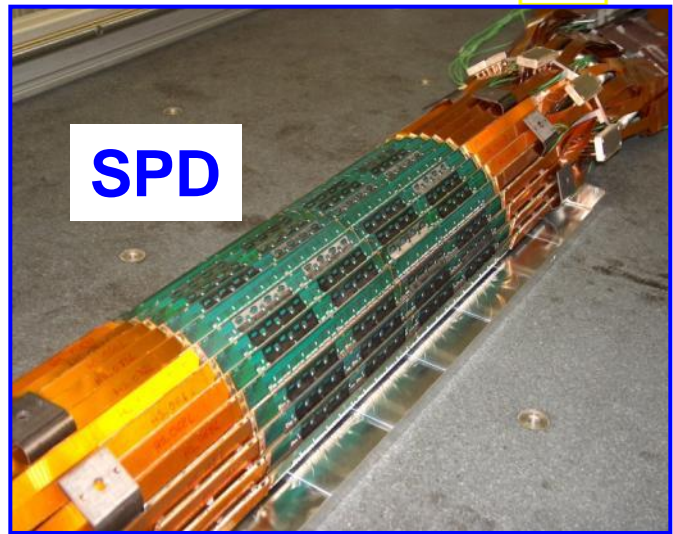
ITS total: 2198 alignable sensitive volumes → 13188 d.o.f.

Radiation damage

Particles (radiation) interact with atoms of the detector material and may cause permanent changes (defects) in the detector bulk.

- **One distinguishes two types of radiation damage:**
    - ➢ damage inside the detector bulk (bulk damage): dislocated atoms from their position in the lattice caused by massive particles.
        - ➜ **Bulk damage is primarily produced by neutrons, protons and pions.**
    - ➢ damage introduced in the surface layers (surface damage) is due to the charges generated in the amorphous oxide
        - ➜ **Surface damage is primarily produced by photons and charged particles.**

- **Defects may change with time:**
    - ➢ one distinguishes between primary defects and secondary defects
    - ➢ the secondary defects appear with time caused by moving primary defects

- **Comulative effects:**
    - ➢ increased leakage current
    - ➢ silicon bulk type inversion (n-type to p-type)
    - ➢ increased depletion voltage
    - ➢ increased capacitance

- **Sensor can stop working :**
    - ➢ noise too high
    - ➢ depletion voltage too high
    - ➢ loss of inter-strip isolation

Typical limits of Si Detectors are at 10^{14}-10^{15} Hadrons/cm^2

Radiation damage

❑ **Defects in the semiconductor lattice create energy levels in the band gap between valence and conduction band. Depending on the position of these energy levels the following effects will occur:**

➢ **Modification of the effective doping concentration**
➔ **shift of the value of the depletion voltage.**

➢ **Trapping of charge carriers**
➔ **reduced lifetime of charge carriers**

➢ **Easier thermal excitement of e- and h+**
➔ **increase of the leakage current**

Interstitial   **Frenkel defect**

Vacancy

A displaced silicon atom produces an empty space n the lattice (Vacancy) and in another place an atom in an inter lattice space (Interstitial, I). A vacancy-interstitial pair is called a Frenkel-defect.

In hard impacts the primary knock-on atom displaces additional atoms. These defects are called cluster defects. The size of a cluster defect is approximately 5 nm and consists of about 100 dislocated atoms.

Surface defects in the oxide
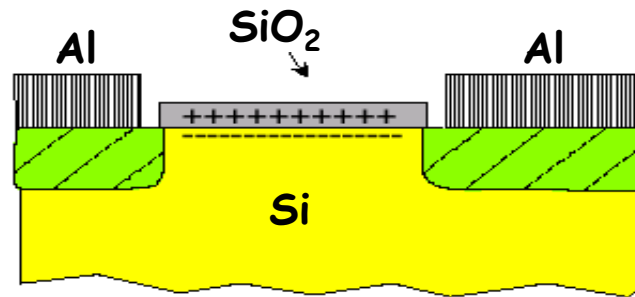
❑ **Ionizing radiation creates charges in the oxide**
   (in the amorphous oxide dislocation of atoms is not relevant)

❑ **The mobility of electrons in SiO2 is much larger than the mobility of holes**
   ➜ **electrons diffuse out of the oxide, holes remain semi permanent fixed**
   ➜ **the oxide becomes positively charged due to these fixed oxide charges.**

➢ **Consequences for the detector:**
   ✓ **reduced electrical separation between implants**
   ✓ **increase of interstrip capacitance**
   ✓ **increase of detector noise**
   ✓ **worsening of position resolution**
   ✓ **increase of surface leakage current**
   ✓ **reduced break down voltage**

Tracking: why

At hadron colliders the challenging aim is the full reconstruction of the events produced in the interaction under study. Therefore primary goals are:

✓ reconstruct the trajectories ("tracking") of charged particles and measure their momenta
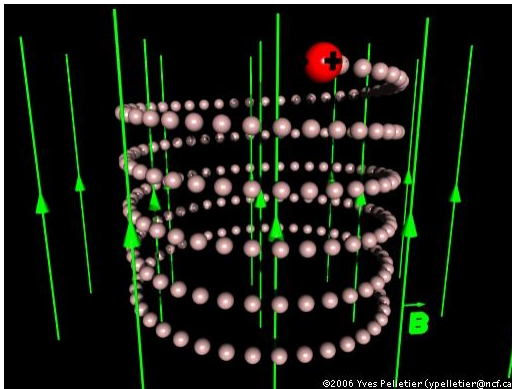
Most common case: in a solenoidal uniform magnetic filed the Lorentz force

$$\vec{F} = \frac{d\vec{p}}{dt} = q\vec{E} + q\left(\vec{v} \times \vec{B}\right)$$

induce charged particles to follow a helicoidal path:
- describe circles in the transverse plane
- move uniformly along the magnetic field direction

$$P_T(GeV) = 0.3 \; B(T) \; R(m)$$

✓ identify the sign of the charge

Positives +

Negatives –

Magnetic field, pointing out of the plane

negative charge

positive charge

$p_1 < p_2 \Leftrightarrow R_1 < R_2$
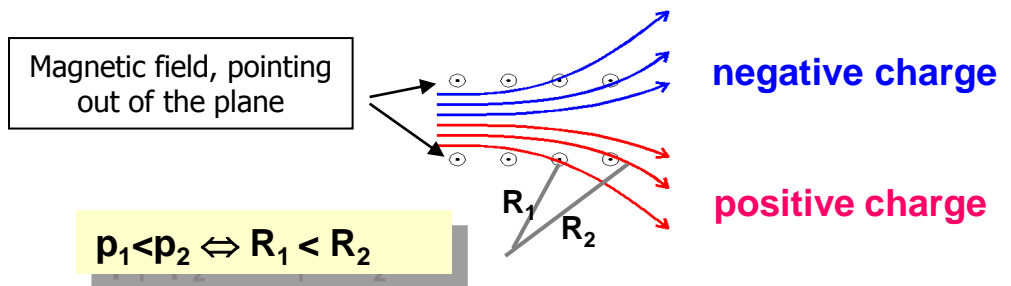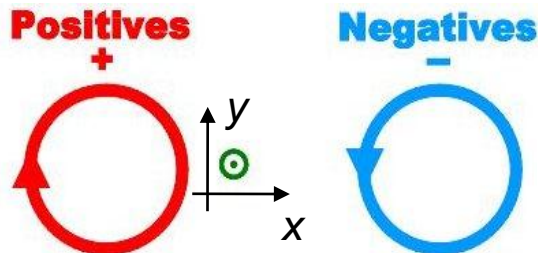
Tracking: why

✓ reconstruct the primary and secondary vertices of the interaction
(at LHC with large pile-up of events in the same bunch crossing !)

jet

Secondary vtx

displaced track

L_{xy}

Primary vtx

d_0

ALEPH Higgs search

$e^+e^- \rightarrow bbqq$

μ

jet

jet

jet

w^+

u

d

b

t

Proton →

← Antiproton

$\bar{t}$

w^-

b

jet

CDF Top Quark Event

W-> c + sbar

b-quark

Top->W+b-quark

Top->W+b-quark

b-quark

W->electron+neutrino
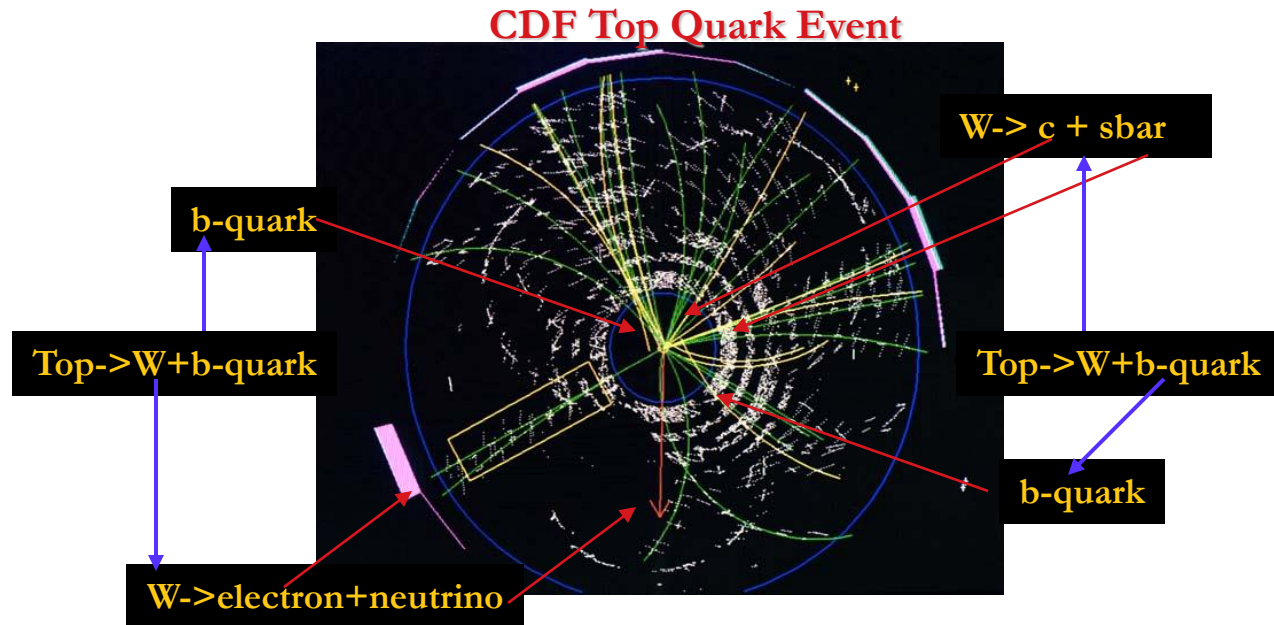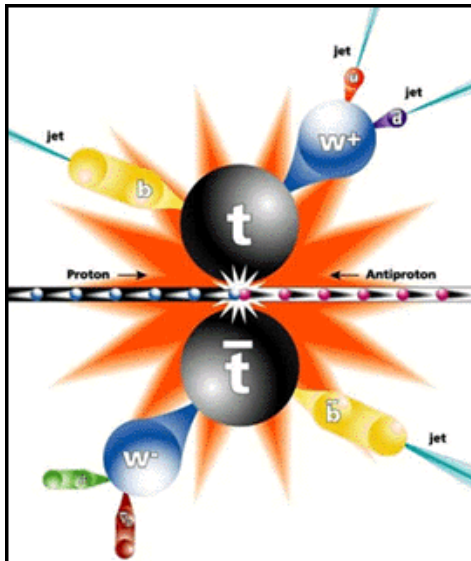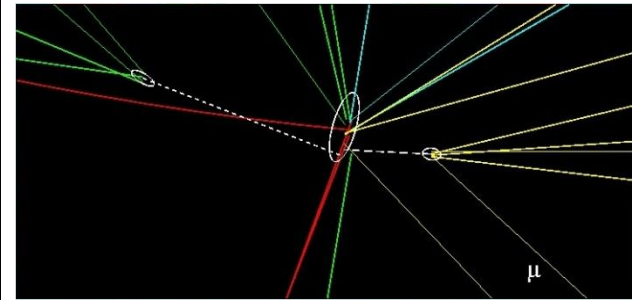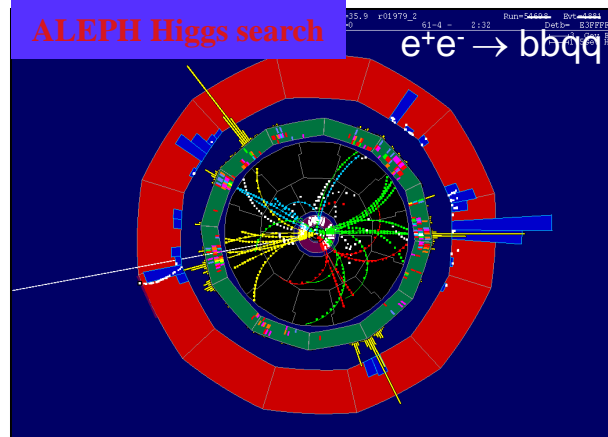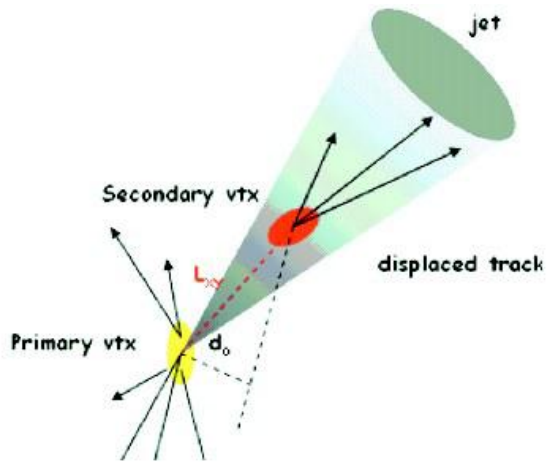
Tracking: a real challenge at LHC

- **Tracking at LHC is a very complex procedure due to the high track density. It needs specific implementation adapted to the detector type and geometry**

- **Precise and efficient detector modules are required to measure where the particle crossed the module**

- **Fast and radiation hard detectors and electronics are needed**

- **Track reconstruction requires specific software implementation:**
    - **track finding (pattern recognition)**
    - **estimation of track parameters (fitting)**

- **Precise alignment of detector modules is a prerequisite for efficient tracking**

After installation in 2008 precise alignments were done by all experiments with millions of cosmic muons
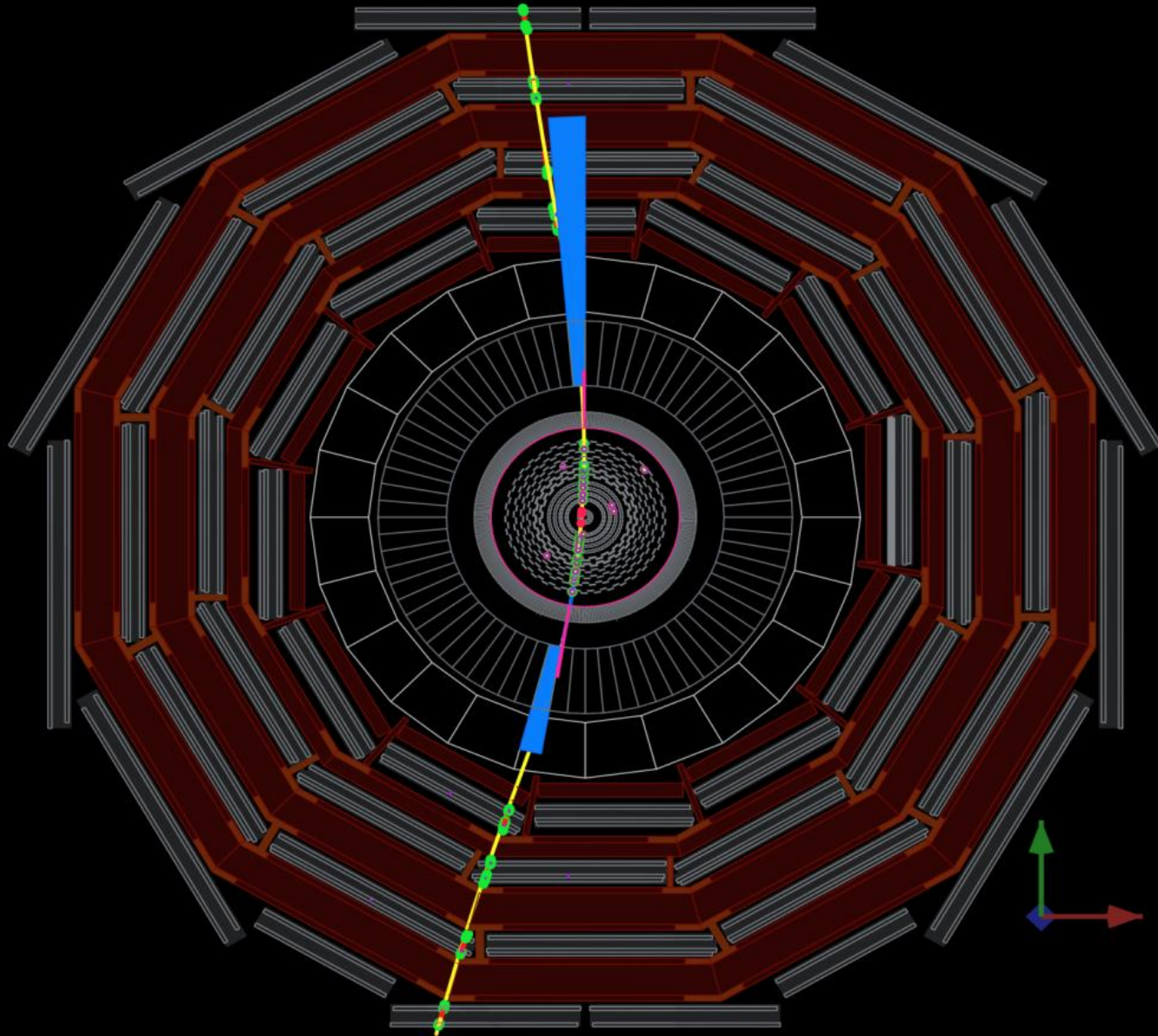
CMS: Cosmic Runs At Four Tesla
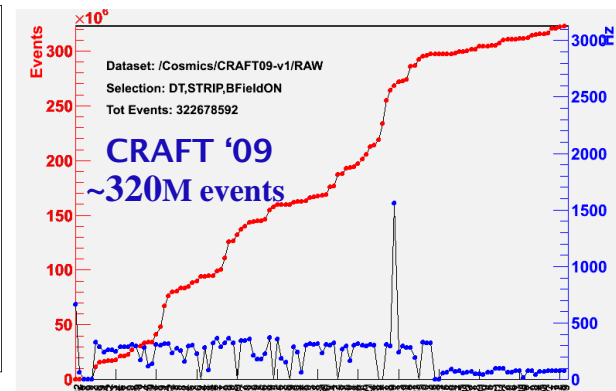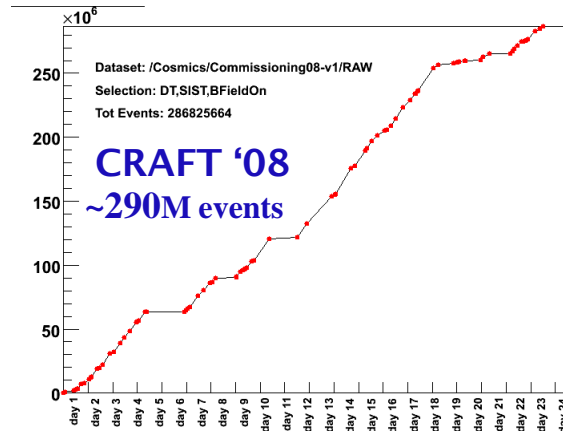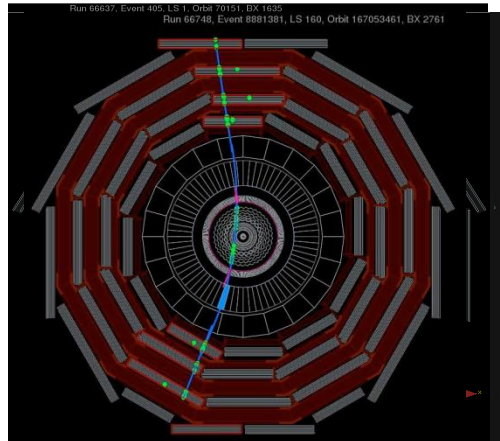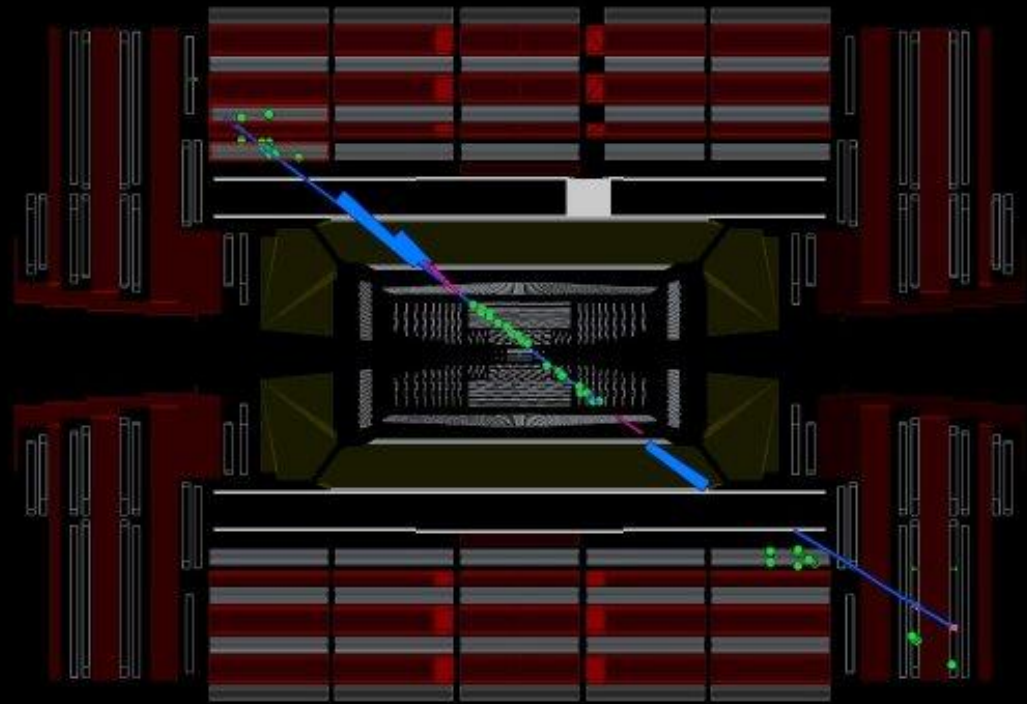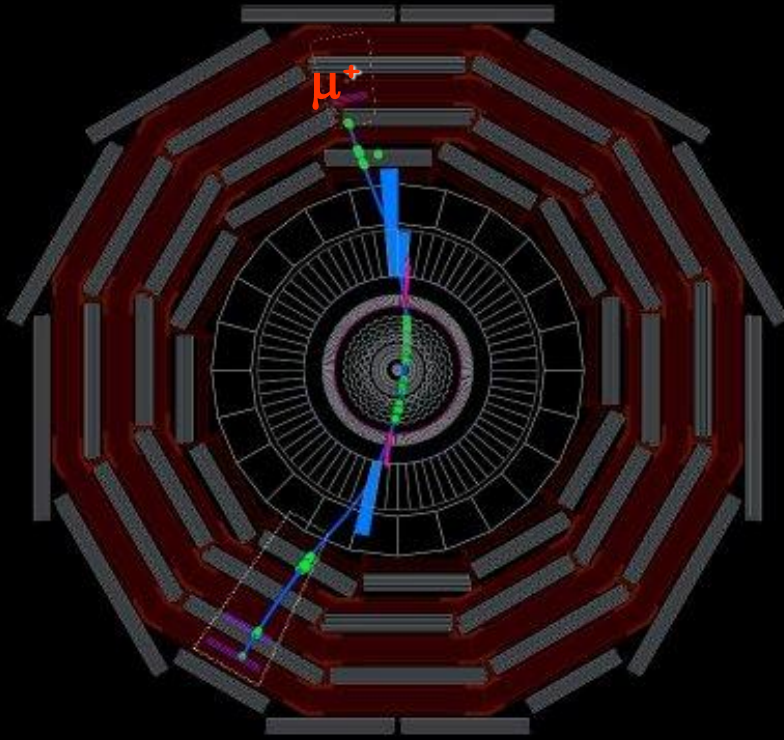
ATLAS: pixel commissioning with cosmics

arXiv:1004.5293v1
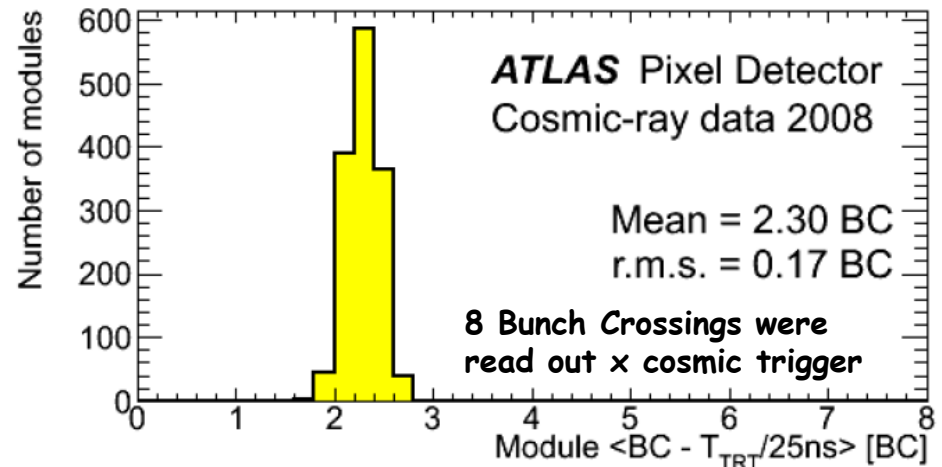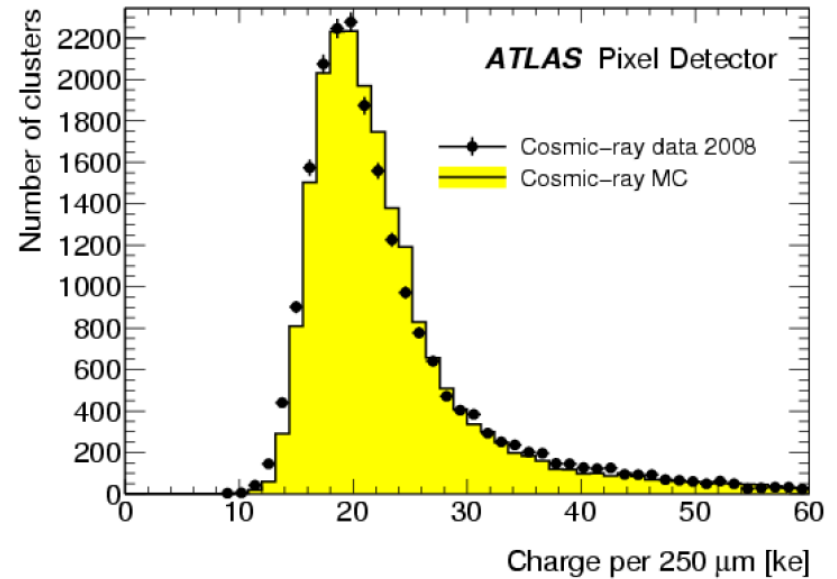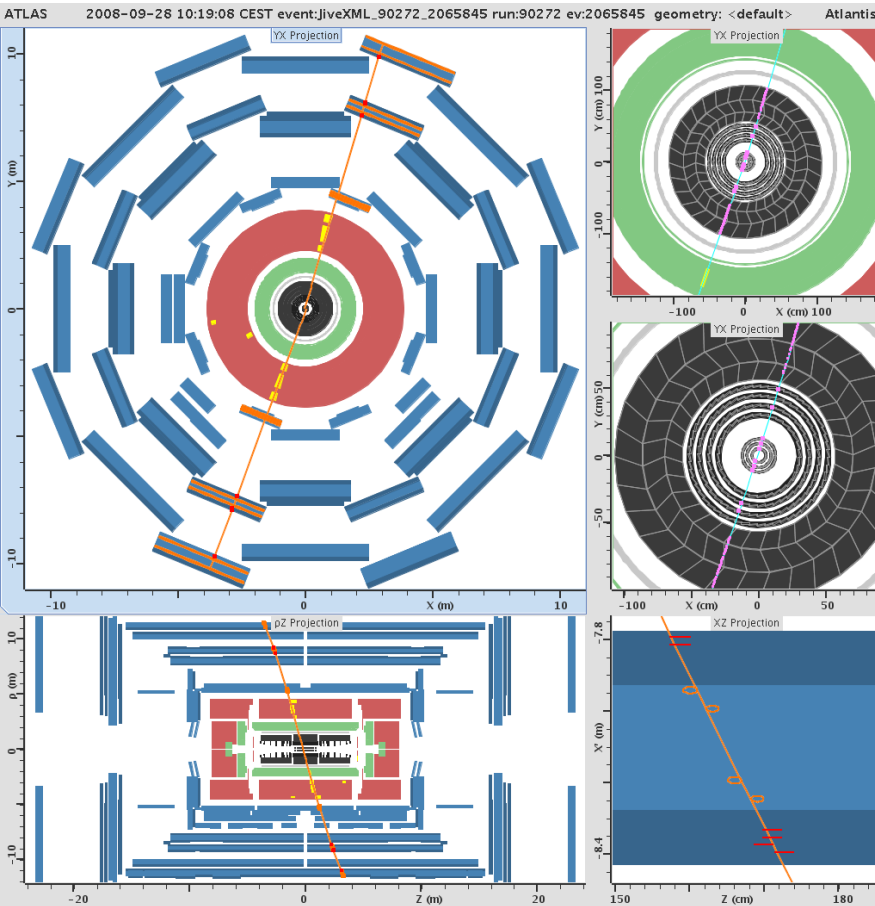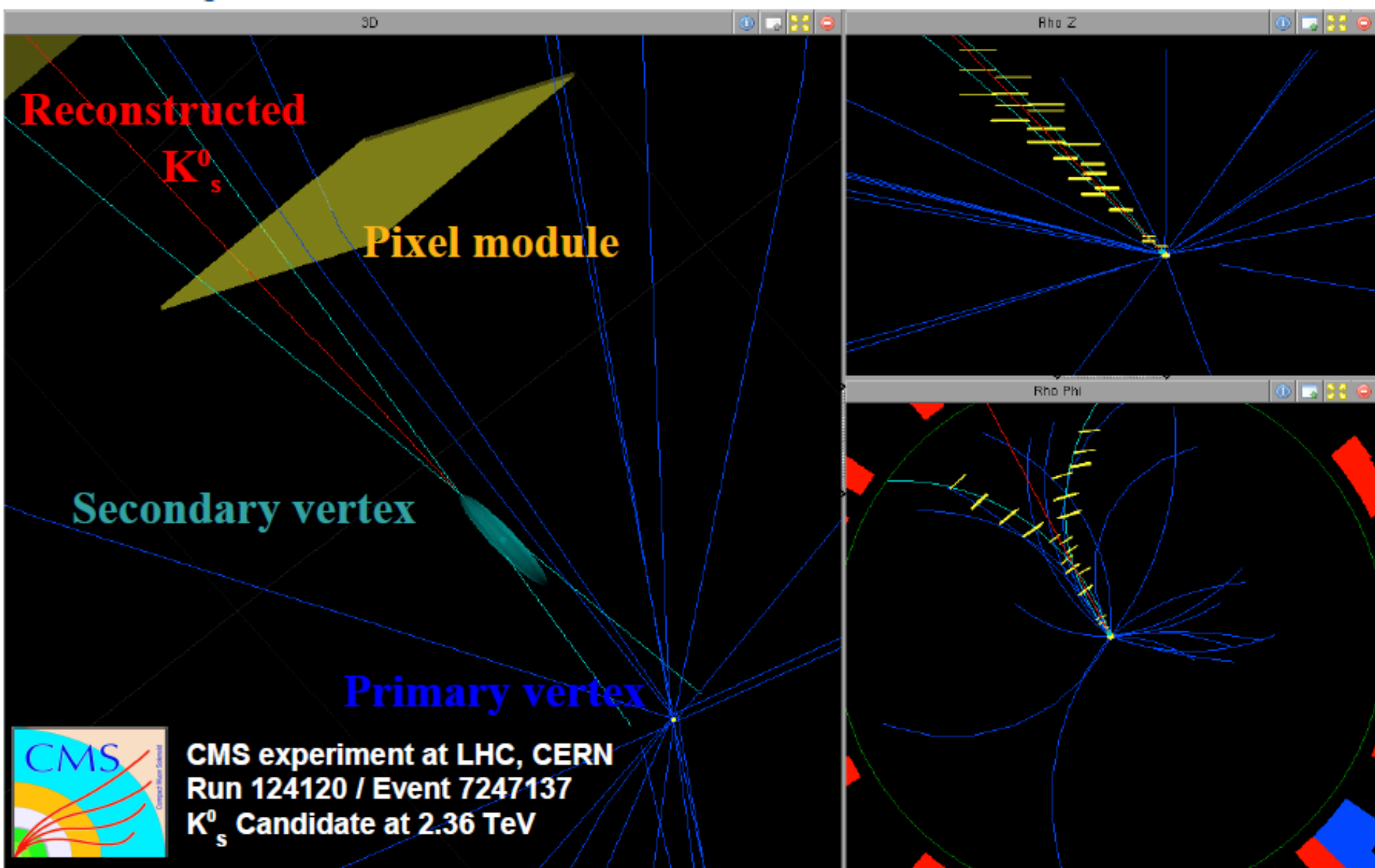
ATLAS Pixel Detector

Cosmic-ray data 2008
Cosmic-ray MC

Number of clusters vs Charge per 250 μm [ke]

ATLAS Pixel Detector
Cosmic-ray data 2008

Mean = 2.30 BC
r.m.s. = 0.17 BC

8 Bunch Crossings were read out × cosmic trigger

Number of modules vs Module $<BC - T_{TRT}/25ns>$ [BC]

K⁰ₛ candidate event in CMS

Reconstructed
K⁰ₛ

Pixel module

Secondary vertex

Primary vertex

CMS experiment at LHC, CERN
Run 124120 / Event 7247137
K⁰ₛ Candidate at 2.36 TeV

K^0_s candidate event in ATLAS
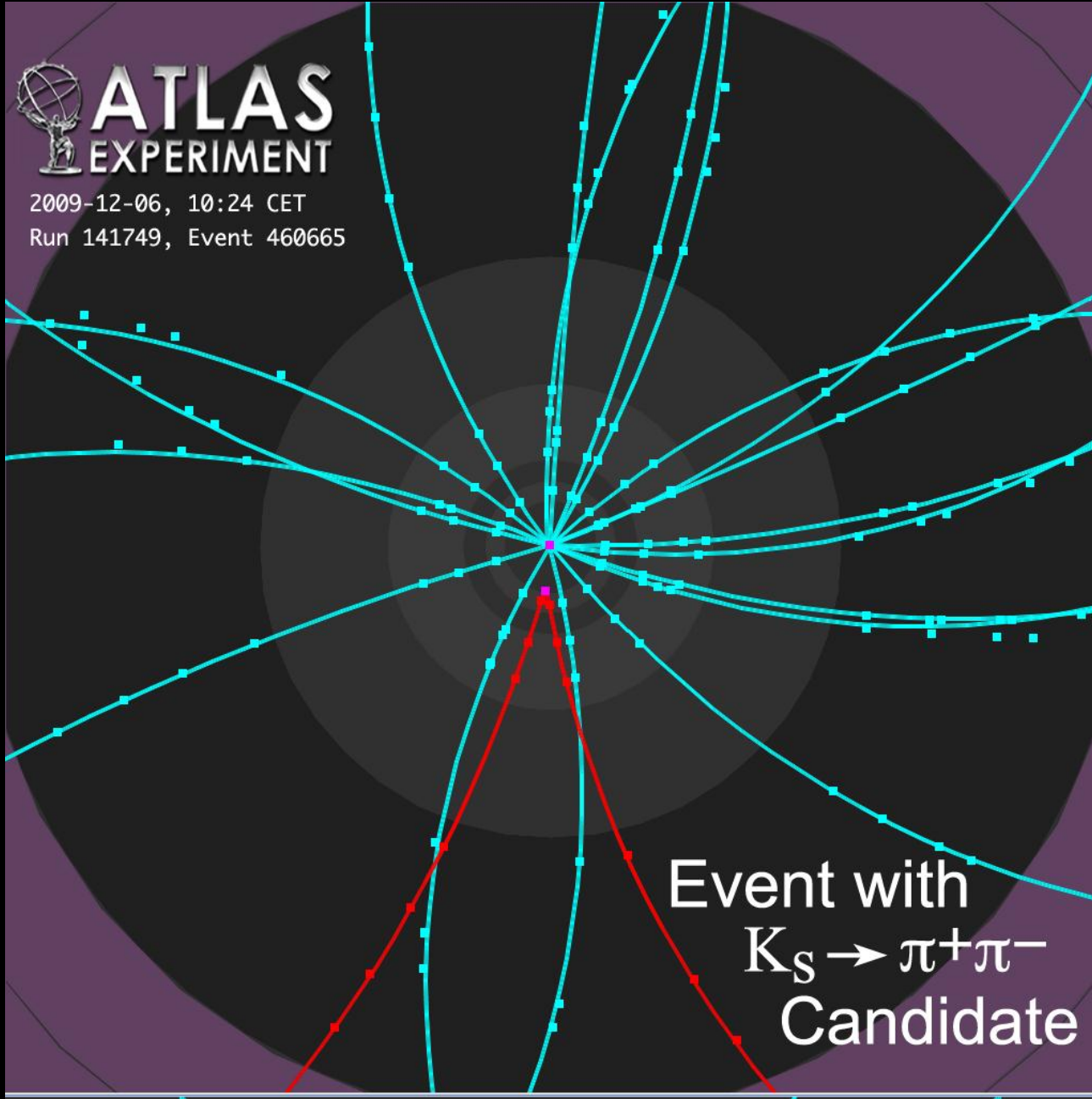
double b-jet candidate
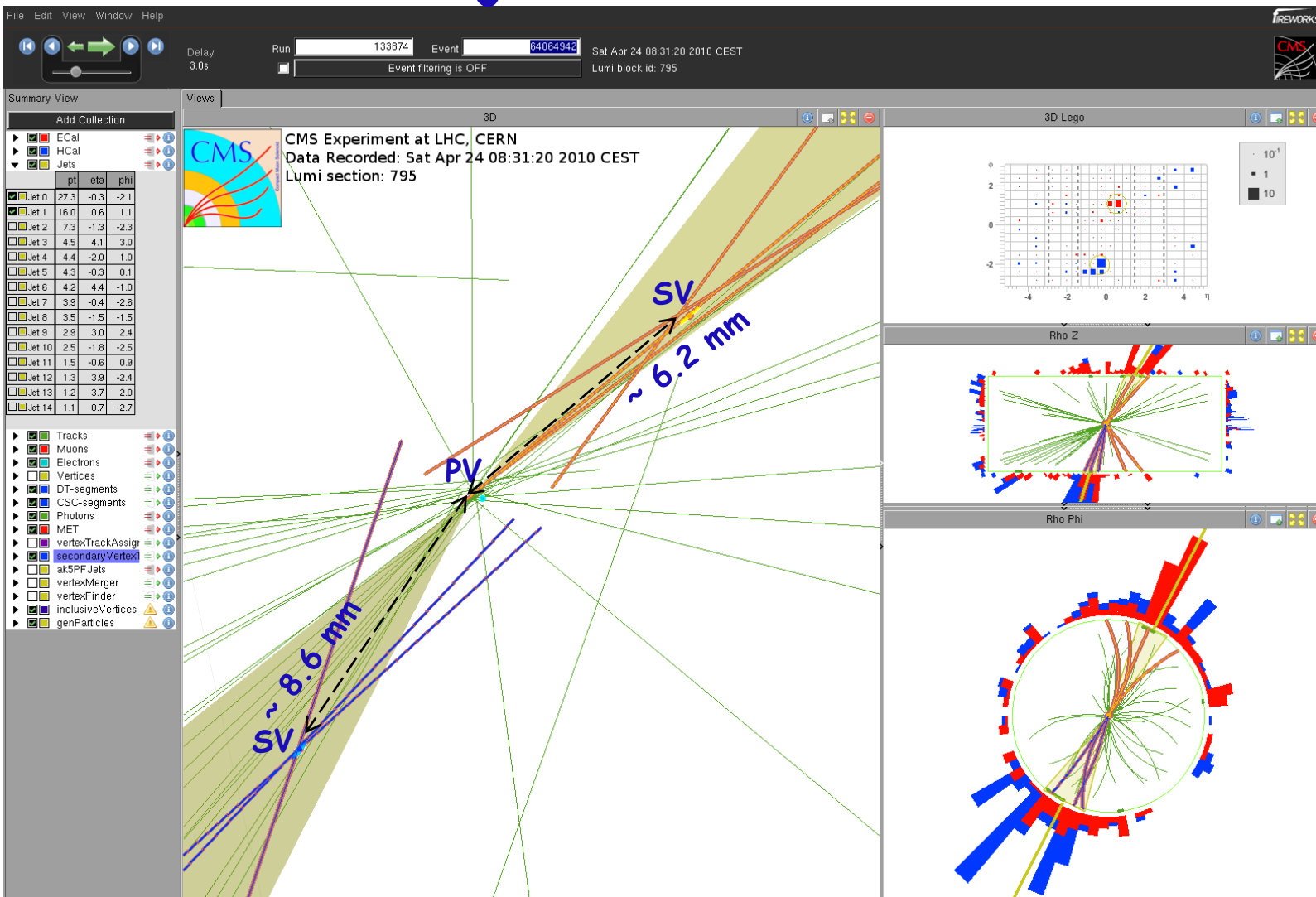
Jets: p_T = 43.7 GeV (top right) / 40.3 GeV (bottom left)

Secondary vertices

    top-right: 3D flight distance (value/ significance) = 6.2 mm / 43 m_{SV} = 2.9 GeV, p_T = 25.7 GeV

    bottom left: 3D flight distance (value / significance) = 8.6mm / 55 m_{SV} = 3.1 GeV, p_T = 17.2 GeV
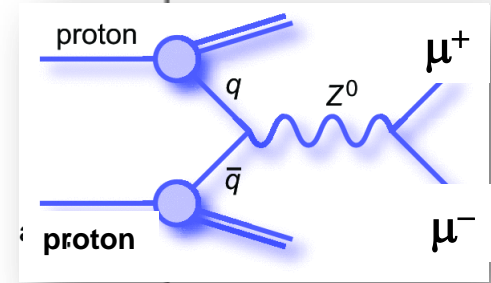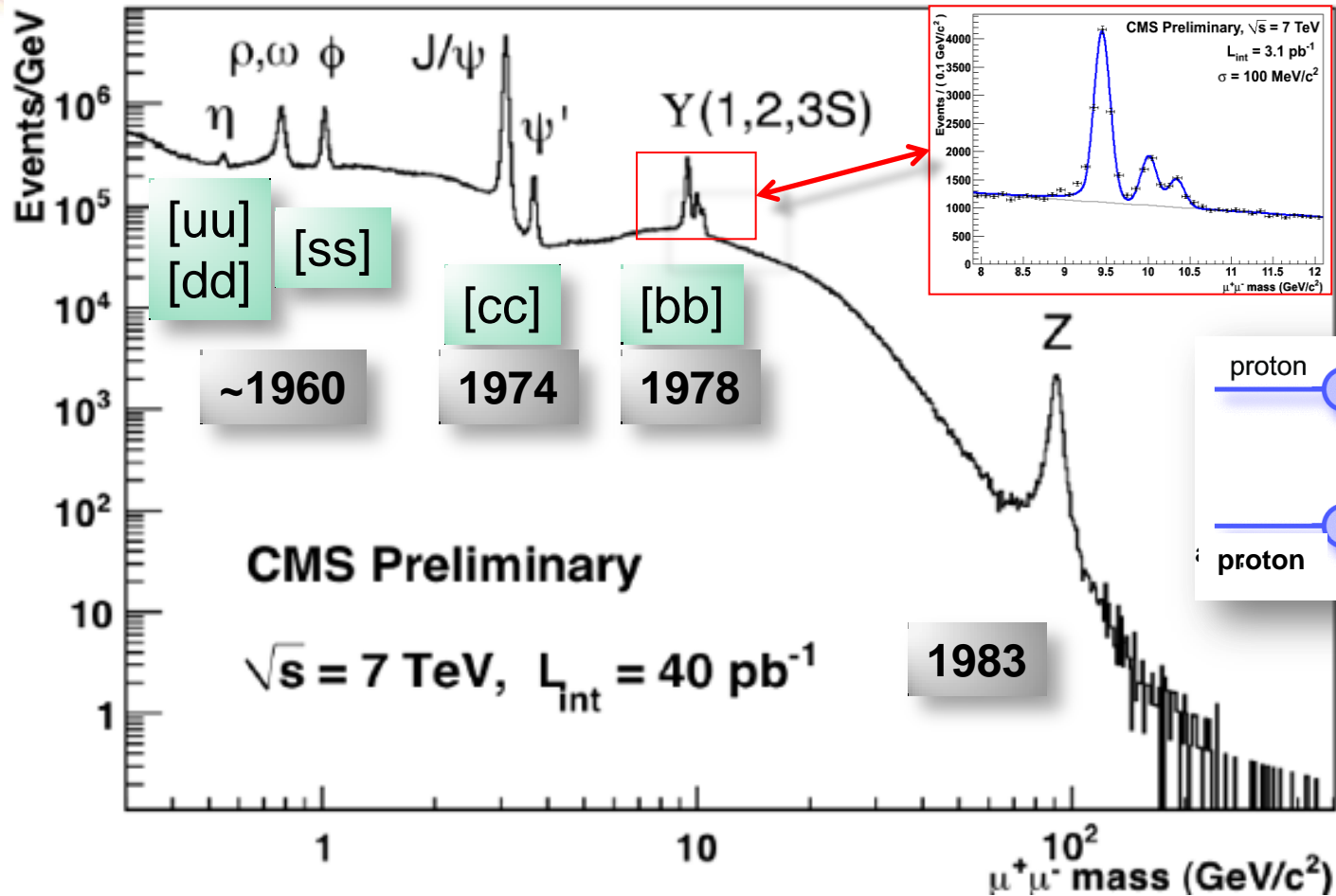
4μ candidate with $m_{4\mu}$ = 125.1 GeV

p_T (muons)= 36.1, 47.5, 26.4, 71.7GeV m_{12}= 86.3 GeV, m_{34}= 31.6 GeV
15 reconstructed vertices
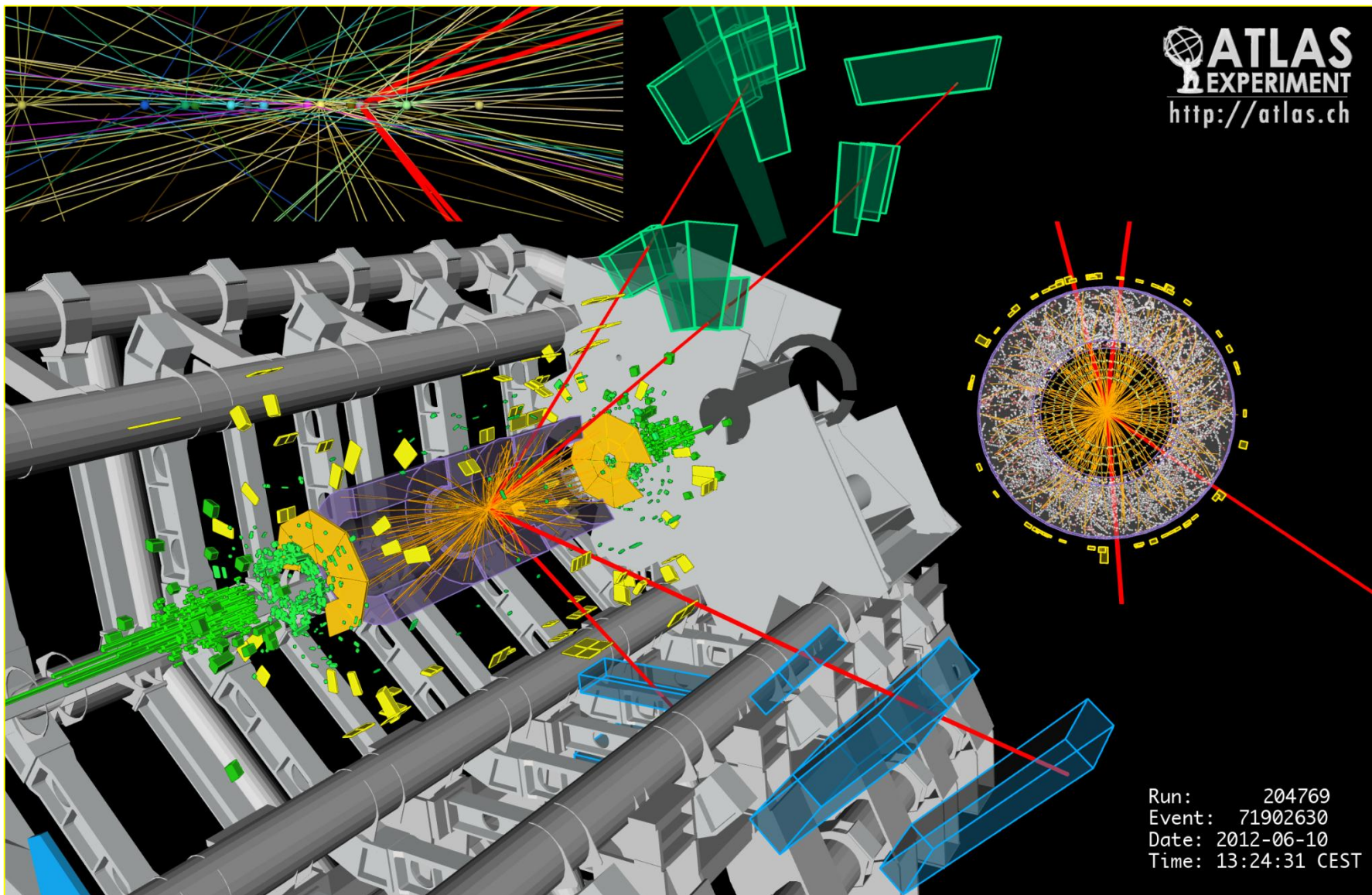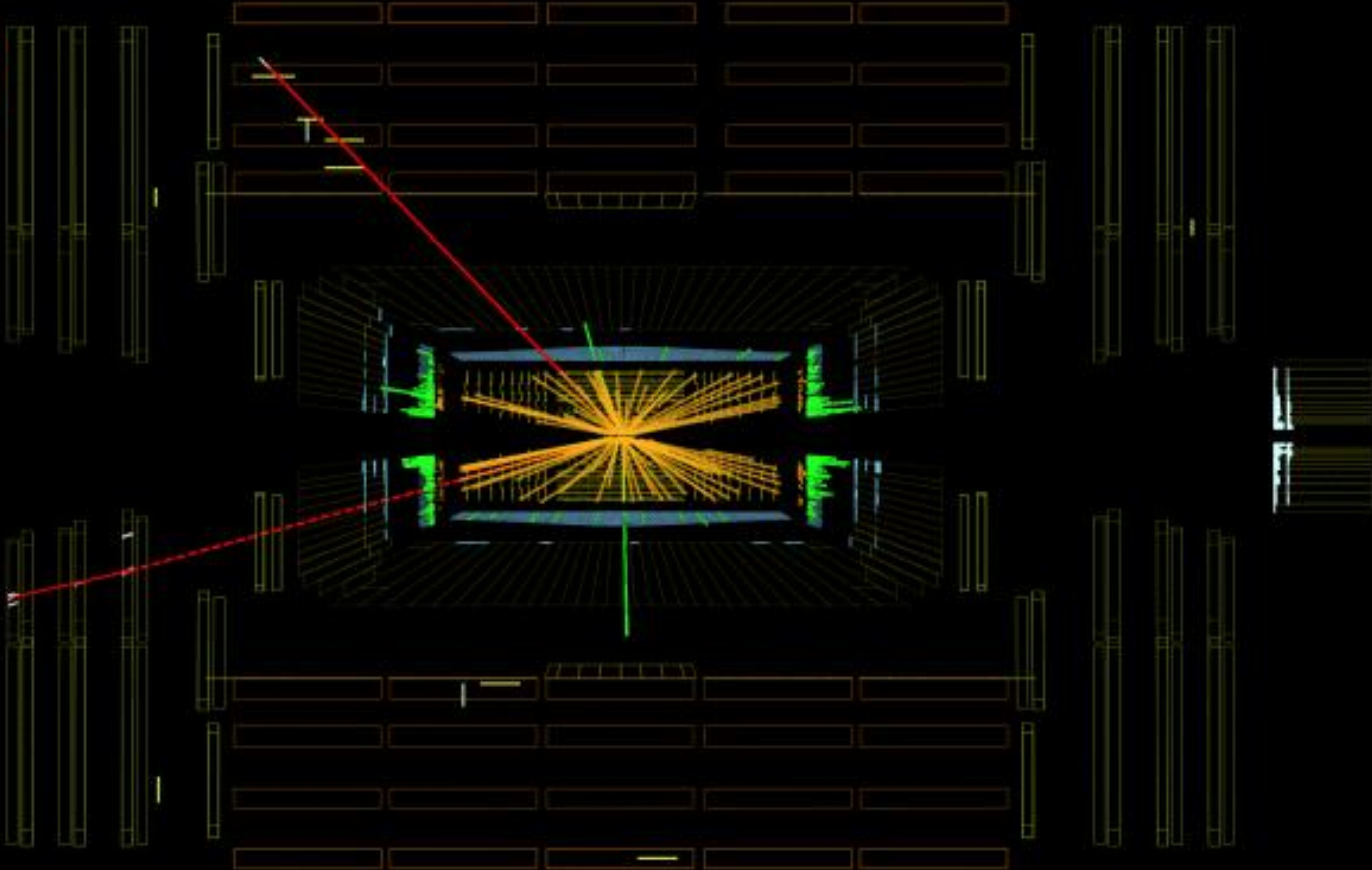
ATLAS
EXPERIMENT
http://atlas.ch

Run: 204769
Event: 71902630
Date: 2012-06-10
Time: 13:24:31 CEST

candidate ZZ event with two electrons and two muons
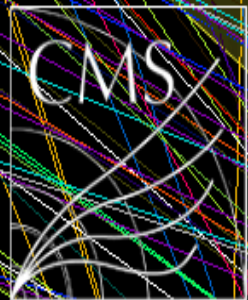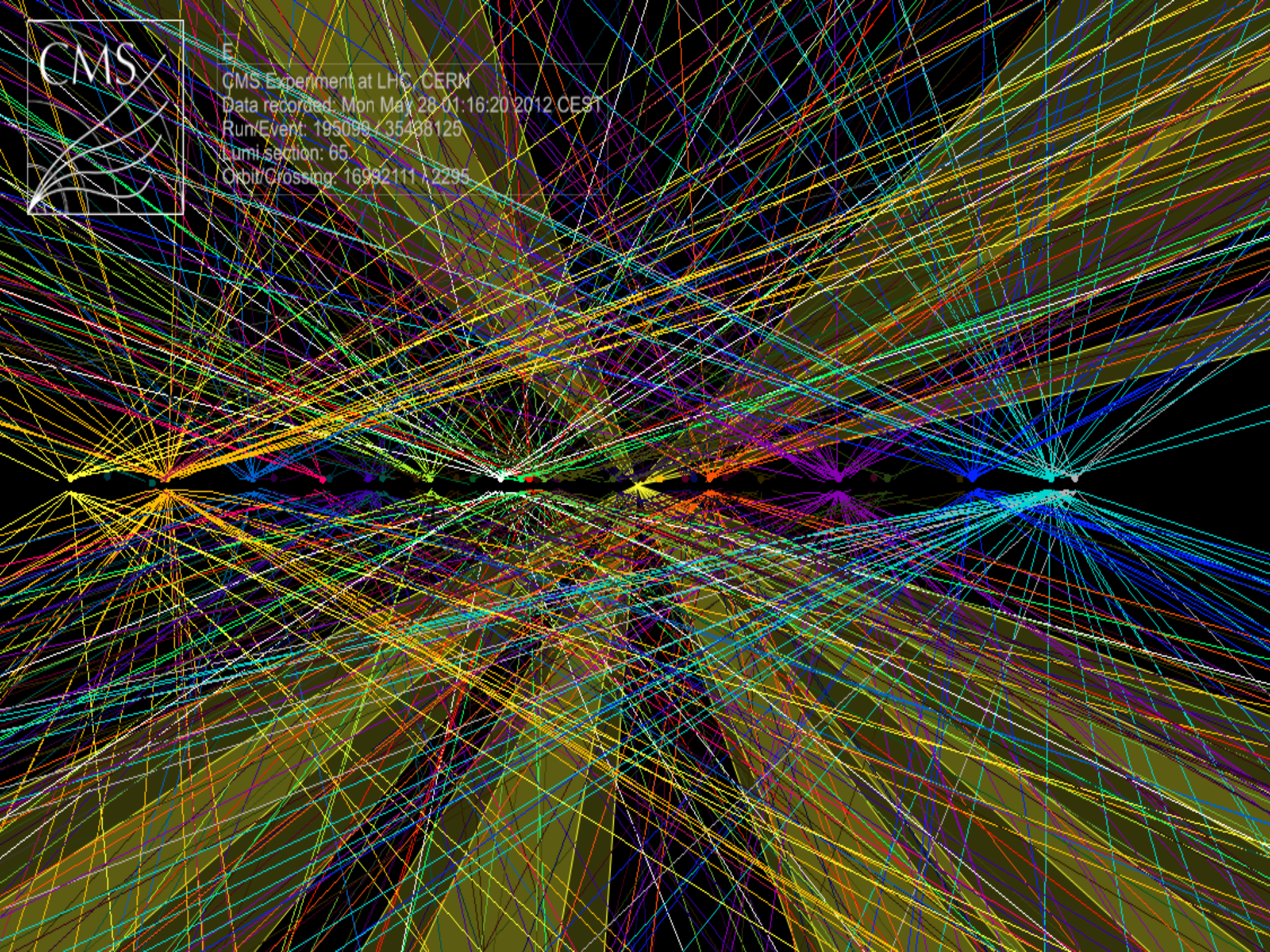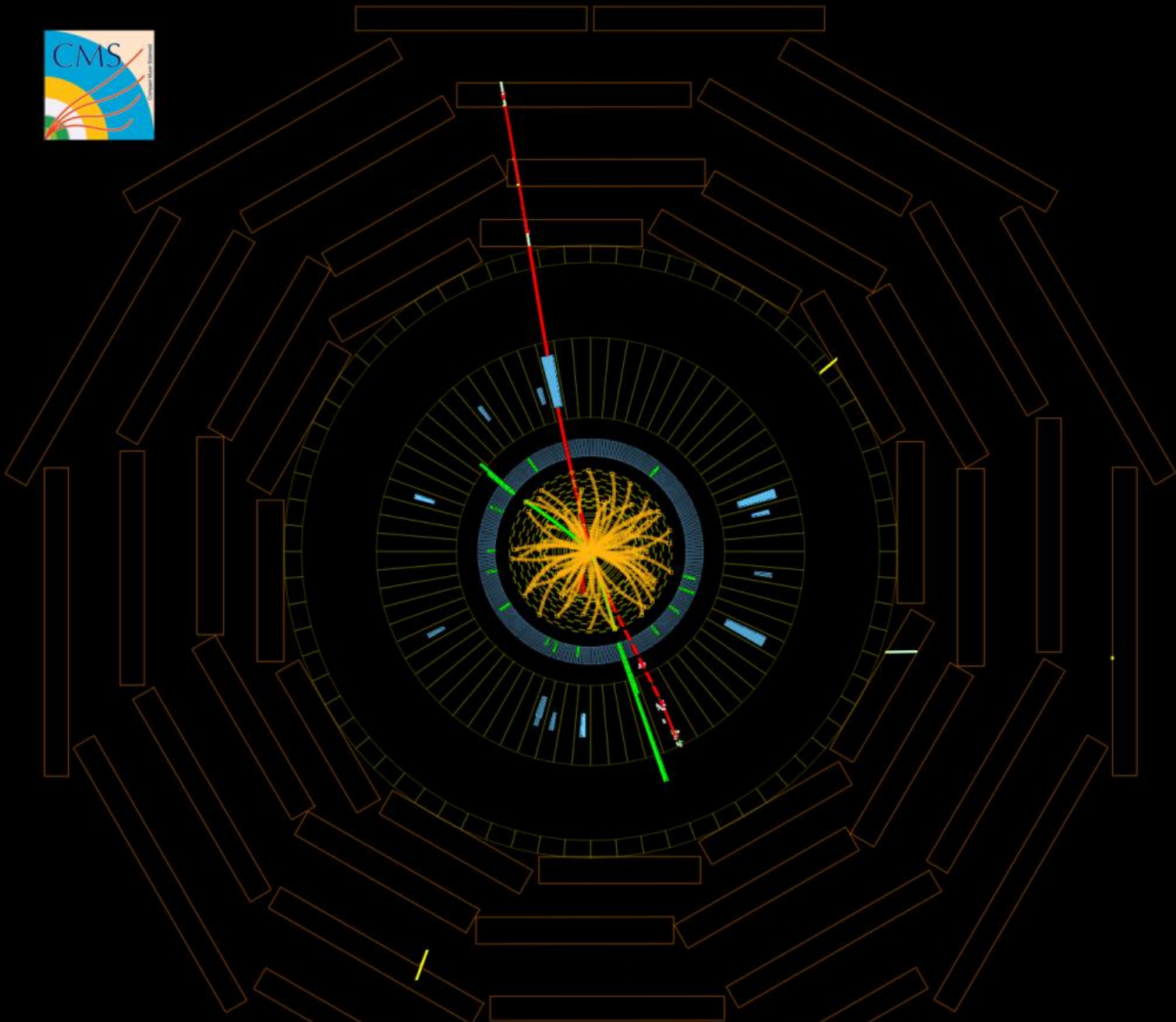
candidate ZZ event with two electrons and two muons
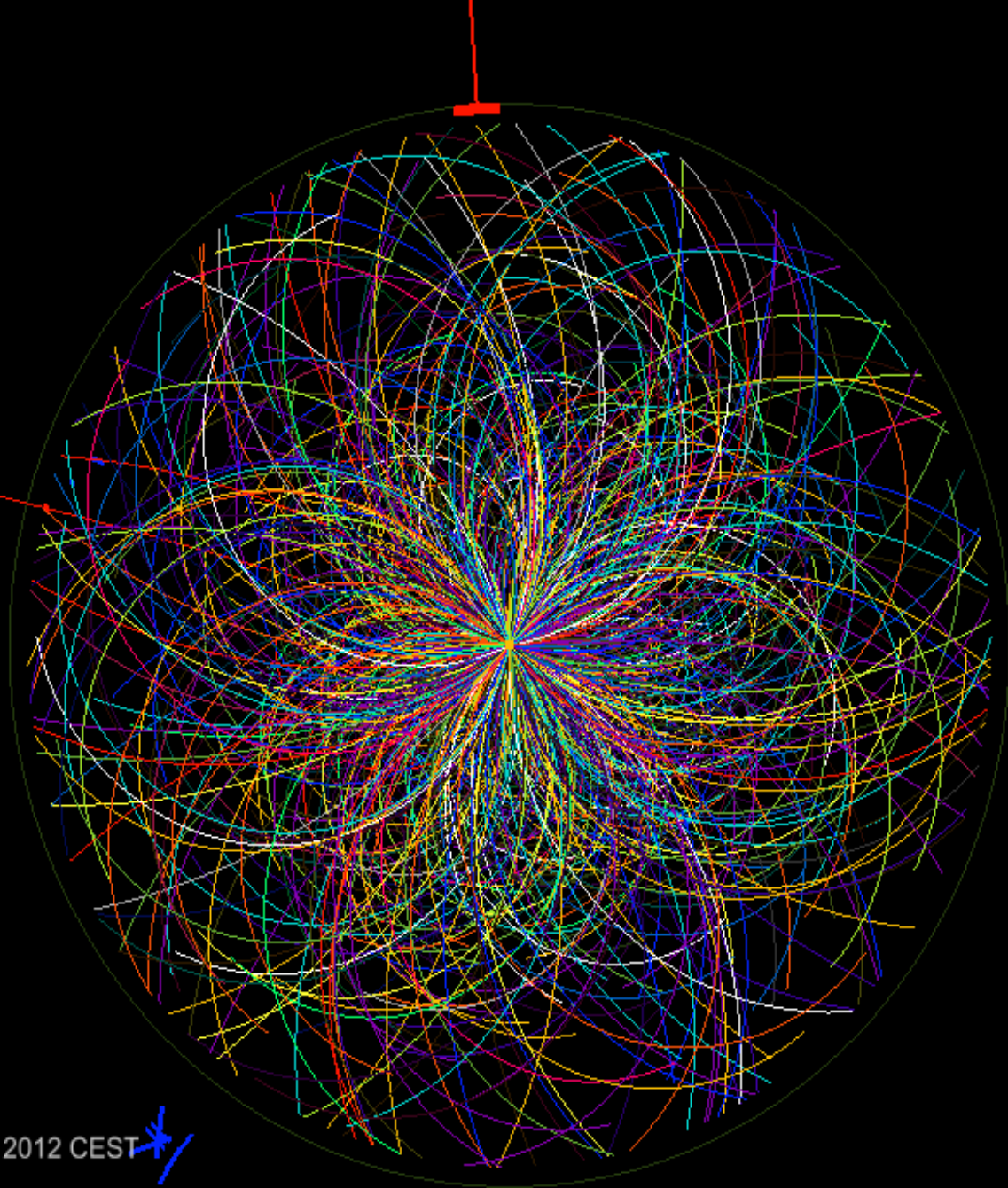
CMS Experiment at LHC, CERN
Data recorded: Mon May 28 01:16:20 2012 CEST
Run/Event: 195099 / 35438125
Lumi section: 65
Orbit/Crossing: 16992111 / 2295

Transition Radiation

Transition Radiation was predicted by Ginzburg and Franck in 1946

When the particle crosses the boundary between two media, (e.g. the boundary between vacuum and a dielectric layer) there is a probability of the order of 1% to produced and X ray photon, called <u>Transition radiation</u>.

$$\varepsilon_1, \omega_1 < \varepsilon_2, \omega_2$$

Photon

charged particle
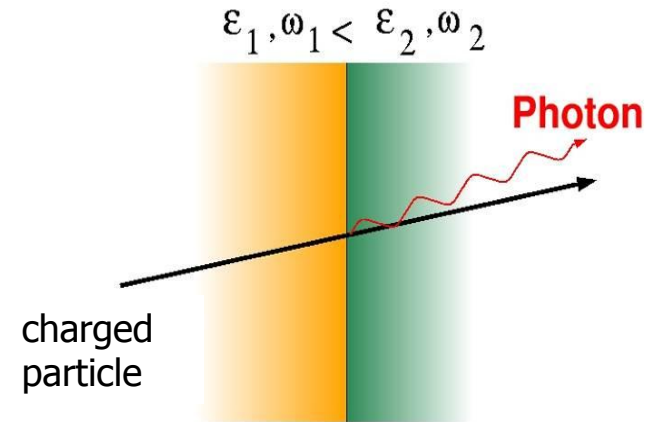
The energy emitted is proportional to the boost γ of the particle
    → Particularly useful for electron ID

A (too) simple picture

medium | vacuum
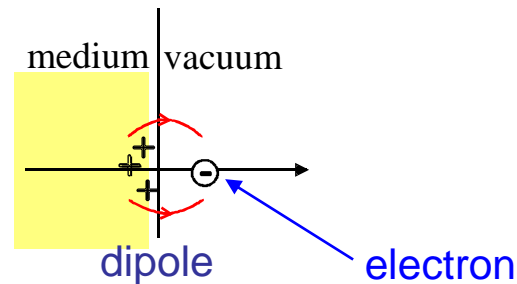
dipole   electron

Medium gets polarized. Electron density displaced from its equilibrium
→ Dipole, varying in time → radiation of energy.

The ATLAS Transition Radiation Tracker (TRT)

R = 1082 mm

TRT

R = 554 mm
R = 514 mm
R = 443 mm

SCT

R = 371 mm
R = 299 mm

TRT

SCT

R = 122.5 mm
R = 88.5 mm
Pixels
R = 50.5 mm
R = 0 mm

Pixels
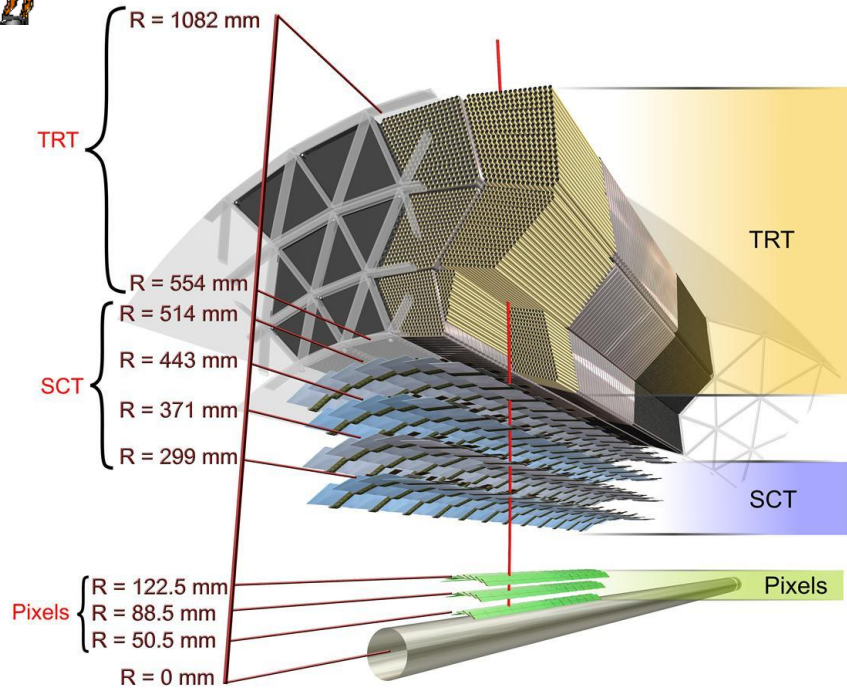
TRT: 4 mm straw tubes, arranged in 2·160 disks (end-cap) and 73 layers (barrel), 40 K channels, acceptance $|\eta| < 2$

HV −
Gas
+

π^+
e^+
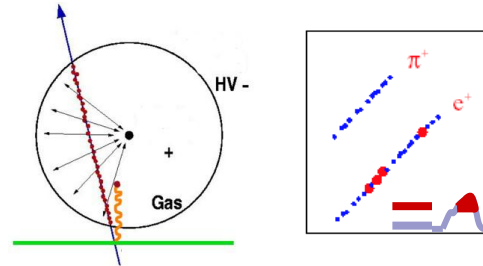
TR (polypropylene foils/fiber): pion-electron separation (TR γ's convert into e's in Xe)

TRT end-cap during assembly

# Hits (Barrel):
3(Pixel)+4 (SCT)+<36>(TRT)

$\sigma/p_T \sim 5 \times 10^{-4}\ p_T \oplus 0.01$

Cosmic ray event in TRT
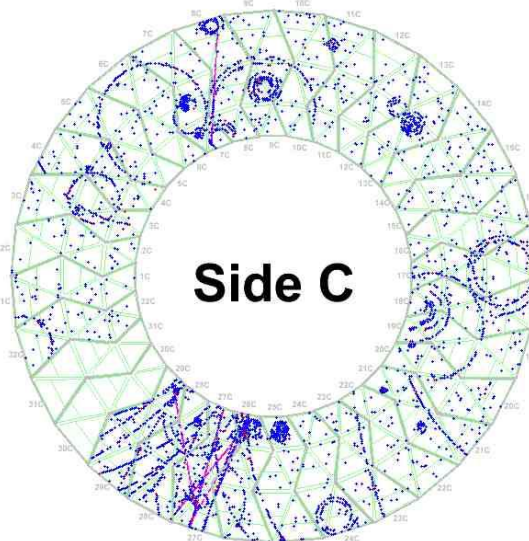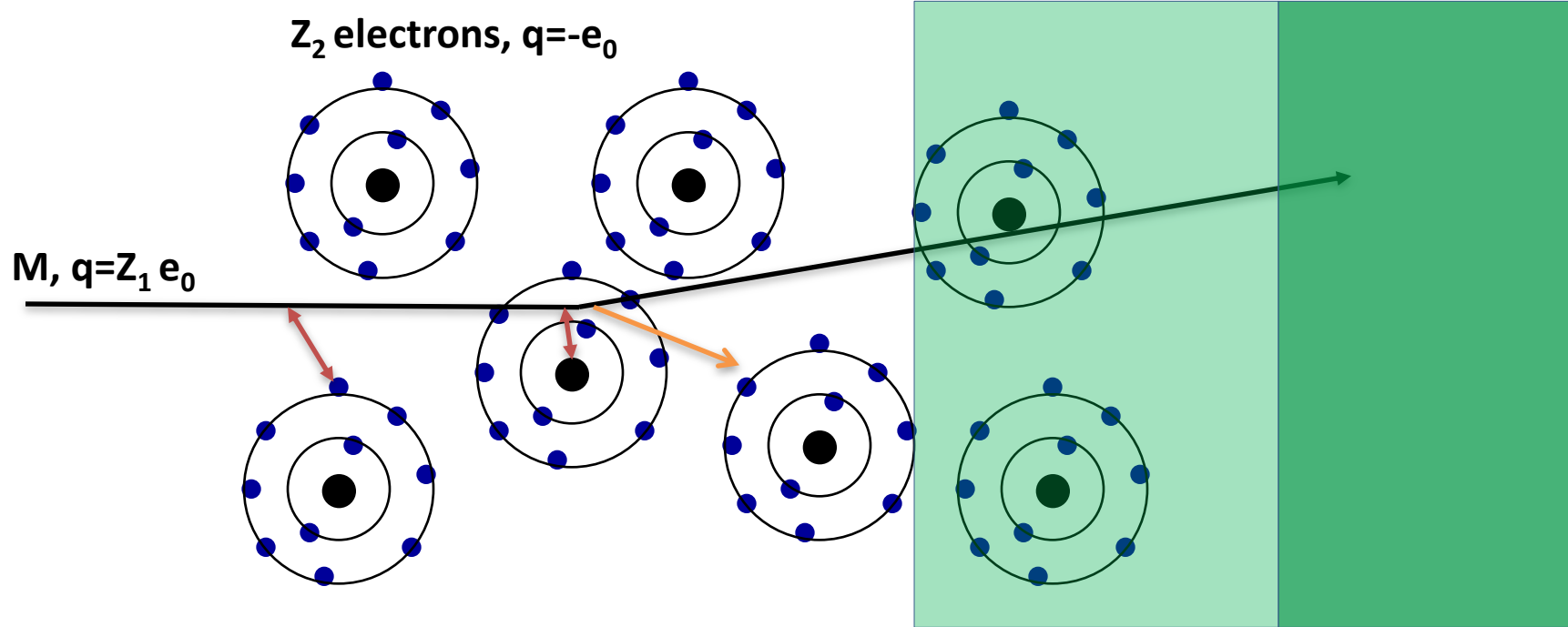
Side C

¼ of TRT barrel during integration

Electromagnetic Interaction of Particles with Matter

Z_2 electrons, $q=-e_0$

M, $q=Z_1 e_0$

Interaction with the atomic electrons. The incoming particle loses energy and the atoms are excited or ionized.

Interaction with the atomic nucleus. The particle is deflected (scattered) causing multiple scattering of the particle in the material. During this scattering a Bremsstrahlung photon can be emitted.

In case the particle's velocity is larger than the velocity of light in the medium, the resulting EM shockwave manifests itself as Cherenkov Radiation. When the particle crosses the boundary between two media, there is a probability of the order of 1% to produced and X ray photon, called Transition radiation.

Cherenkov light

- Named after the Russian scientist P. Cherenkov who was the first to study the effect in depth (he won the Nobel Prize for it in 1958)

- From Relativity, nothing can go faster than the speed of light c (in vacuum)

- **Due to the refractive index n of a material, a particle *can* go faster than the *local* speed of light in the medium $c_{\mathrm{p}} = c/n$**

- **This is analogous to the bow wave of a boat travelling over water or the sonic boom of an aeroplane travelling faster than the speed of sound**

Propagating waves

- A stationary boat bobbing up and down on a lake, producing waves

Propagating waves

- Now the boat starts to move, but slower than the waves

- No coherent wavefront is formed
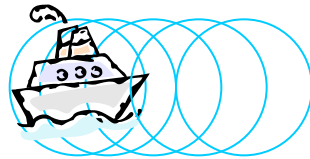
Propagating waves

- Next the boat moves faster than the waves
- A coherent wavefront is formed
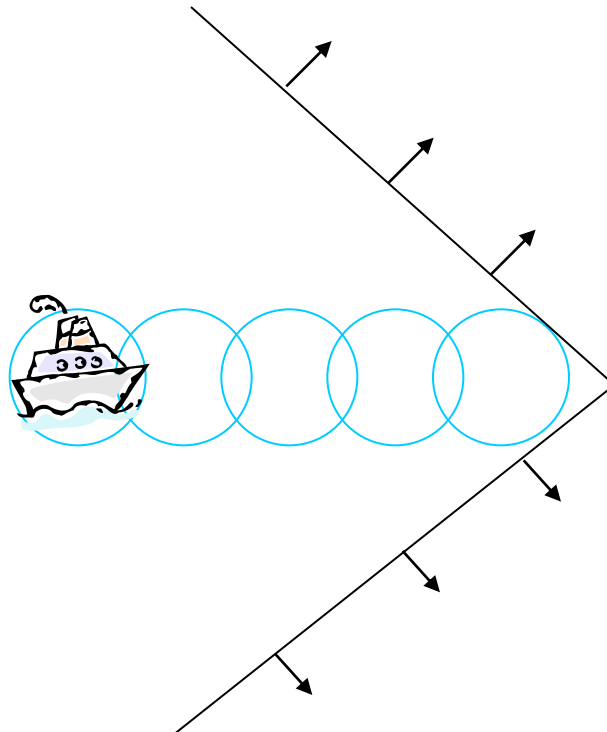
Propagating waves

- Finally the boat moves even faster
- The angle of the coherent wavefront changes
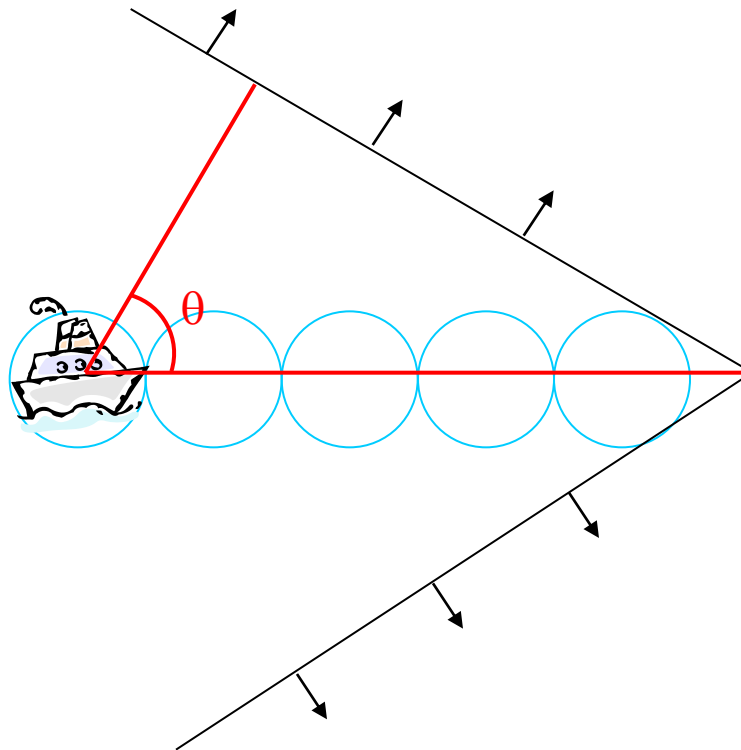
$$\cos\theta = \frac{v_{\mathrm{wave}}}{v_{\mathrm{boat}}}$$

Speed calculation

- Using this construction, we can determine (roughly) the boat speed:
  $\theta \approx 70º$, $v_{\text{wave}} = 2$ knots on water
  $\rightarrow$ $v_{\text{boat}} = v_{\text{wave}}/\cos \theta \approx 6$ knots

- Cherenkov light is produced when charged particle ($v_{\text{boat}} = \beta c$) goes faster than the speed of light ($v_{\text{wave}} = c/n$)

  $\rightarrow$ $\cos \theta_C = 1 / \beta n$

- Produced in three dimensions, so the wavefront forms a *cone* of light around the particle direction

- Measuring the opening angle of cone $\rightarrow$ particle velocity can be determined

$\theta \approx 70º$

For Ne gas ($n = 1.000067$)
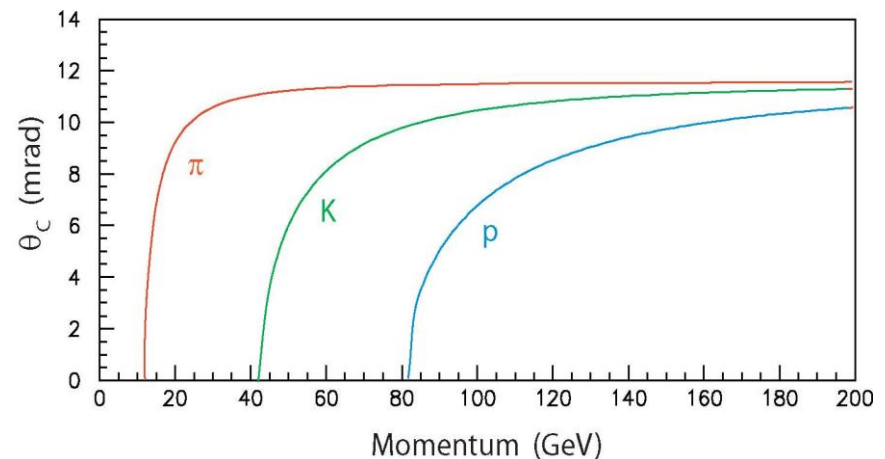
Cherenkov detectors

Cherenkov radiation is emitted when a charged particle passes through a dielectric medium with velocity

$$\beta \geq \beta_{thr} = \frac{1}{n} \quad n : \text{refractive index}$$

- Cherenkov light is emitted with $\cos \theta_C = 1 / \beta n$

- The light is produced equally distributed over photon energies, which when transformed to a wavelength distribution implies it is peaks at low wavelengths – it is responsible for the blue light seen in nuclear reactors

- There is a threshold for light production at $\beta = 1/n$
  - Tracks with $\beta < 1/n$ give no light
  - Tracks with $\beta > 1/n$ give light

$$\beta_{thr} = \frac{1}{n} \quad \rightarrow \quad \theta_C \approx 0$$

θ_C
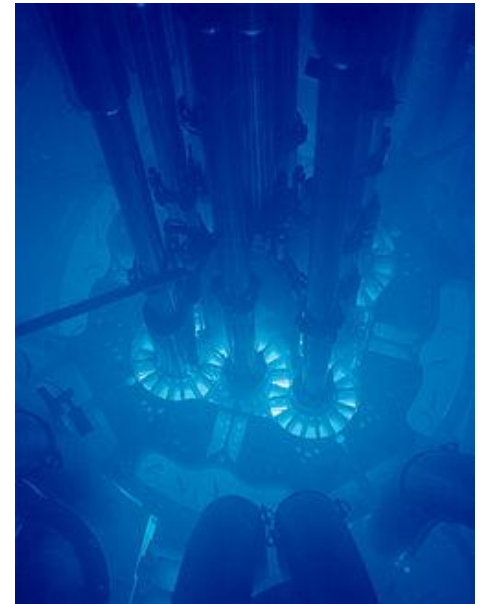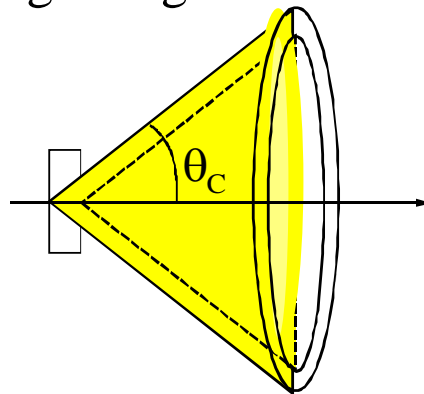
Threshold detectors

- This is the principle of "threshold Cherenkov detectors" which are useful to identify particles in a beam line (with fixed momentum) for example a 50 GeV π^+ beam with some proton contamination

- By choosing a medium with a suitable refractive index, it can be arranged that the π will produce light, but the protons will not

Ne gas
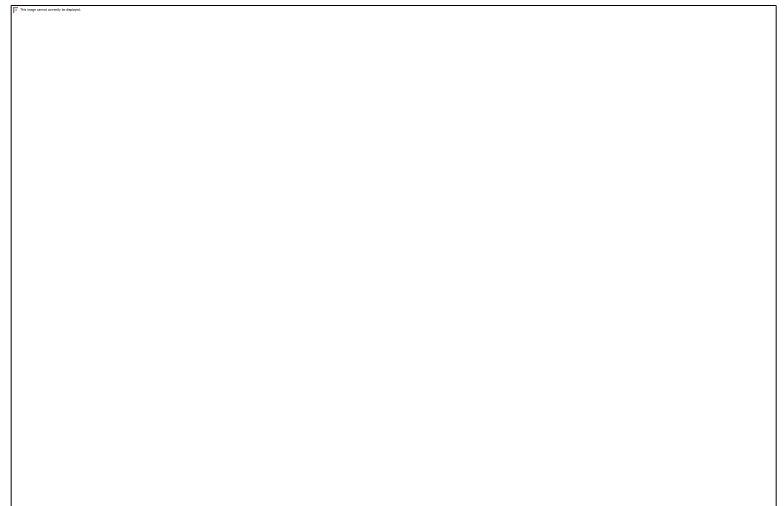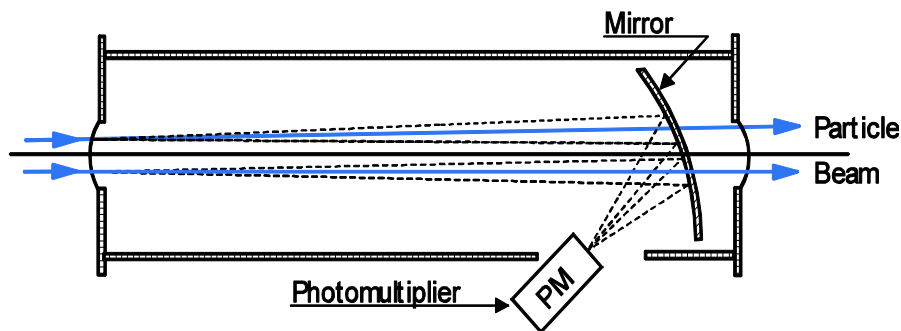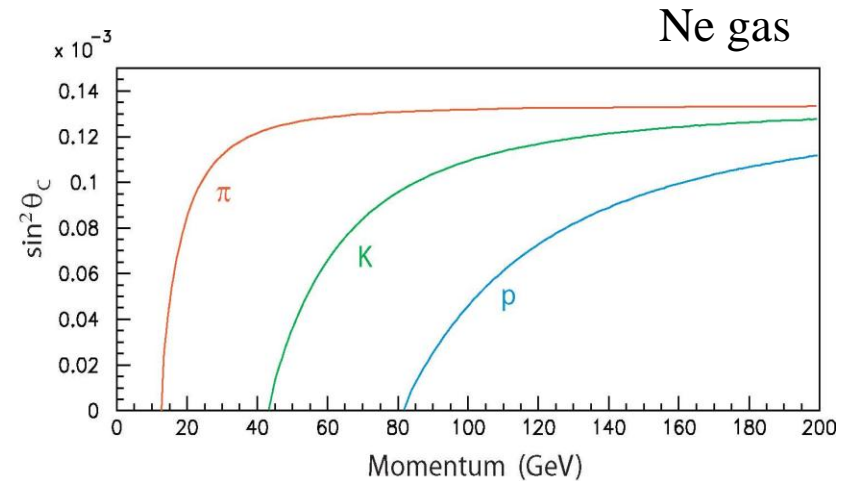
Ring imaging

- Threshold counters just give a yes/no answer, and are less useful when the tracks have a wide momentum range
  However, more information can be extracted from the Cherenkov angle

- From a classic paper by J. Seguinot and T. Ypsilantis [NIM 142 (1977) 377] the Cherenkov cone can be imaged into a ring, using a spherical mirror

Interaction point

Track

Photons

r

Detector plane
radius R/2

Radiator
medium

Spherical mirror
radius R
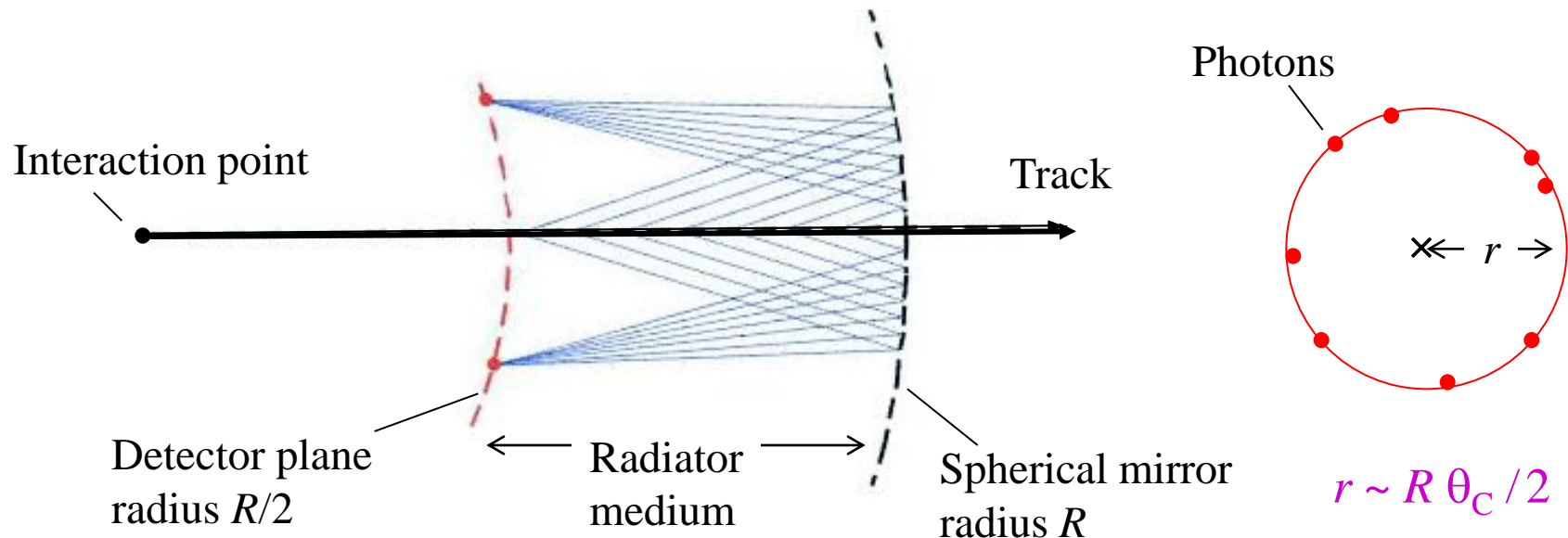
$r \sim R\, \theta_C\, /\, 2$

- Measuring the ring radius r allows the Cherenkov angle θ_C to be determined

LHCb RICH
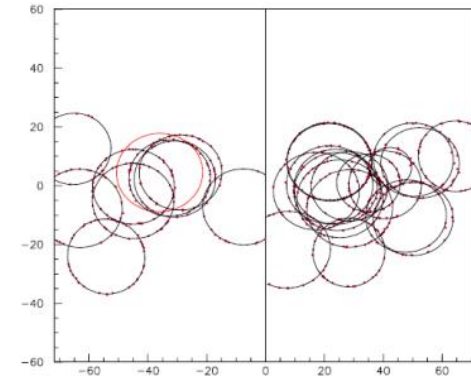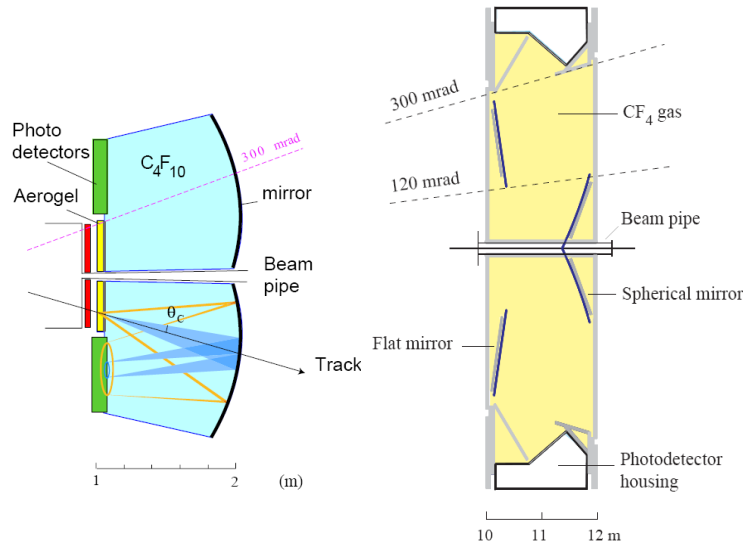
$$r \sim R\, \theta_C\, /2$$
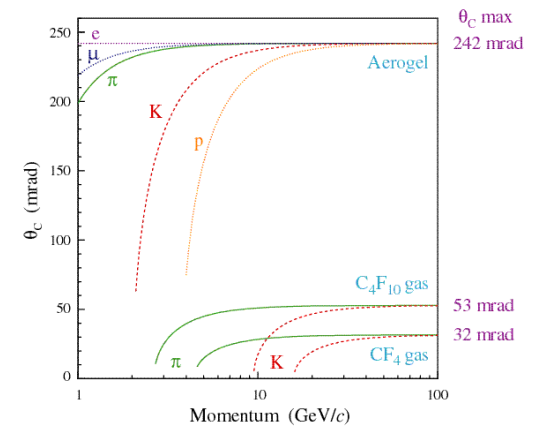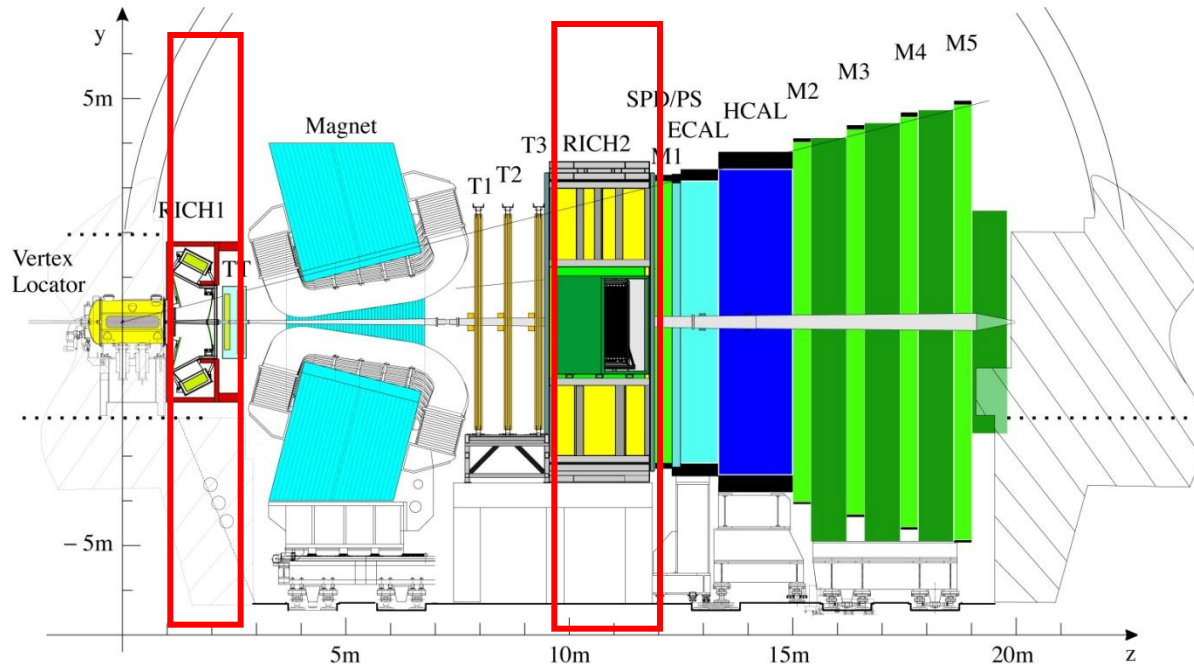
Scintillators

measureable signals occur via the interaction of charged particles with the detector material.

Dominant interaction is due to the coulomb interactions with the atomic *electrons* of the detector.
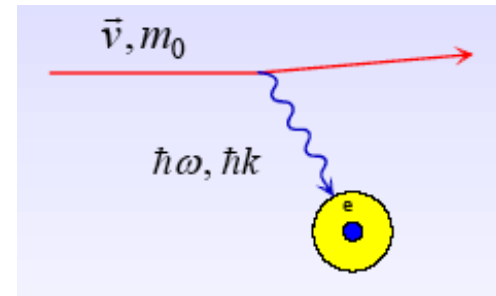
Depending on the $\hbar\omega$ value we may have:

❑ **ionization**   **or**   ❑ **excitation/scintillation**
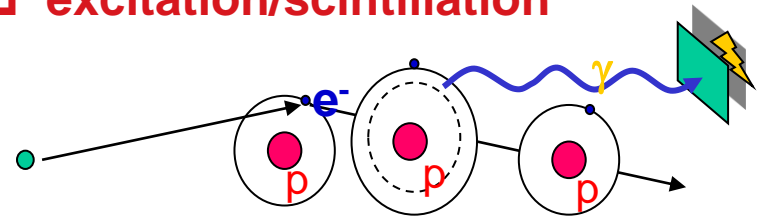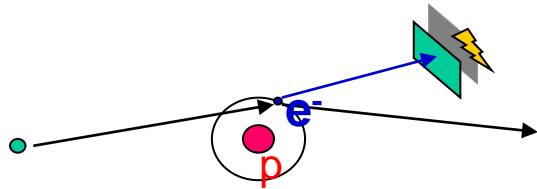
Ionization and excitation of atomic electrons in matter are the most common processes and allow to detect charged particles.

Introduction to Scintillators

scintillator   photodetector
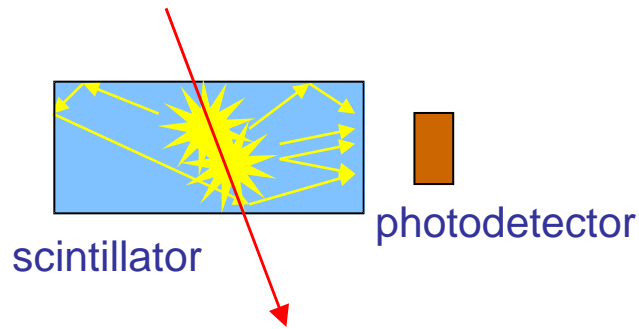
Energy deposition by an ionizing particle or photon (γ)

$\rightarrow$ generation
$\rightarrow$ transmission $\Big\}$ of scintillation light
$\rightarrow$ detection

Two categories

Inorganic
(crystalline structure)

- Up to 40000 photons per MeV
- High Z (good for photoeffect Z^5)
- Large variety of Z and ρ
- Undoped and doped
- ns to μs decay times
- Expensive
- Fairly Rad. Hard (100 kGy/year)

- E.m. calorimetry (e, γ)
- Medical imaging

Organic
(crystals, plastics or liquid solutions)

- Up to 10000 photons per MeV
- Low Z (not good for photoeffect)
- Low density $\rho \sim 1 g/cm^3$
- Doped, large choice of emission wavelength
- ns decay times
- Relatively inexpensive
- Medium Rad. Hard (10 kGy/year)

Scintillators readout

Readout has to be adapted to geometry, granularity and emission spectrum of scintillator.

Geometrical adaptation:

- Light guides: transfer by total internal reflection   (+outer reflector)

Light guide

PM

Scintillator   PMT

Light guide
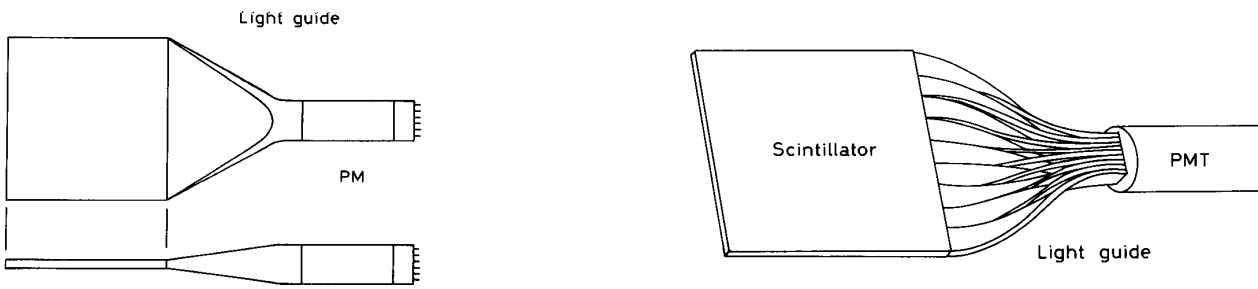
- Wavelength shifter (WLS) bars

small air gap

WLS   green

Photo detector

blue (secondary)

UV (primary)

scintillator

primary particle

WLS bars/fibres

plastic scintillators

a)

SCINTILLATOR (emission at λ_1)

ABSORBER

articles

WAVELENGTH SHIFTER (fluorescent emission at $\lambda_2 > \lambda_1$)

b)

c)
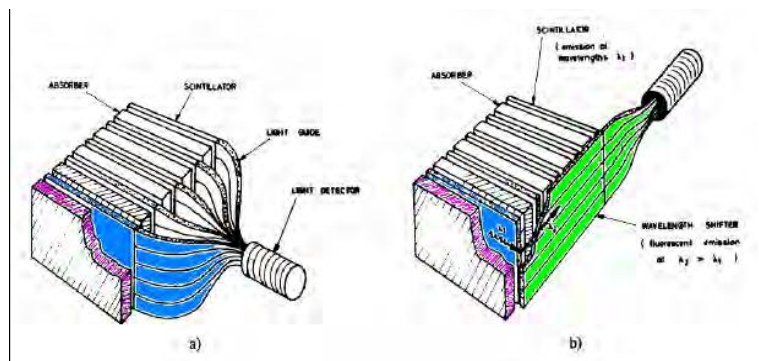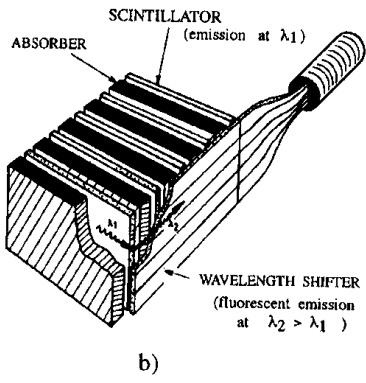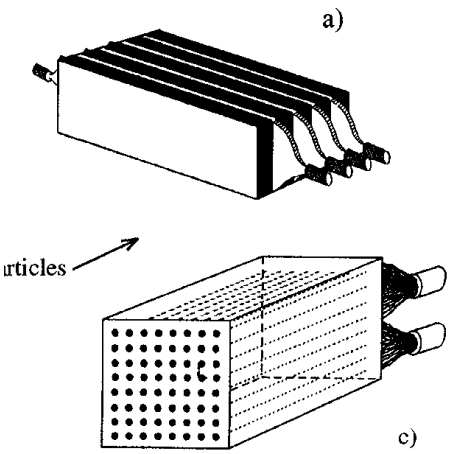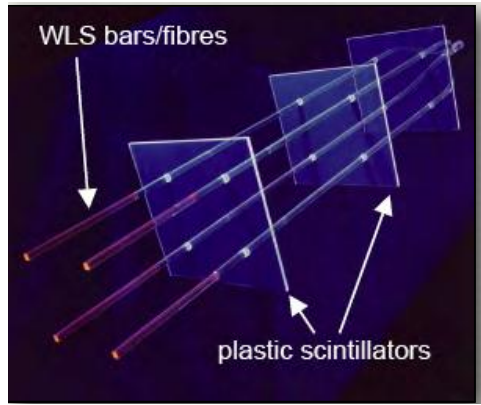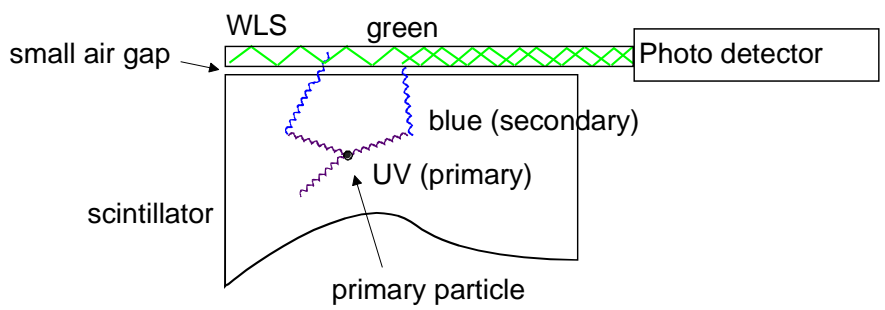
Photo-multiplier tubes (PMT's)

Basic principle:

- Photo-emission from photo-cathode

- Secondary emission from N dynodes:

  - dynode gain $g \approx$ 3-50 (function of incoming electron energy E);

  - total gain M:

$$M = \prod_{i=1}^{N} g_i$$

- Example:

  - 10 dynodes with $g = 4$

  - $M = 4^{10} \approx 10^6$

(Hamamatsu)

Incoming Photon
Window
Photo-cathode
Dynodes
Anode
Focusing Electrode
pe
Voltage Dropping Resistors
Power Supply
Output Meter
Figure 1
(http://micro.magnet.fsu.edu)
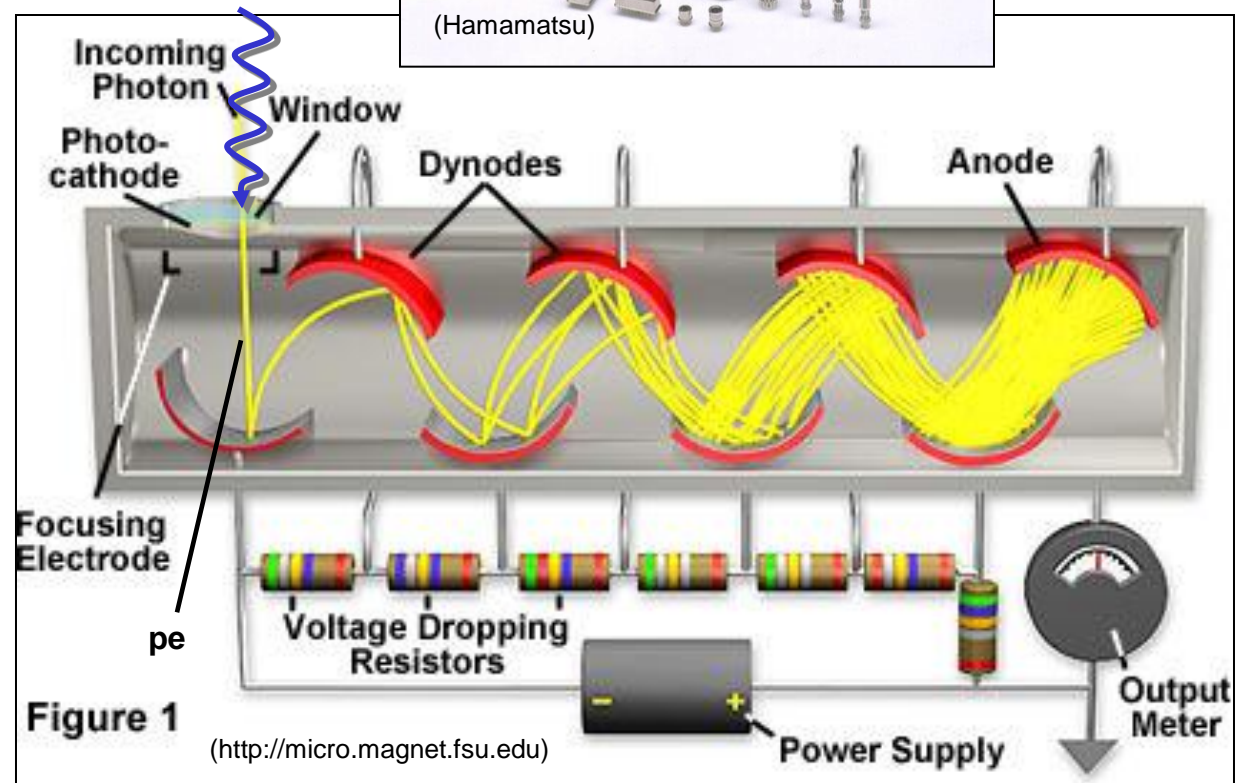
Most common applications of organic scintillators

- Large volume liquid or solid detectors
- neutron detection
- underground experiments
- sampling calorimeters (HCAL in CMS or ATLAS, etc.),
- trigger counters,
- TOF counters,
- Fibre tracking

Michigan University: 'neutron wall'. The flat-sided glass tubes contain liquid scintillator.

Plastic scintillators in various shapes (Saint Gobain)
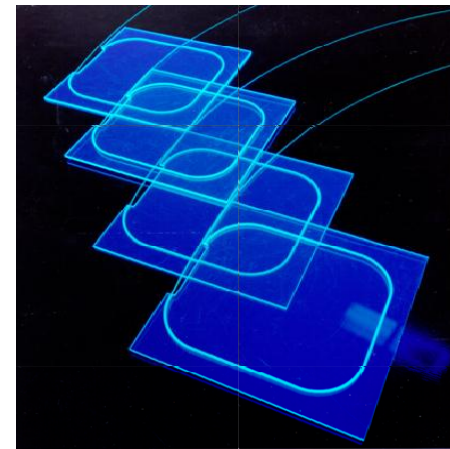
Scintillating tiles of CMS HCAL.
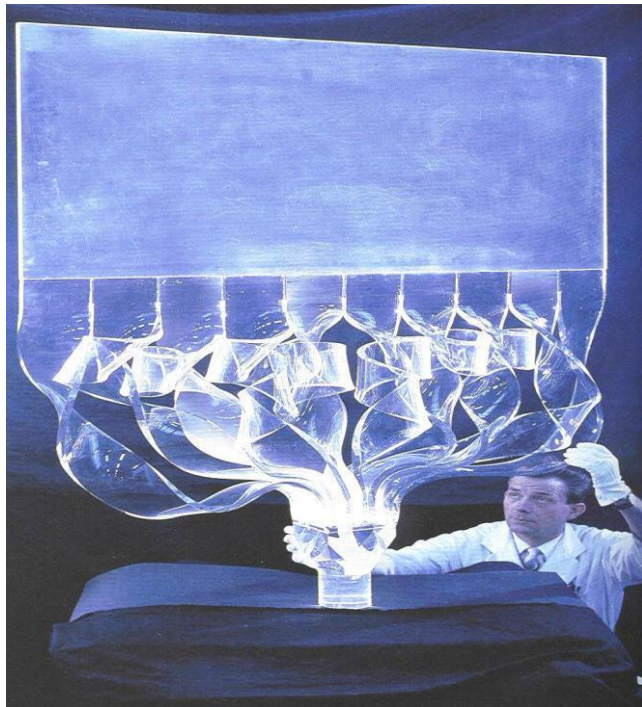
Time Of Flight

- Simple concept: measure the time difference between two detector planes $\beta = d/c\Delta t$

- At high energy, particle speeds are relativistic, closely approaching to c

- For a 10 GeV K, the time to travel 12 m is 40.05 ns, whereas for a π it would be 40.00 ns, so the difference is only 50 ps

- TOF gives good ID at low momentum Very precise timing required for $p > 5$ GeV

- Traditional approach to TOF uses scintillator hodoscopes

- Organic scintillators provide light on a timescale of ~ 100 ps (Inorganic are slower)
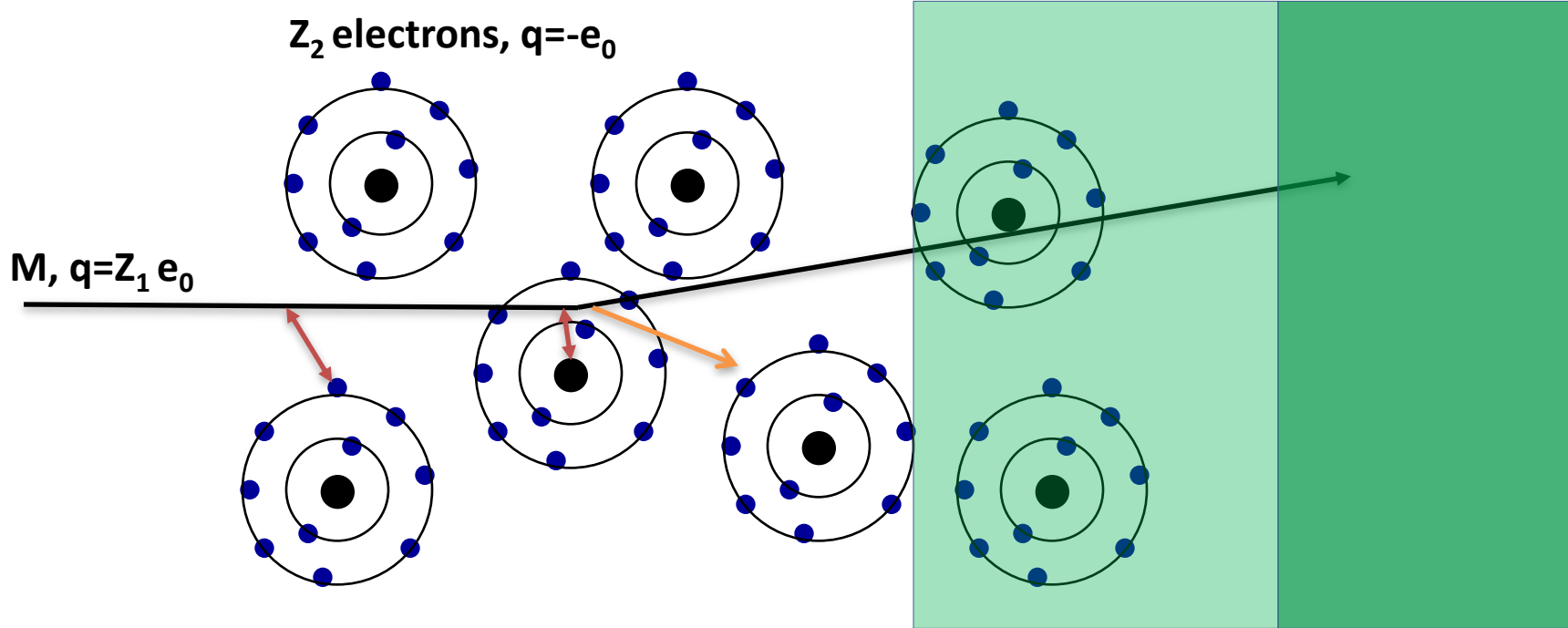
Detectors

Track

d

TOF difference for $d = 12$ m

K-π TOF difference (ps)

Momentum (GeV)

ALICE Performance
15/05/2011
TOF PID - Pb-Pb, $\sqrt{s_{NN}}$=2.76 TeV, min. bias

β

p (GeV/c)

all plots:
preliminary calibration & alignment !

TOF

Alice

Protons

Kaons

Pions

p_T [GeV/c]

velocity v/c β

Electromagnetic Interaction of Particles with Matter

Z_2 electrons, $q=-e_0$

M, $q=Z_1 e_0$

Interaction with the atomic electrons. The incoming particle loses energy and the atoms are <u>excited</u> or <u>ionized.</u>

Interaction with the atomic nucleus. The particle is deflected (scattered) causing <u>multiple scattering</u> of the particle in the material. During this scattering a <u>Bremsstrahlung</u> photon can be emitted.

In case the particle's velocity is larger than the velocity of light in the medium, the resulting EM shockwave manifests itself as <u>Cherenkov Radiation</u>. When the particle crosses the boundary between two media, there is a probability of the order of 1% to produced and X ray photon, called <u>Transition radiation</u>.

Multiple Scattering

A particle traversing material undergoes successive deflections due to multiple elastic scattering from nuclei.

The probability that the particle is defected by an angle θ after travelling a distance x in the material is well approximated (actually tails are larger than Gaussian tails) by a Gaussian distribution with sigma of:

$$\theta_{MCS} = \theta_{rms} = \frac{13.6\,MeV}{\beta c\,p}\,z\sqrt{\frac{x}{X_0}}\left[1 + 0.038\ln\left(\frac{x}{X_0}\right)\right]$$

X_0 Radiation length of the material
z Charge of the particle
p Momentum of the particle

Radiation Length X_0 has 2 definitions:

◇ Mean distance over which high energy electron losses all but 1/e of its energy by Bremsstrahlung.

◇ 7/9ths of the mean free path for pair production by a high energy photon.

$$X_0 \approx \frac{716.4\,gcm^{-2}A}{Z(Z+1)\ln(287/\sqrt{Z})}$$
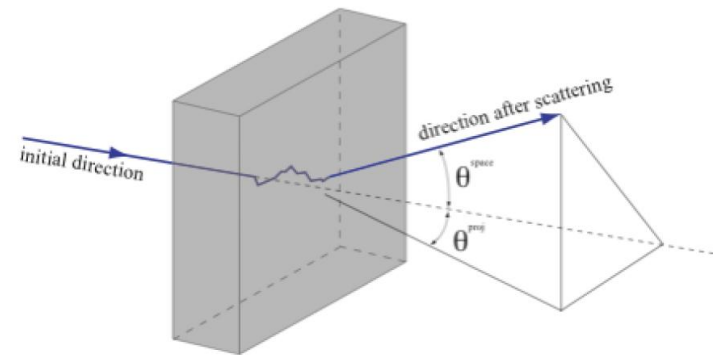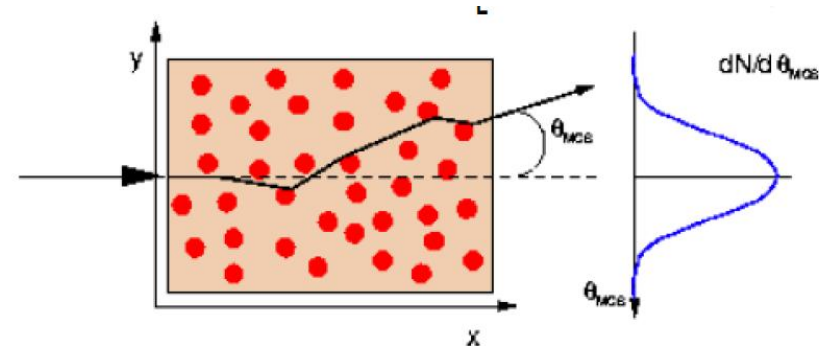
	X_0 (g cm^{-2})	X_0 (cm)
Air	37	30,000
Silicon	22	9.4
Lead	6.4	0.56

Bremsstrahlung

A charged particle of mass m and charge q traversing material not only interacts with the atomic electrons loosing energy via ionization and excitation, but also can be deflected by the atomic nuclei of charge Z of the material. This deflection (Rutherford scattering) results in an acceleration of the charge q that causes emission of photons. The radiation energy (Bremsstrahlung) emitted by the accelerated particle for a given momentum transfer can be evaluated by the Maxwell's equations and comes out to be:

➤ proportional to $1/m^2$ of the incoming particle
➤ proportional to E of the incoming particle
➤ proportional to q^4 of the incoming particle
➤ proportional to Z^2 of the material
➤ proportional to ρ of the material
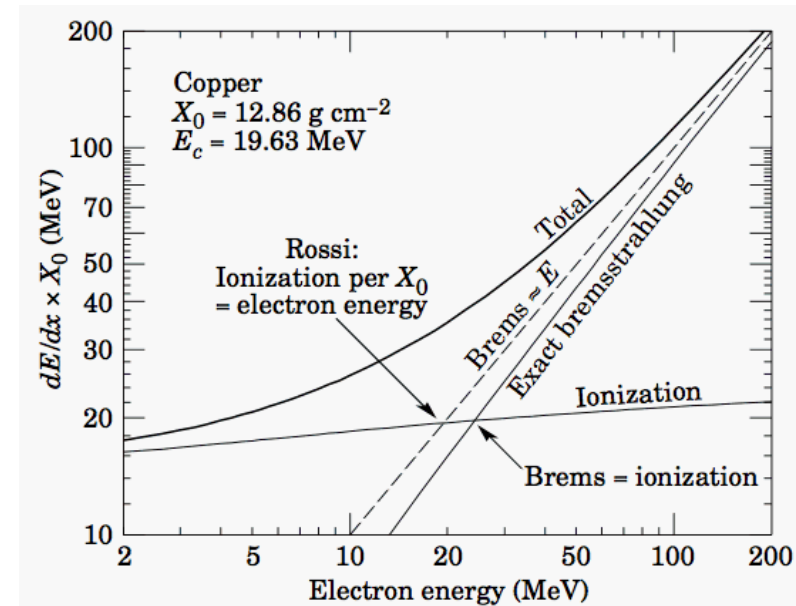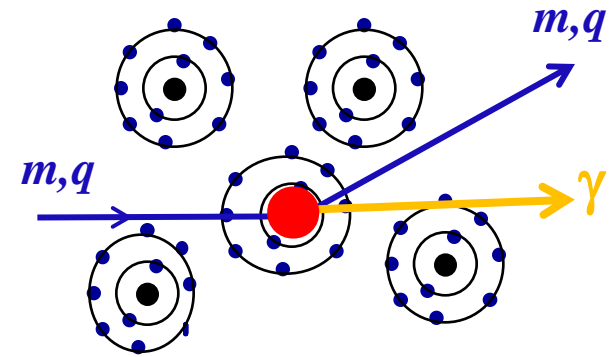
Critical Energy E_C is defined the energy at which
dE/dx (Ionization)=dE/dx (Bremsstrahlung)
Muon in Copper: $E_C \approx$ 400 GeV
Electron in Copper: $E_C \approx$ 20 MeV
Electrons lose energy via ionization as other charged particles, however because of their small mass the Bremsstrahlung becomes the dominant process for energies ≥ 20 MeV

Copper
X_0 = 12.86 g cm^{-2}
E_c = 19.63 MeV

Rossi:
Ionization per X_0
= electron energy

Total

Brems = E

Exact bremsstrahlung

Ionization

Brems = ionization

Bremsstrahlung

$$-\frac{dE}{dx} = 4\alpha N_A \frac{Z^2}{A} z^2 \left(\frac{1}{4\pi\varepsilon_0}\frac{e^2}{mc^2}\right)^2 E \ln\frac{183}{Z^{1/3}} \left(\propto \frac{E}{m^2}\right)$$
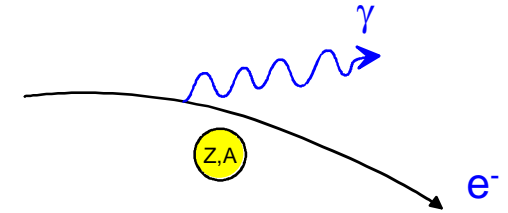
Effect is only relevant for $e^{\pm}$ and ultra-relativistic μ (>1000 GeV)

$$\frac{m_\mu^2}{m_e^2} = \frac{105^2\,\mathrm{MeV}^2}{0.5^2\,\mathrm{MeV}^2} = 4.4\cdot 10^4$$

Synchrotron Radiation

■ Energy loss per revolution

$$\Delta E = \frac{e^2}{3\varepsilon_0}\frac{\beta^3\gamma^4}{2\pi R} \qquad \beta = \frac{v}{c} \qquad \gamma = \frac{E}{m} \qquad R = \text{orbit radius}$$

$$\Delta E[GeV] = 5.7\times 10^{-7}\frac{E^4[GeV]}{R[km]}$$
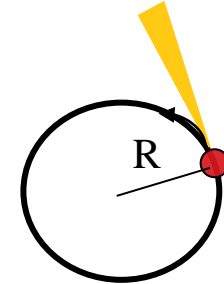
■ Example : LEP, $2\pi R$=27km, E=100 GeV (in 2000)

 □ **ΔE = 2 GeV!!**

 □ **LEP at limit, need more and more energy just to compensate energy loss**

■ Note : for ultrarelativistic protons/electrons (b $\cong$ 1)

$$\Delta E[p]/\,\Delta E[e] = (m_e/m_p)^4 = \mathbf{10^{-13}}\ \mathbf{!!}$$

Muon Energy Loss

(Limits of applicability for Bethe Bloch)

μ at minimum ionization
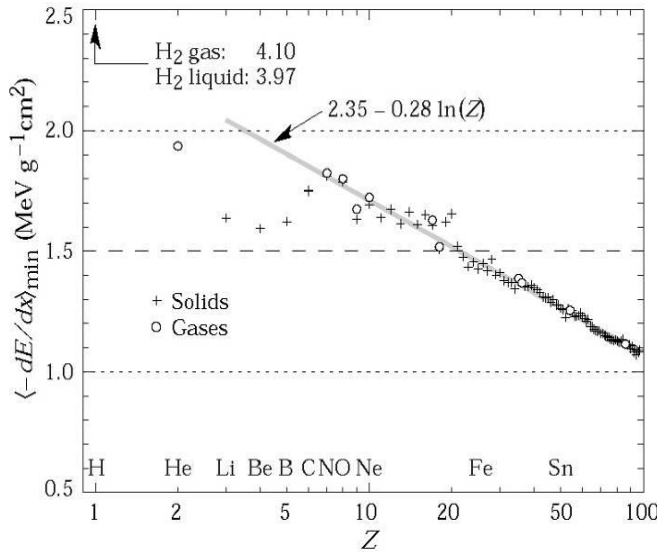
a 1TeV muon hitting copper is not a MIP !

$1/\beta^2$

$\ln \beta\gamma$
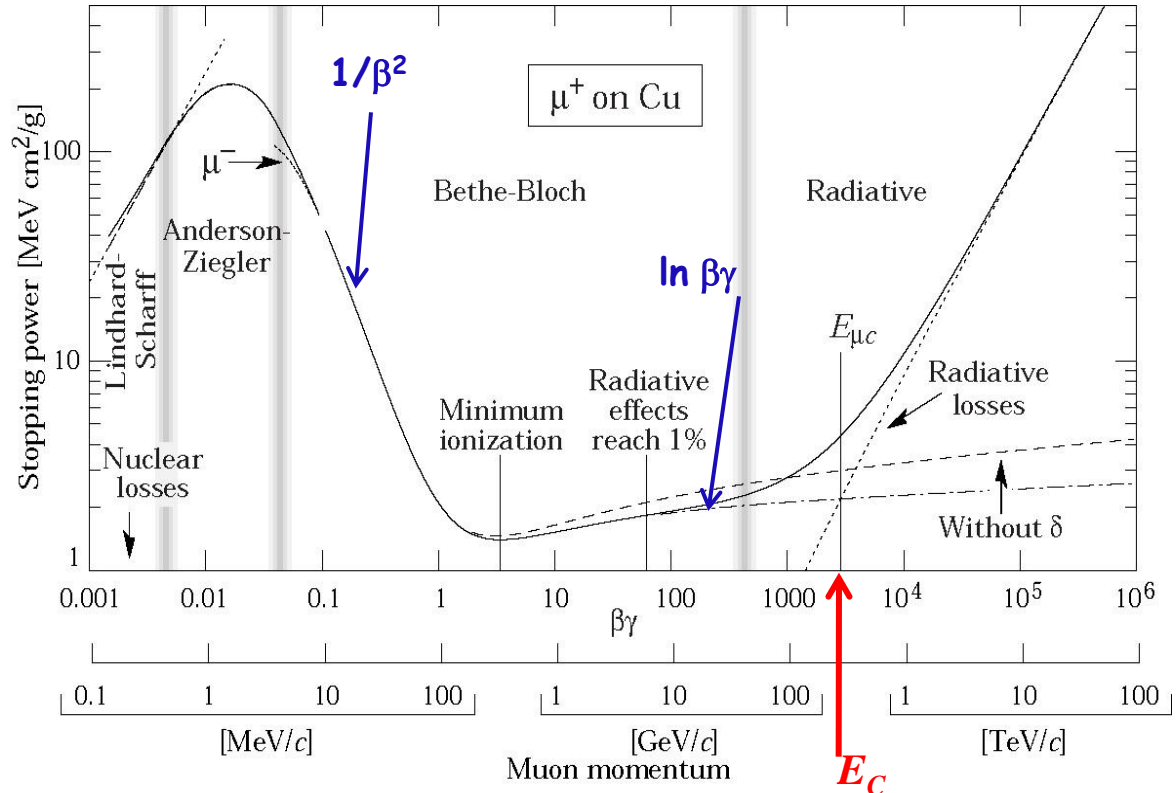
Example: a 1 GeV μ in Iron

Fe: Thickness = 100 cm; ρ = 7.87 g/cm³

$\Delta E \approx 1.4 * 100 * 7.87 = 1102$ MeV

→ a 1 GeV μ can traverse 1 m of Iron

E_c = energy for which ionization matches bremsstrahlung

Search for Hidden Chambers in the Pyramids

The structure of the Second Pyramid of Giza is determined by cosmic-ray absorption.

Luis W. Alvarez, Jared A. Anderson, F. El Bedwei,
James Burkhard, Ahmed Fakhry, Adib Girgis, Amr Goneid,
Fikhry Hassan, Dennis Iverson, Gerald Lynch, Zenab Miligy,
Ali Hilmy Moussa, Mohammed-Sharkawi, Lauren Yazolino

Fig. 2 (bottom right). Cross sections of (a) the Great Pyramid of Cheops and (b) the Pyramid of Chephren, showing the known chambers: *(A)* Smooth limestone cap, *(B)* the Belzoni Chamber, *(C)* Belzoni's entrance, *(D)* Howard-Vyse's entrance, *un* descending passageway, *(F)* ascending passageway, *(G)* underground chamber, *(/-1)* Grand Gallery, *(I)* King's Chamber, *(I)* Queen's Chamber, *(K)* center line of the pyramid.

6 FEBRUARY 1970

Luis Alvarez used the attenuation of muons to look for chambers in the Second Giza Pyramid → Muon Tomography

He proved that there are no chambers present.

Fig. 13. Scatter plots showing the three stages in the combined analytic and visual analysis of the data and a plot with a simulated chamber, (a) Simulated "x-ray photograph" of uncorrected data. (b) Data corrected for the geometrical acceptance of the apparatus. (c) Data corrected for pyramid structure as well as geometrical acceptance. (d) Same as (c) but with simulated chamber, as in Fig. 12.

Interaction of photons

In order to be detected, a photon has to create charged particles and / or transfer energy to charged particles

Photo-electric effect

Compton scattering

Pair production

✓1-Photoelectric effect
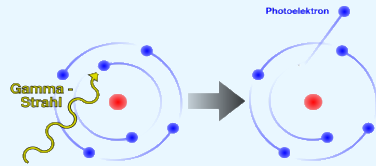
cross section scales with $Z^{4,5}$ and E^{-3}

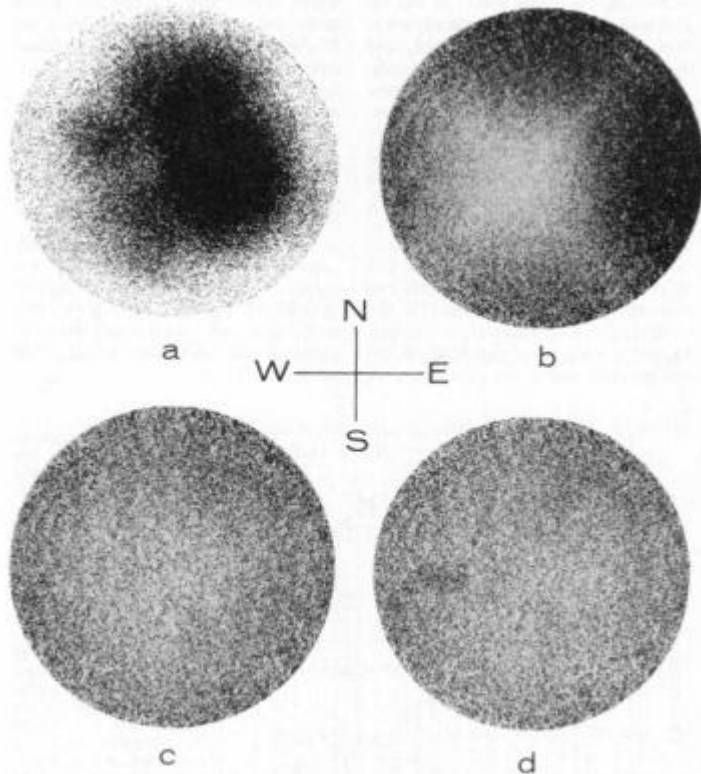✓2-Coherent (Rayleigh) scattering
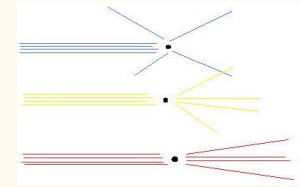
elastic scattering of g by the atomic electron, no energy loss just change of direction at low energy ... $s \sim 1/l^4$

✓3-Compton scattering

Compton scattering

Recoil electron

$p_e = \dfrac{\sqrt{E^2 - (m_e c^2)^2}}{c}$

Incident photon λ_i

Target electron at rest

Φ

$p_i = \dfrac{E_i}{c} = \dfrac{h\upsilon_i}{c} = \dfrac{h}{\lambda_i}$

θ

$p_f = \dfrac{E_f}{c} = \dfrac{h\upsilon_f}{c} = \dfrac{h}{\lambda_f}$

Scattered photon λ_f

$\lambda_f - \lambda_i = \Delta\lambda = \dfrac{h}{m_0 c}(1 - \cos\theta)$
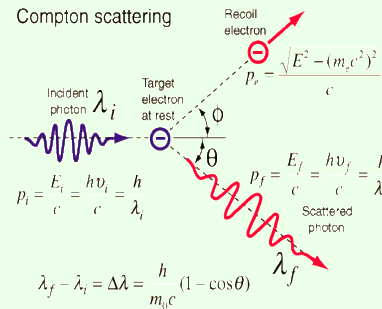
cross section scales with Z and 1/E

✓4-Electron positron pair production

Nucleus — Electron (e⁻)

Photon (y) — Positron (e⁺)
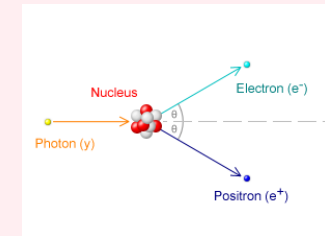
cross section raises with Z and energy and reaches an asymptotic value above 1 GeV

✓5-Photo nuclear reactions   between 5-20 MeV, cross section does not exceed 1% of all other processes.

gn, gp or induced nuclear fission

Photon Interactions

$$I_\gamma = I_0 e^{-\mu x}$$

μ: attenuation coefficient :

$$\mu_i = \frac{N_A}{A} \sigma_i \quad \left[cm^2 / g \right] \qquad \mu = \mu_{photo} + \mu_{Compton} + \mu_{pair} + \dots$$

- **low energies (< 100 keV): Photoelectric effect**

- **medium energies (~1 MeV): Compton scattering**

- **high energies (> 10 MeV): e⁺e⁻ pair production**

- **Note that each of these processes leads to the ejection of electrons from atoms!**

- **"electromagnetic showers"**
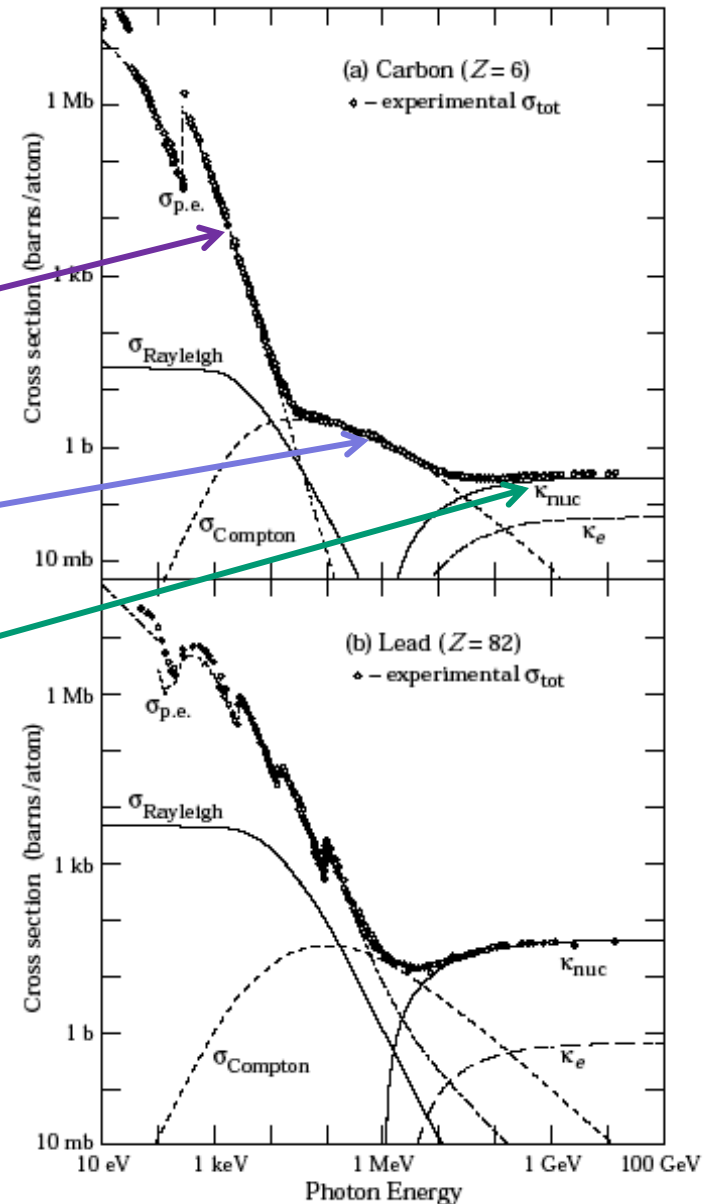
electromagnetic interactions: e⁺/e⁻ versus γ

e⁺ / e⁻

- **Ionisation**
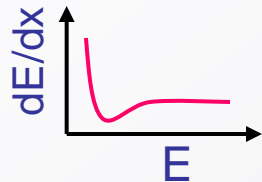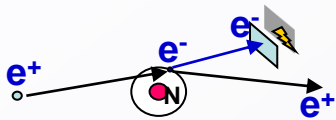
- **Bremsstrahlung**
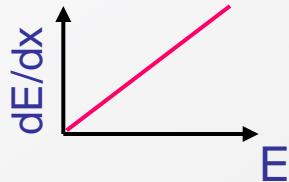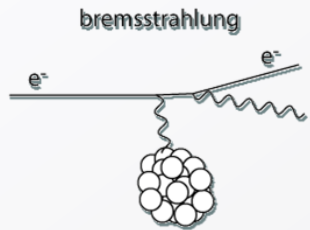
Brems is more important at high energies.

$$R = \frac{\left(\frac{dE}{dx}\right)_{Brem}}{\left(\frac{dE}{dx}\right)_{ion}} \sim \frac{ZE}{580MeV}$$

$$E_c = \frac{580MeV}{Z}$$

R: ratio of the energy loss for the two processes

E_c: critical energy when R=1

γ

- Photoelectric effect

- Compton effect
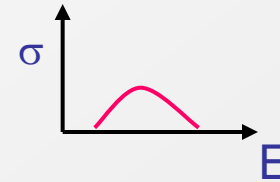
- Pair production

At high energy, when e⁺/e⁻ interactions in matter are dominated by Brems, the interactions of γs are dominated by e⁺e⁻ pair production.

Electromagnetic Showers

- **A photon impinging on solid matter produce a e⁺e⁻ pair. Each e⁺/e⁻ of the pair will generate a γ-Brem which in turn will produce a e⁺e⁻ pair, and so on…(with a linear absorption coefficient of $1/X_0$**

- **Shower can be initiated by electron OR positron**

- **this process repeats, giving rise to an e.m. shower:**
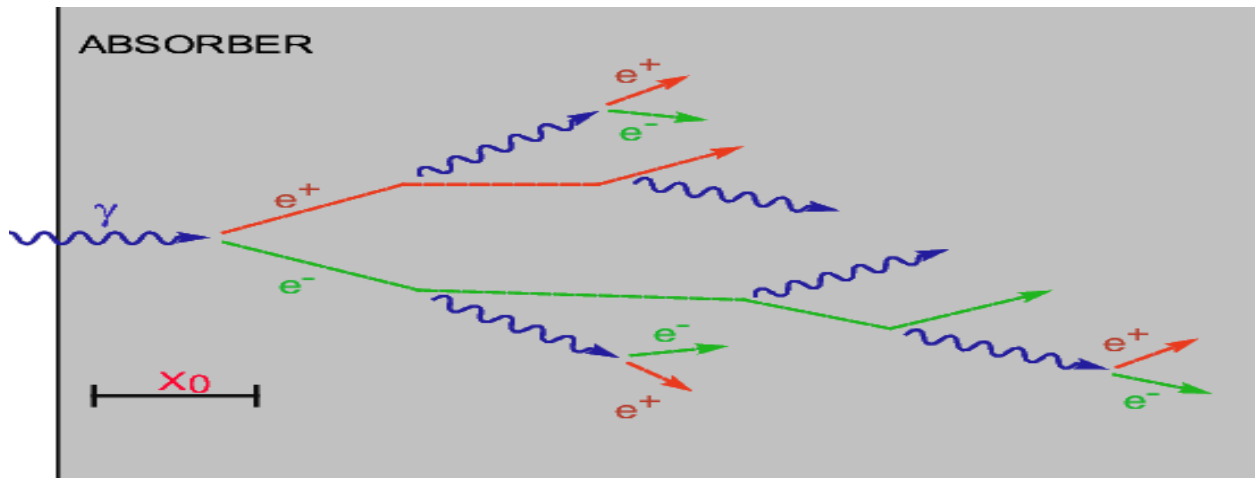
- **the process continues until the resulting photons and electrons fall below threshold**

- **so how do we get some sort of signal out?**

- **the (total) ionization (scintillation) produced by the e⁺e⁻ pairs during the e.m. shower can be detected.**

- **the amount of ionization (scintillation) is proportional to the energy of the incoming electro/positron**

Electromagnetic Calorimeter Types

❑ Sampling Calorimeter

- "lead-scintillator sandwich" calorimeter $\otimes E/E \sim 20\%/\sqrt{E}$

- liquid argon calorimeter $\otimes E/E \sim 10\%/\sqrt{E}$
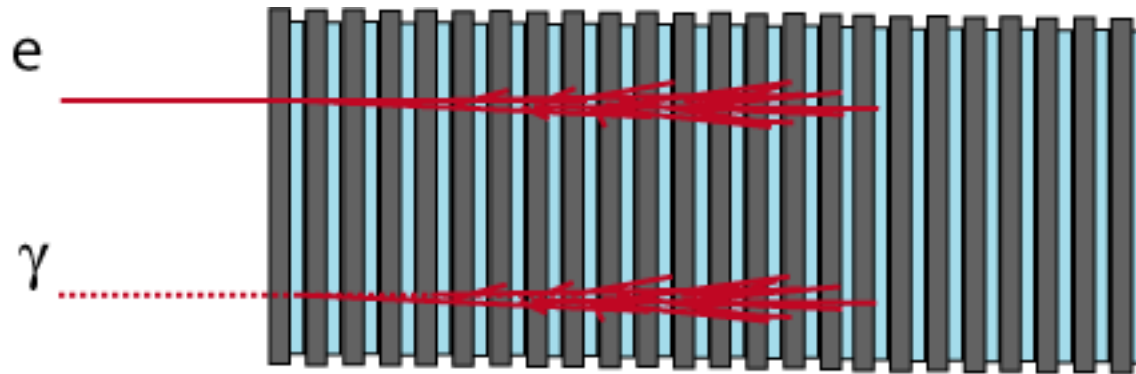
❑ Omogeneous Calorimeter

- A single medium serves both as absorber and detector: exotic crystals (BGO, $PbWO_4$, ...)

$\otimes E/E \sim 1 \div 3 \%/\sqrt{E}$
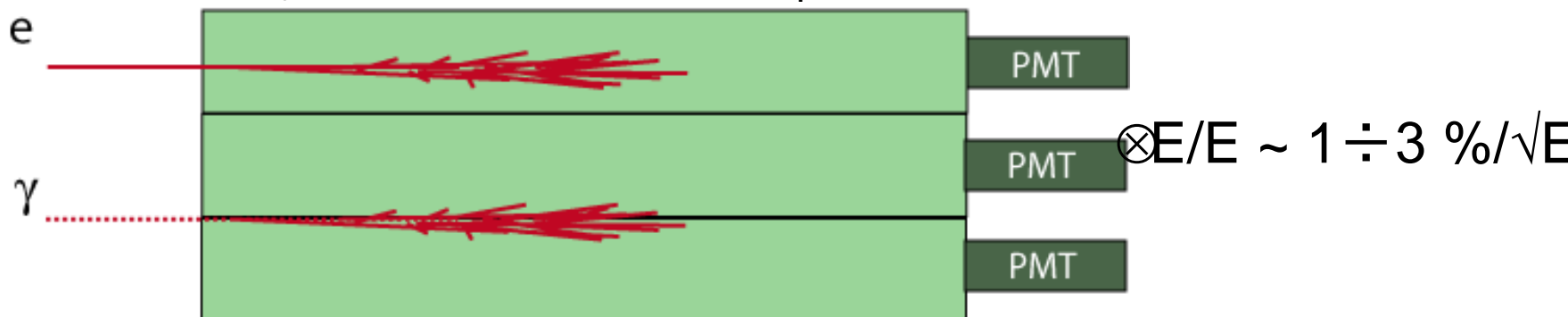
ECAL

75.000 lead tungstate crystals (very compact); fast (95% light emitted in 25ns; highly granular (2.19cm Moliere radius)

Excellent energy resolution

Stochastic term (Photostatistics APD 4p.e./MeV)

Noise (electronics and pile-up)

Constant term (uniformity and calibration)

$$\frac{\sigma(E)}{E} = \frac{3\%}{\sqrt{E}} \oplus \frac{150 MeV}{E} \oplus 0.40\%$$

e⁻

23 25 27 X_0
1 X_0 = 0.9 cm
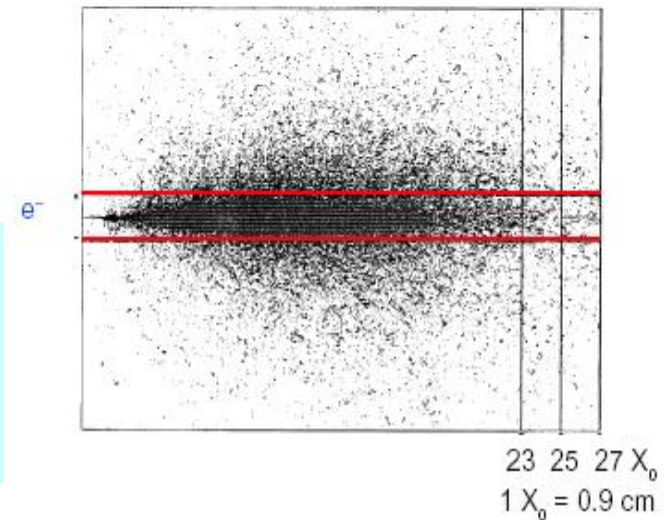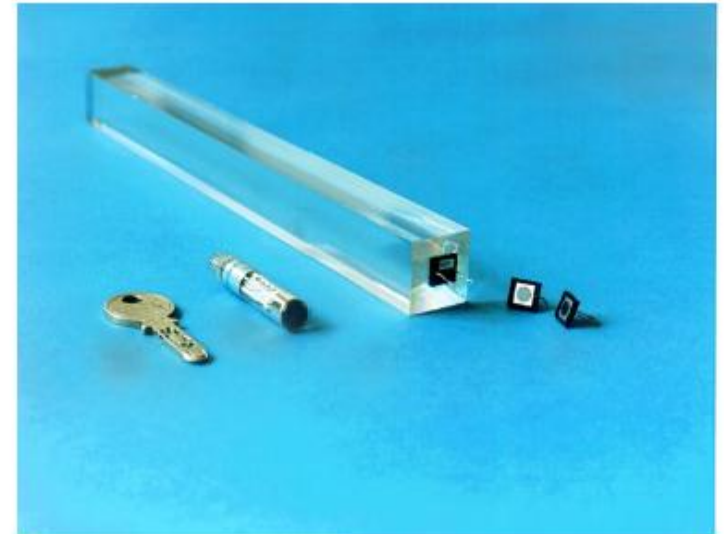
Lead Tungstate production

- ✓ **From high-purity Lead Oxide and Tungsten Oxide in high-T oven at 1200⁰C**

- ✓ **Ingots machined to size**

- ✓ **Lapping and polishing to obtain optical quality surface (for total reflection of light)**

dimensions: 26 x 26 x 230 mm^3
X_0 = 8.9 mm , r_M = 20 mm, r = 8.3 g/cm^3
weight = 1.2 kg, polished to R_a ~ 0.02 mm
dLY/dT (18⁰ C) = -1.9%/⁰ C
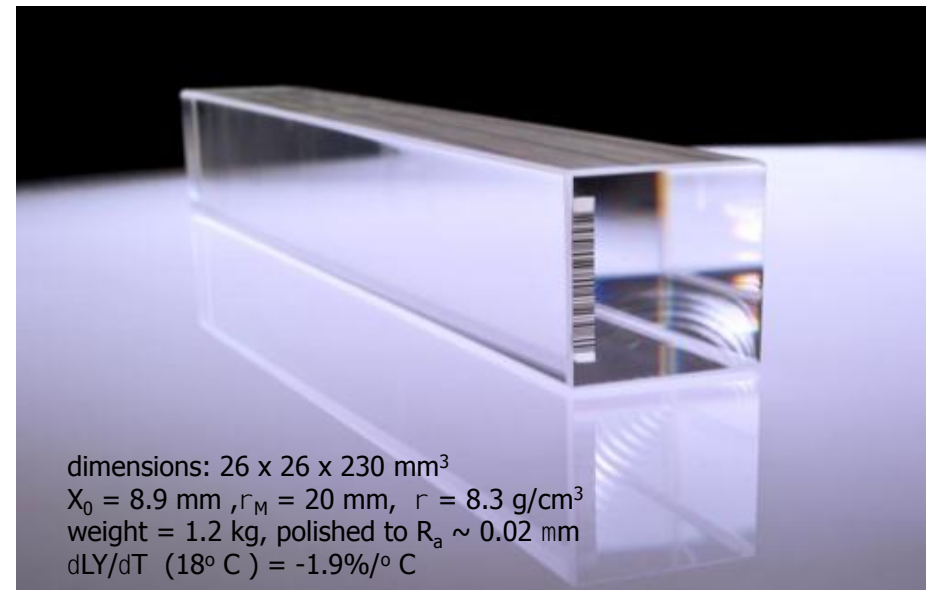
CMS crystals: PbWO$_4$

Excellent energy resolution

$X_0 = 0.89$cm $\rightarrow$ compact calorimeter (23cm for 26 X_0)

$R_M = 2.2$ cm $\rightarrow$ compact shower development

Fast light emission (80% in less than 15 ns)

Radiation hard (10^5Gy)

But

Low light yield (150 γ/MeV)

Response varies with dose

Response temperature dependance

γ
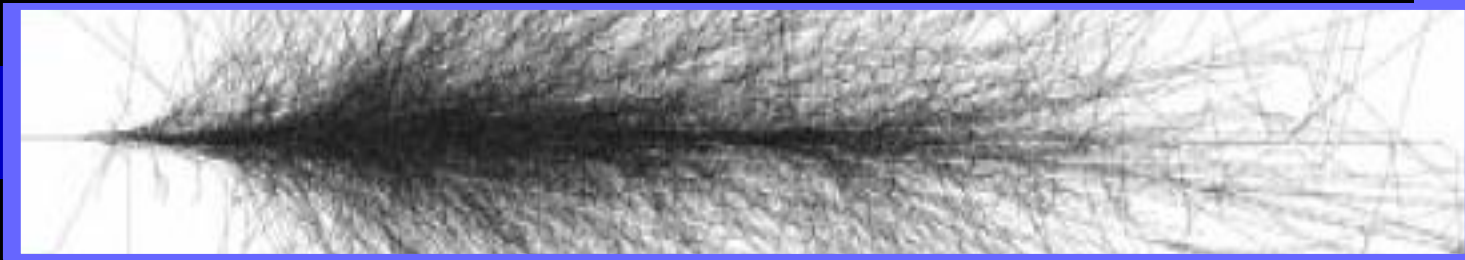
Lead Tungstate Scintillating Crystals
(75.000 crystals)

Submodule
2x5 crystals

CERN PH/CMA.
5 Feb. 2004
CMS ECAL Submodules
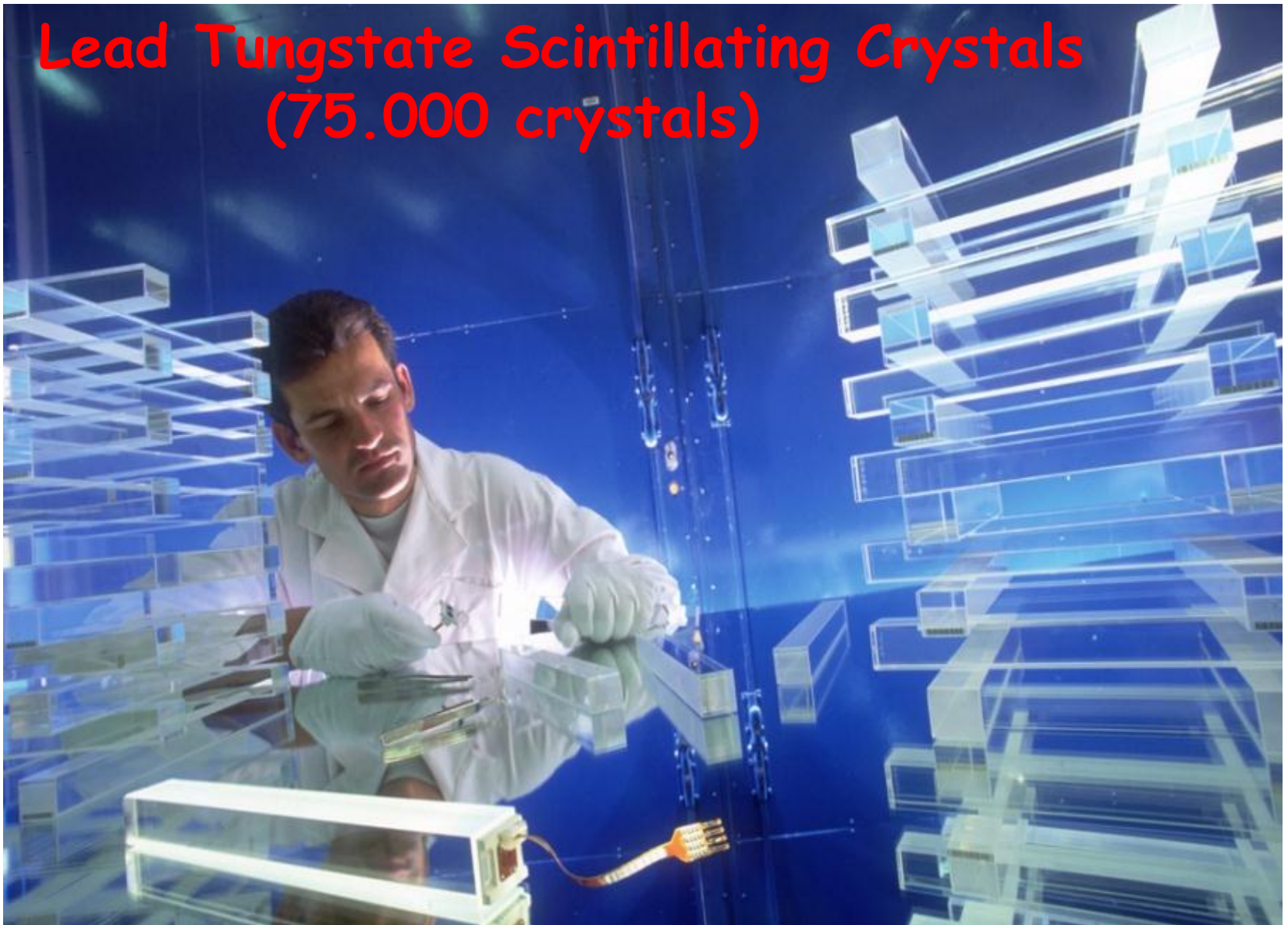
Module
400 crystals

Supermodule
1700 crytsals
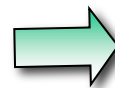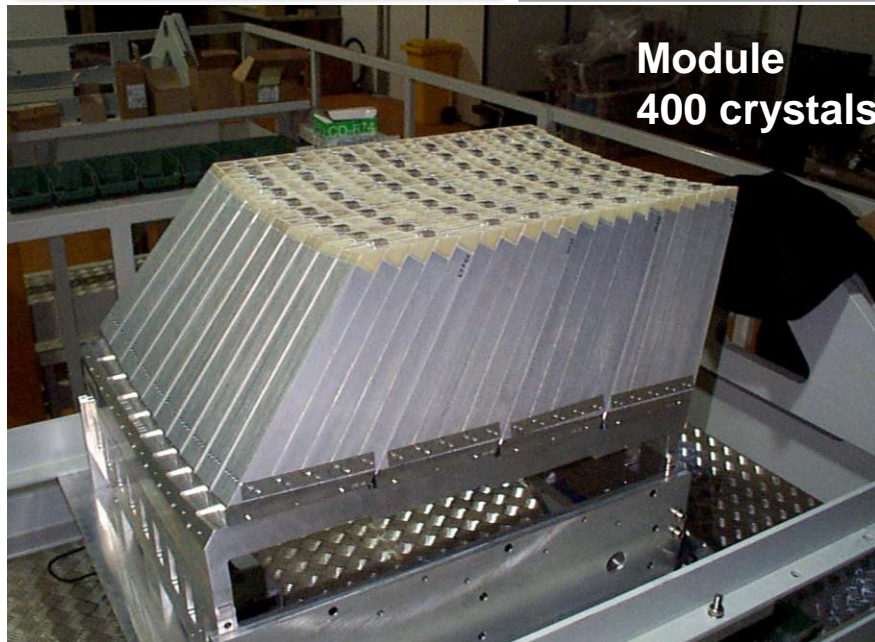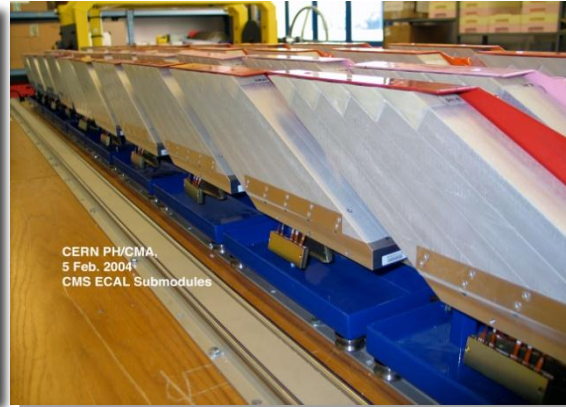
Total 36 Supermodules

Jul'07
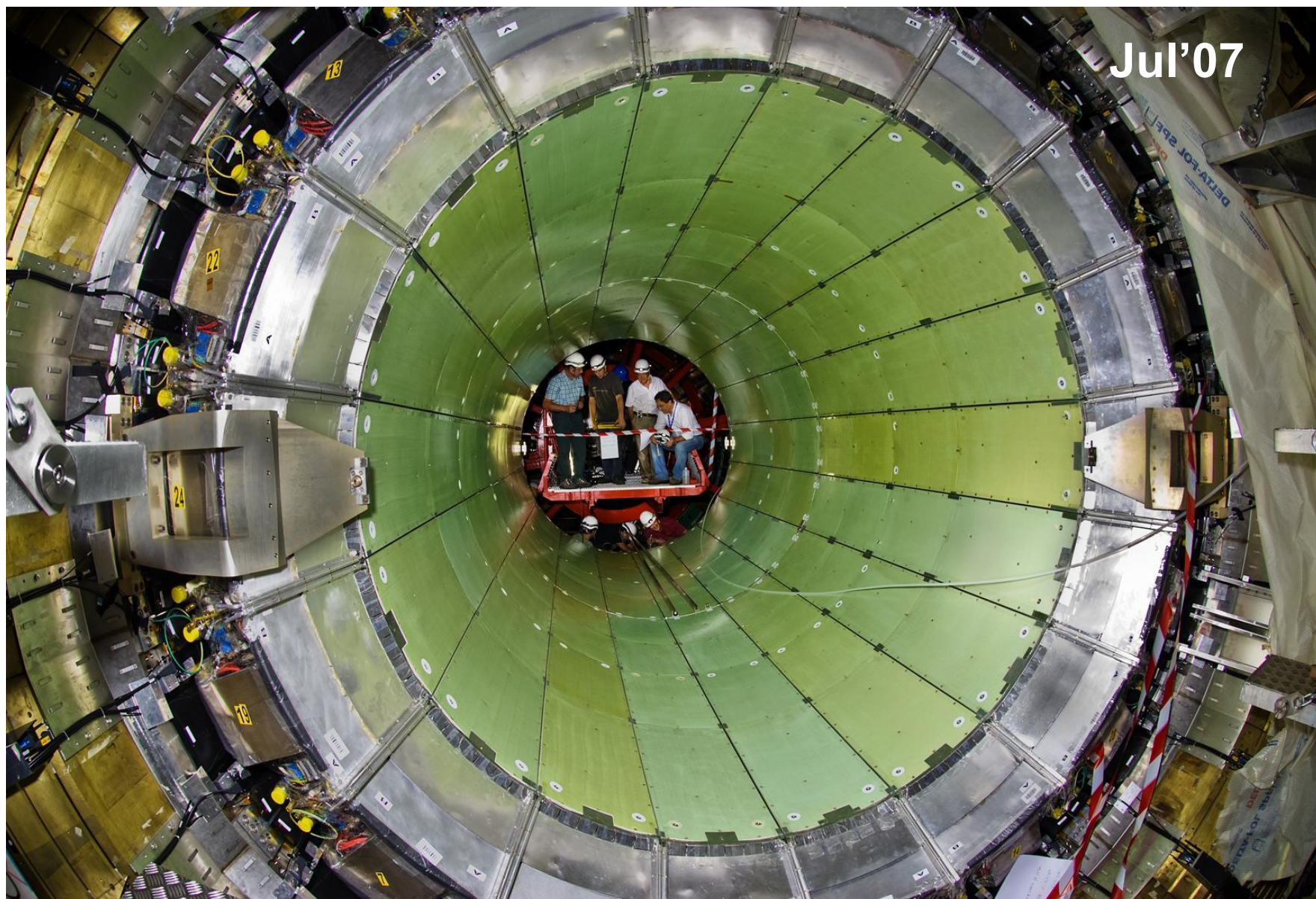
Sampling Calorimeters

Possible setups

Scintillators as active layer; signal readout via photo multipliers

Absorber Scintillator Light guide Photo detector
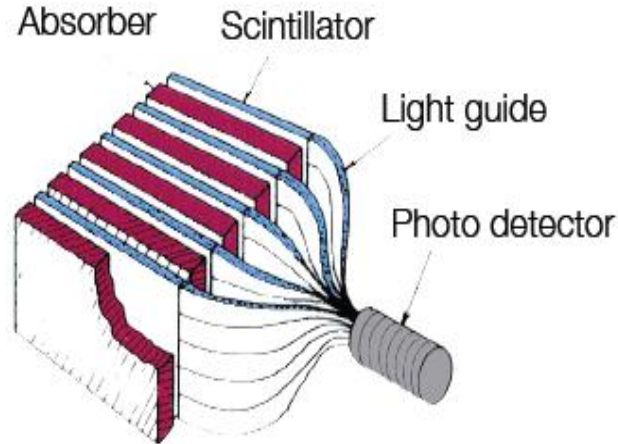
Scintillators as active layer; wave length shifter to convert light

Scintillator (blue light) Wavelength shifter
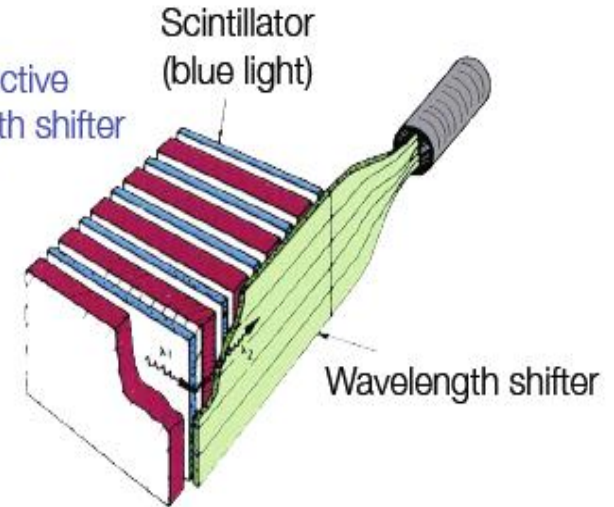
Charge amplifier Absorber as electrodes HV

Argon

Active medium: LAr; absorber embedded in liquid serve as electrods
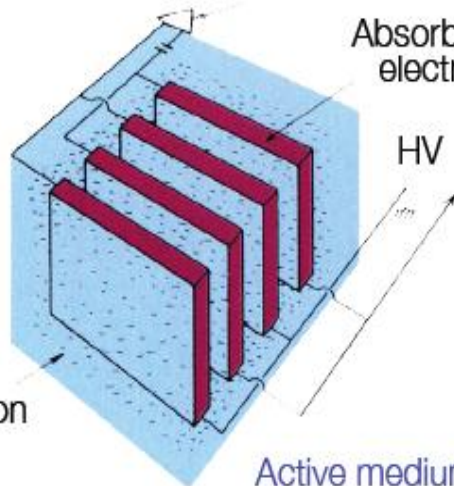
Ionization chambers between absorber plates Electrodes Analogue signal

ATLAS LAr Accordion Calorimeter

1.9 L Ar

6.4

40.1

25

kapton

0.1 inox

2.2

0.1 inox

1.8 Lead
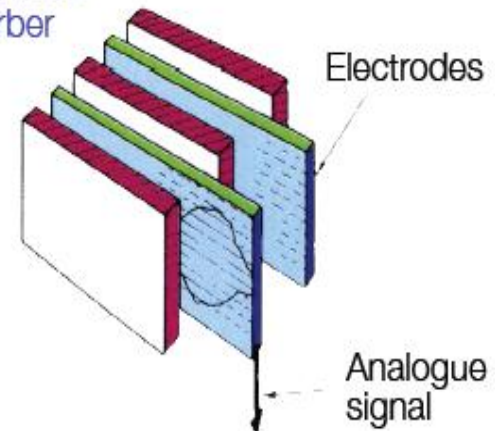
✓ **Sampling at 45^0, accordion concept**

✓ **New readout concept, to make it fast (~40 ns)**
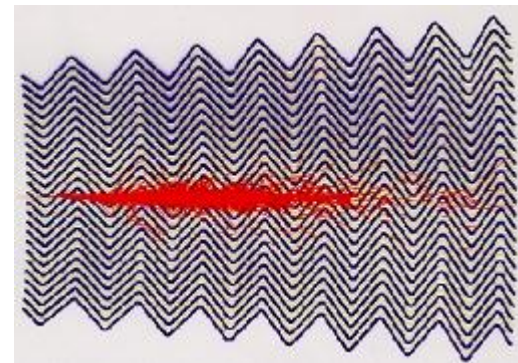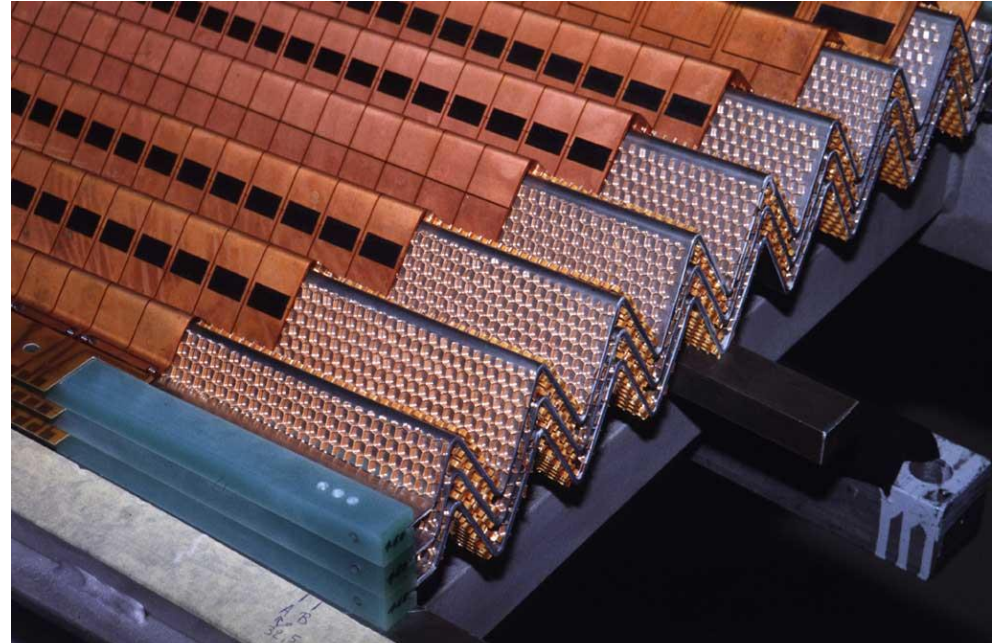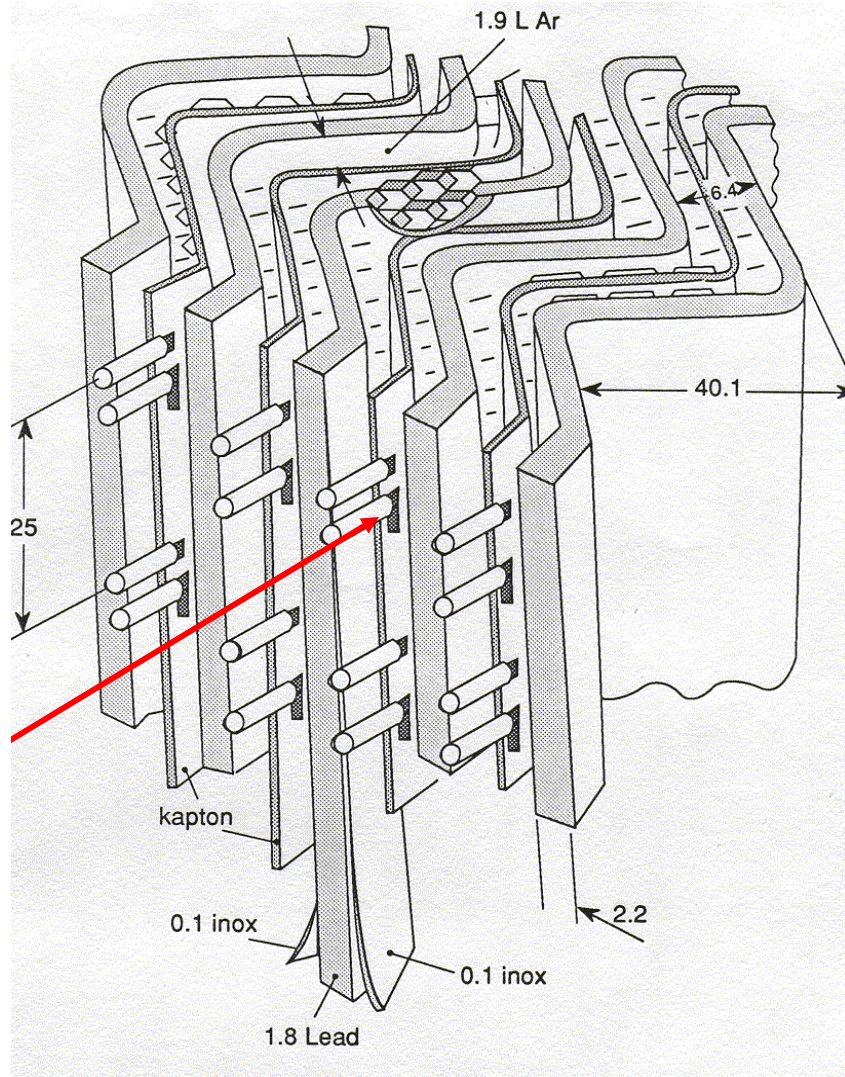
ATLAS LAr Calorimeter
Accordion structure

47 cm

readout electrode

absorber

outer copper layer
inner copper layer
kapton
outer copper layer

(~2 mm)

liquid argon gap

liquid argon gap

stainless steel

glue
lead

HV   HV

P
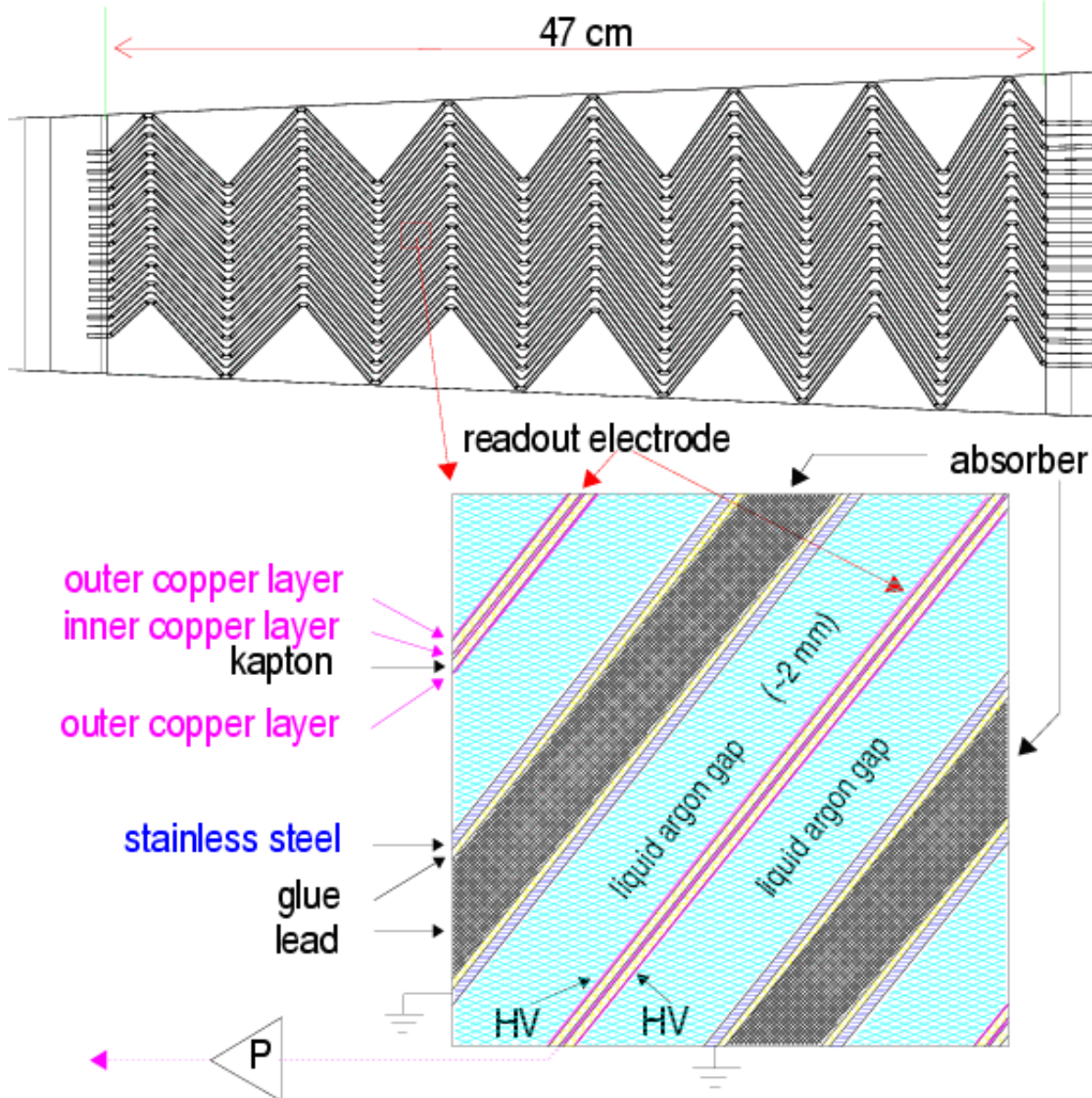
Detector uniformity (constant term) defined by the control of the thickness distribution of the various layers (absorber, electrodes, LAr, ...)

$$\frac{\sigma(E)}{E} \approx \frac{10\%}{\sqrt{E}} \oplus 0.7\%$$
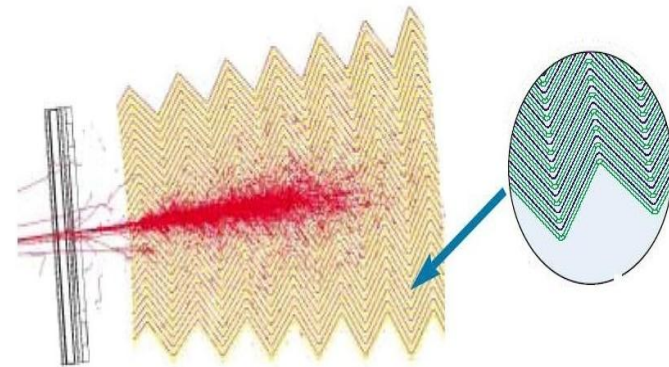
ATLAS Lar Accordion Calorimeter
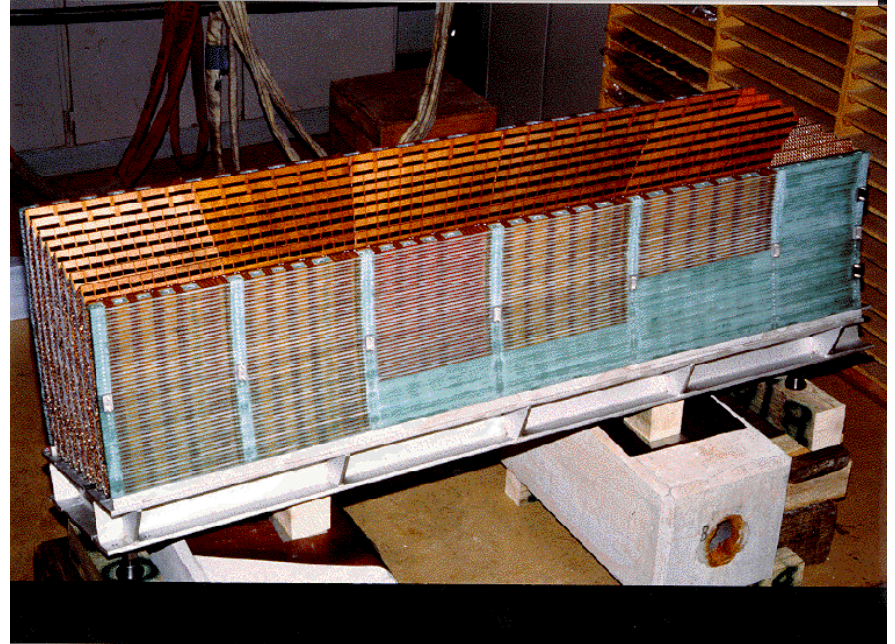
ATLAS Lar Accordion Calorimeter

Fine segmentation and granularity :
(longitudinally 3 compartments)
   compartment 1 : 4 mm strips in η direction
   compartment 2 : ~ 4 x 4 cm^2
   compartment 3 : ~ 8 x 4 cm^2 in η x ϕ

Total:
~ 200 000
channels

Readout: warm preamps + 3-gain
shapers (t_p ~ 40 ns) + 40 MHz
analog pipeline + 12-bit ADC

Towers in Sampling 3
$\Delta\varphi \times \Delta\eta = 0.0245 \times 0.05$

Trigger Tower
$\Delta\eta = 0.1$

$2X_0$

$\eta = 0$

470 mm

$16X_0$

Trigger
Tower
$\Delta\varphi = 0.0982$

$4.3X_0$

1500 mm

$1.7X_0$
$\Delta\varphi = 0.0245 \times 4$
36.8mm x 4
=147.3mm

Square towers in
Sampling 2

$\Delta\varphi = 0.0245$

φ

37.5mm/8 = 4.69 mm
$\Delta\eta = 0.0031$

$\Delta\eta = 0.025$

Strip towers in Sampling 1

η
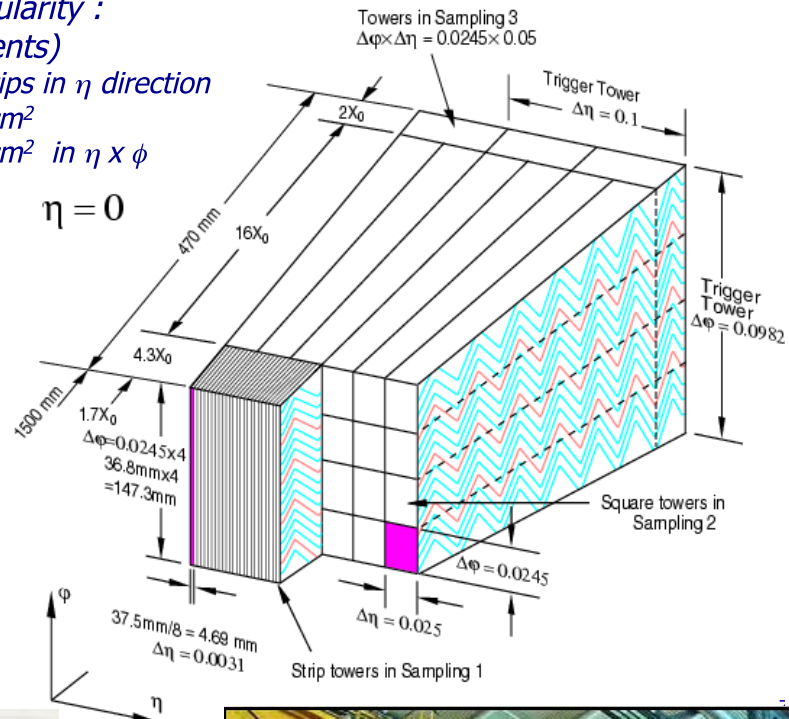
ATLAS LAr

ECAL calibration

$\mathcal{L} > 1$ nb^{-1} : beginning to use π^0's and η's in ECAL calibration.

1.46M $\pi^0 \rightarrow \gamma\gamma$ pairs

25.5k $\eta \rightarrow \gamma\gamma$ pairs

7 TeV DATA

CMS Preliminary Data √s=7 TeV

M = 133.82 ± 0.02 MeV

σ = 10.6 %

S/B$_{\pm 2\sigma}$ = 0.81

CMS Preliminary Data √s=7 TeV

M = 537.37 ± 0.53 MeV

σ = 6.1± 0.1 %

S/B$_{\pm 2\sigma}$ = 0.34

8 TeV DATA

CMS 2012 Preliminary, √s= 8 TeV, L = 2.4 fb^{-1}

ECAL Barrel

Electrons with low or no Bremsstrahlung

CMS 2012 Preliminary
√s = 8 TeV   L = 3.95 fb^{-1}

with LM correction
without LM correction
1 / LM correction

ECAL Barrel: Prompt Reco
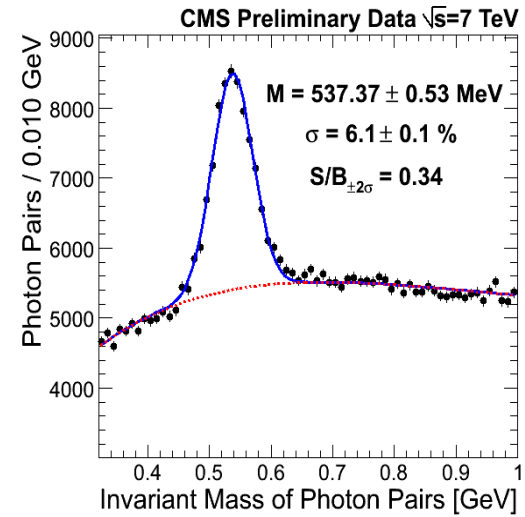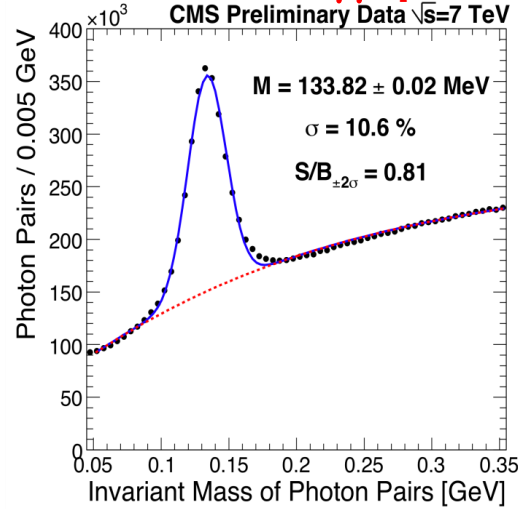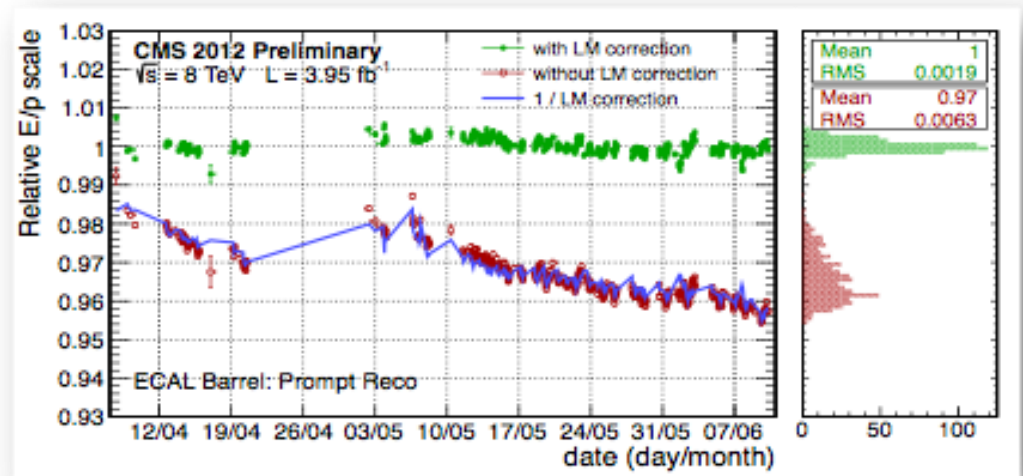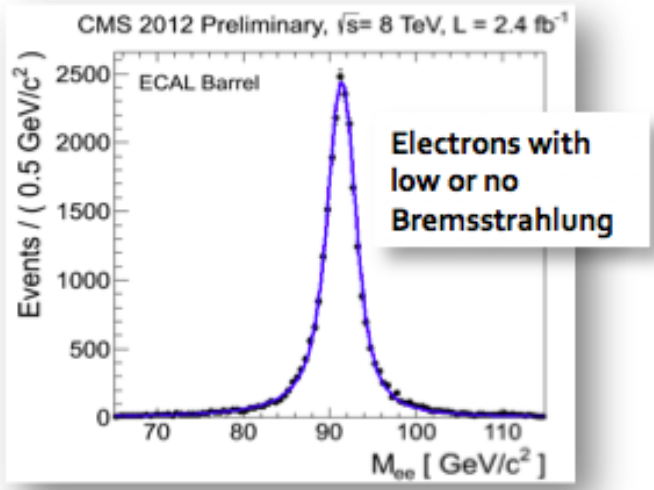
Mass resolution

$$m^2_{\gamma\gamma} = 2 \, E_1 \, E_2 \, (1-cos\alpha)$$

Present understanding of calorimeter E response (from Z, J/ψ → ee, W→ ev data and MC):
- ❏ E-scale at m_Z known to ~ 0.3%
- ❏ Linearity better than 1% (few-100 GeV)
- ❏ "Uniformity" (constant term of resolution): ~ 1% (2.5% for 1.37<|η|<1.8)

Stability of EM calorimeter response vs time (and pile-up) **during full 2011 run better than 0.1%**

RMS: 0.054%
RMS: 0.052%

● W→en E/p
○ Z→ee inv. mass

Data 2011, √s=7 TeV, ∫ Ldt = 4.9 fb⁻¹

ATLAS Preliminary

Relative energy scale

Date (Day/Month)

1/N dN/dm$_{\gamma\gamma}$ / 0.5 GeV

- μ < 10
- 10 ≤ μ < 15
- 15 ≤ μ < 20
- 20 ≤ μ

ATLAS Simulation

gg → H → γγ
m_H = 125 GeV
√s = 8 TeV

m$_{\gamma\gamma}$ [GeV]
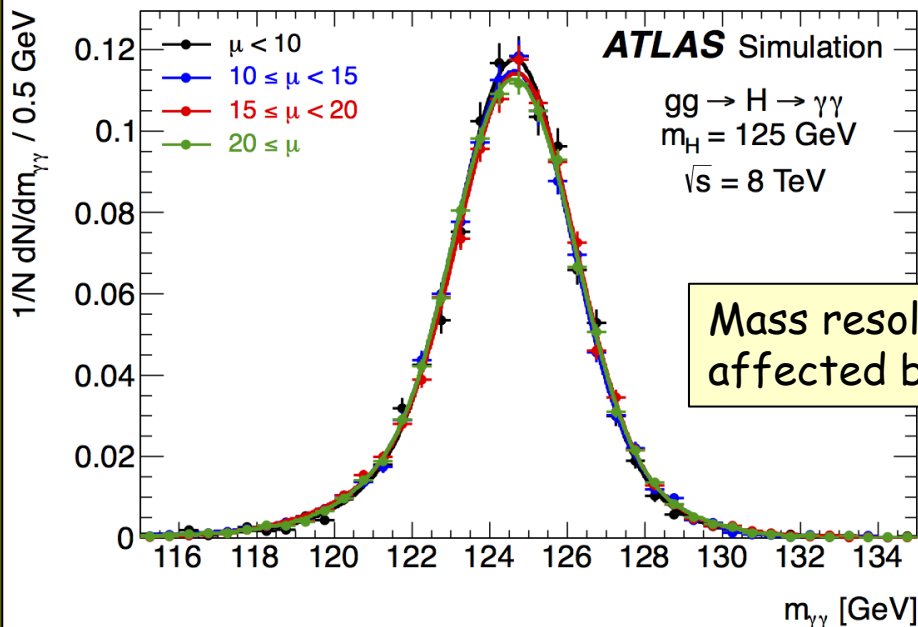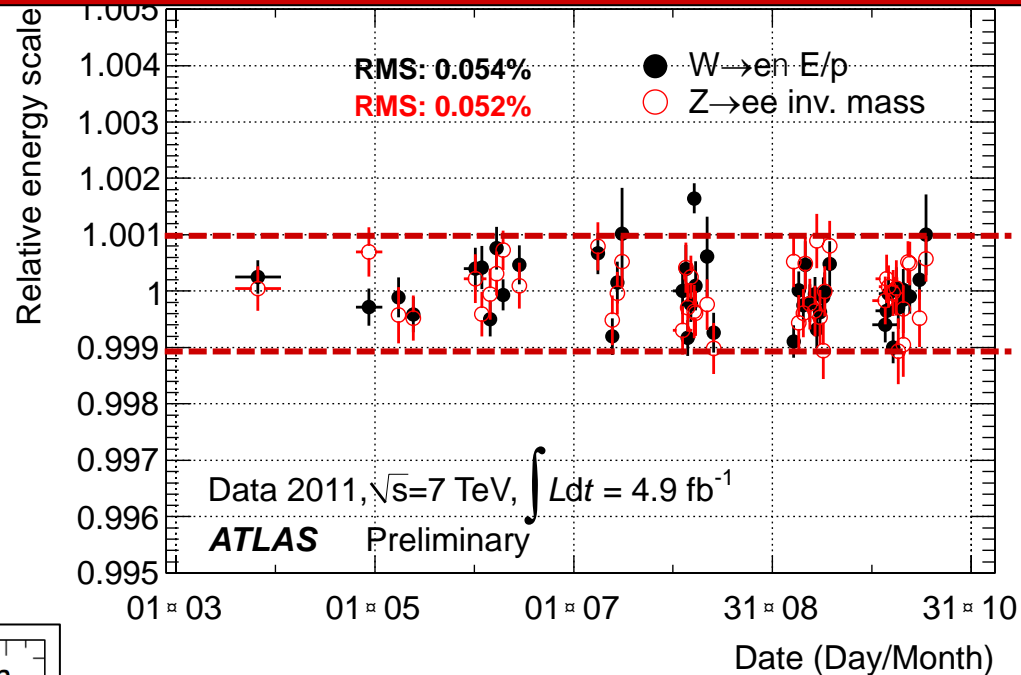
Mass resolution not affected by pile-up

Electron scale transported to photons using MC (small systematics from material effects)

Mass resolution of inclusive sample: 1.6 GeV
Fraction of events in ±2σ: ~90%
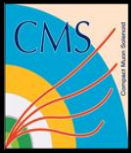
H → γγ
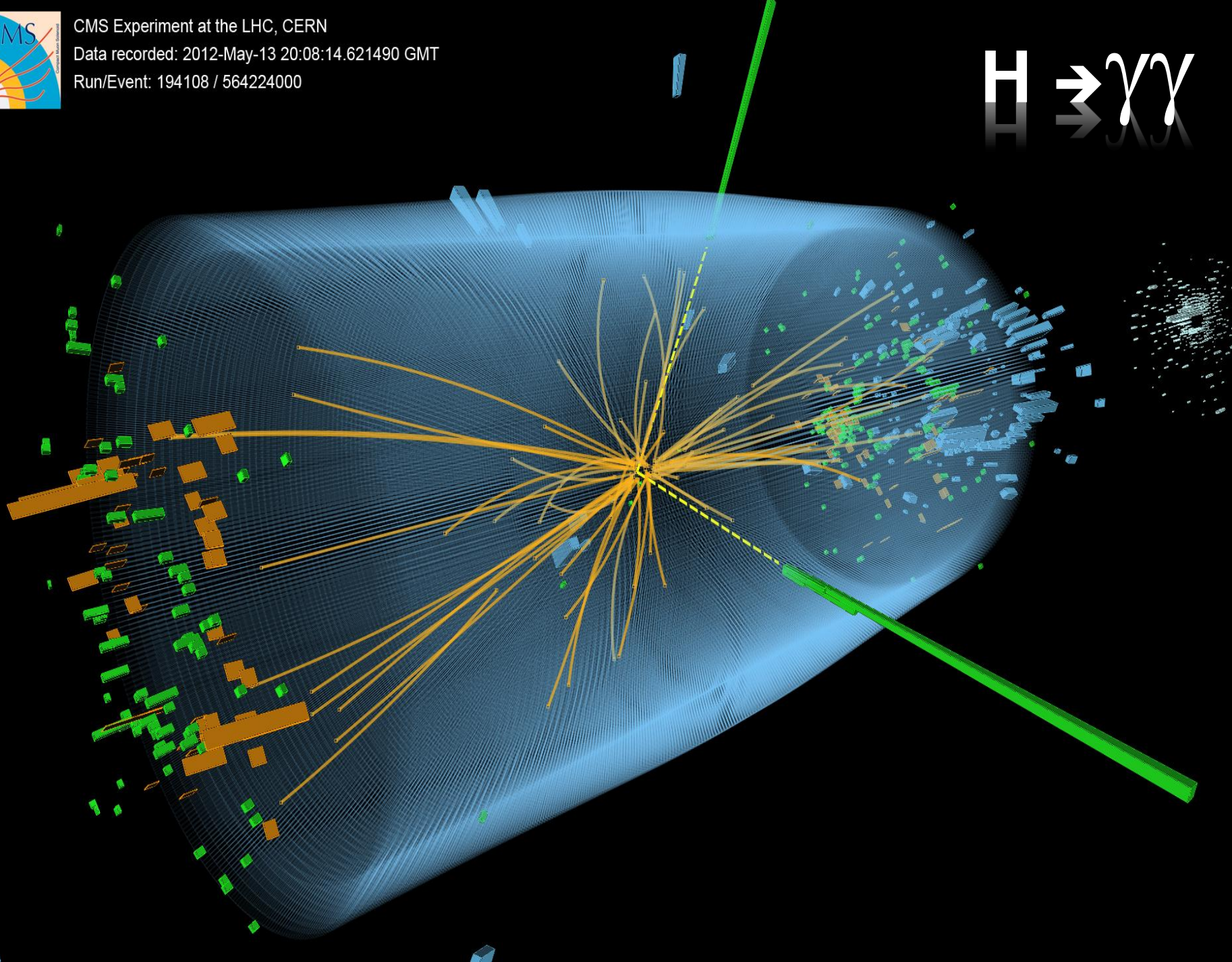
4e candidate with m_{4e} = 124.6 GeV

p_T (electrons)= 24.9, 53.9, 61.9, 17.8 GeV m_{12}= 70.6 GeV, m_{34}= 44.7 GeV
12 reconstructed vertices
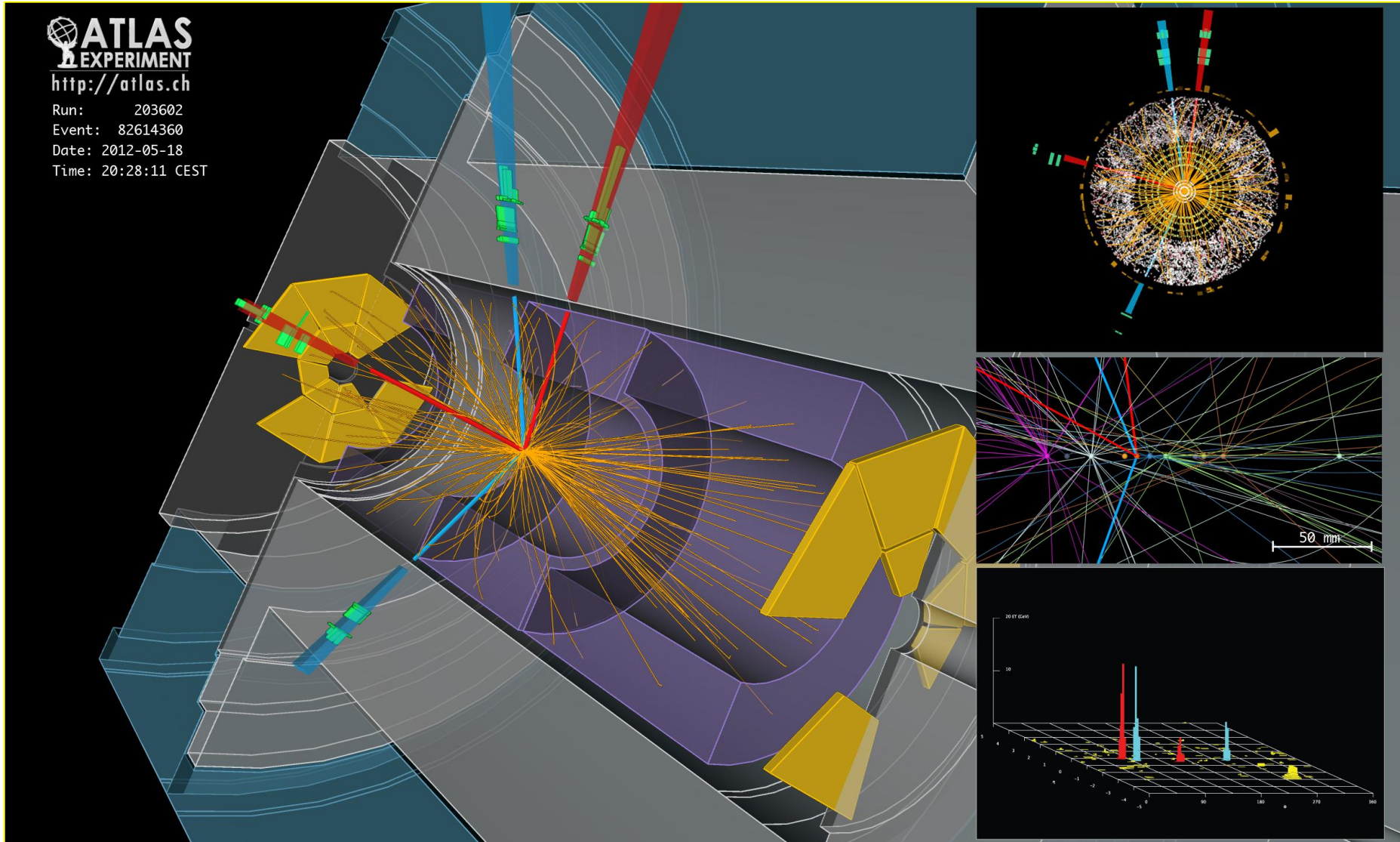
2e2μ candidate with $m_{2e2\mu}$ = 123.9 GeV

p_T (e,e,μ,μ)= 18.7, 76, 19.6, 7.9 GeV,   m(e⁺e⁻)= 87.9 GeV, m(μ⁺μ⁻) =19.6 GeV
12 reconstructed vertices
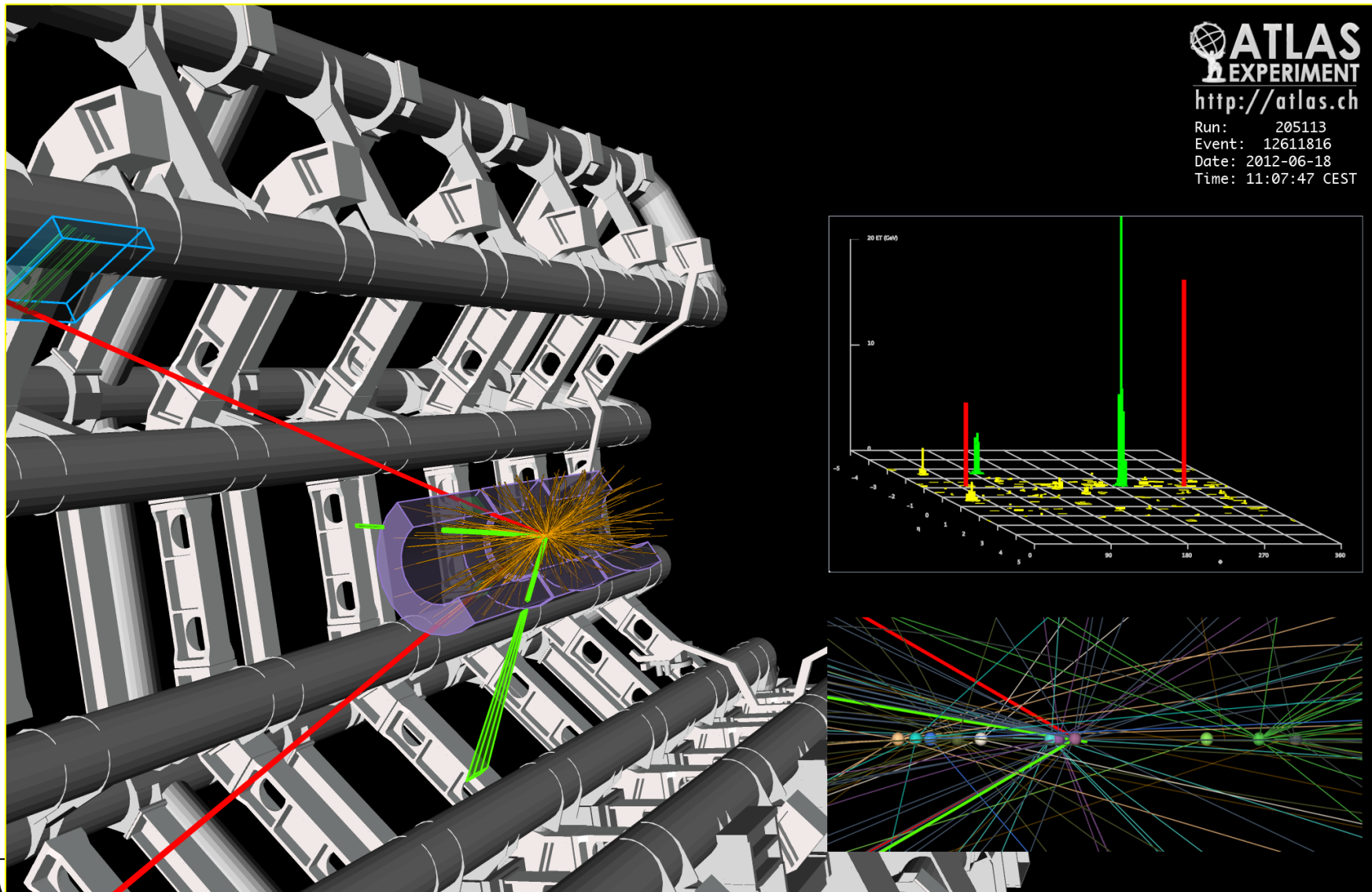
Nuclear Interactions

The interaction of energetic hadrons (charged or neutral) with matter is dominated by inelastic nuclear processes.

→ **Excitation and breakup of the nucleus**
  → **Nucleus fragments**
  → **Production of secondary particles:**
     Charged hadrons: $\pi^\pm$, p, …
     Neutral hadrons: n, π^0, …
     Charged leptons: $\mu^\pm$, …
     Neutral leptons: ν
     Low energy γ, etc…
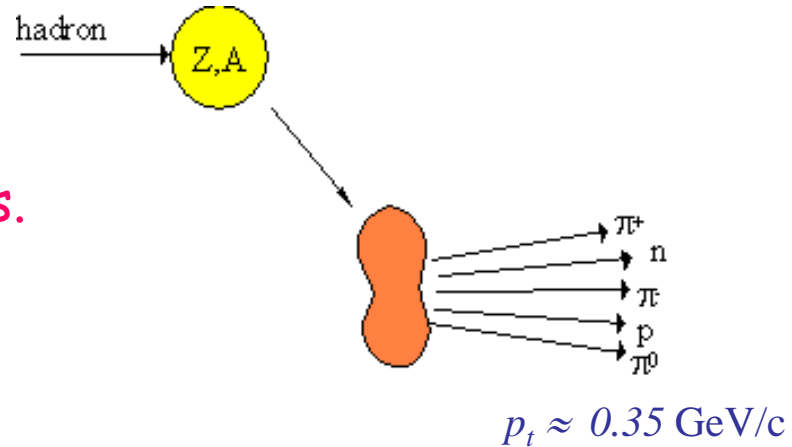
$p_t \approx 0.35$ GeV/c

Hadrons create showers via strong interactions just like electrons and photons create them via E.M.

E. M. component

hadronic component
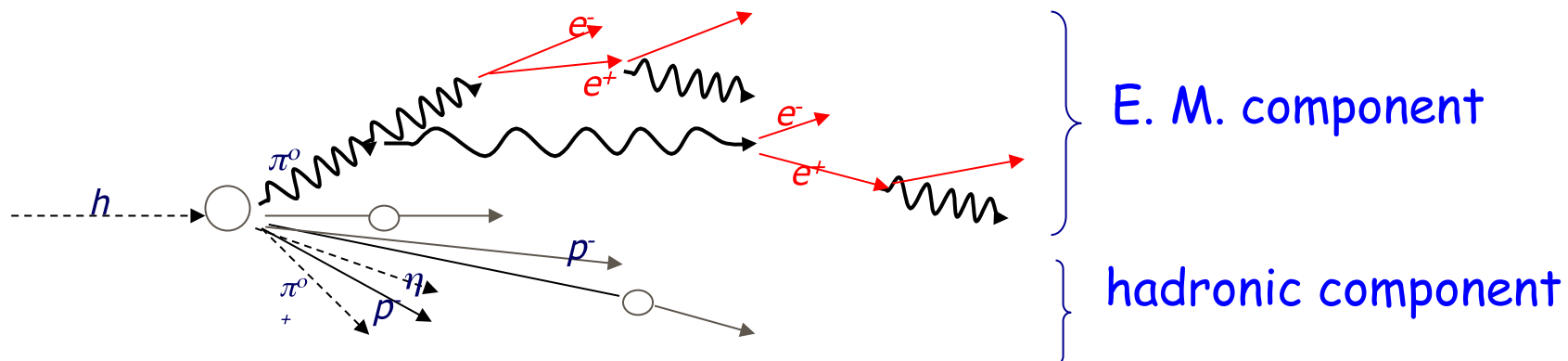
Hadronic showers

→ Process similar to EM shower:

    → Secondary particles interact and produces:
    → tertiary particles
    → tertiary particles interact and produces
    → …… (and so forth)

→ However, processes involved are much more complex

    → Many more particles produced
    → Multiplicity ~ log(E) (E = energy of the primary hadron)

→ Shower ceases when hadron energies are small enough for energy loss by ionization or to be absorbed in a nuclear process.

→ The secondary particles are produced with large transverse momentum

→ Consequently, hadronic showers spread more laterally than EM showers.

→ Only (about) half of the primary hadron energy is passed on to fast secondary particles

→ The other half is consumed in production of slow pions and other process:

    → Nuclear excitation
    → Nucleon spallation → slow neutrons
    → etc..
    → Great part of this energy is "lost" : binding energy of the nucleus, production of neutrinos, etc
    → Part can be recovered: slow neutrons can interact with H atoms in active material like scintillator
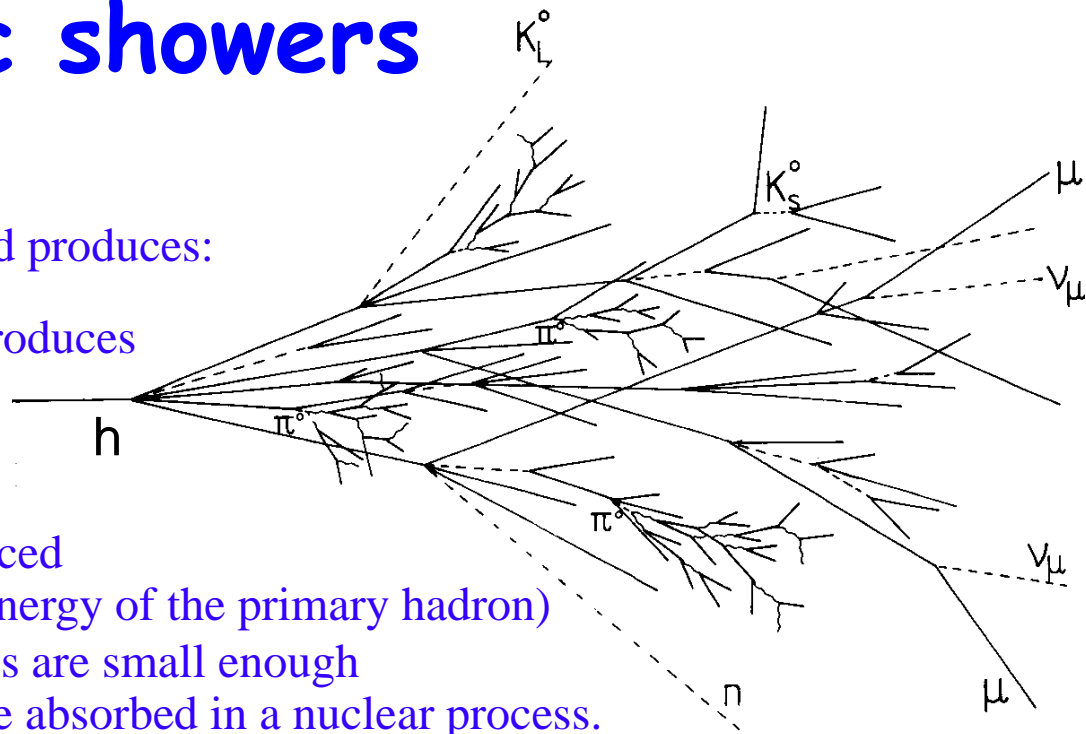
For example, in lead (Pb):
Nuclear break-up (invisible) energy: 42%
Ionization energy: 43%
Slow neutrons (E_K ~ 1 MeV): 12%
Low energy γ's (E_γ ~ 1 MeV): 3%

Hadronic showers
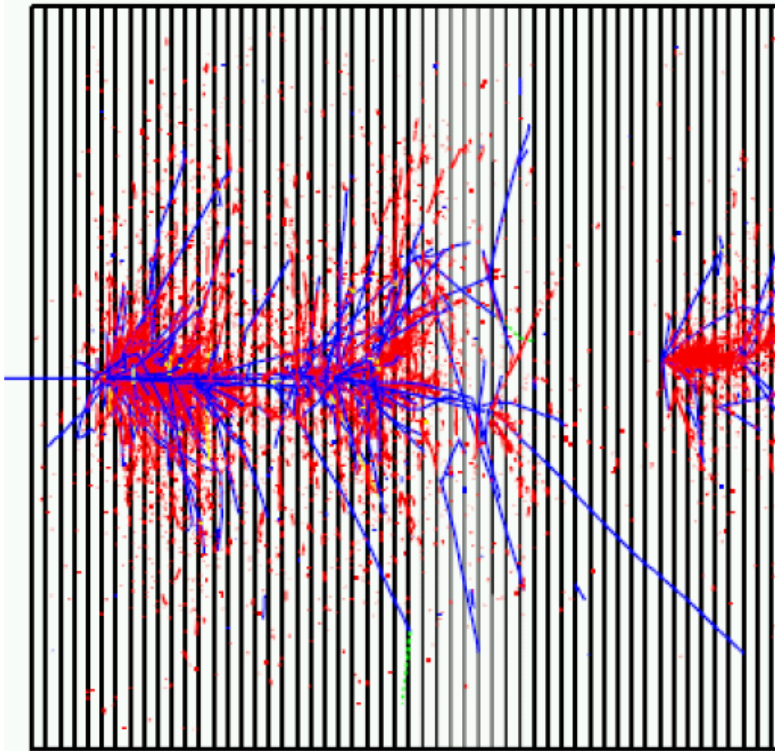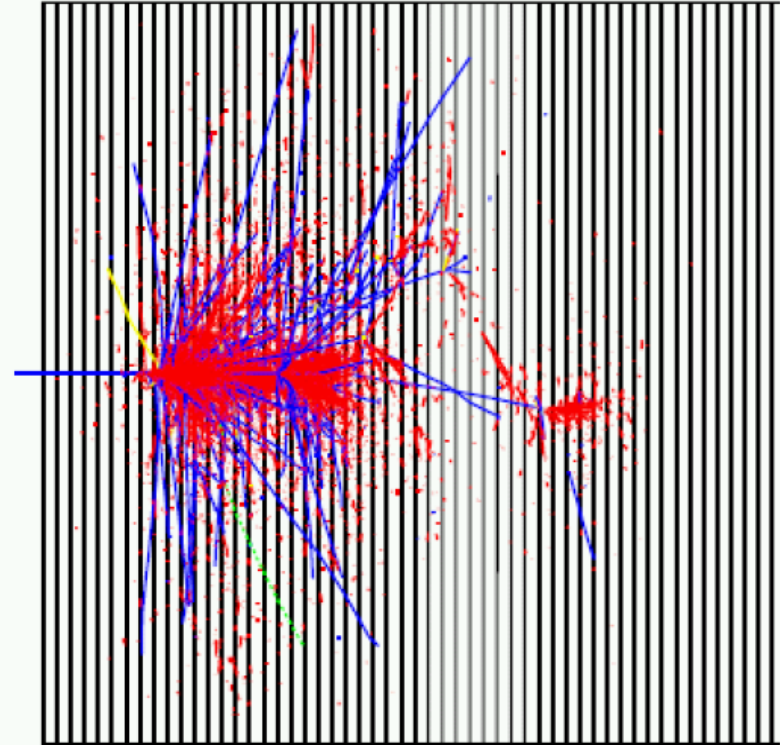
RED – e. m. component   BLUE – charged hadron

Unlike electromagnetic showers, hadron showers do not show a uniform deposition of energy throughout the detector medium

Shower development determined by the mean free path, λ_I, between inelastic collisions The nuclear interaction length is given by $\lambda_I = A / (N_A \cdot \sigma_{inel})$,

Simple model, expect $\sigma_I \propto A^{2/3}$ and thus $\bot_I \propto A^{1/3}$. In practice $\bot_I \sim 35\ A^{1/3}$

Hadronic Calorimeter (HCAL)

→ Hadronic calorimeters are usually sampling calorimeters

→ The active medium made of similar material as in EM calorimeters:

    → Scintillator (light), gas (ionization chambers, wired chambers), silicon (solid state detectors), etc
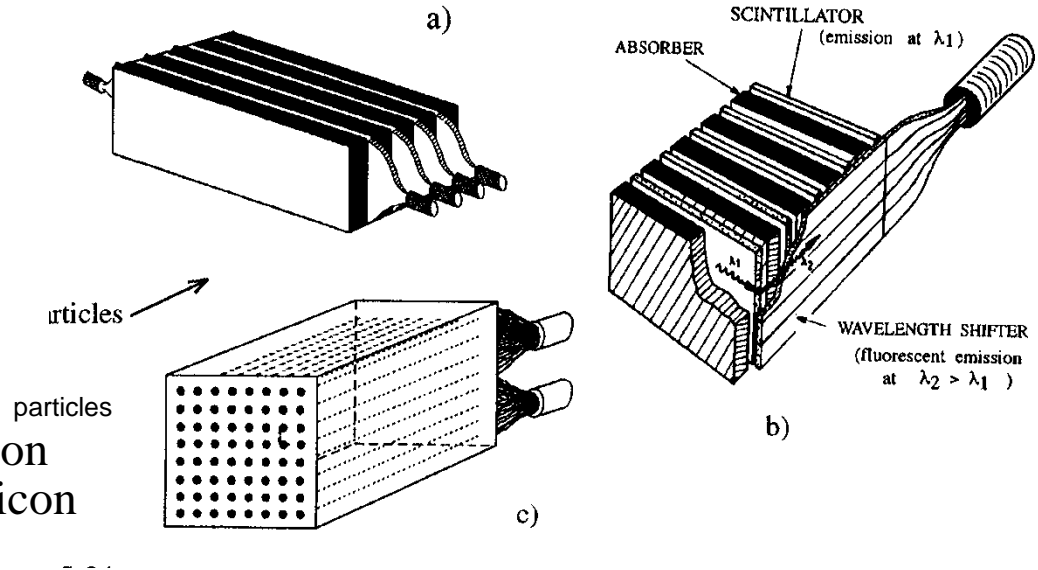
→ The passive medium is made of materials with longer interaction length λ_I

    → Iron, uranium, etc

→ Resolution is worse than in EM calorimeters (discussion in the next slides), usually in the range:

$$\frac{\sigma(E)}{E} \propto \frac{(35\% - 80\%)}{\sqrt{E}}$$

Can be even worse depending on the goals of an experiment and compromise with other detector parameters

→ Response of calorimeters is usually higher for electromagnetic (e) than hadronic (h) energy deposit → e/h>1 → non linearity: try to compensate!

ATLAS Hadronic Tiles calorimeter

Ext. Barrel

P

Barrel

PMT

Fibra WLS

Double readout

Scintillatore

h
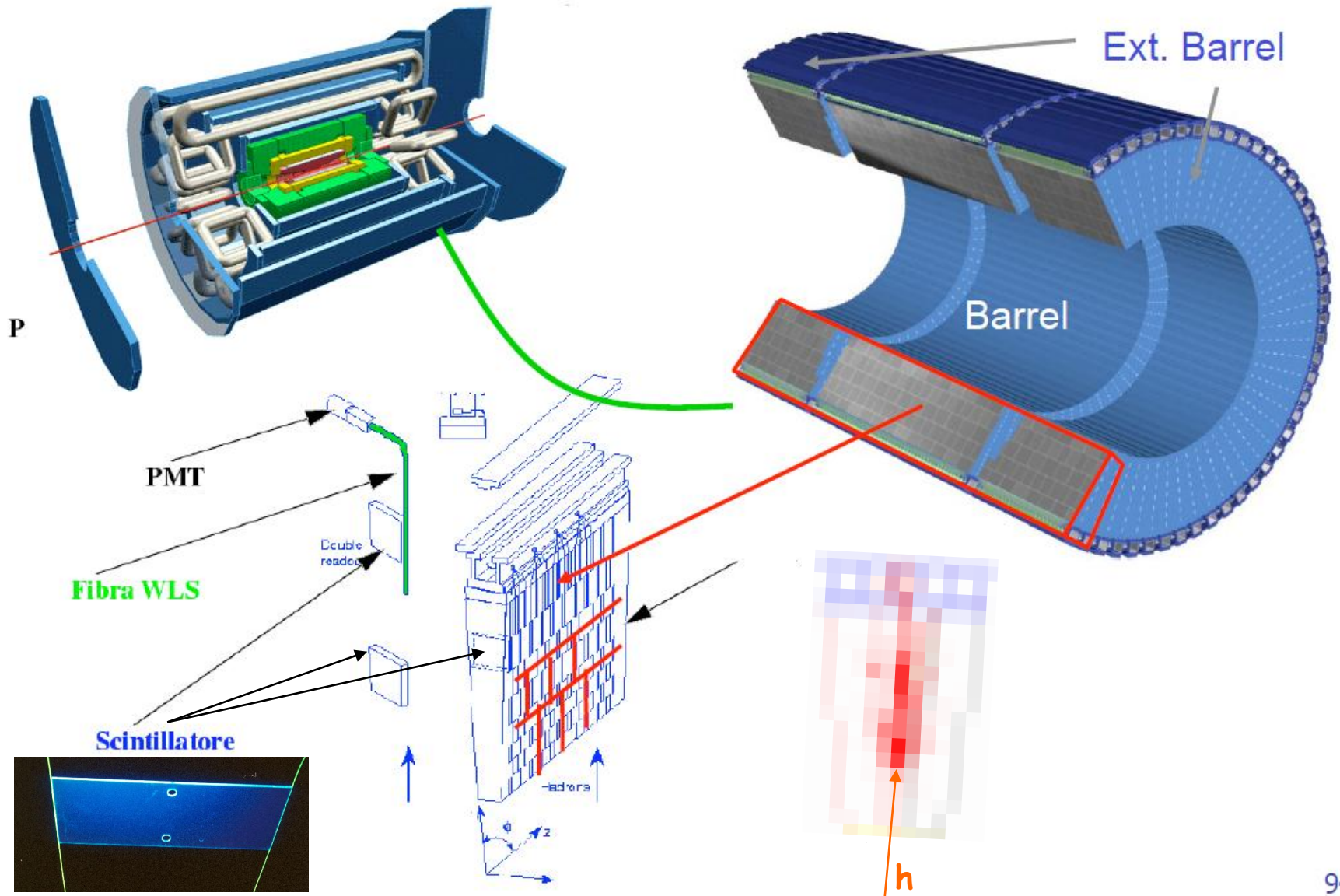
ATLAS tile calorimeter

ATLAS tile calorimeter

ATLAS

14mm iron/3mm scintillator,
WLS optical fibres, PMT readout

The CMS hadron calorimeter HCAL

CMS
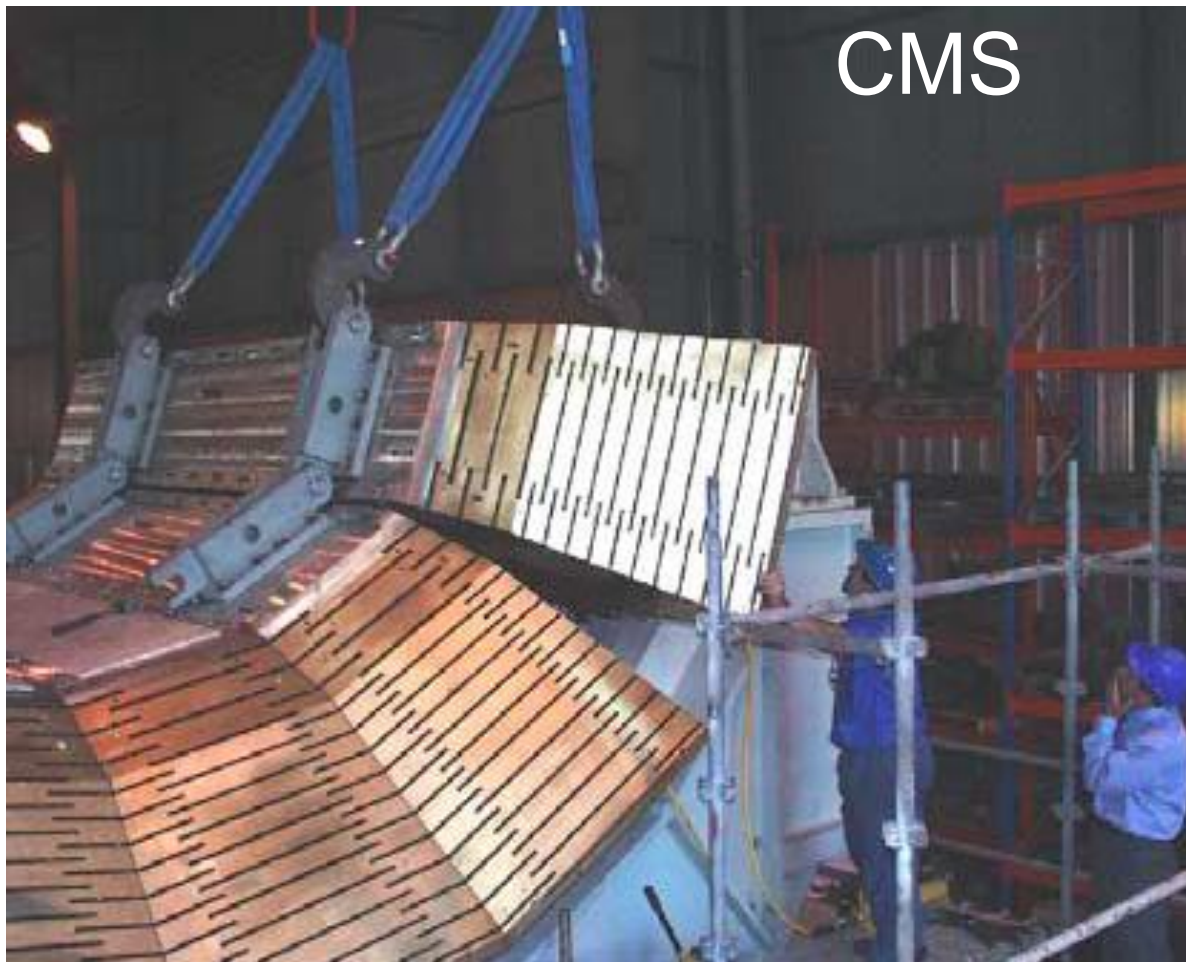
50mm brass/3.7mm scintillator, embedded WLS fibres, HPD readout
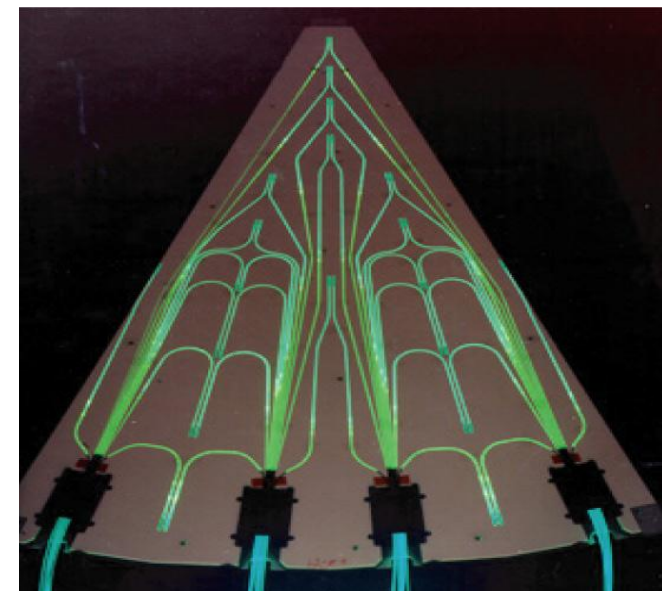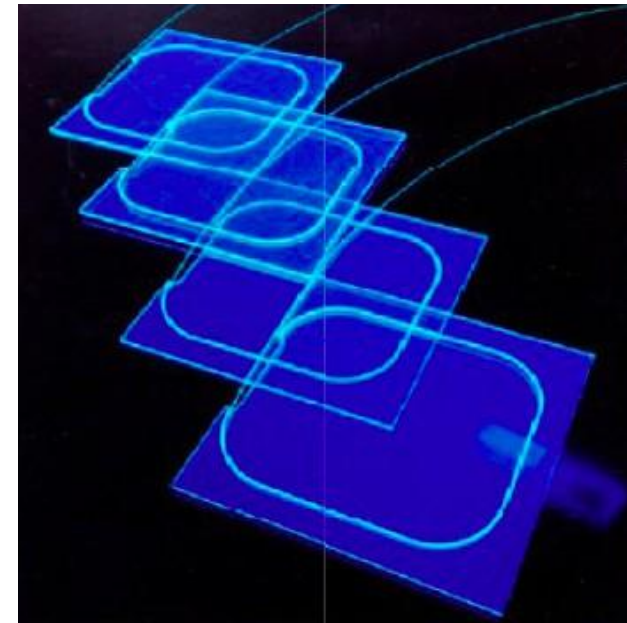
HB+ insertion complete on 3 April

Rino Castaldi   **Apparati Sperimentali – I semestre 2006**
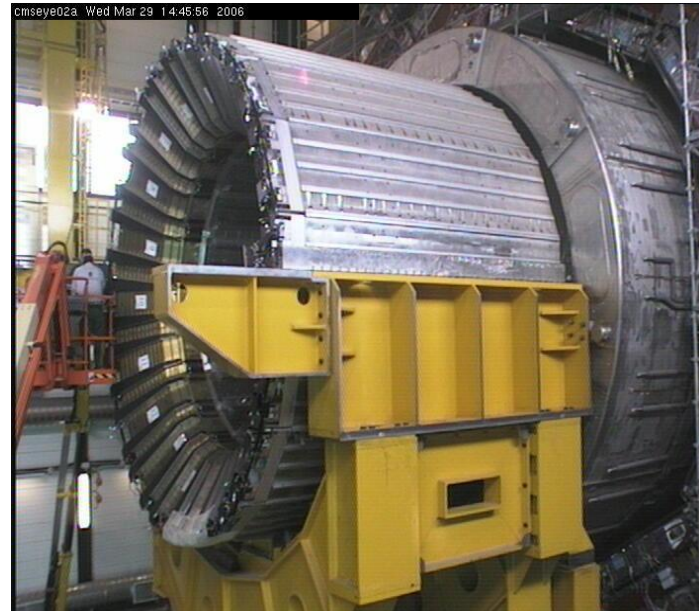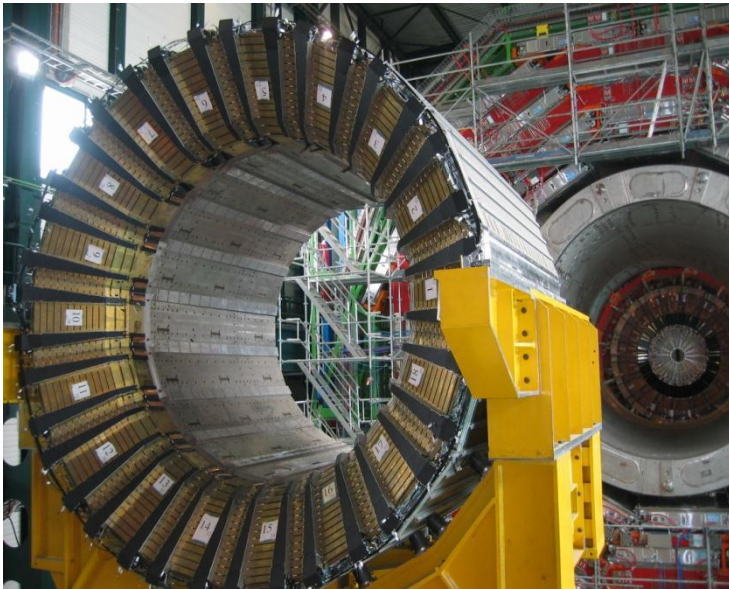
Hadronic Calorimeter (HCAL)

→ CMS hadron calorimeter

    → 16 scintillator 3.7 mm thick plates (active material) Interleaved with 50 mm thick plates of brass

    → Energy resolution:

$$\frac{\sigma(E)}{E} \propto \frac{(120\%)}{\sqrt{E}} \oplus 5\%$$

Hadronic energy resolution compromised in favor of a much higher EM energy resolution

Relative Energy Res.

- π interacting in HCAL only

π interacting in ECAL or HCAL

- ■ no weighting
- ○ passive weighting
- □ dynamic weighting

CMS TB '04

$$\frac{\sigma(E)}{E} = \frac{120\%}{\sqrt{E}} \oplus 5\%$$

pion beam momentum (GeV)

The HCAL being inserted into the solenoid

http://www.flickr.com/photos/naezmi/365114338/

125
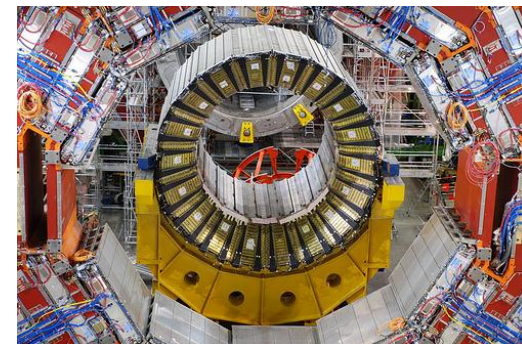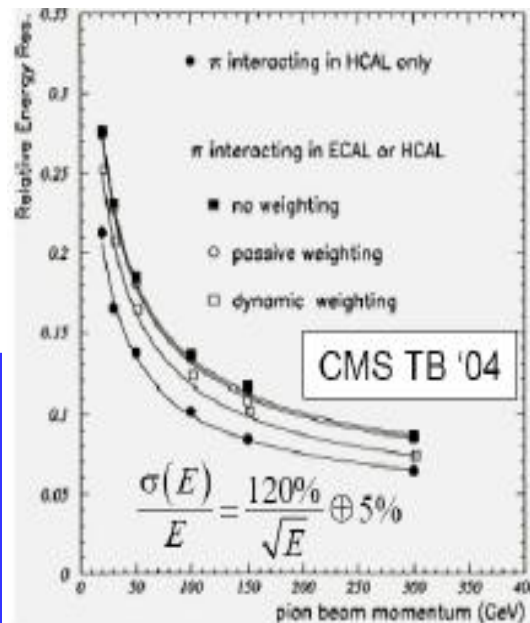
Typical detector concept

- **Combine different detector types/technologies into one large detector system**

Key:
- Muon
- Electron
- Charged Hadron (e.g. Pion)
- Neutral Hadron (e.g. Neutron)
- Photon

Transverse slice through CMS

4T

Silicon Tracker

Electromagnetic Calorimeter

Hadron Calorimeter

Superconducting Solenoid

2T

Muon Chambers

0m 1m 2m 3m 4m 5m 6m 7m
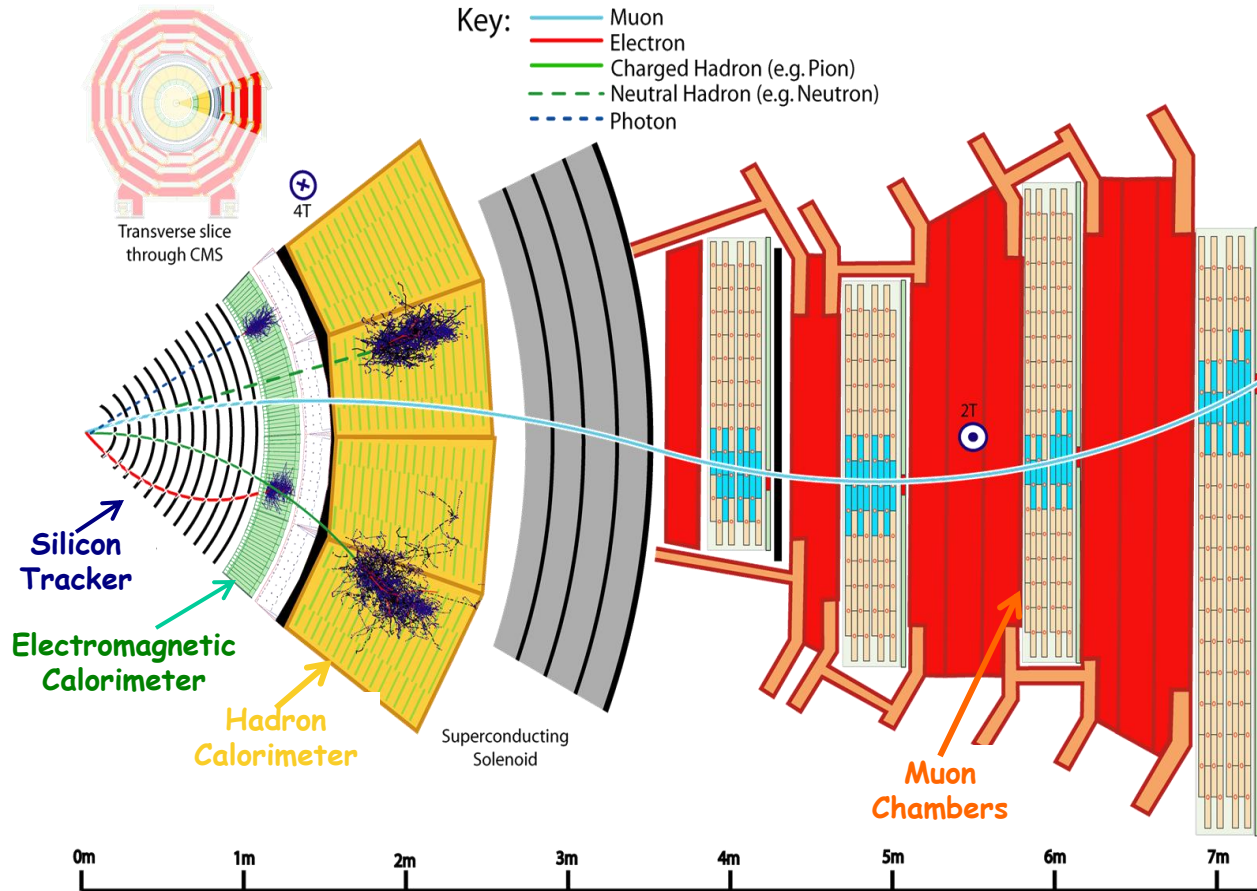
❑ Electrons ionize and show bremsstrahlung due to the small mass
❑ Muons ionize and bremsstrahlung is less important
❑ Photons do no ionize but undergo pair production in high Z material
❑ Charge hadrons ionize and produce hadron shower in dense material
❑ Neutral hadron do not ionize but produce hadron shower in dense material

Transverse slice of ATLAS
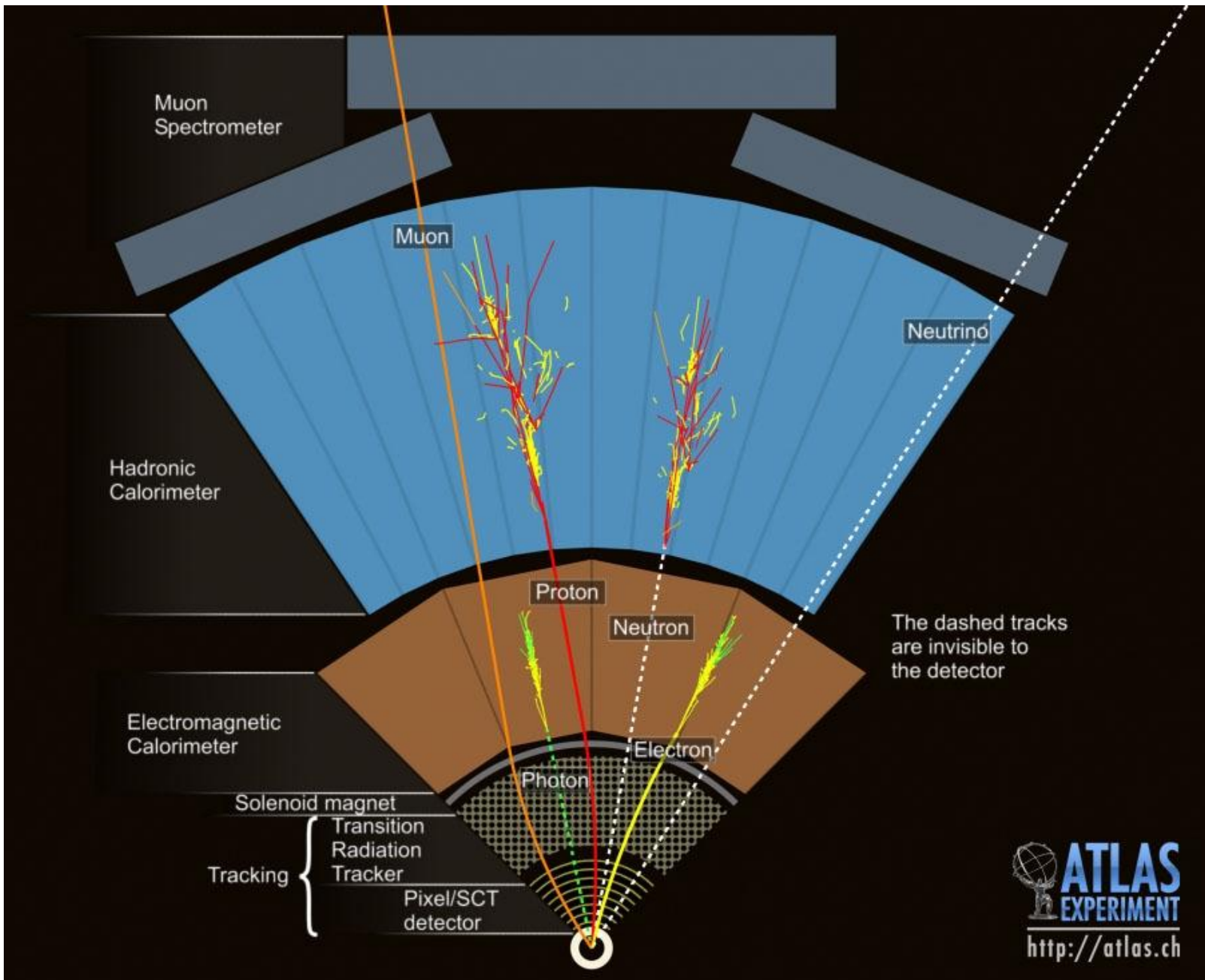
Macchina fotografica digitale di 12500 tonnellate con migliaia di milioni di pixels capace di scattare una foto tridimensionale delle collisioni protone-protone a 14 TeV di LHC 40 milioni di volte al secondo.
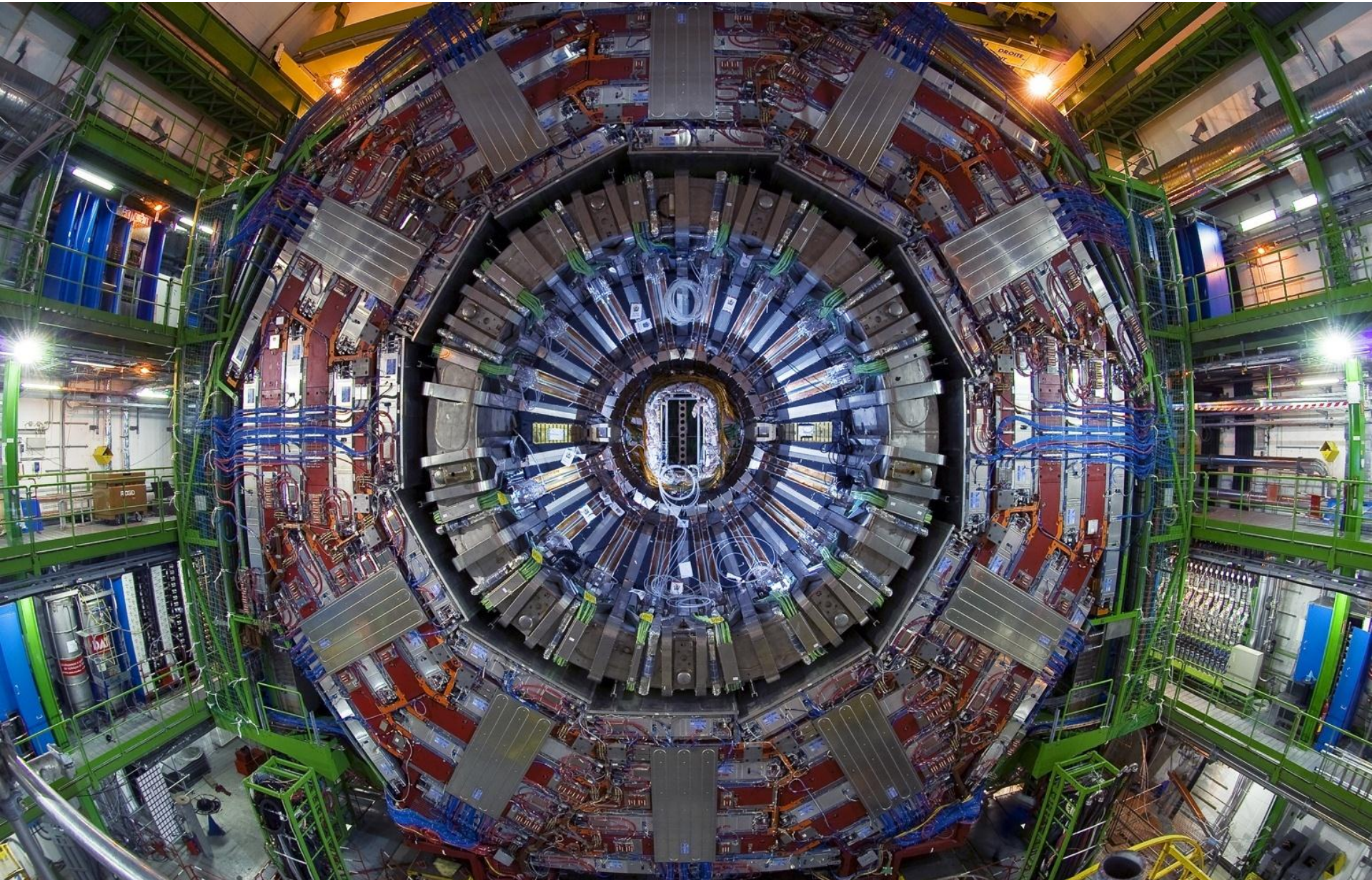
CMS Experiment at LHC, CERN
Data recorded: Mon May 28 01:35:47 2012 CEST
Run/Event: 195099 / 137440354
Lumi section: 115

$\mu^+(Z_1)$ p_T : 43 GeV

$e^-(Z_2)$ p_T : 10 GeV

4-lepton Mass : 126.9 GeV

$e^+(Z_2)$ p_T : 21 GeV

$\mu^-(Z_1)$ p_T : 24 GeV
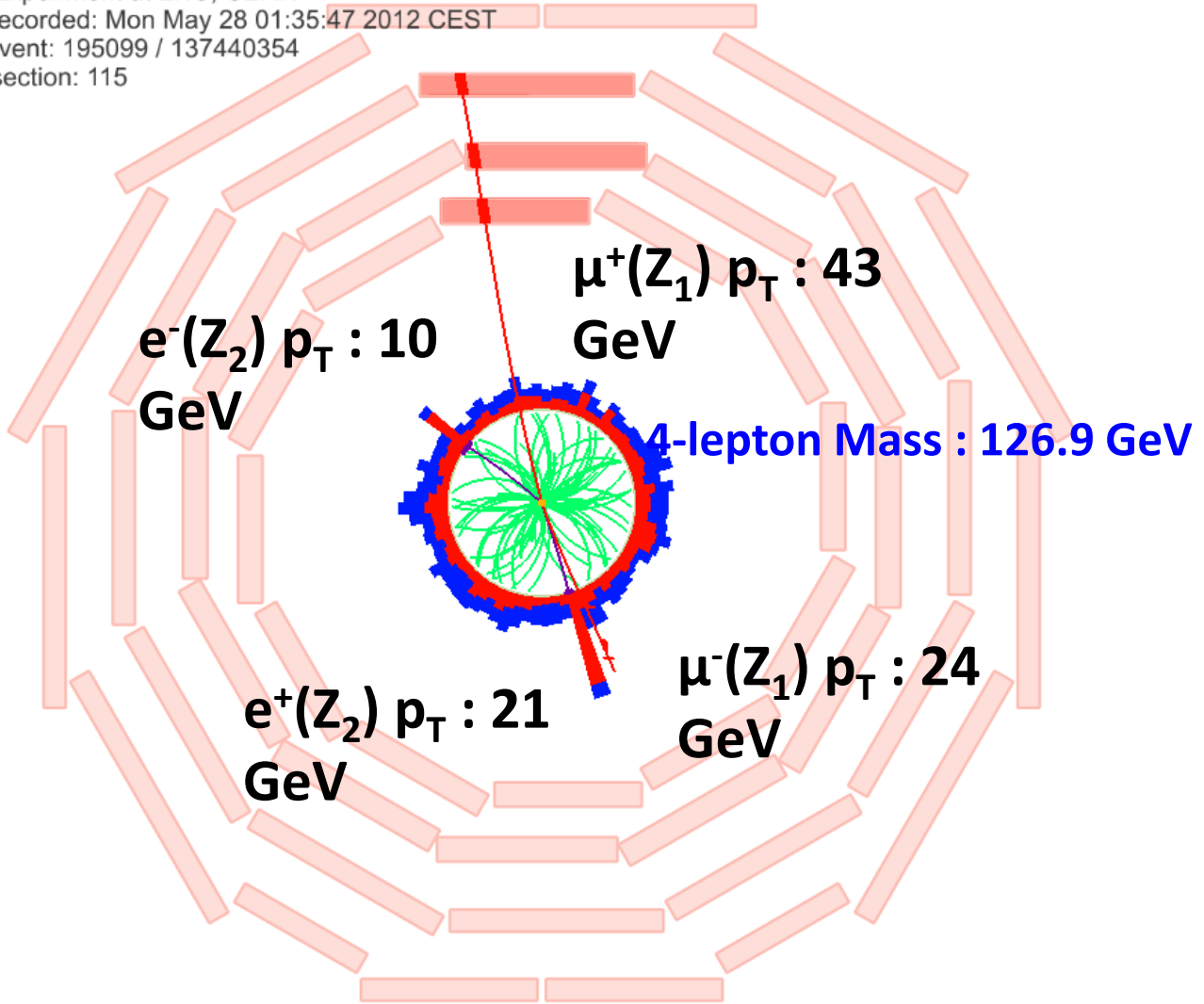
CMS Experiment at LHC, CERN
Data recorded: Mon May 28 01:35:47 2012 CEST
Run/Event: 195099 / 137440354
Lumi section: 115

$\mu^+(Z_1)$ p_T : 43 GeV

$e^-(Z_2)$ p_T : 10 GeV

4-lepton Mass : 126.9 GeV

$\mu^-(Z_1)$ p_T : 24 GeV

$e^+(Z_2)$ p_T : 21 GeV
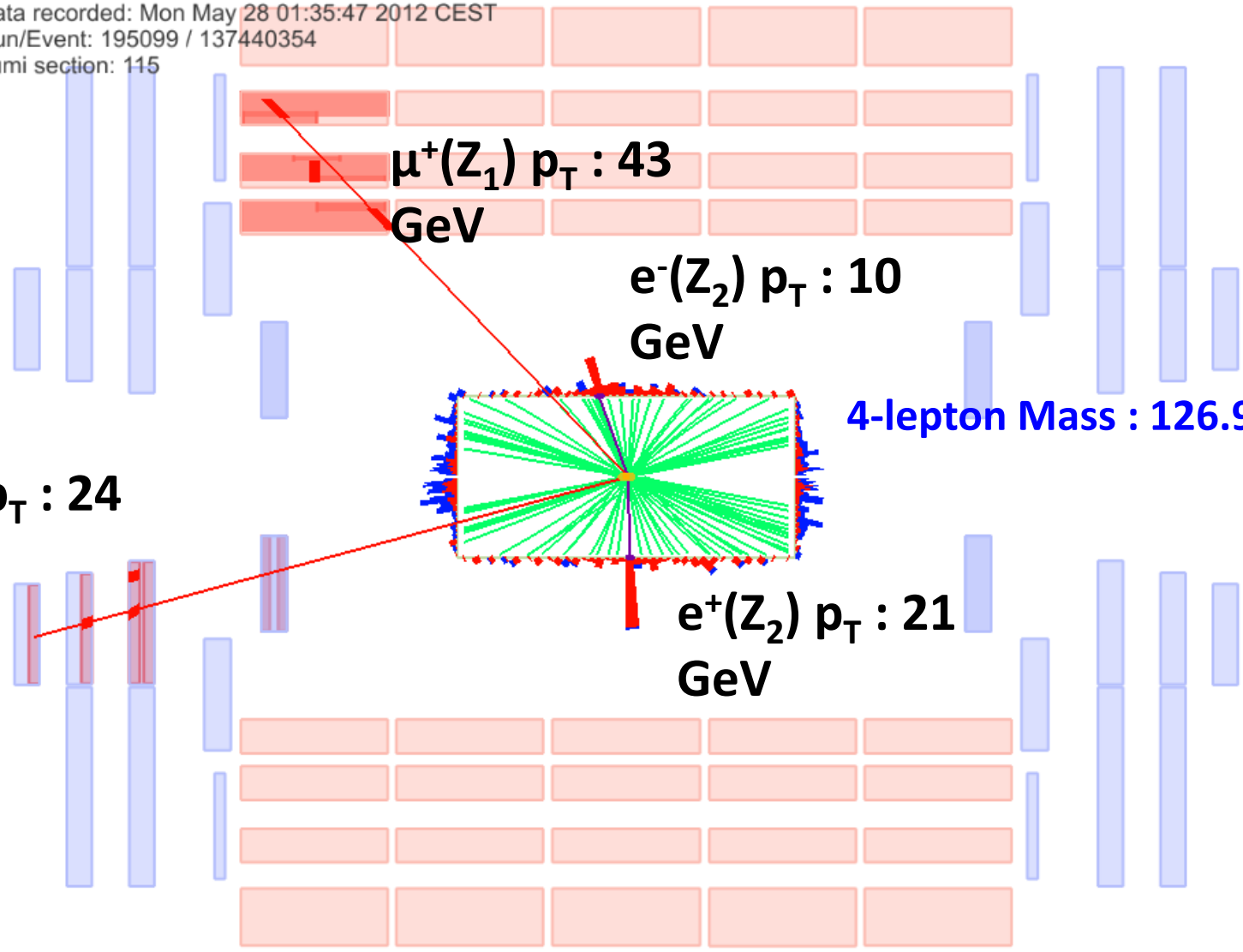
μ$^+$(Z$_1$) p$_T$: 43 GeV

e$^-$(Z$_2$) p$_T$: 10 GeV

8 TeV DATA

4-lepton Mass : 126.9 GeV
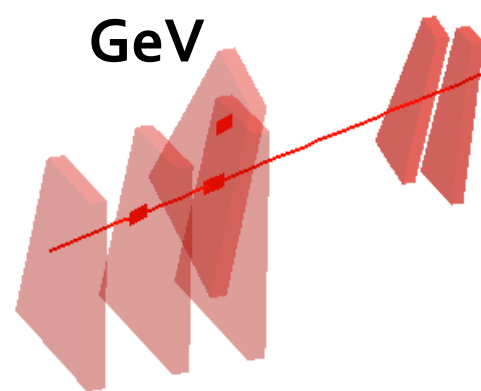
μ$^-$(Z$_1$) p$_T$: 24 GeV
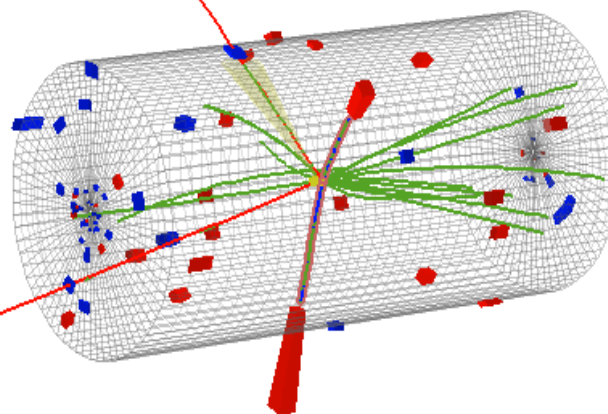
e$^+$(Z$_2$) p$_T$: 21 GeV

CMS Experiment at LHC, CERN
Data recorded: Mon May 28 01:35:47 2012 CEST
Run/Event: 195099 / 137440354
Lumi section: 115

2e2μ candidate with $m_{2e2\mu}$ = 123.9 GeV
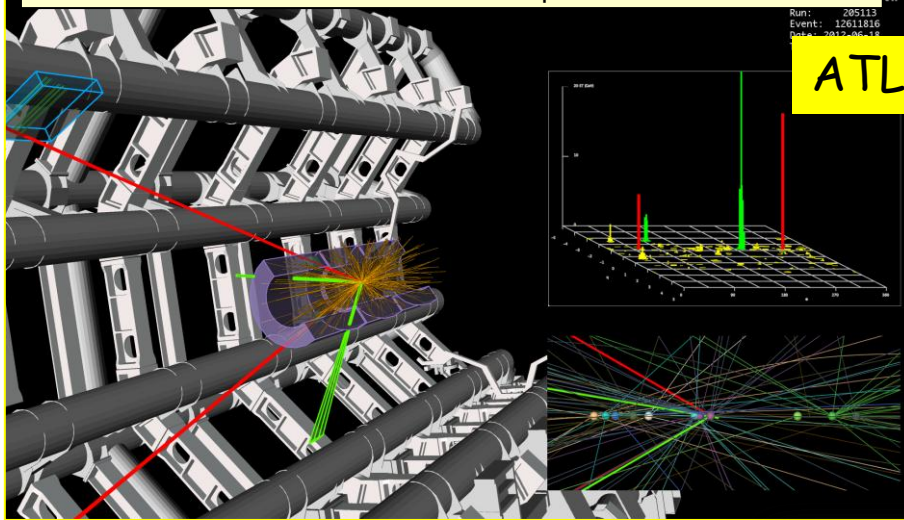
H → ZZ$^{(*)}$ → 4l (4e, 4μ, 2e2μ)
σ × BR ~ 2.5 fb m_H ~ 126 GeV

ATLAS

In the region 125 ± 5 GeV

Dataset	2011	2012	2011+2012
Expected B only	2±0.3	3±0.4	5.1±0.8
Expected S m_H=125 GeV	2±0.3	3±0.5	5.3±0.8
Observed in the data	4	9	13

2011+ 2012	4μ	2e2μ	4e
Data	6	5	2
Expected S/B	1.6	1	0.5
Reducible/total background	5%	45%	55%

H → γγ
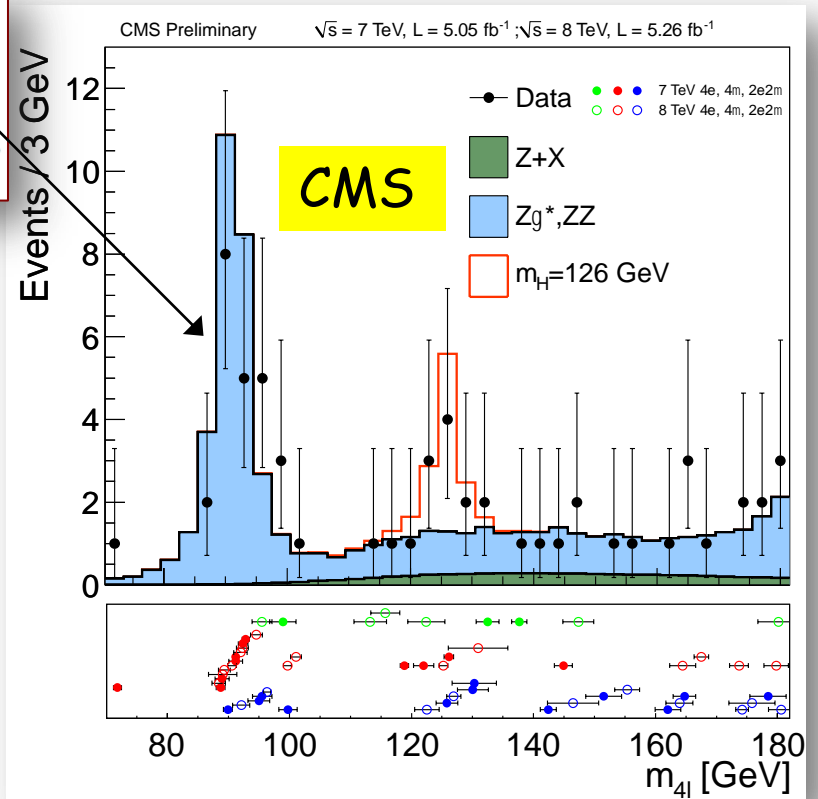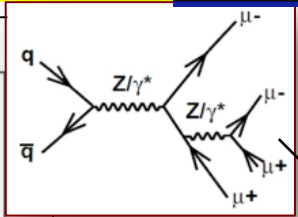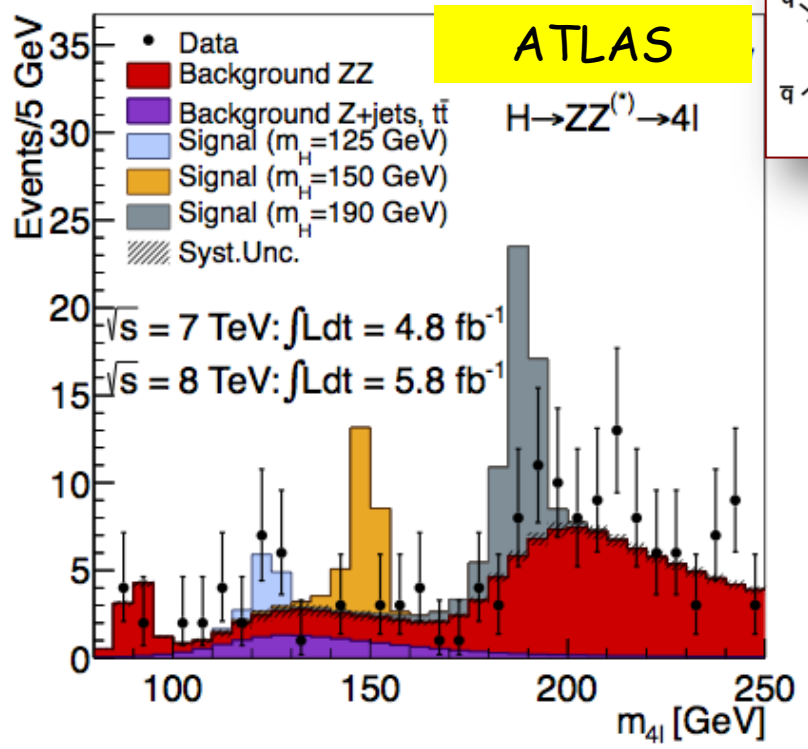
σ x BR ~ 50 fb m_H ~ 126 GeV

- ❑ Simple topology: two high-p_T isolated photons $E_T (\gamma_1, \gamma_2)$ > 40, 30 GeV
- ❑ Main background: γγ continuum (irreducible, smooth, ..)

ATLAS: after all selections, expect (10.7 fb^{-1}, m_H~ 126 GeV)
~ 170 signal events (total signal efficiency ~ 40%)
~ 6340 background events in mass window
→ S/B ~ 3% inclusive (~ 20% 2jet category)

H →γγ candidate

ATLAS

Selected diphoton sample
- Data 2011 and 2012
- Sig + Bkg inclusive fit (m_H = 126.5 GeV)
- 4th order polynomial

$\sqrt{s}$ = 7 TeV, $\int Ldt$ = 4.8 fb^{-1}
$\sqrt{s}$ = 8 TeV, $\int Ldt$ = 5.9 fb^{-1}

CMS

CMS Preliminary
$\sqrt{s}$ = 7 TeV, L = 5.1 fb^{-1}
$\sqrt{s}$ = 8 TeV, L = 5.3 fb^{-1}

- S/B Weighted Data
- S+B Fit
- Bkg Fit Component
- ±1 σ
- ±2 σ
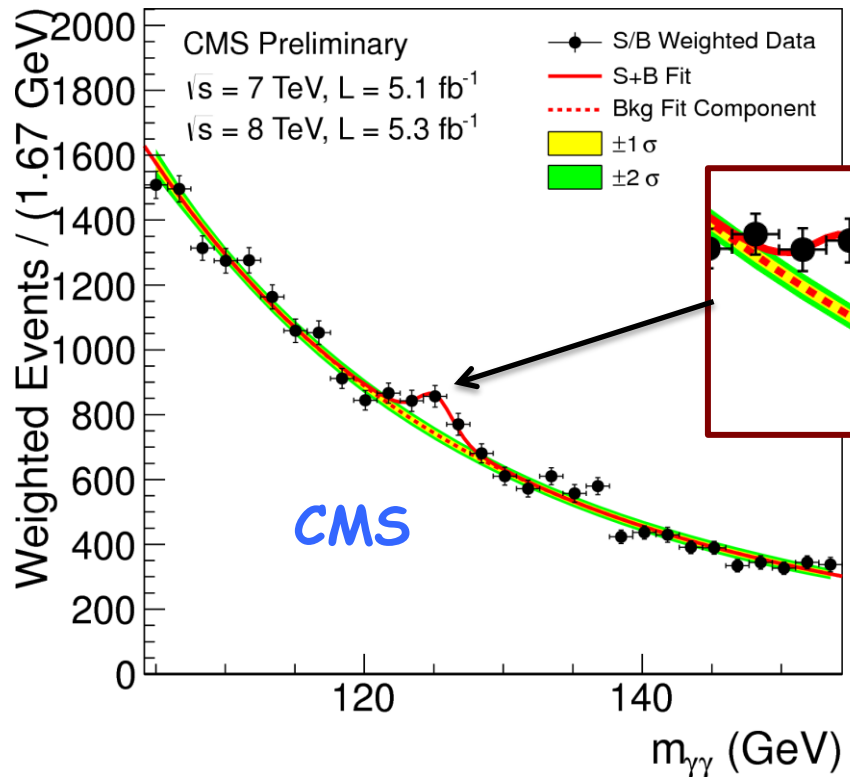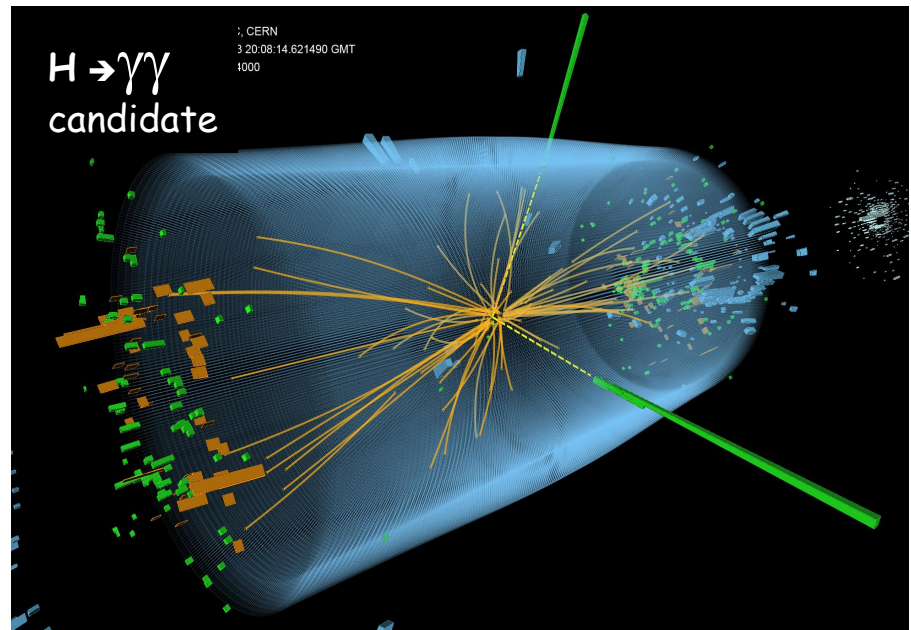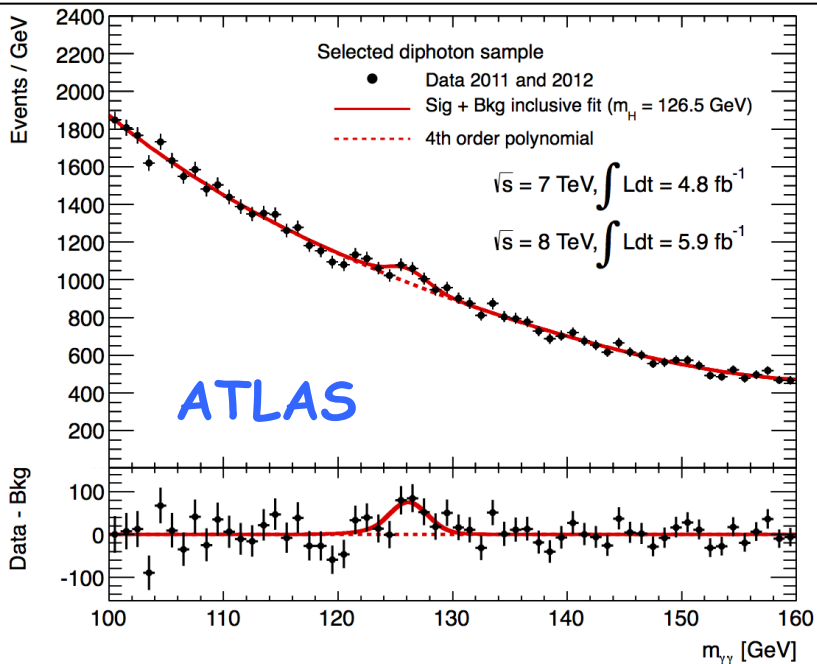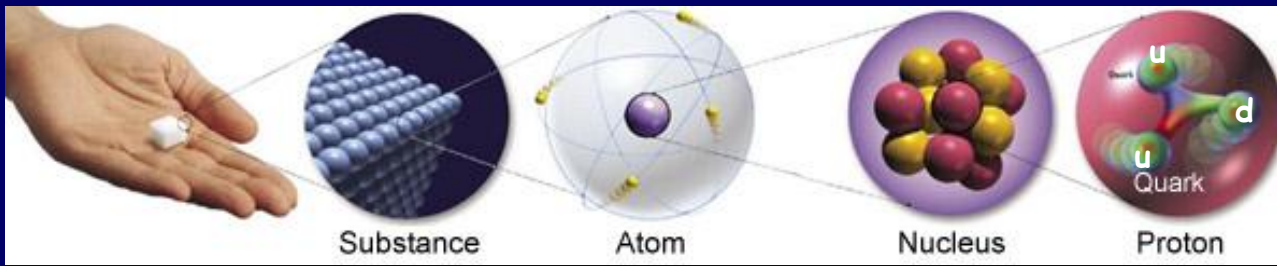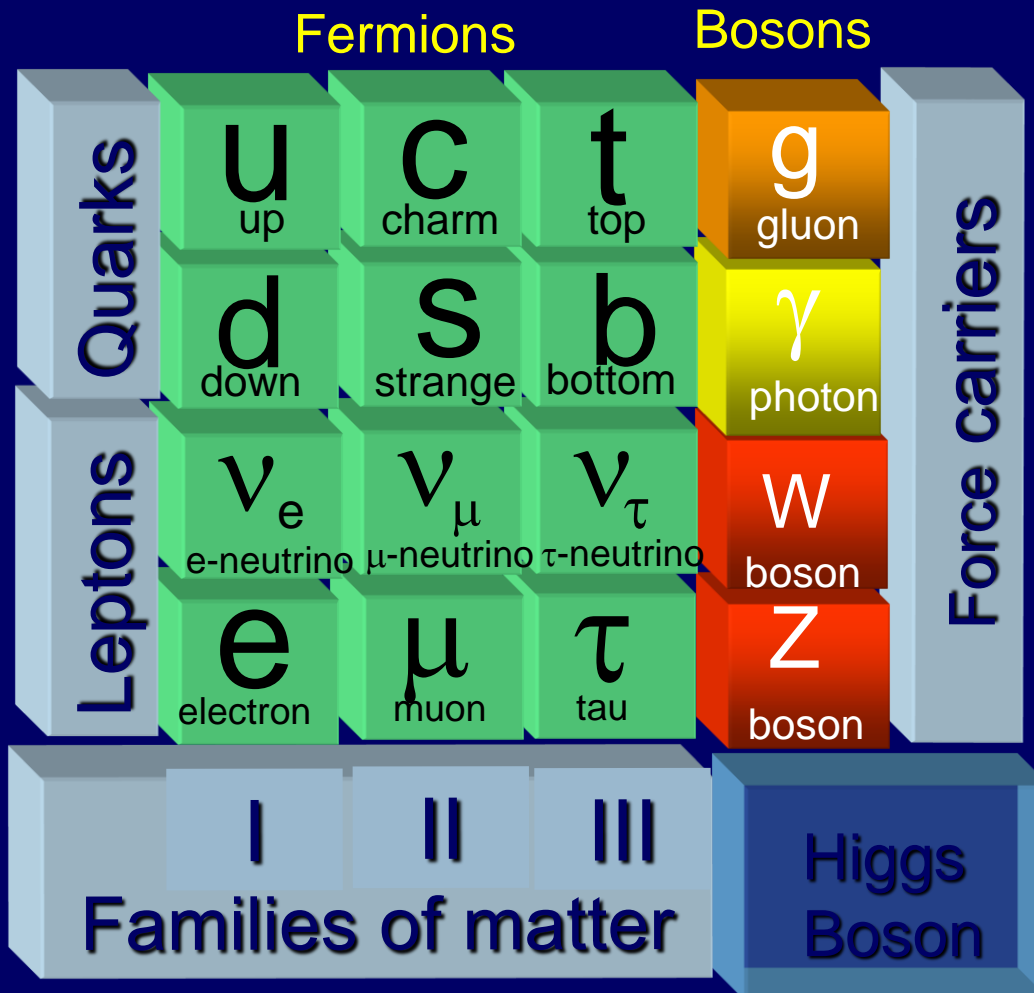
Backup slides

Several drawings of this presentation have been borrowed (sometimes with small changes only for the sake of my presentation) from very good lectures that can be found in the Web.

See for instance:

W. Riegler; Summer Student Lectures 2009
M. Krammer; XI ICFA School on Instrumentation

Why use higher and higher energies?
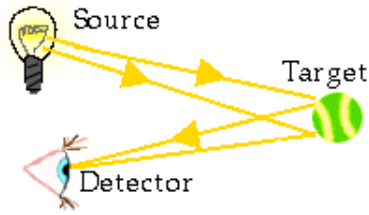
$$\lambda = h/p$$
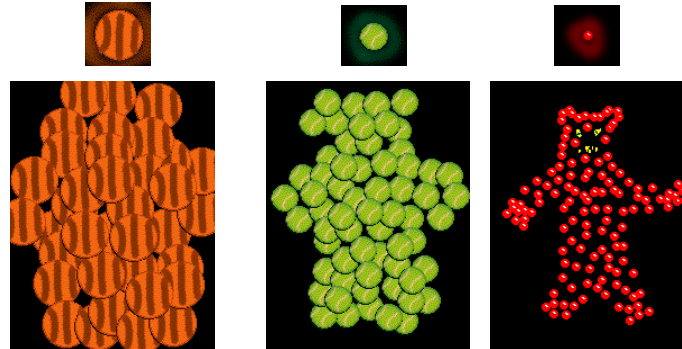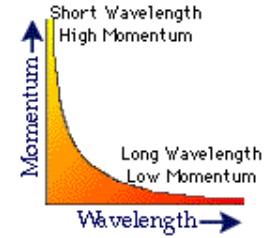
∴ **The more energetic the probe, the finer the accessible detail**
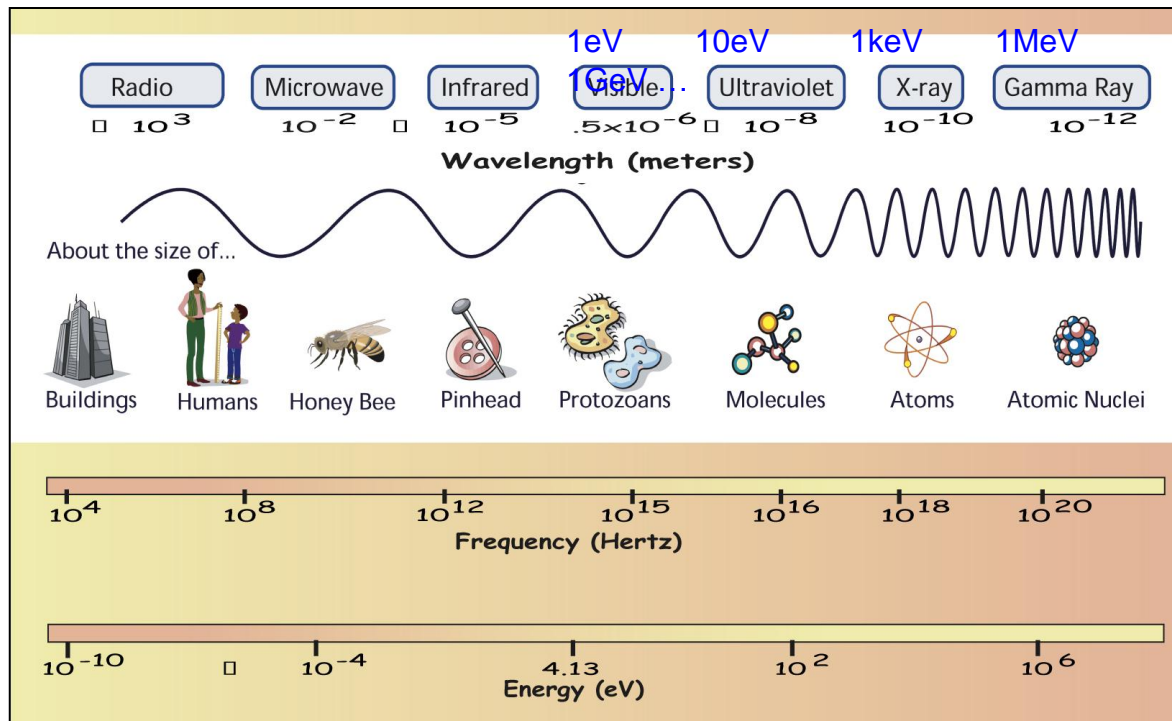
1 keV = 10^3 eV
1 MeV = 10^6 eV
1 GeV = 10^9 eV
1 TeV = 10^{12} eV
1 PeV = 10^{15} eV
1 EeV = 10^{18} eV

Why do we need accelerators?

✳ Resolution of "Matter" Microscopes

↪ Wavelength of Particles (γ, e, p, ...) (de Broglie, 1923)

$$\boxed{\lambda \;=\; h\,/\,p} \quad = 1.2 \text{ fm}/p\,[\text{ GeV/c}]$$

↪ Higher momentum => shorter wavelength => better the resolution

✳ Energy to Matter

↪ Higher energy produces heavier particles

$$E = mc^2 = \frac{m_o c^2}{\sqrt{1 - \dfrac{v^2}{c^2}}} = \gamma\, m_o c^2$$

✳ Penetrate more deeply into matter

Raggi Cosmici

I raggi cosmici primari producono sciami di particelle nell'atmosfera

Sulla superficie della Terra :~ 1/sec/dm²

Raggi cosmici primari:
p 80 %, α 9 %, n 8 %
e 2 %, heavy nuclei 1 %
γ 0.1 %, ν 0.1 %

p
π⁰
π±
μ
ν
e,γ
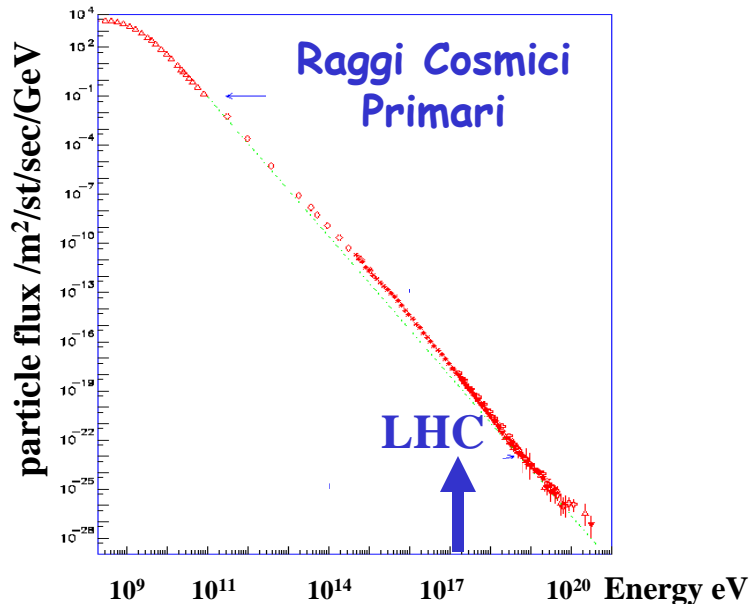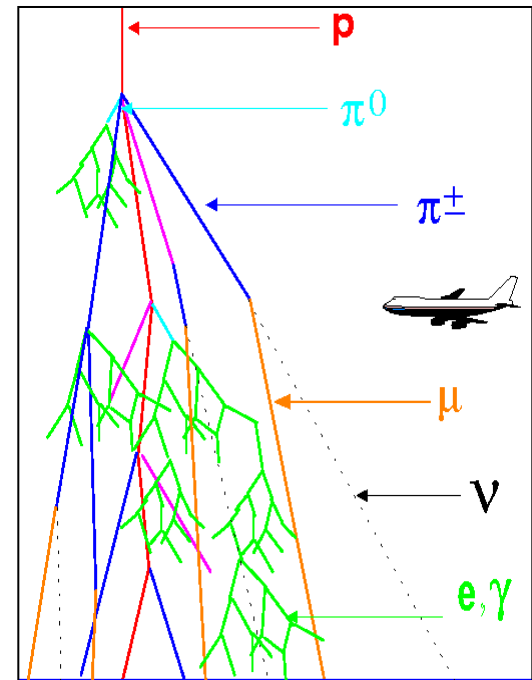
Raggi cosmici secondari sulla superficie della Terra:
ν 68 % ; μ 30 %
p, n, ... 2 %

Raggi Cosmici Primari

particle flux /m²/st/sec/GeV

LHC

10^9 10^{11} 10^{14} 10^{17} 10^{20} **Energy eV**

1931, P. Dirac : e⁺ is predicted

cloud chamber

e^+
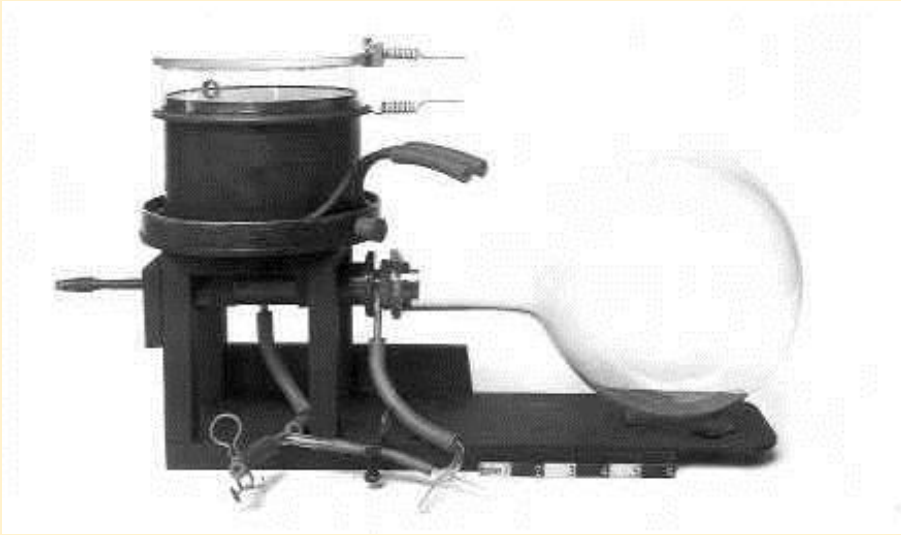
1932, C. Anderson : positron discovery in cosmic rays
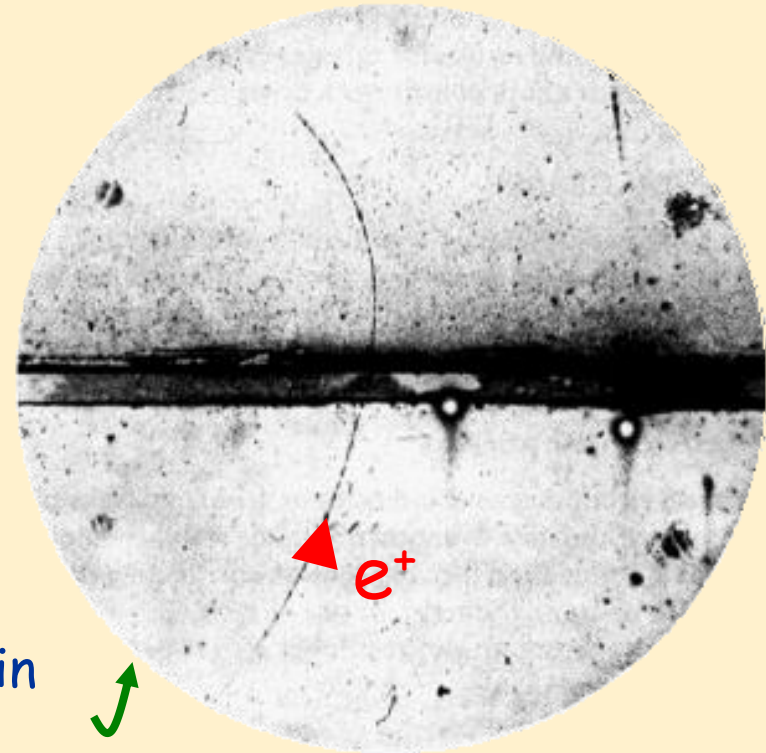
Neutrinos are predicted

1930, ν ipostulated to preserve energy conservation in β decays   [W. Pauli]

1956, 1ˢᵗ Evidence of ν @ reactor [Reines & Cowan]

β^-

p

β^-

n

$\bar{\nu}_e$
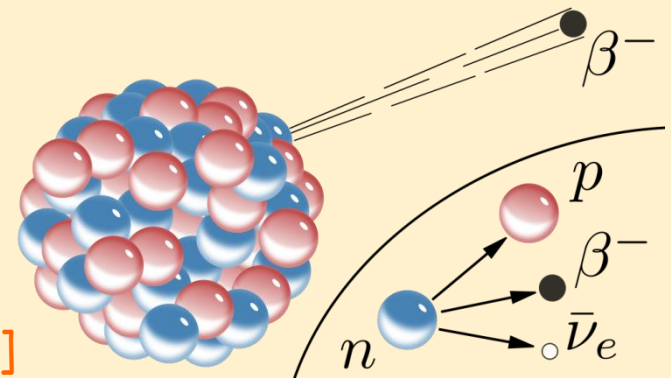
Beyond ordinary matter ...

1937, muon discovery (C. Anderson & S. Neddermeyer)
1947, pion discovery (C. Powell)
1947, discovery of neutral and charged kaons (G. Rochester & C. Butler)

$K^0 \rightarrow \pi^+ \pi^-$

$K^{\pm} \rightarrow \mu^{\pm} \nu$
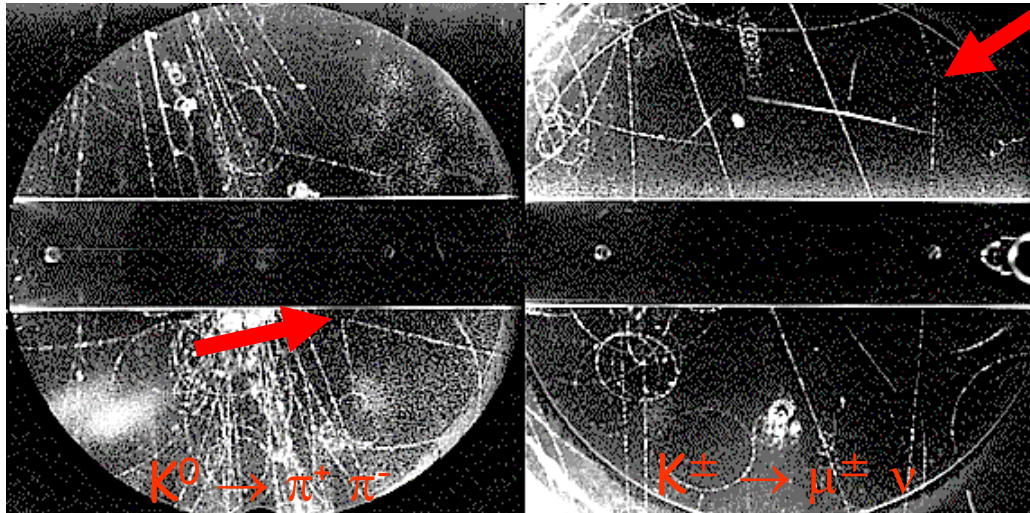
Photographs of cloud chamber exposed to cosmic rays

1955, antiproton discovery with accelerator (Chamberlain et al.)
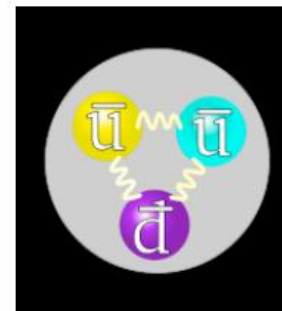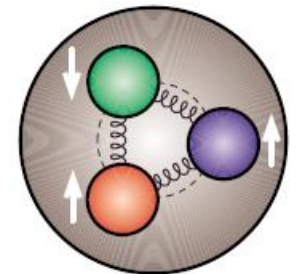
Antibaryon ($\bar{q}\bar{q}\bar{q}$)   Baryon (qqq)

Le interazioni fondamentali tra particelle

nucleo **protone**

$$1$$
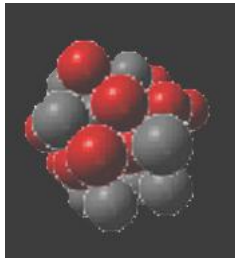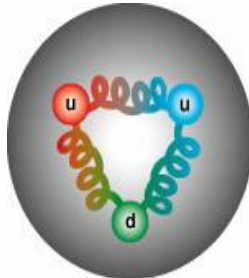
Forza forte
g (Gluone)

atomo

$$10^{-2}$$
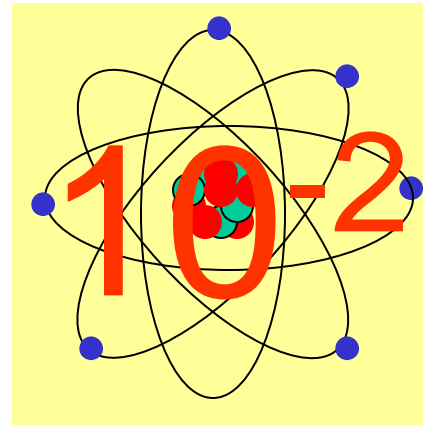
Forza elettromagnetica
γ (Fotone)

$$10^{-40}$$

Forza gravitazionale

(Gravitone)

Radioattività Beta

$\bar{\nu}_e$

$$10^{-5}$$

nucleo **elettrone**

Forza debole
$z, w^{\pm}$
(Bosoni)

$n \rightarrow p + e^- + \bar{\nu}_e$
$d \rightarrow u + e^- + \bar{\nu}_e$
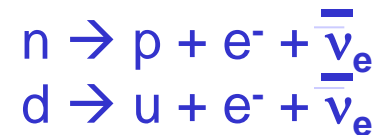
Ionization: the Bethe-Bloch formula

- Bethe-Block formula only gives the average energy loss, and do not take into account fluctuations from event to event.
- Large high energy tail – δ rays

δ-rays : electrons that have sufficient energy to ionize further atoms through subsequent interactions on their own.

Landau distribution:

$f(\Delta/X)$: Probability for energy loss Δ in a thickness X of matter.

Very asymmetric distribution: average and most probable energy loss must be distinguished !
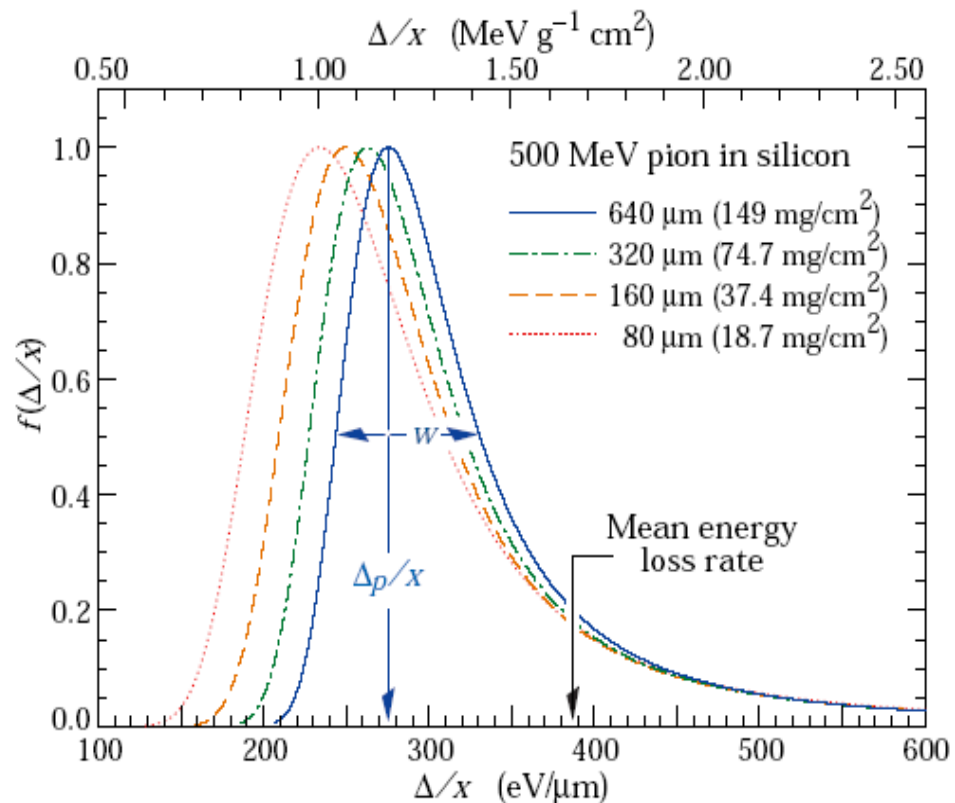
Gas Detectors: the avalanche multiplication

As the electric field increases to sufficient high value (~100kV/cm) more and more electrons gain kinetic energy in excess of the ionization energy so that they can ionize in turn other atoms (secondary ionzation) and so on.

Cathode

Ions

E

λ

x

Electrons

Anode
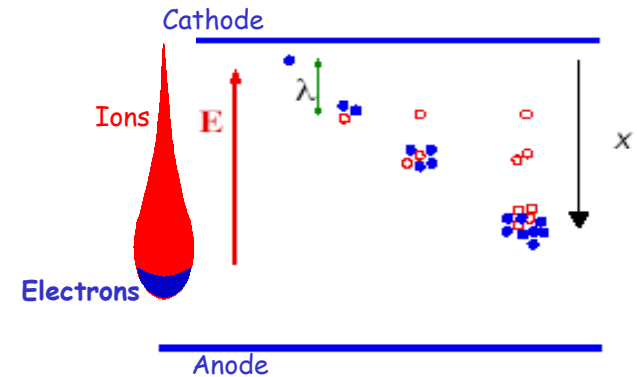
The mean free path λ is defined as the average distance that an electron must walk before another ionizing collision may occurs. On average every λ the number of ion pairs is doubled. $\alpha=1/\lambda$ is called Townsend coefficient:

$dN = N \, \alpha \, dx$

$N(x) = N_0 \exp (\alpha \, x)$ $N/N_0 = A =$ Amplification or Gas Gain

The problem with an avalanche multiplication with an homogeneous electric field is that very high field on are needed and may easily cause breakdown
The solution is to obtain the avalanche multiplication in an inhomogeneous field:

$\alpha(E) \rightarrow N(x)/N_0 = A = \exp [\int \alpha (E(x'))dx']$

Solid State Detectors

In solid state detectors the charges produced by the ionization due to the incoming particle are sufficient to provide a measurable signal.

❑ Solid state detectors have a high density
  ➜ large energy loss in a short distance:
    116 (78) keV = mean (most probable) energy loss
    for 300μm Silicon thickness

❑ Low ionisation energy (few eV per e-hole pair)
  compared to gas detectors (20-40 eV per e-ion pair)
    3.6 eV for silicon to create an e-hole pair
    $\Rightarrow$ 72 e-h/μm (most probable); 108 e-h/μm (mean)
    $\Rightarrow$ most probable charge 300μm Silicon thickness:
            $\approx$ 21600 e $\approx$ 3.6 fC

❑ Drift velocity much faster than in gas detectors:
  ➜ Very fast signals of only a few ns length !

❑ Diffusion effect is smaller than in gas detectors:
  ➜ achievable position resolution of less than 10 μm
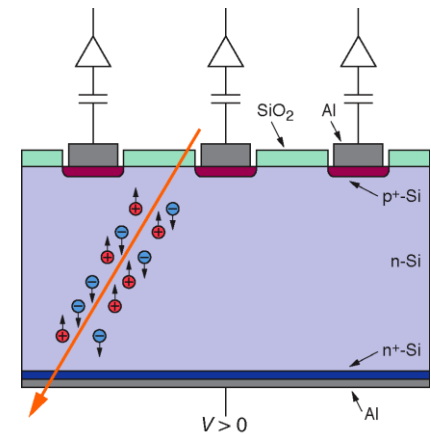
Solid State Detectors

In an isolated atom of a gaseous detector the electrons have only discrete energy levels and when are liberated from the atoms by an ionizing particle they (and the ions) can freely move under an applied electric field. In solid state (crystal) material the atomic levels merge to energy bands. Inner shell electrons, in the lower energy bands, are closely bound to the individual atoms. However electrons in the **conduction band** and the holes in the lower **valence band** (bands that are still bound states of the crystal, but they belong to the entire crystal) can freely move around the crystal, if an electric field is applied.
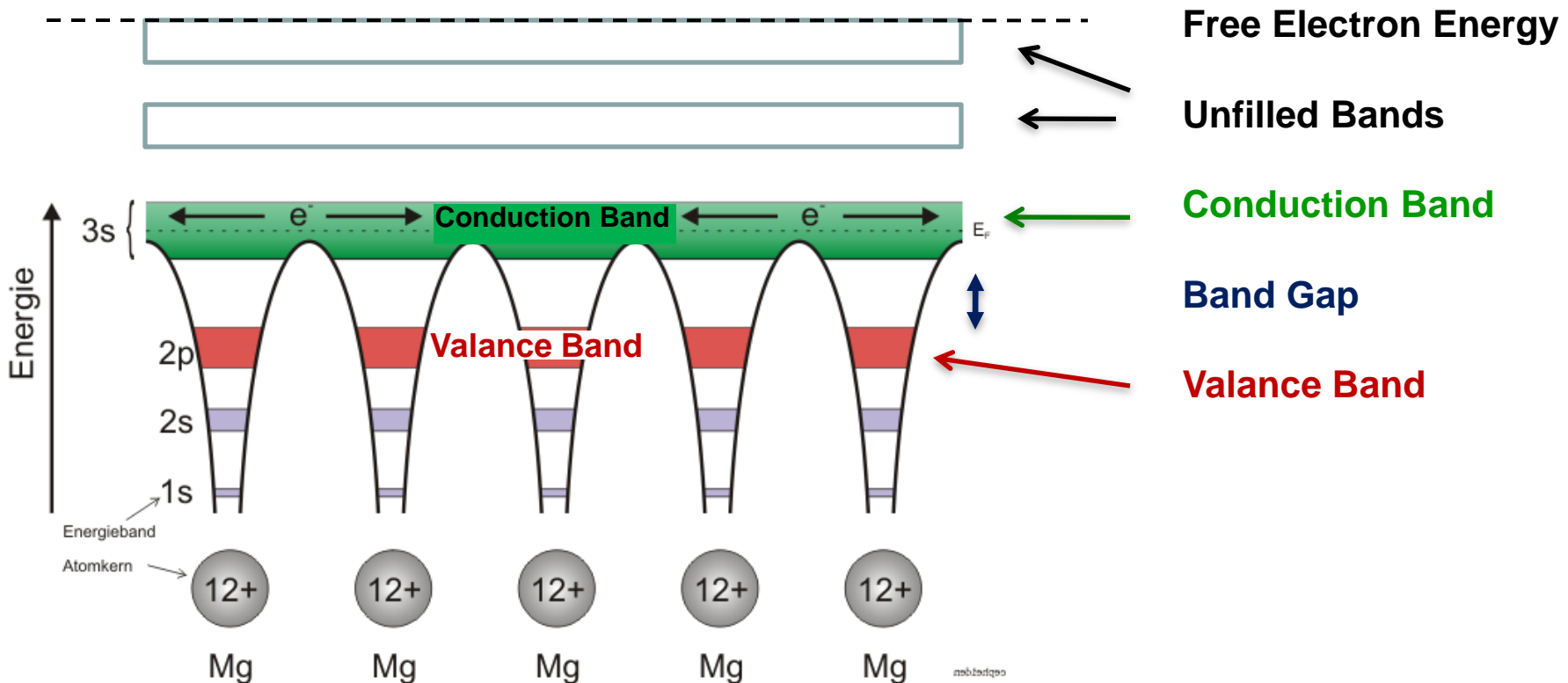
Solid State Detectors

Fermi distribution $f(E)$ describes the probability that an electronic state with energy E is occupied by an electron:

$$f(E) = \frac{1}{1 + e^{\frac{E-E_F}{kT}}}$$
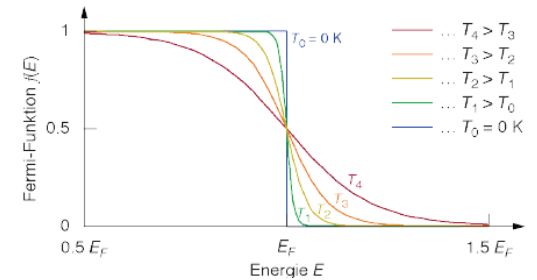
The Fermi level E_F is the energy at which the probability of occupation is 50%. For metals E_F is in the conduction band, for semiconductors and isolators E_F is in the band gap.
In metals the conduction and the valence band partially overlap, whereas in isolators and semiconductors these levels are separated by an energy gap.
This energy gap E_g is called band gap. In isolators this gap is large.
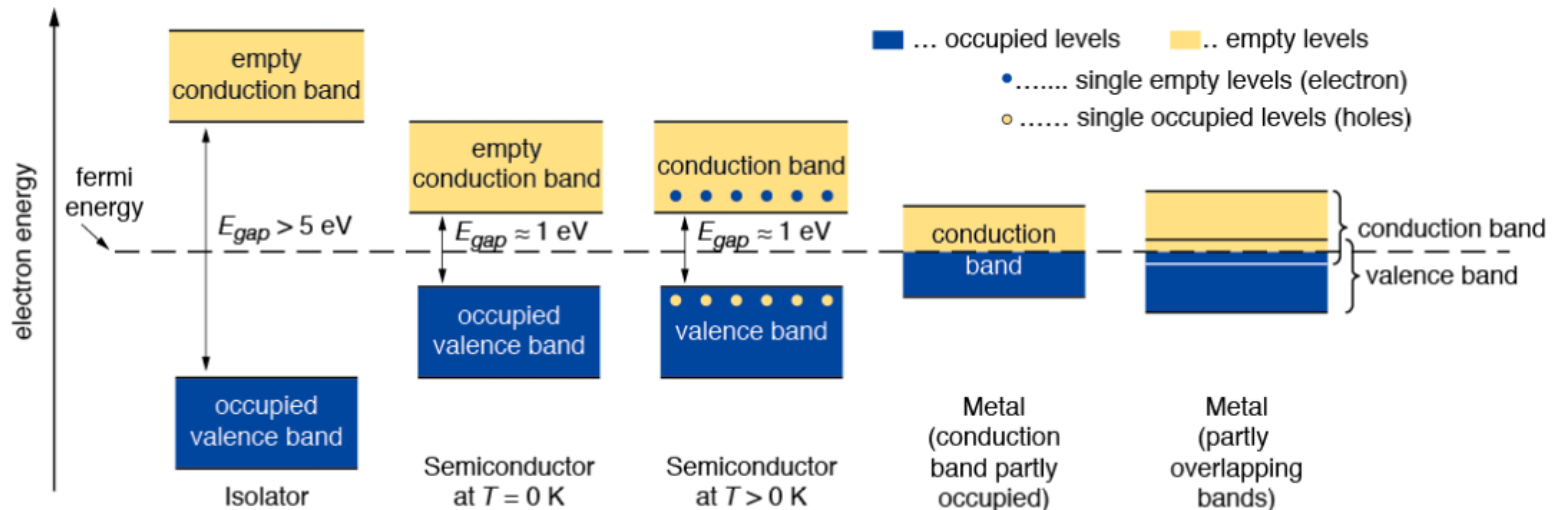
Solid State Detectors

❖ The energy gap E_g (band gap) of Diamond/Silicon/Germanium is 5.5,1.12,0.66 eV

❖ Due to the small band gap, electrons already occupy the conduction band gap in many semiconductors at room temperature.

❖ Electrons from the conduction band may recombine with holes

❖ The thermal excitation excites electrons into the conduction band leaving a hole in the valence band. Thermal equilibrium is reached at intrinsic carrier concentration:

$$n_i = n_e = n_h \propto T^{\frac{3}{2}} \cdot \exp\left(-\frac{E_g}{2kT}\right)$$

❖ Therefore the number of electrons in the conduction band, and thus also the conductivity of the semiconductor, increases with temperature.
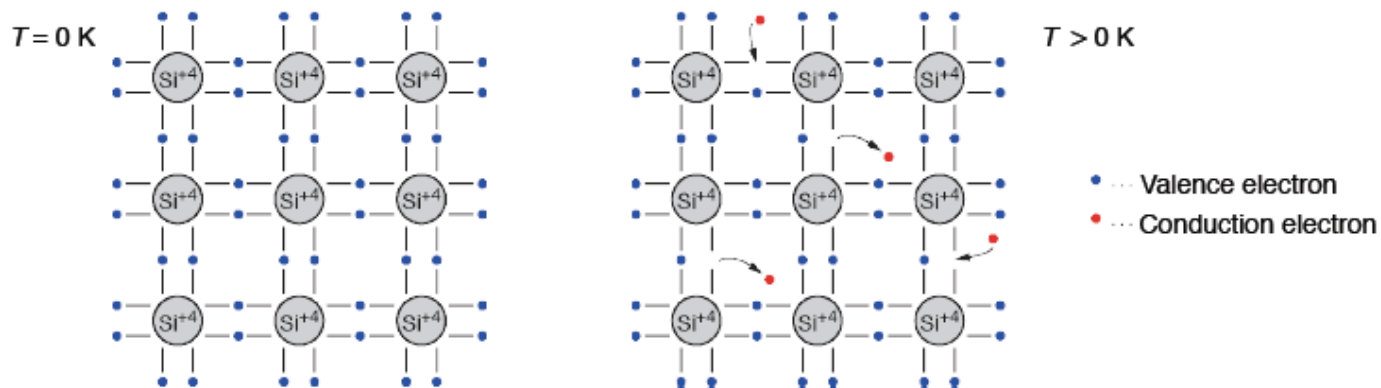
In silicon at room temperature the intrinsic carrier concentration is $1.45 \cdot 10^{10}$ cm^{-3}. With approximately 10^{22} Atoms/cm^3 about 1 in 10^{12} silicon atoms is ionised. This yields an intrinsic resistivity of: $\rho \approx 230$ kΩcm

Solid State Detectors
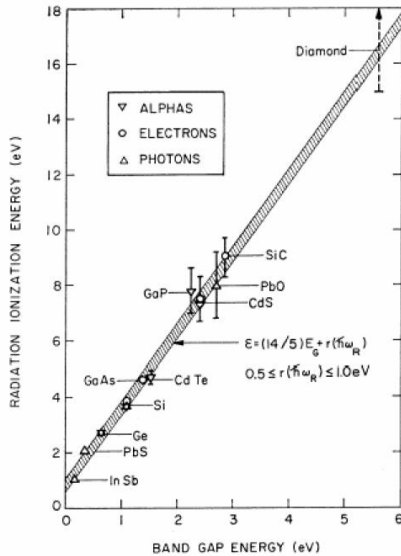
	Diamond	Silicon	Germanium
Band gap E_g [eV]	5.5	1.12	0.66
Energy $E_{e/h}$ for e-h pair [eV]	13	3.6	2.9
Density [g/cm^3]	3.51	2.33	5.32
e-mobility μ_e [cm^2/Vs]	1800	1450	3900
h-mobility μ_h [cm^2/Vs]	1200	450	1900
Intrinsic charge carrier:			
n_i [cm^{-3}] (T=300 K)	$\approx 10^{-27}$	$1.45 \cdot 10^{10}$	$2.4 \cdot 10^{13}$

In Diamond detectors there are very few charge carriers at room temperature (n_i[cm^{-3}] $\approx 10^{-27}$) due to large band gap while many e-h pairs are produced by an ionizing particle
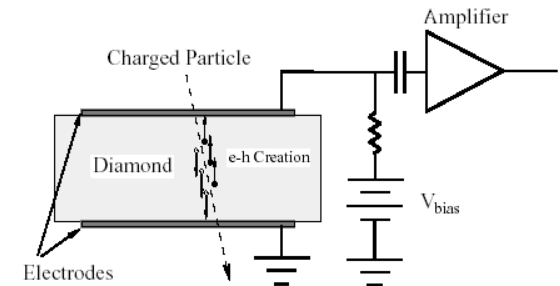
In a 300μm Silicon detector the number (mean) of e-h pairs produced by the passage of a charged particle at the minimum ionizing is given by:

$$n_{e/h} = dE/dx \cdot d / E_{e/h} = 3.87 \cdot 10^6 eV/cm \cdot 0.03cm / 3.6eV \approx 3.2 \cdot 10^4 \text{ e-h pairs}$$

In the same detector of an area A=1cm^2 the intrinsic charge carrier (T=300 K) is:

$$n_i \cdot d \cdot A = 1.45 \cdot 10^{10} cm^{-3} \cdot 0.03cm \cdot 1cm^2 \approx 4.35 \cdot 10^8 \text{ e-h pairs}$$

In silicon the thermal e-h pairs are four orders of magnitude larger than signal !!!
➔ remove the charge carrier !

n-Doping in Silicon

Doping with an element +5 atom with one valence electron more than silicon (e.g. P,As).
The 5th valence electrons is weakly bound. The doping atom is called donor.
The n-doped silicon becomes a n-type conductor (more electrons than holes)
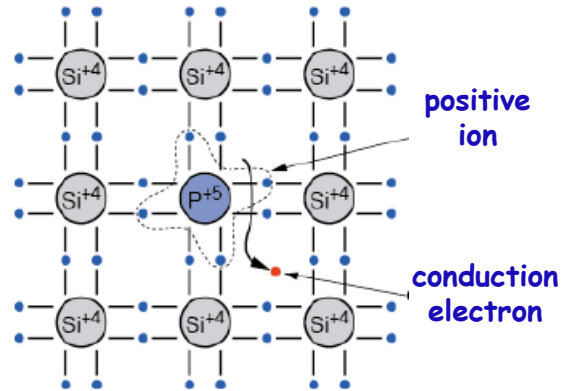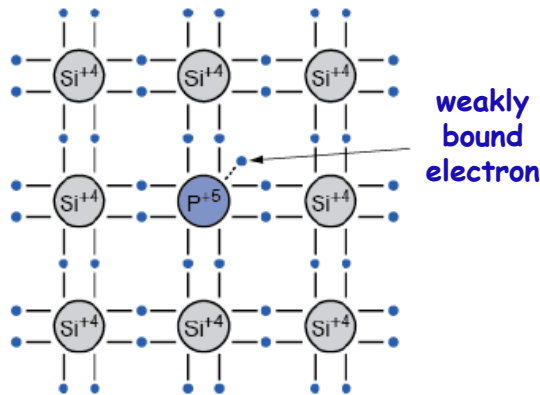
Typical doping concentrations for Si detectors are $\approx 10^{12}$ atoms/cm^3
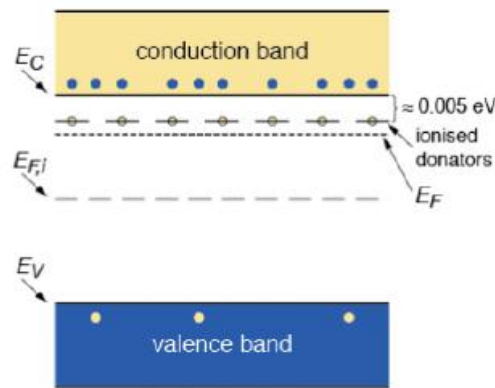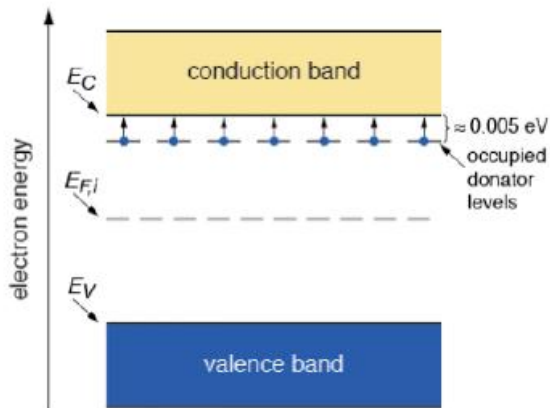
**The energy level of the donor is just below the edge of the conduction band.
At room temperature most electrons are raised to the conduction band.
The Fermi level E_F moves up.**

p-Doping in Silicon

Doping with an element +3 atom with one valence electron less than silicon (e.g. B,Ga).
One valence bond remains open and attracts electrons from the neighbor atoms.
The doping atom is called acceptor.
The p-doped silicon becomes a p-type conductor (more holes than electrons)
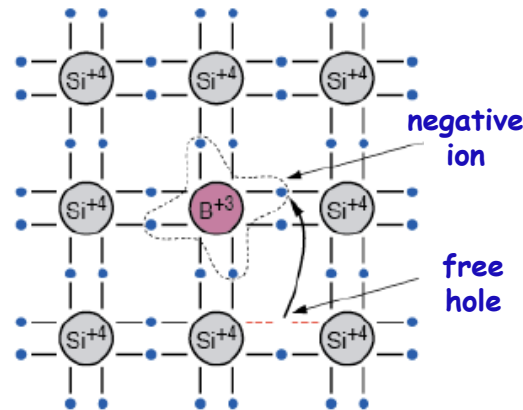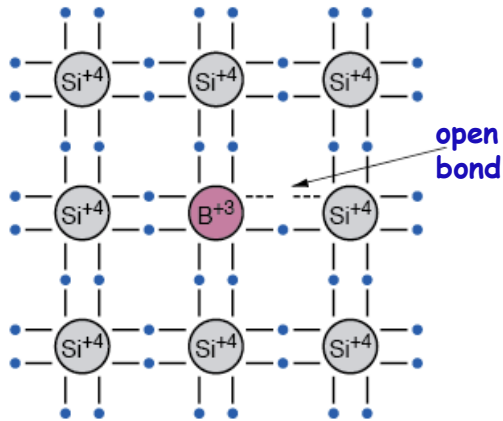
Typical doping concentrations for Si detectors are ≈10^{12} atoms/cm^3
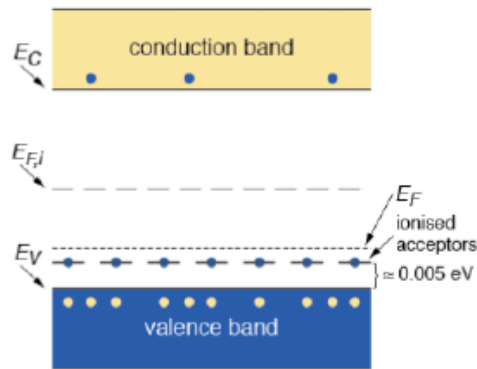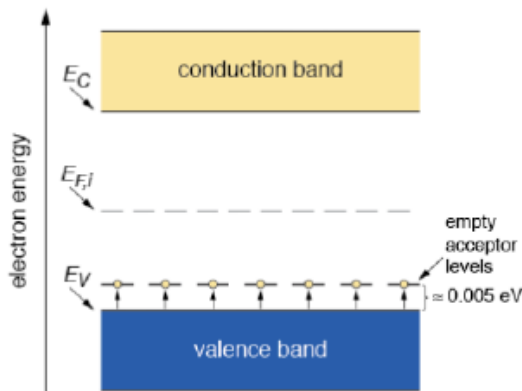
The energy level of the acceptor is just above the edge of the valence band.
At room temperature most levels are occupied by electrons leaving holes in the valence band.
The Fermi level E_F moves down.

Si-Diode as Si-Detector

At the p-n junction the difference in the fermi levels cause diffusion of charge carries until thermal equilibrium is reached and the electric field thus created stops further diffusion. At this point the fermi level is equal.
A zone free of charge carries, called **depletion region**, is thus established .
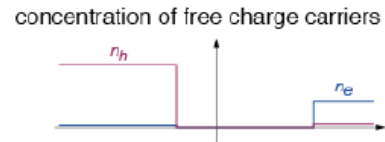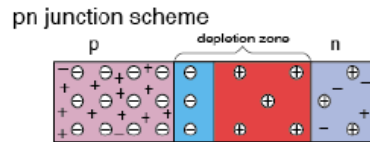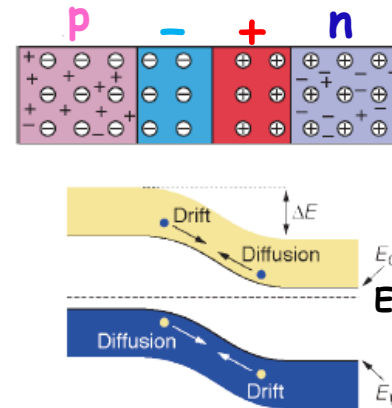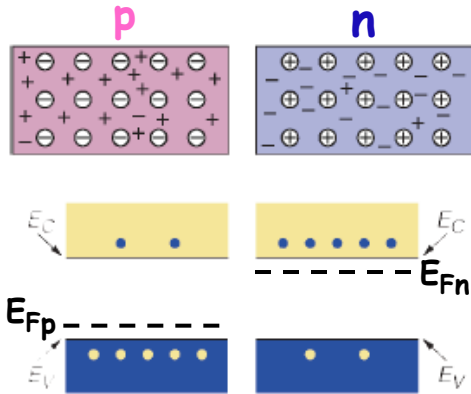
+ hole   ⊖ acceptor

– electron   ⊕ donator
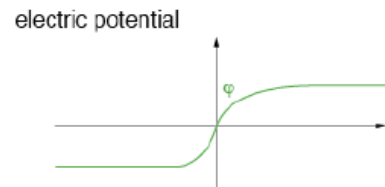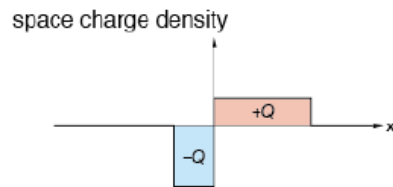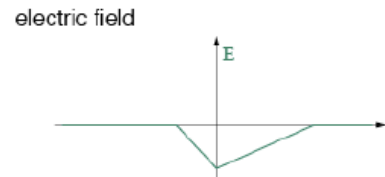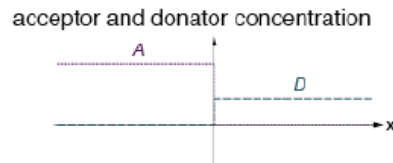
Si-Diode as Si-Detector

By applying an external voltage V, the depletion zone can be extended to the entire diode.

An incoming particle can then produce by ionization free charge carriers in the diode. The charges carriers drift in the electric field and induce an electrical signal on the electrodes.
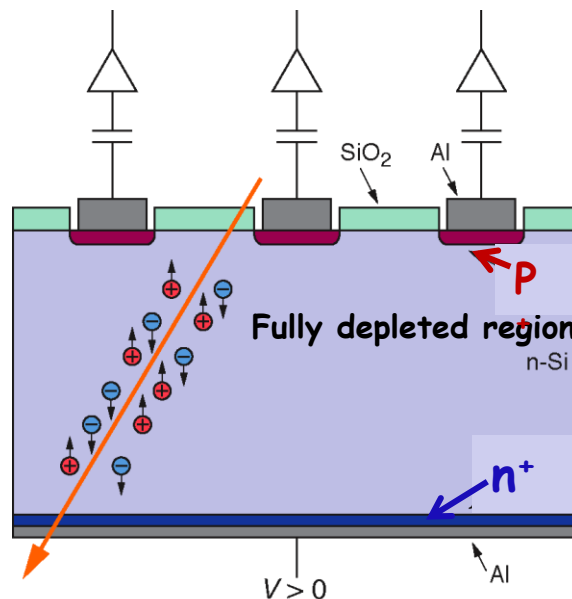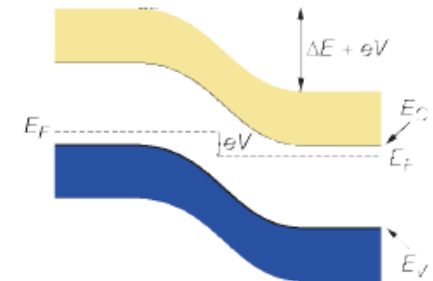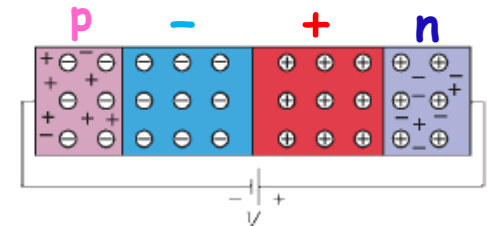
➔ **That is the way a Silicon detector can work !**

Detector Structures
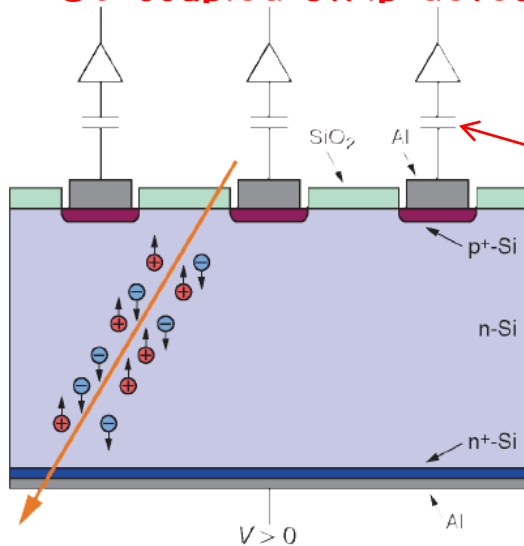
coupling capacitors
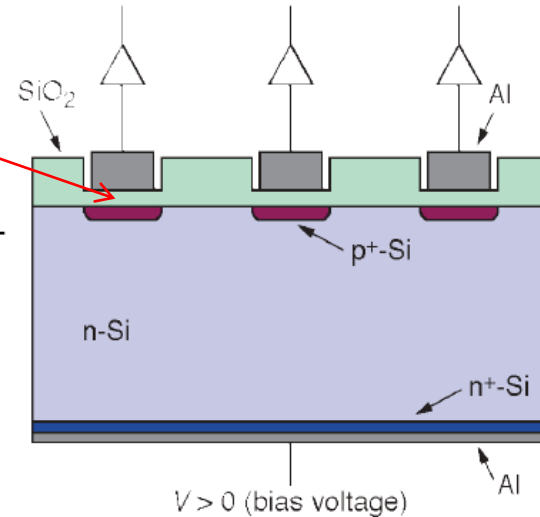
A typical n-type Si strip detector:
- ✓ about 30.000 e-h+ pairs in 300 μm detector thickness
- ✓ p+n junction:
  $N_a \approx 10^{15}$ cm^{-3}, $N_d \approx 1-5 \cdot 10^{12}$ cm^{-3}
- ✓ n-type bulk: $\rho > 2$ kΩcm
- ✓ operating voltage < 200 V.
- ✓ n+ layer on backplane to improve ohmic contact
- ✓ Aluminum metallization

Using p-type silicon and exchanging p+ and n+ would give a perfectly working p-type detector.

➢ **Deposition of SiO2 with a thickness of 100–200 nm between p+ and aluminum strip**

➢ **AC coupling blocks leakage current from the amplifier.**

➢ **Problems are shorts through the dielectric (pinholes). Usually avoided by a second layer of Si3N4.**

➢ **Need to isolate strips from each other to collect charge from each strip:**
  several methods for high impedence bias voltage connection (≈ 1MΩ resistor): polysilicon resistor, punch through bias, FOXFET bias.

Radiation environment at the LHC
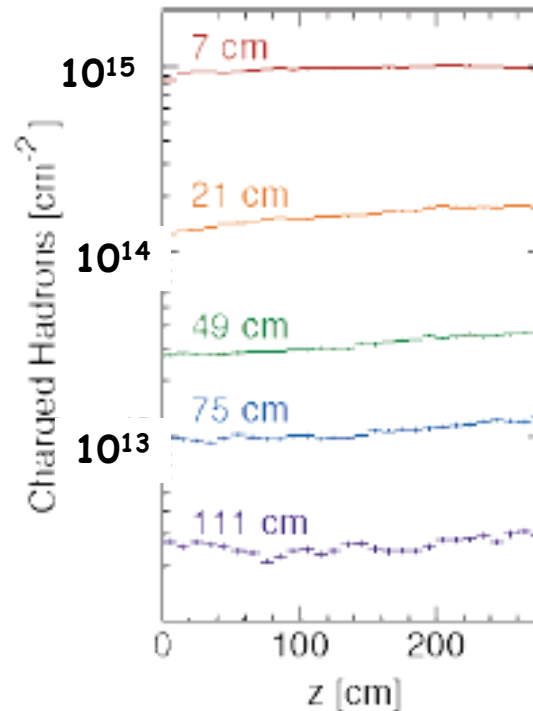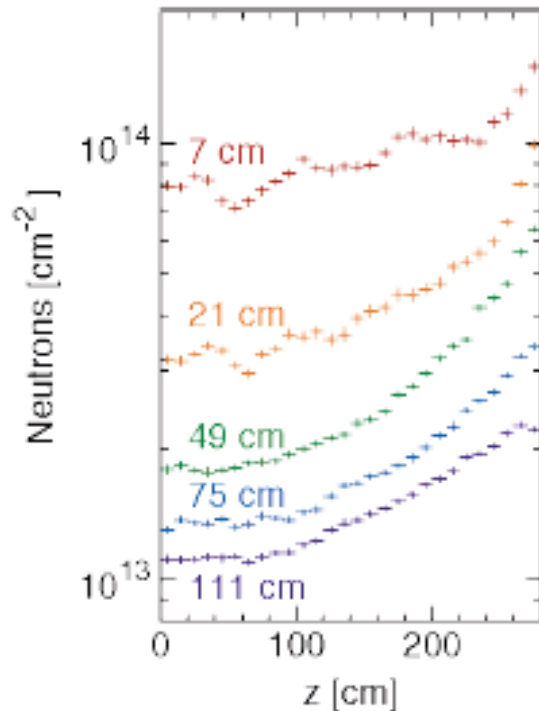
Expected particle fluences for the silicon detector inner layers in CMS integrated over 10 years as a function of the distance from the vertex point and for various radii.

Left: neutrons   Right: charged hadrons

Radiation damage

Particles (radiation) interact with atoms of the detector material and may cause permanent changes (defects) in the detector bulk.

■ **One distinguishes two types of radiation damage:**
  ➤ damage inside the detector bulk (bulk damage): dislocated
    atoms from their position in the lattice caused by massive particles.
      ➜ Bulk damage is primarily produced by neutrons, protons and pions.
  ➤ damage introduced in the surface layers (surface damage) is due to the
    charges generated in the amorphous oxide
      ➜ Surface damage is primarily produced by photons and charged particles.

■ **Defects may change with time:**
  ➤ one distinguishes between primary defects and secondary defects
  ➤ the secondary defects appear with time caused by moving primary defects

■ **Comulative effects:**
  ➤ increased leakage current
  ➤ silicon bulk type inversion (n-type to p-type)
  ➤ increased depletion voltage
  ➤ increased capacitance

■ **Sensor can stop working :**
  ➤ noise too high
  ➤ depletion voltage too high
  ➤ loss of inter-strip isolation

Typical limits of Si Detectors are at 10^{14}-10^{15} Hadrons/cm^2

Radiation damage

❑ **Defects in the semiconductor lattice create energy levels in the band gap between valence and conduction band. Depending on the position of these energy levels the following effects will occur:**

➢ **Modification of the effective doping concentration**
  ➔ **shift of the value of the depletion voltage.**

➢ **Trapping of charge carriers**
  ➔ **reduced lifetime of charge carriers**

➢ **Easier thermal excitement of e- and h+**
  ➔ **increase of the leakage current**

Vacancy **Interstitial** **Frenkel defect**

A displaced silicon atom produces an empty space n the lattice (Vacancy) and in another place an atom in an inter lattice space (Interstitial, I). A vacancy-interstitial pair is called a Frenkel-defect.

In hard impacts the primary knock-on atom displaces additional atoms. These defects are called cluster defects. The size of a cluster defect is approximately 5 nm and consists of about 100 dislocated atoms.

Radiation damage

Increase of leakage current as function of irradiation fluence (different materials)

M. Moll, *Radiation Damage in Silicon Particle Detectors*, PhD-Thesis (1999)
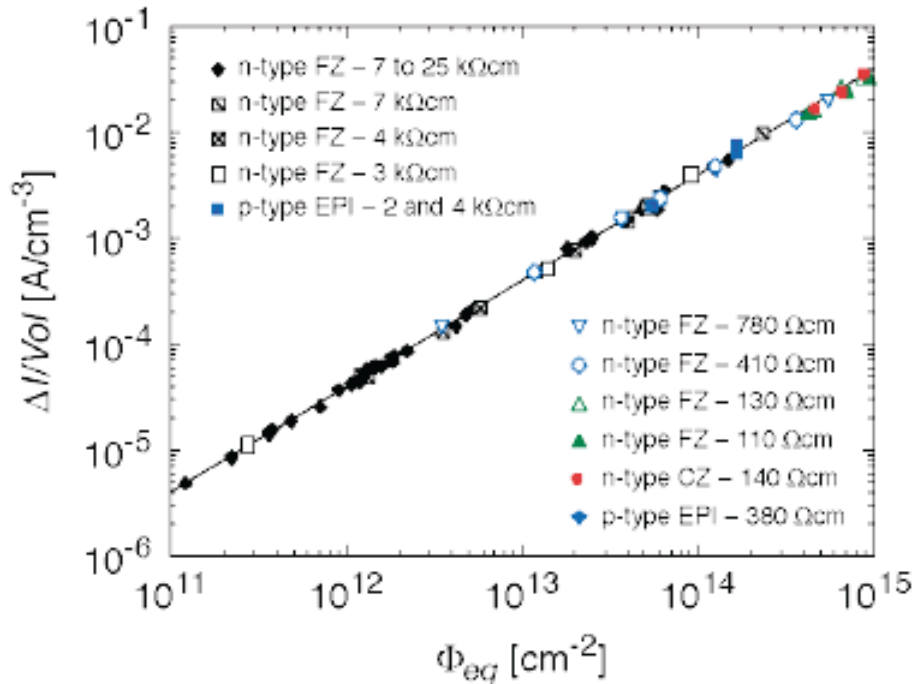
In ten years of LHC operation the currents of the innermost layers increase by 3 orders of magnitude!

- $\Delta I = \alpha \Phi_{eq} V$

α damage constant $\cong 3 \times 10^{-17}$ A/cm

Radiation damage

Full depletion voltage and effective doping concentration of an originally n type silicon detector as a function of the fluence Φeq:

type inversion

"Donor removal"

$10^{14} cm^{-2}$

≈ 600 V

"Acceptor creation"

n - type

"p - type"

[Data from R. Wunstorf 92]

voltage may becomes too high to fully deplete:
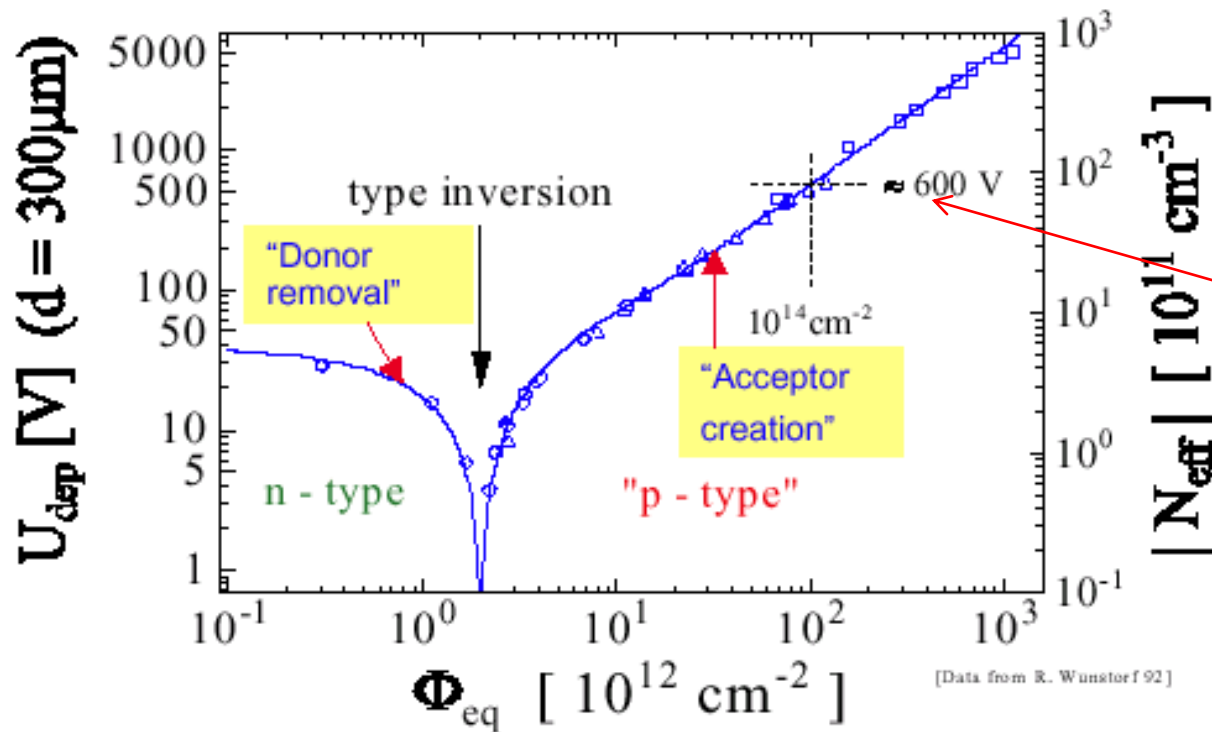
Type inversion ! an n-tyle Si detector becomes a p-type Si detector !

Radiation damage

In n type sensors with p+ implants the depletion zone grows from the p+ implants to the backplane n+ implant.
After type inversion the p+ bulk is now depleted from the backside (polarity of bias voltage remains the same)

Unirradiated detector:
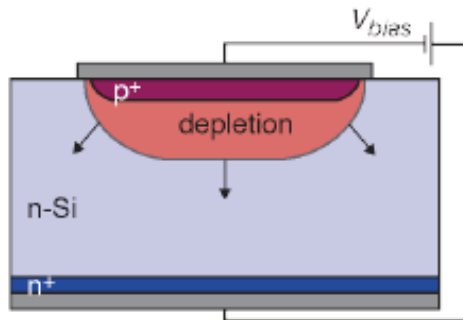
Detector after type inversion:
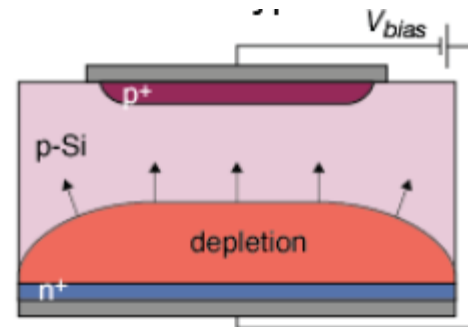
n–type detectors before type inversion can be operated below full depletion

after type inversion, the depletion zone has to reach the strips.

(a possible solution is to use n+p or n+n detectors)

Surface defects in the oxide
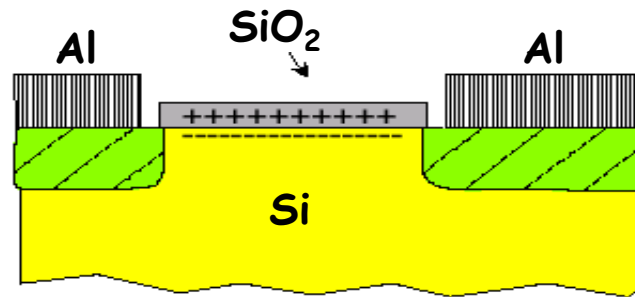
❑ **Ionizing radiation creates charges in the oxide**
   (in the amorphous oxide dislocation of atoms is not relevant)

❑ **The mobility of electrons in SiO2 is much larger than the mobility of holes**
   ➔ **electrons diffuse out of the oxide, holes remain semi permanent fixed**
   ➔ **the oxide becomes positively charged due to these fixed oxide charges.**

➢ **Consequences for the detector:**
   ✓ **reduced electrical separation between implants**
   ✓ **increase of interstrip capacitance**
   ✓ **increase of detector noise**
   ✓ **worsening of position resolution**
   ✓ **increase of surface leakage current**
   ✓ **reduced break down voltage**

Resonances @ √s = 900 GeV
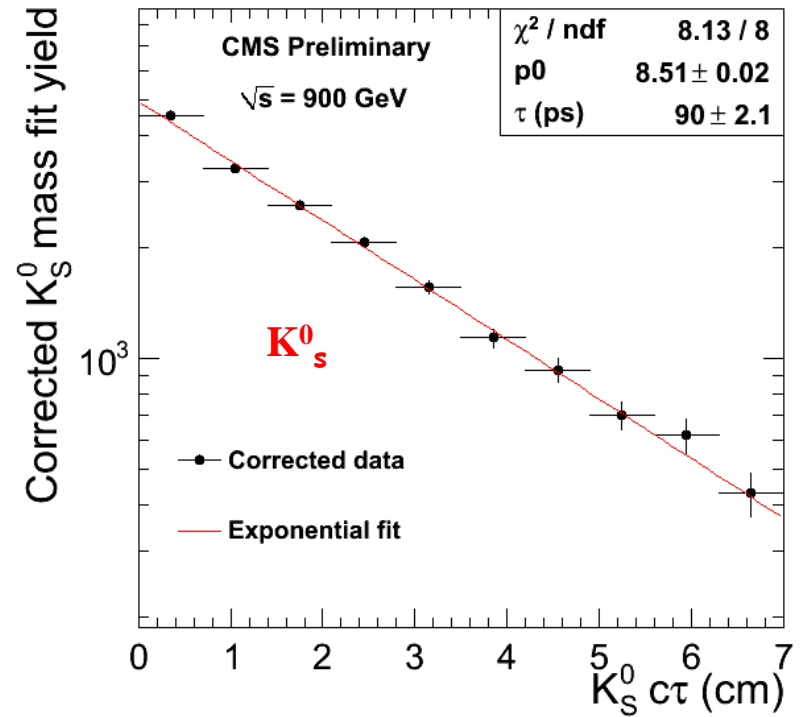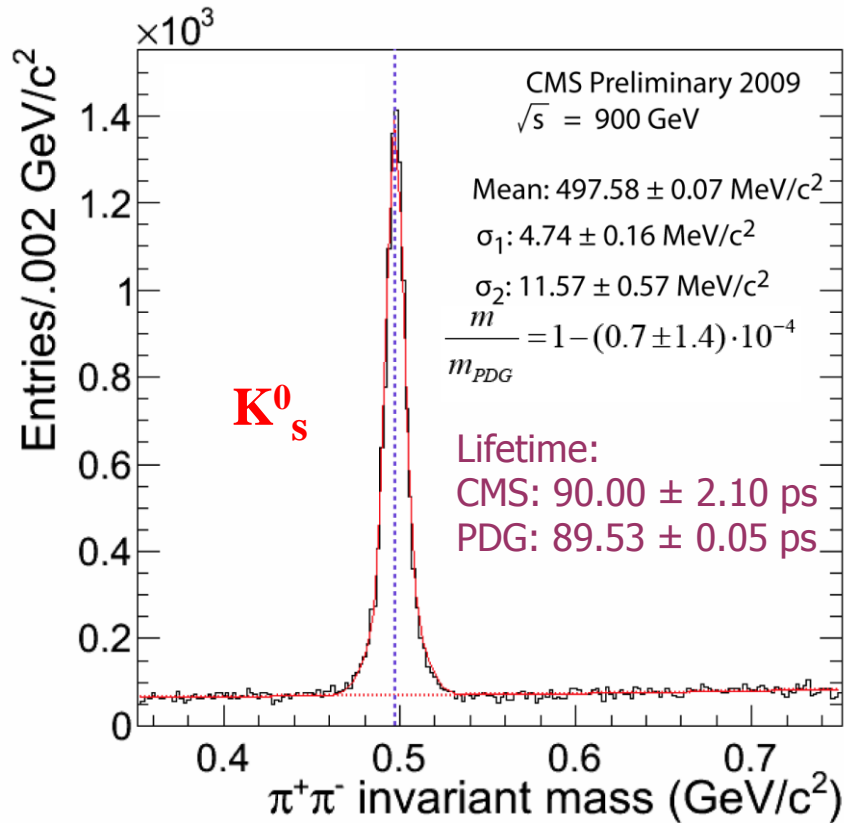
Excellent understanding of the momentum scale for low mass resonances

⇒ **Accurate tracking, vertexing, alignment, magnetic field, ….**

Resonances @ √s = 900 GeV
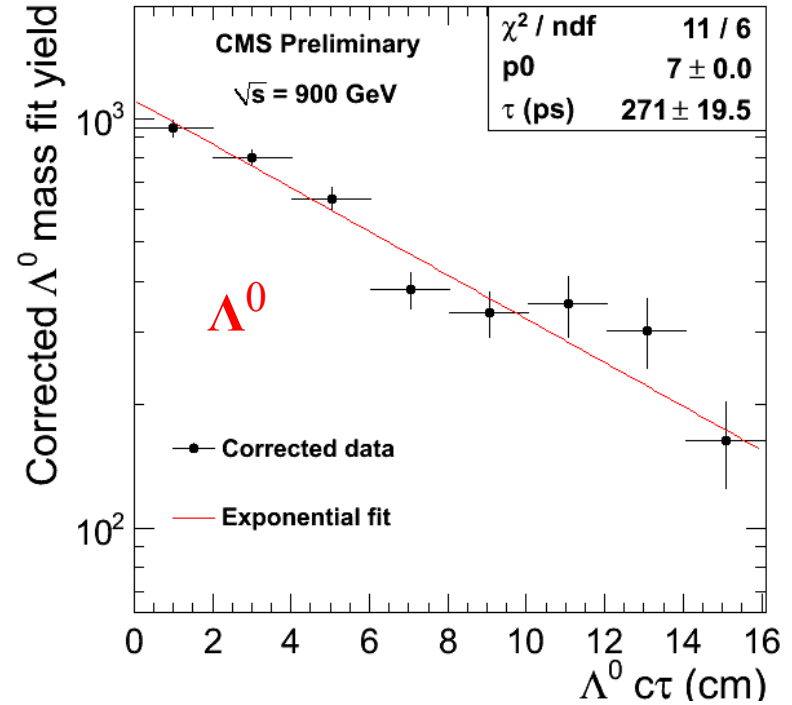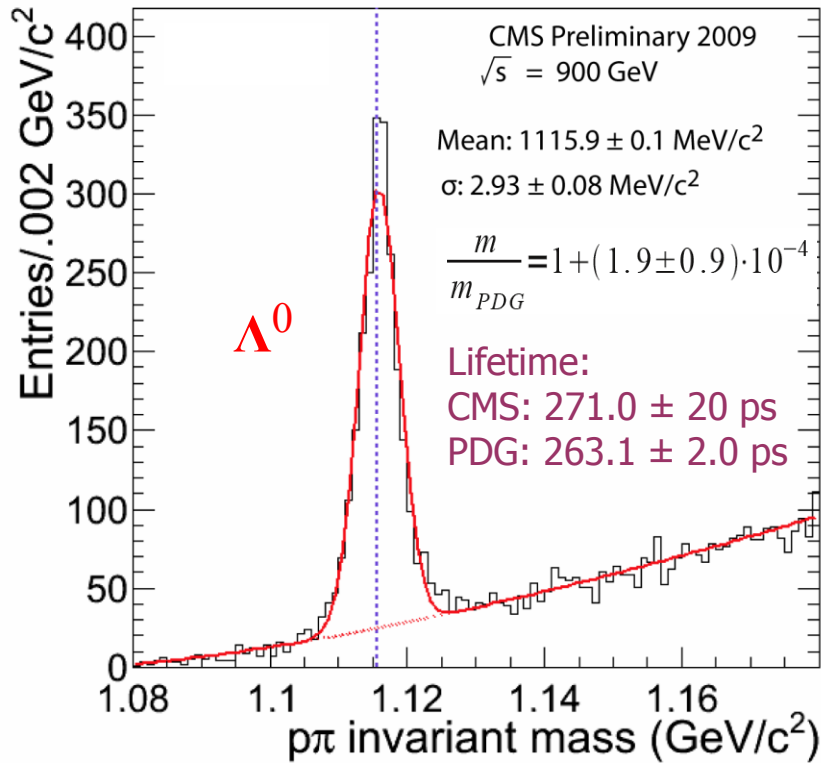
Excellent understanding of the momentum scale for low mass resonances

⇒ **Accurate tracking, vertexing, alignment, magnetic field, ….**

... and the $\Xi^\pm$

CMS Experiment at LHC/CERN
Run/Event 124024/3693969
Candidate Xi- Event

Yield: 49.7 ± 9.0
Mean: 1322.8 ± 0.8 MeV/c^2
Width: 4.0 ± 0.8 MeV/c^2
PDG $\Xi^\pm$ mass: 1321.71 ± 0.07 MeV/c^2

CMS Preliminary

$\sqrt{s}$ = 900 GeV and 2360 GeV

$\Xi^\pm$

Candidates / 5 MeV/c^2

$\Lambda^0 \pi^-$ (+ c.c.) invariant mass (MeV/c^2)

$\Xi^\pm \longrightarrow \Lambda\pi^\pm$
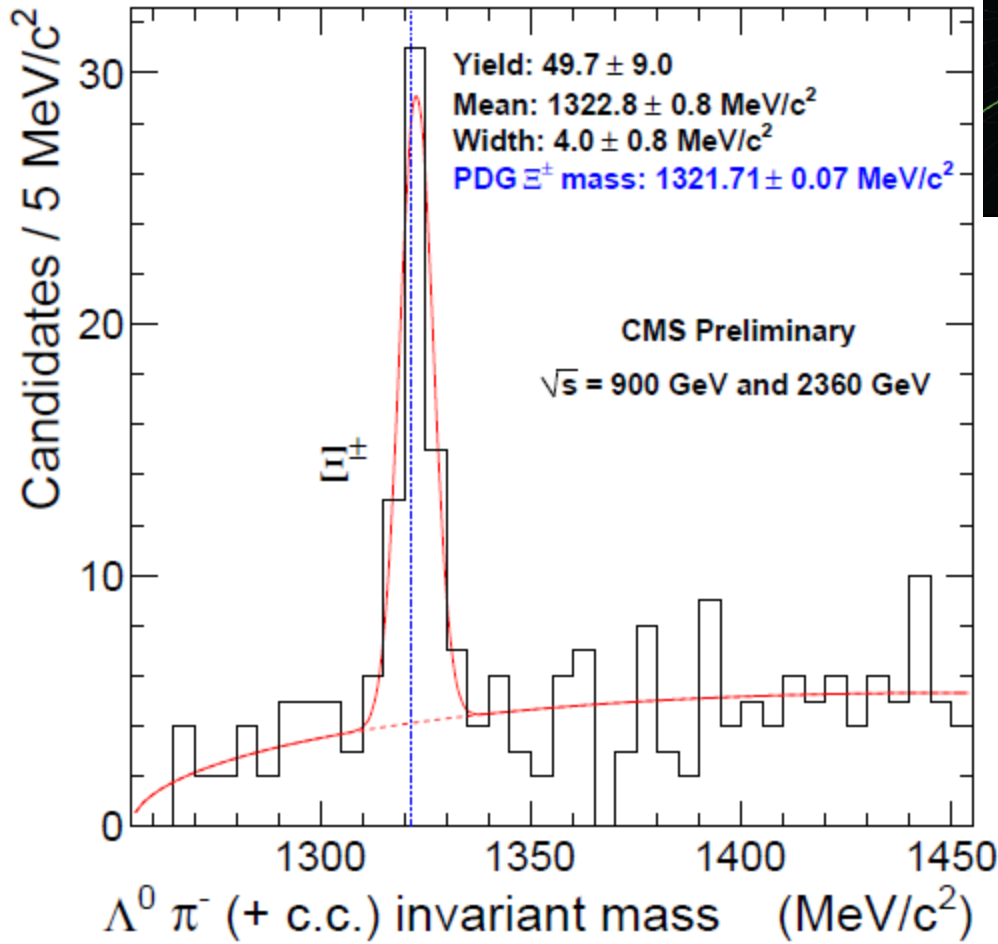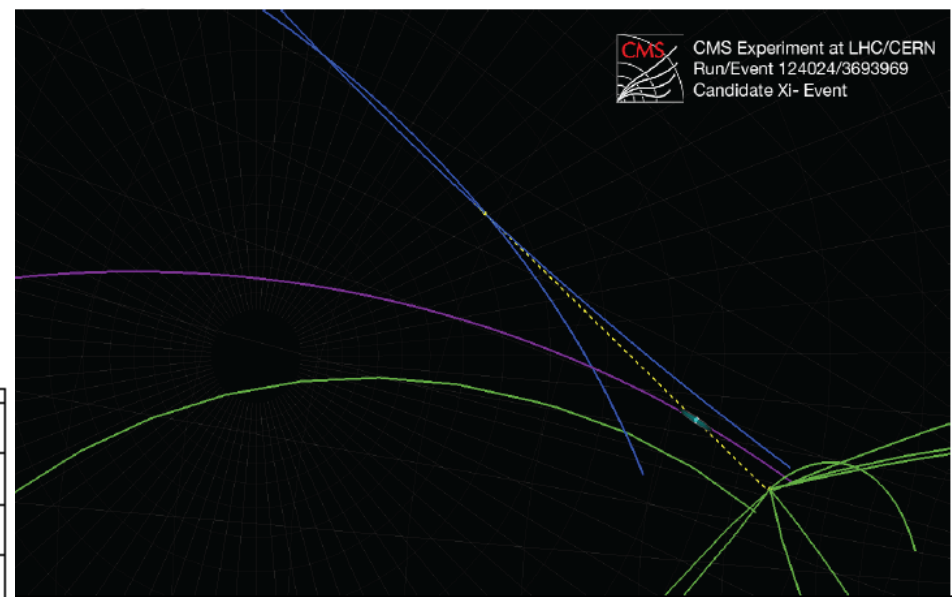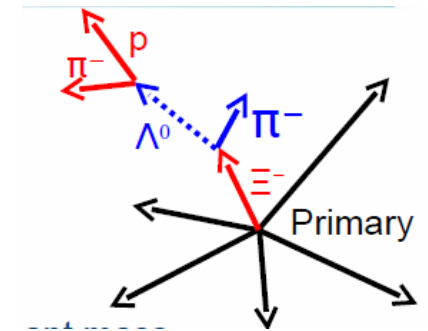
$\Lambda\pi$ Invariant mass
- tracks displaced from primary vertex ($d_{3D} > 3\sigma$)
- constrain Λ mass to PDG world average value in Ξ fit
- require same sign π's

7 TeV Data: Resonances

$\Xi^{\pm} \longrightarrow \Lambda\pi^{\pm}$

$\Lambda\pi^-$ or anti-$\Lambda\pi^+$ invariant mass

$\Omega^{\pm} \rightarrow \Lambda K^{\pm}$

ΛK^- or anti-ΛK^+ invariant mass

CMS Preliminary

Yield: 2344.8 ± 58.2
Mean: 1321.92 ± 0.09 MeV/c^2
Sigma: 3.24 ± 0.09 MeV/c^2
Statistical uncertainties only

CMS Preliminary

Yield: 187.6 ± 19.9
Mean: 1672.2 ± 0.4 MeV/c^2
Sigma: 2.9 ± 0.3 MeV/c^2
Statistical uncertainties only

Charm Production

D⁰→K⁻π⁺

CMS preliminary

μ: 1.867 ± 0.002 GeV
σ: 0.016 ± 0.002 GeV
N: 493 ± 45
S/√S+B: 13.1

D⁺→K⁻π⁺π⁺

**CMS Preliminary
7 TeV data**

Yield = 417 ± 42
Mean = 1.8708 ± 0.0018
Sigma = (16.38 ± 1.97) MeV/c²

D*⁺→D⁰(K⁻π⁺)π⁺

**CMS Preliminary
√s = 7 TeV**

Yield = 669 ± 43
Mean = (1.864 ± 0.001) GeV/c²
Sigma = (14.3 ± 1.0) MeV/c²

**CMS Preliminary
√s = 7 TeV**

Yield = 665 ± 62
Mean = (145.43 ± 0.06) MeV/c²
Sigma = (0.67 ± 0.06) MeV/c²

Collision Event at 7 TeV with 2 Pile Up Vertices
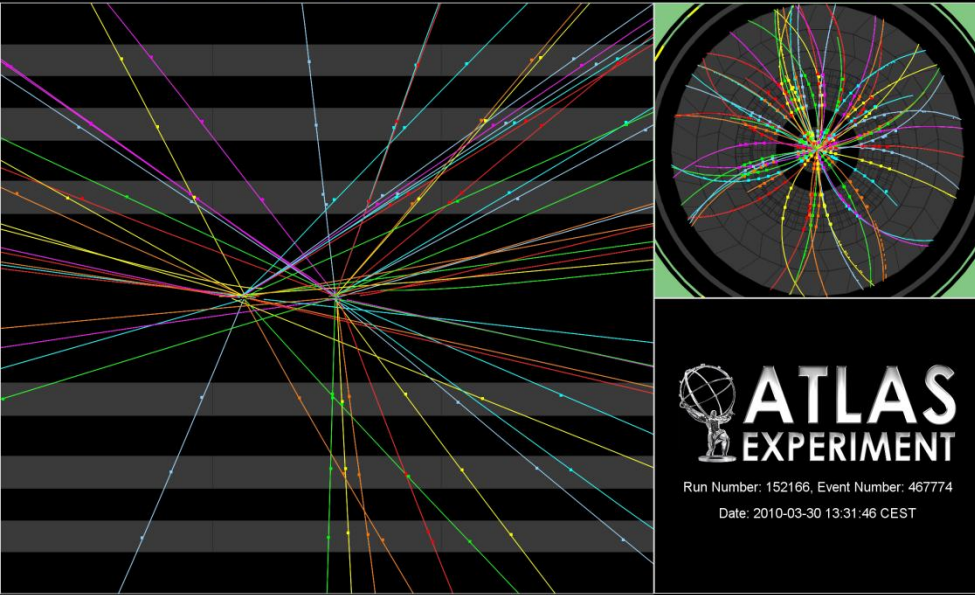
ATLAS EXPERIMENT

Run Number: 152166, Event Number: 467774

Date: 2010-03-30 13:31:46 CEST

http://atlas.web.cern.ch/Atlas/public/EVTDISPLAY/events.html
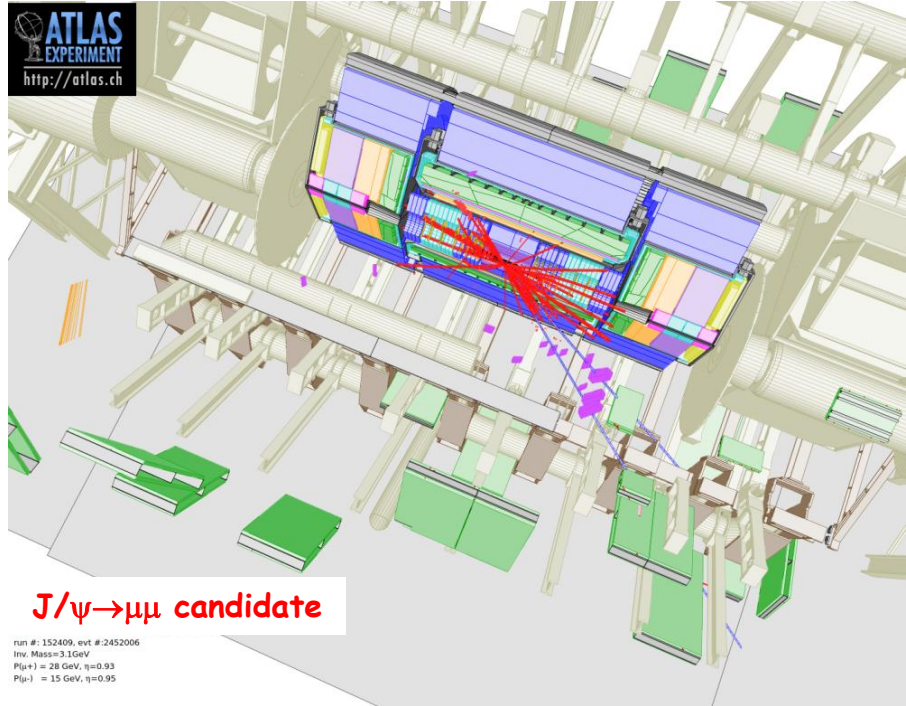
J/ψ→μμ candidate

run #: 152409, evt #:2452006
Inv. Mass=3.1GeV
P(μ+) = 28 GeV, η=0.93
P(μ-) = 15 GeV, η=0.95

Run: 152845, Event: 3338173
Date: 2010-04-12 16:56:44 CEST

ATLAS EXPERIMENT

$p_T(\mu-) = 40$ GeV
$\eta(\mu-) = 2.0$
$E_T^{miss} = 41$ GeV
$M_T = 83$ GeV
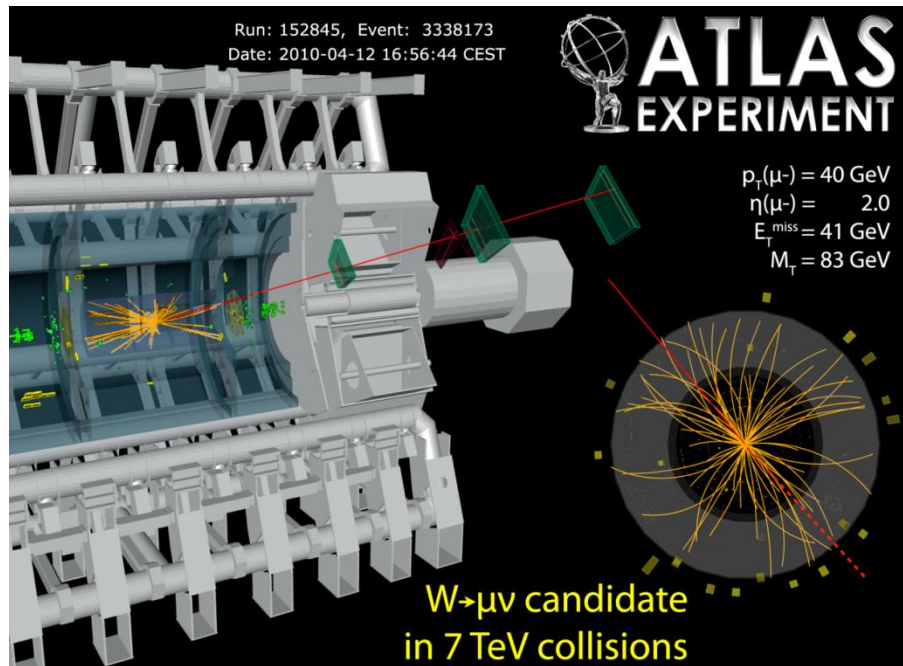
W→μν candidate
in 7 TeV collisions

ATLAS EXPERIMENT

Run: 154822, Event: 14321500
Date: 2010-05-10 02:07:22 CEST

$p_T(\mu^-) = 27$ GeV $\eta(\mu^-) = 0.7$
$p_T(\mu^+) = 45$ GeV $\eta(\mu^+) = 2.2$
$M_{\mu\mu} = 87$ GeV

Z→μμ candidate
in 7 TeV collisions

2 pile up vertices

double b-jet candidate

W→μν candidate

Z+jets candidate

CMS Experiment at the LHC, CERN
Run 135149, Event 125426133
Sunday May 9 2010, 05:24:09

M = 93.2 GeV/c²
pT = 97.0 GeV/c

MET=15.1 GeV

jet-2

jet-1

jet-2

jet-1

μ+

μ−

μ+

μ−

pT = 67.3 GeV/c

pT = 50.6 GeV/c

CMS Experiment at LHC, CERN
Run 133875, Event 1228182
Lumi section: 16
Sat Apr 24 2010, 09:08:46 CEST

Muon p_T = 38.7 GeV/c
ME$_T$ = 37.9 GeV
M$_T$ = 75.3 GeV/c²

$\not{E}_T$

μ

μ

CMS Experiment at LHC, CERN
Data Recorded: Sat Apr 24 08:31:20 2010 CEST
Lumi section: 795
Run / Event : 133874 / 64064942

Additional new particles are found at the LHC….. !

SU4 20-plets

$J=1/2^+$

$J=3/2^+$

Ξ^{*0}_b by CMS

$$\Xi_b^{*0} \rightarrow \Xi_b^- \pi^+ \rightarrow \Xi^- J/\psi \, \pi^+ \rightarrow \Lambda \pi^- \mu^+ \mu^- \pi^+ \rightarrow p^+ \pi^- \pi^- \mu^+ \mu^- \pi^+$$

CMS
pp, √s = 7 TeV
L = 5.3 fb⁻¹

● Opposite-sign data
— Signal+background fit
⋯ Background

(b)
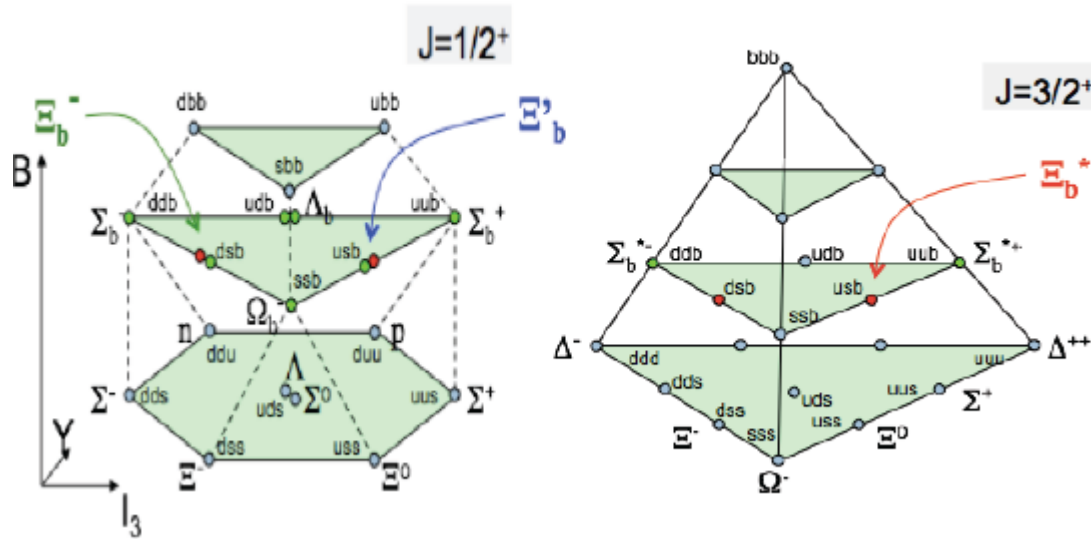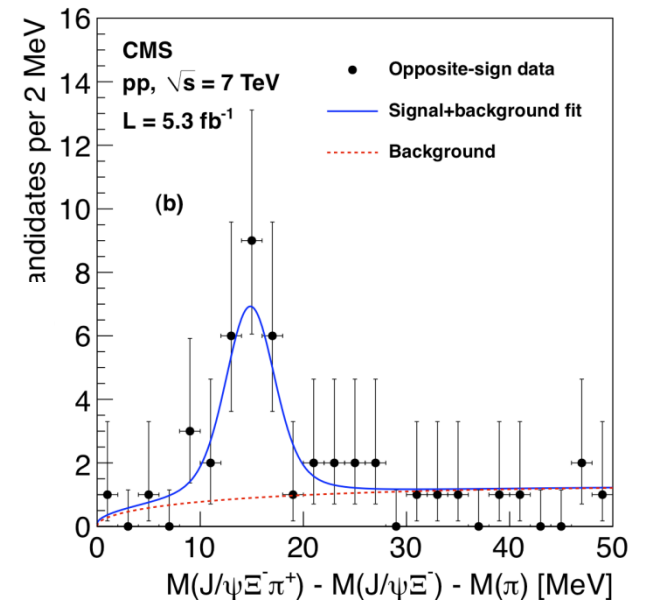
PhotoElectric Effect

Interaction between photon and whole atom.

Photons with energies above the binding energy of an electron, can eject an atomic electron, with kinetic energy T:

$$T = h\nu - W$$

Einstein: Quantized photon energies

Feynman: QED!

$E_{photon} = h\nu$

$v_{max} = 6.22 \times 10^5$ m/s

700 nm
1.77 eV

550 nm
2.25 eV

$v_{max} = 2.96 \times 10^5$ m/s

400 nm
3.1 eV

no electrons

Potassium - 2.0 eV needed to eject electron

Photoelectric effect
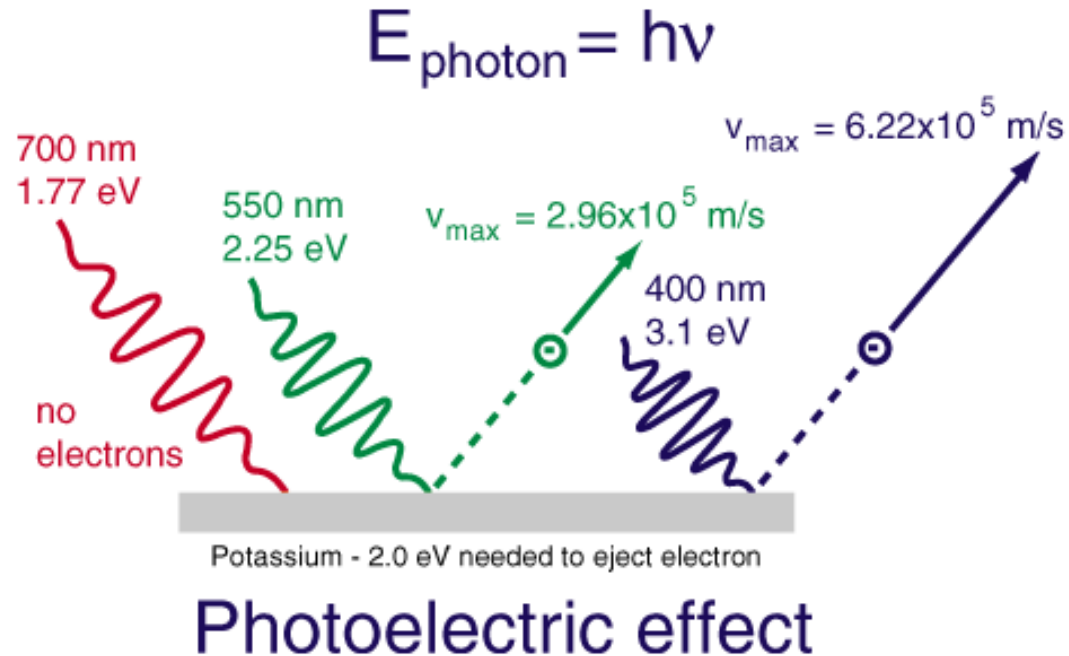
Compton scattering:

e⁻

$$E'_\gamma = E_\gamma \frac{1}{1+\varepsilon(1-\cos\theta_\gamma)} \qquad \varepsilon = \frac{E_\gamma}{m_e c^2}$$

$$E_e = E_\gamma - E'_\gamma$$

θ_γ
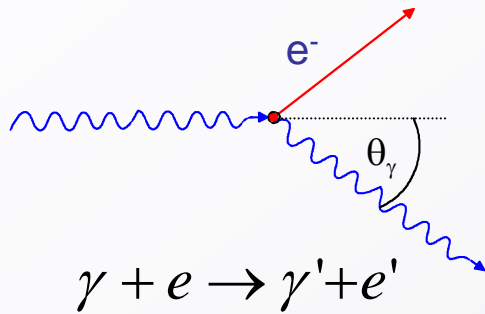
$$\gamma + e \rightarrow \gamma' + e'$$

Compton cross-section (Klein-Nishina)
example: E_γ = 0 … 511 keV

Assume electron as quasi-free.

Klein-Nishina $\frac{d\sigma}{d\Omega}(\theta,\varepsilon)$ →

At high energies approximately

$$\sigma^e_c \propto \frac{\ln\varepsilon}{\varepsilon}$$

Atomic Compton cross-section:

$$\sigma^{atomic}_c = Z \cdot \sigma^e_c$$

XI ICFA School on Instrumentation in Elementary Particle Physics
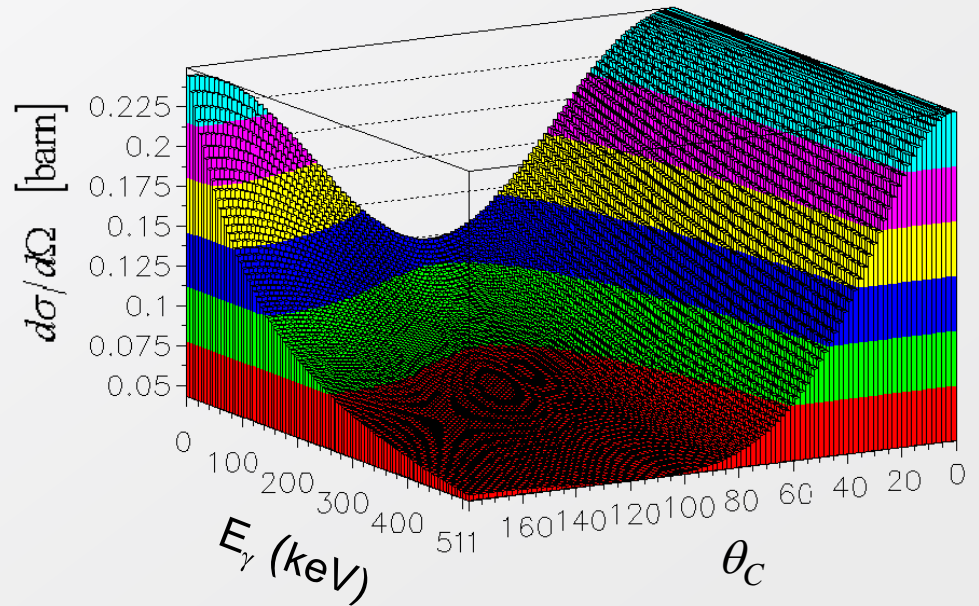
Pair production
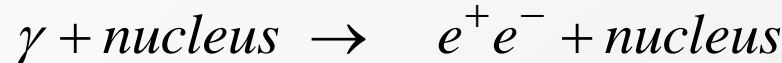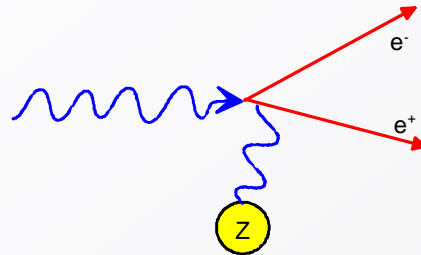
$$\gamma + nucleus \;\rightarrow\; e^+e^- + nucleus$$

Only possible in the Coulomb field of a nucleus (or an electron) if $\quad E_\gamma \geq 2m_e c^2$

Cross-section (high energy approximation)

$$\sigma_{pair} \approx 4\alpha r_e^2 Z^2 \left(\frac{7}{9} \ln \frac{183}{Z^{\frac{1}{3}}} \right)$$

independent of energy !

$$\approx \frac{7}{9}\frac{A}{N_A}\frac{1}{X_0}$$

$$\approx \frac{A}{N_A}\frac{1}{\lambda_{pair}}$$

$$\lambda_{pair} = \frac{9}{7}X_0$$

Energy sharing between e$^+$ and e$^-$ becomes asymmetric at high energies.

$$\gamma + e^- \rightarrow e^+e^- + e^-$$

$$\gamma + nucleus \rightarrow e^+e^- + nucleus$$
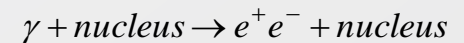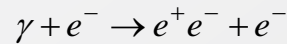
Hadronic Interactions

- Hadrons create showers via strong interactions just like electrons and photons create them via EM.

- Mean energy of pion with initial energy E_0 after traversing material depth λ:

$$\langle E \rangle = E_0 e^{-X/\lambda}$$

- Mean energy of electron with initial energy E_0 after traversing material depth X_0 :

$$\langle E \rangle = E_0 e^{-X/X_0}$$

X_0 = radiation length

λ = interaction length or hadronic absorption length

X_0 and λ for some materials

| Material | X_0 | λ |

	X_0	λ
H_2	63	52.4
Argon	18.9	119.7
Iron	13.8	131.9
BGO	8.0	164

Units of g/cm^2

E.g., a pion takes ~10x the depth in Iron to loose its energy than an electron with the same energy.

E.g. within the depth of X_0 in BGO, a pion looses only 5% of its energy, while an electron looses 63% of its energy, on average.

Longitudinal profile example
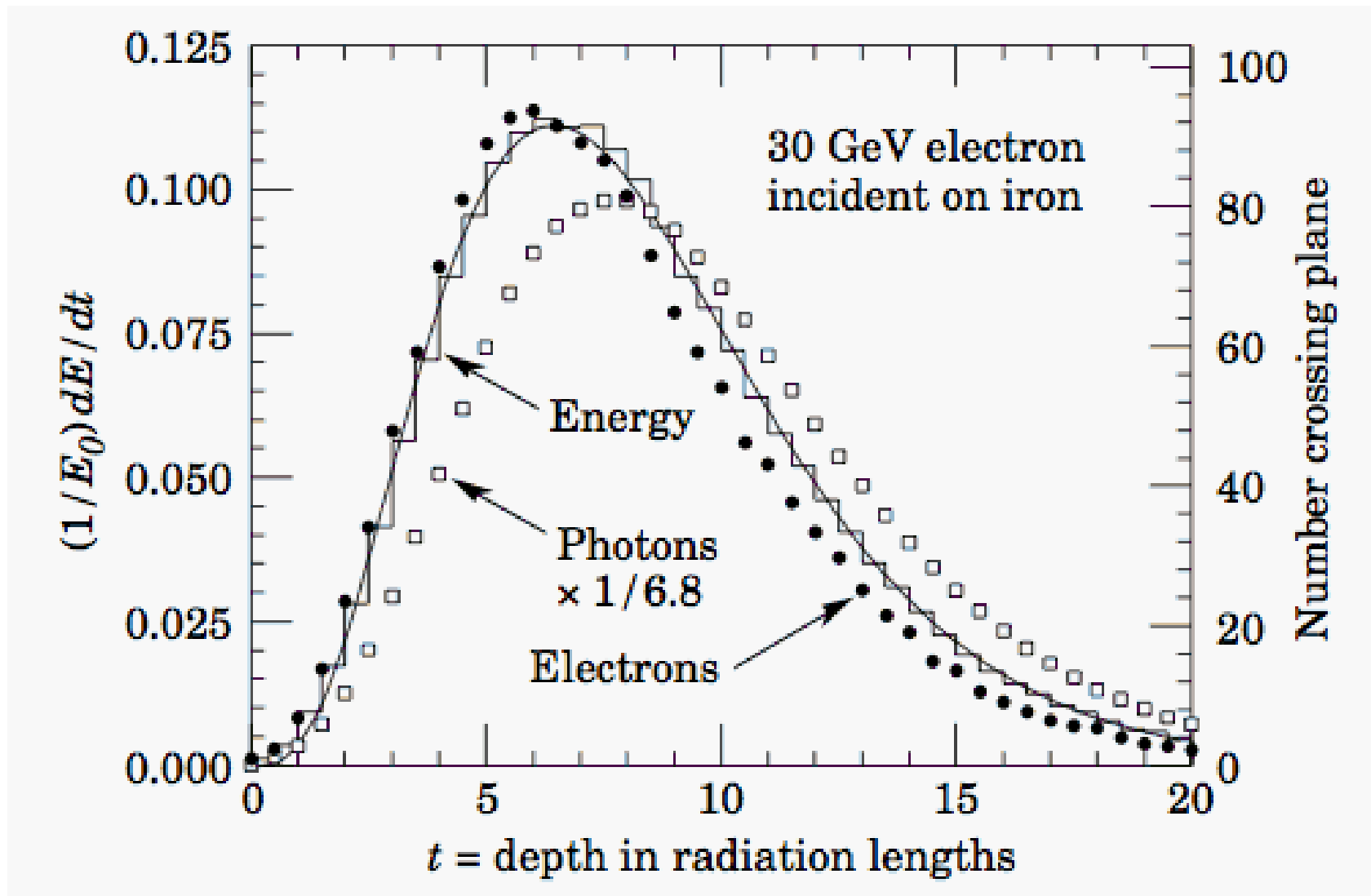
Transverse profile

- Determined by Molier radius, R_M

$$R_M = 21 MeV \bullet \frac{X_0}{E_c}$$

- 99% of energy is within $3R_M$
- E_c and X_0 and thus R_M depend on material.
- Typically, transverse granularity of ECAL is chosen to match R_M .

Development of Hadronic Showers

Hadronic shower

→ At **energies > 1 GeV**, cross-section depends little on energy:

$$\sigma_{abs} \approx \sigma_0 A^{0.7} \, , \quad \sigma_0 \approx 35 \, mb \quad \Rightarrow$$

$$\lambda_I \propto A^{1/3}$$

→ For $Z > 6$ → $\lambda_I > X_0$

Material	Z	A	ρ [g/cm^3]	X_0 [g/cm^2]	λ_I [g/cm^2]
Hydrogen (gas)	1	1.01	0.0899 (g/l)	63	50.8
Helium (gas)	2	4.00	0.1786 (g/l)	94	65.1
Beryllium	4	9.01	1.848	65.19	75.2
Carbon	6	12.01	2.265	43	86.3
Nitrogen (gas)	7	14.01	1.25 (g/l)	38	87.8
Oxygen (gas)	8	16.00	1.428 (g/l)	34	91.0
Aluminium	13	26.98	2.7	24	106.4
Silicon	14	28.09	2.33	22	106.0
Iron	26	55.85	7.87	13.9	131.9
Copper	29	63.55	8.96	12.9	134.9
Tungsten	74	183.85	19.3	6.8	185.0
Lead	82	207.19	11.35	6.4	194.0
Uranium	92	238.03	18.95	6.0	199.0
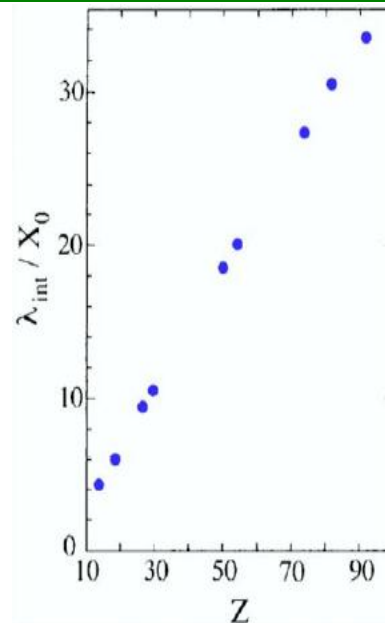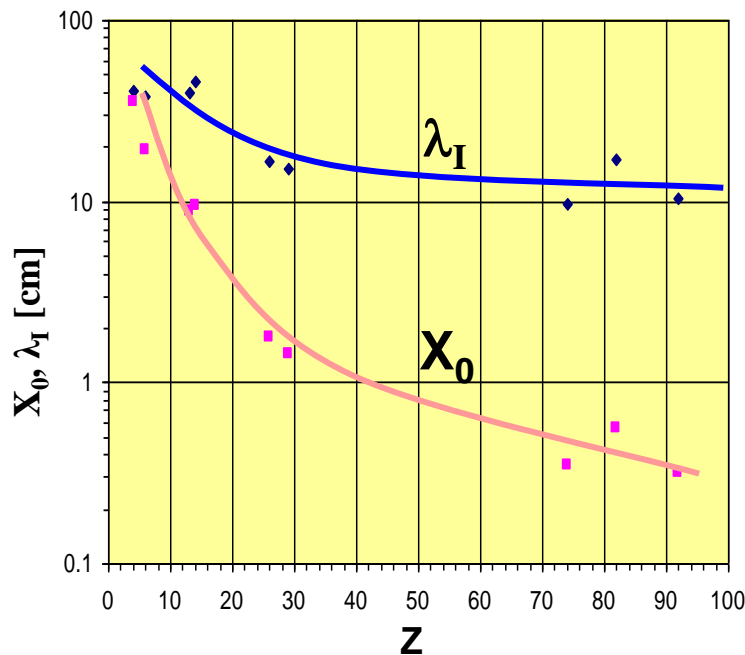
Comparing X_0 and λ_I, we understand why Hadronic calorimeters are in general larger than EM calorimeters

Interaction of neutrons

Neutrons have no charge, i.e. their interaction is based only on strong (and weak) nuclear force. To detect neutrons, we have to create charged particles.

Possible neutron conversion and elastic reactions …

$$n + {}^6Li \rightarrow \alpha + {}^3H$$
$$n + {}^{10}B \rightarrow \alpha + {}^7Li$$
$$n + {}^3He \rightarrow p + {}^3H$$
$E_n < 20$ MeV

$$n + p \rightarrow n + p$$
$E_n < 1$ GeV

(H. Neuert, Kernphysikalische Messverfahren, G. Braun Verlag, 1966)

E_n

high energy

100 MeV — fast

100 keV — epithermal

10^{-1} eV —
10^{-2} eV — thermal
10^{-3} eV — cold ultracold
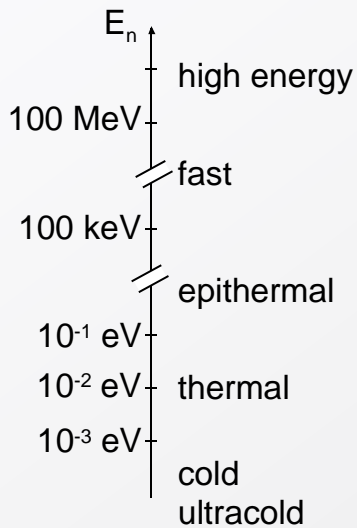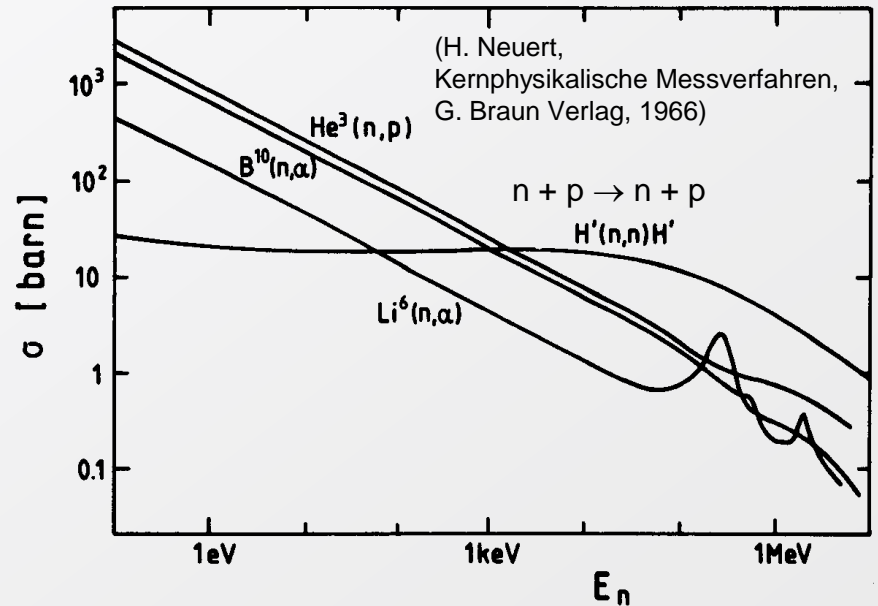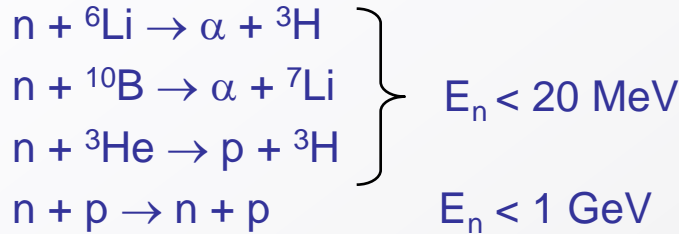
In addition there are …

- neutron induced fission $E_n \approx E_{th} \approx 1/40$ eV
- inelastic reactions → hadronic cascades (see below) $E_n > 1$ GeV

XI ICFA School on Instrumentation in Elementary Particle Physics

LHC: a very hostile environment for tracking
(high event rate, high multiplicity of charged tracks, high radiation flux)

Collisions at LHC
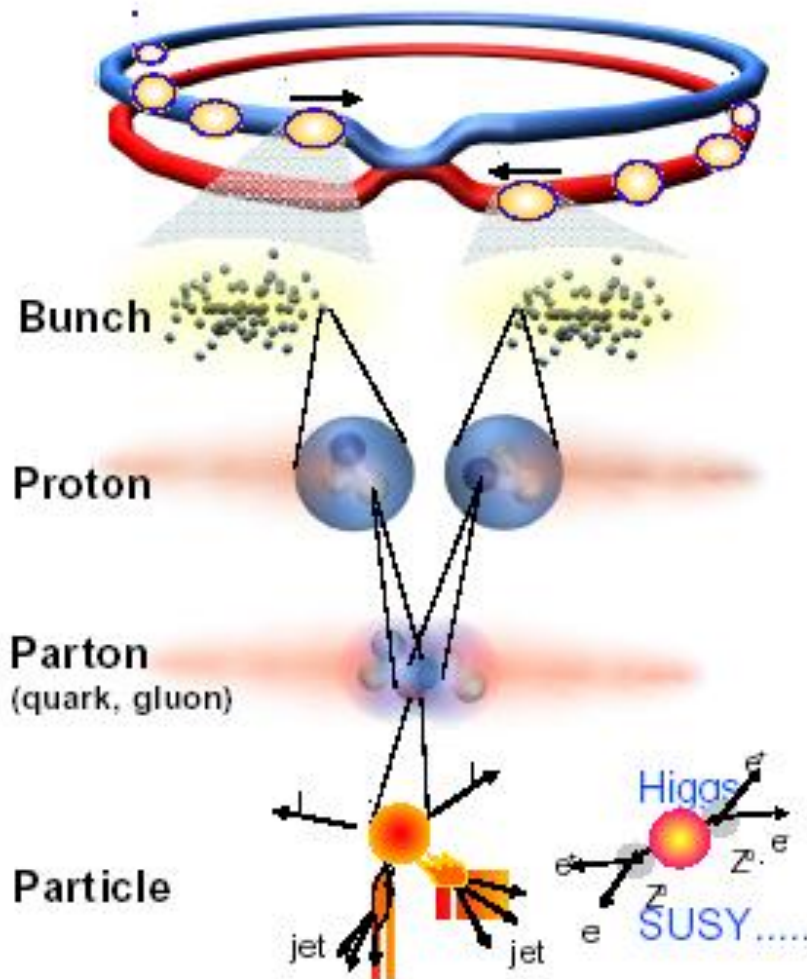
Proton-Proton	2835 bunch/beam
Protons/bunch	10^{11}
Beam energy	7 TeV (7×10^{12} eV)
Luminosity	10^{34} cm^{-2} s^{-1}

Crossing rate   40 MHz

Collisions rate $\approx 10^7 - 10^9$ Hz

New physics rate $\approx$ .00001 Hz

Event selection:
1 in 10,000,000,000,000

Bunch

Proton

Parton
(quark, gluon)

Particle

jet   jet   e

Higgs

Z^0 e

Z^0

SUSY.....

Signal and background → $\mathcal{L}=10^{34}$ cm^{-2}s^{-1}

Cross sections for various physics processes vary over many orders of magnitude

Higgs (600 GeV/c^2): 1pb @10^{34} →10^{-2} Hz
Higgs (100 GeV/c^2): 10pb @10^{34}→0.1 Hz
t t production: →10 Hz
W→ $\ell\,\nu$:   →10^2 Hz
Inelastic: →10^9 Hz

Selection needed: 1:10^{10-11}
Before branching fractions...
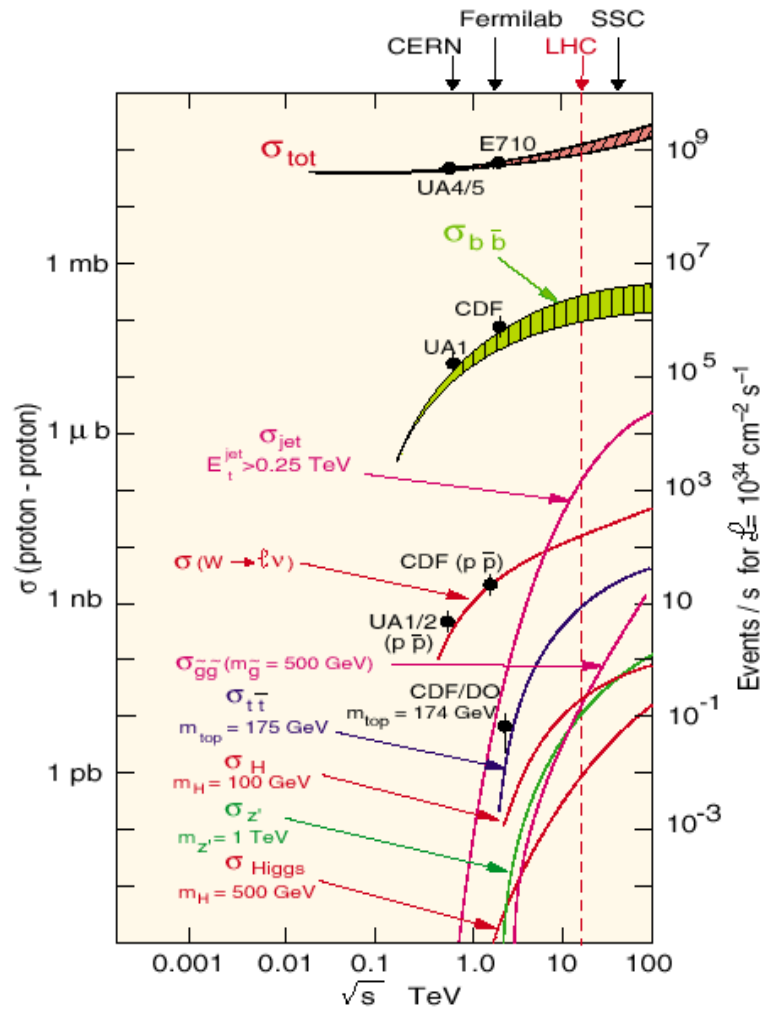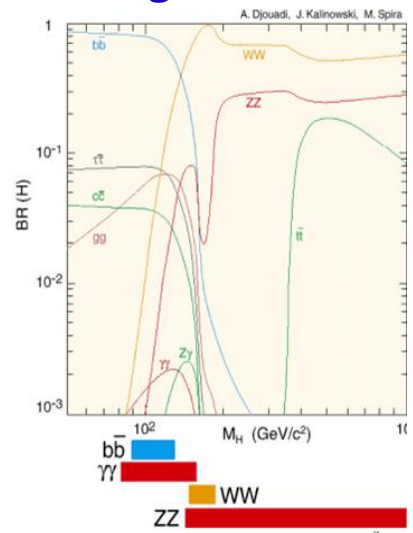
$\Rightarrow$ **Needle in a Hay Stack**

Impact on detector design

LHC detectors must have fast response

    Otherwise will integrate over many bunch crossings

        $\rightarrow$ large "pile-up"

    Typical response time : 20-50 ns

        $\rightarrow$integrate over 1-2 bunch crossings

        $\rightarrow$ pile-up of 25-50 min-bias

        $\rightarrow$ very challenging readout electronics

LHC detectors must be highly granular

    Minimize probability that pile-up particles be in the
same detector element as interesting object

        $\rightarrow$ large number of electronic channels

        $\rightarrow$ high cost

LHC detectors must be radiation resistant:

    high flux of particles from pp collisions

        $\rightarrow$ high radiation environment

Different Strategies...

13m x 6m Solenoid: 4 Tesla Field

Tracking up to $\eta \sim 2.4$

Muon system in return yoke

First muon chamber just after solenoid $\rightarrow$ extended lever arm for p_t measurement

CMS
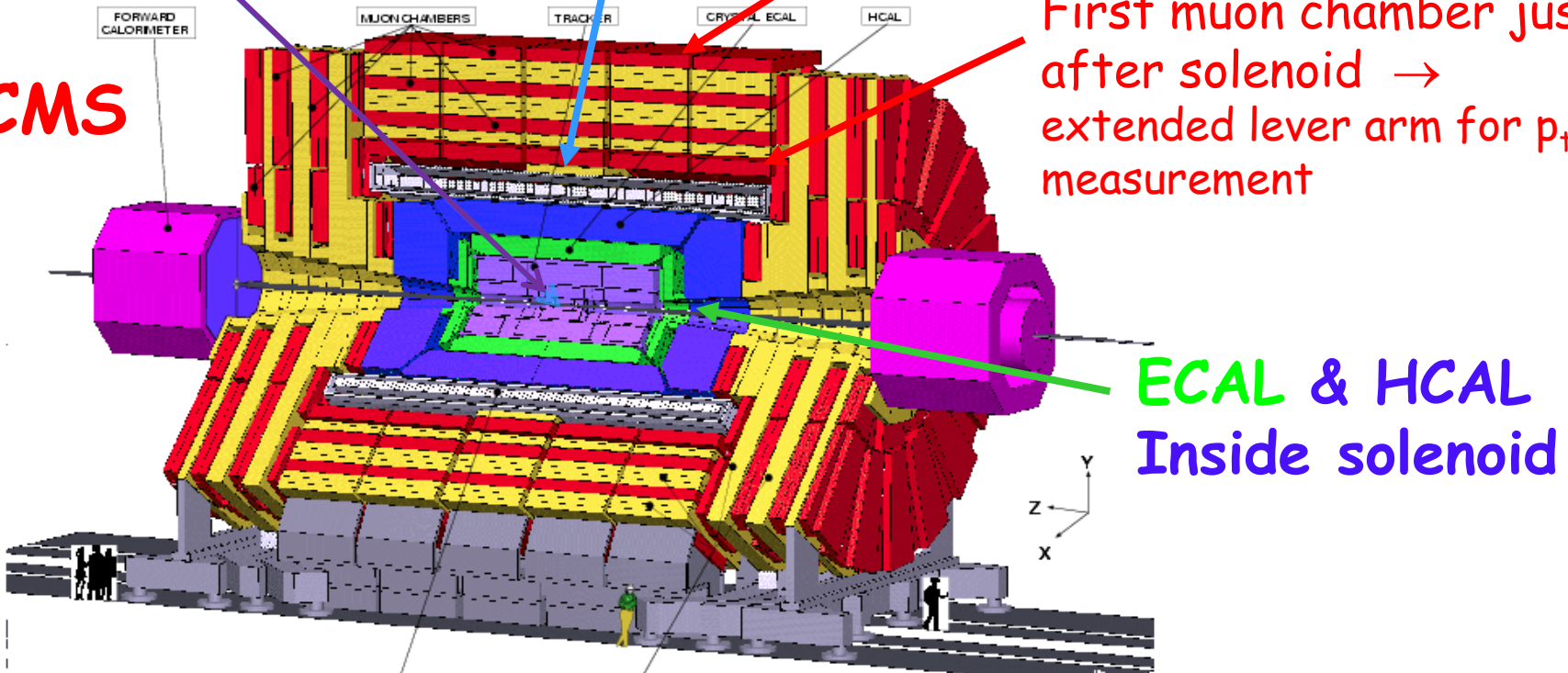
ECAL & HCAL Inside solenoid

22m Long, 15m Diameter, 14'000 Ton Detector
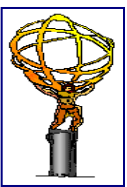
Different Strategies....

2.3mx5.3m Solenoid ~ 2 Tesla Field

End Cap Toroid

ATLAS

muon detectors   electromagnetic calorimeters

forward calorimeters

Barrel Toroid
<B> = 0.4 T

inner detector   hadron calorimeter
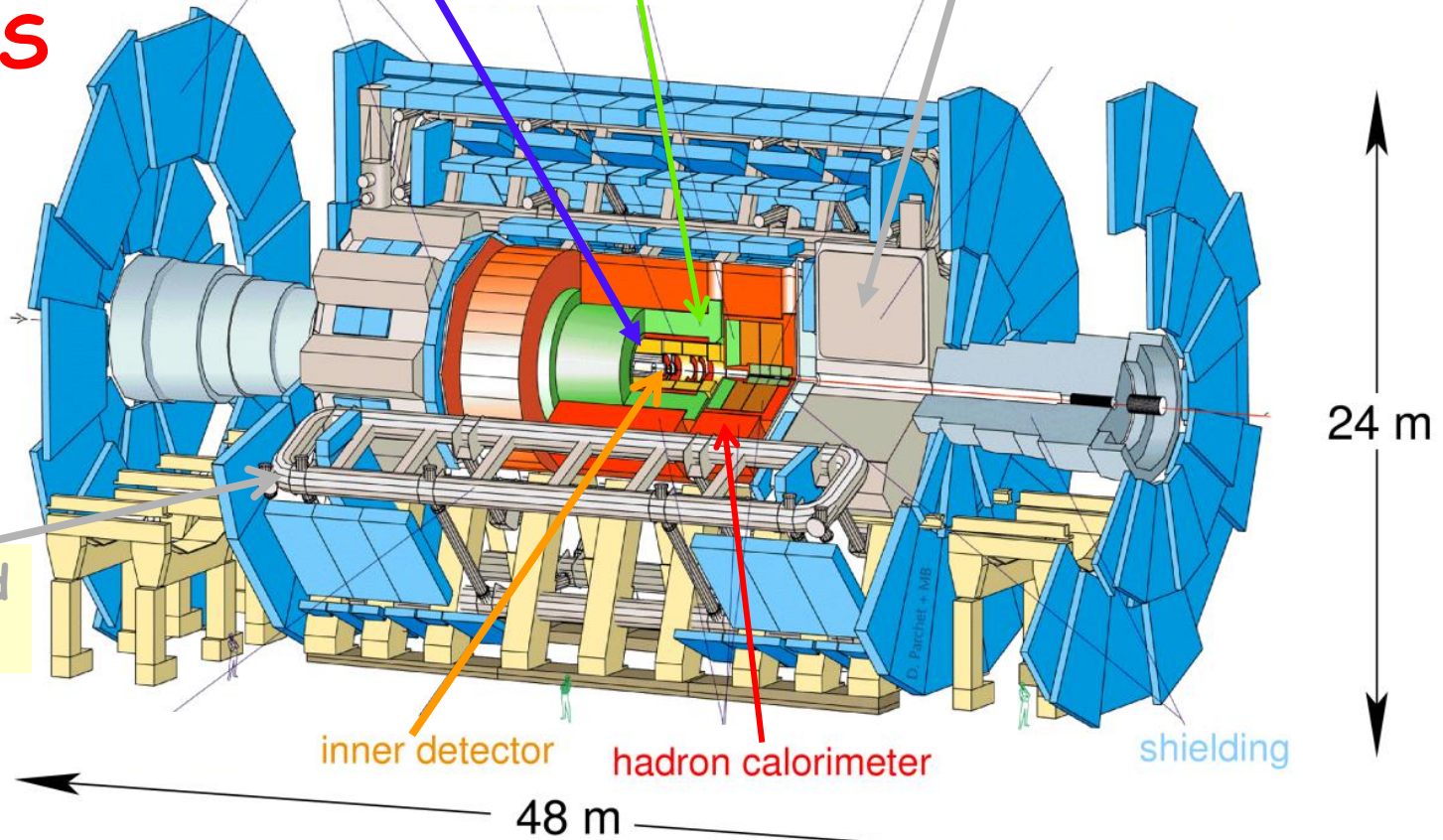
shielding

24 m

48 m

48m Long, 24m Diameter, 7'000 Ton Detector

Total weight   14000 t
Overall diameter   15 m
Overall length   28.7 m

CMS

ECAL 76k scintillating PbWO$_4$ crystals

HCAL Scintillator/brass Interleaved ~7k ch

3.8T Solenoid

IRON YOKE

MUON ENDCAPS

473 Cathode Strip Chambers (CSC)
432 Resistive Plate Chambers (RPC)

Preshower
Si Strips ~16 m^2
~137k ch

YE1-3

Foward Cal
Steel + quartz
Fibers ^{2}~k ch

YBO

YB1-2

Pixels & Tracker
• Pixels (100x150 μm^2)
  ~ 1 m^2 ~66M ch
• Si Strips (80-180 μm)
  ~200 m^2 ~9.6M ch

Pixel
Tracker
ECAL
HCAL
Muons
Solenoid coil

MUON BARREL
250 Drift Tubes (DT) and
480 Resistive Plate Chambers (RPC)

Muon Spectrometer ($|\eta|$<2.7) : air-core toroids with gas-based muon chambers
Muon trigger and measurement with momentum resolution < 10% up to E_μ ~ 1 TeV

Length : ~ 46 m
Radius : ~ 12 m
Weight : ~ 7000 tons
~10^8 electronic channels
3000 km of cables

3-level trigger reducing the rate from 40 MHz to ~200 Hz

Muon Detectors   Tile Calorimeter   Liquid Argon Calorimeter

Toroid Magnets   Solenoid Magnet   SCT Tracker   Pixel Detector   TRT Tracker
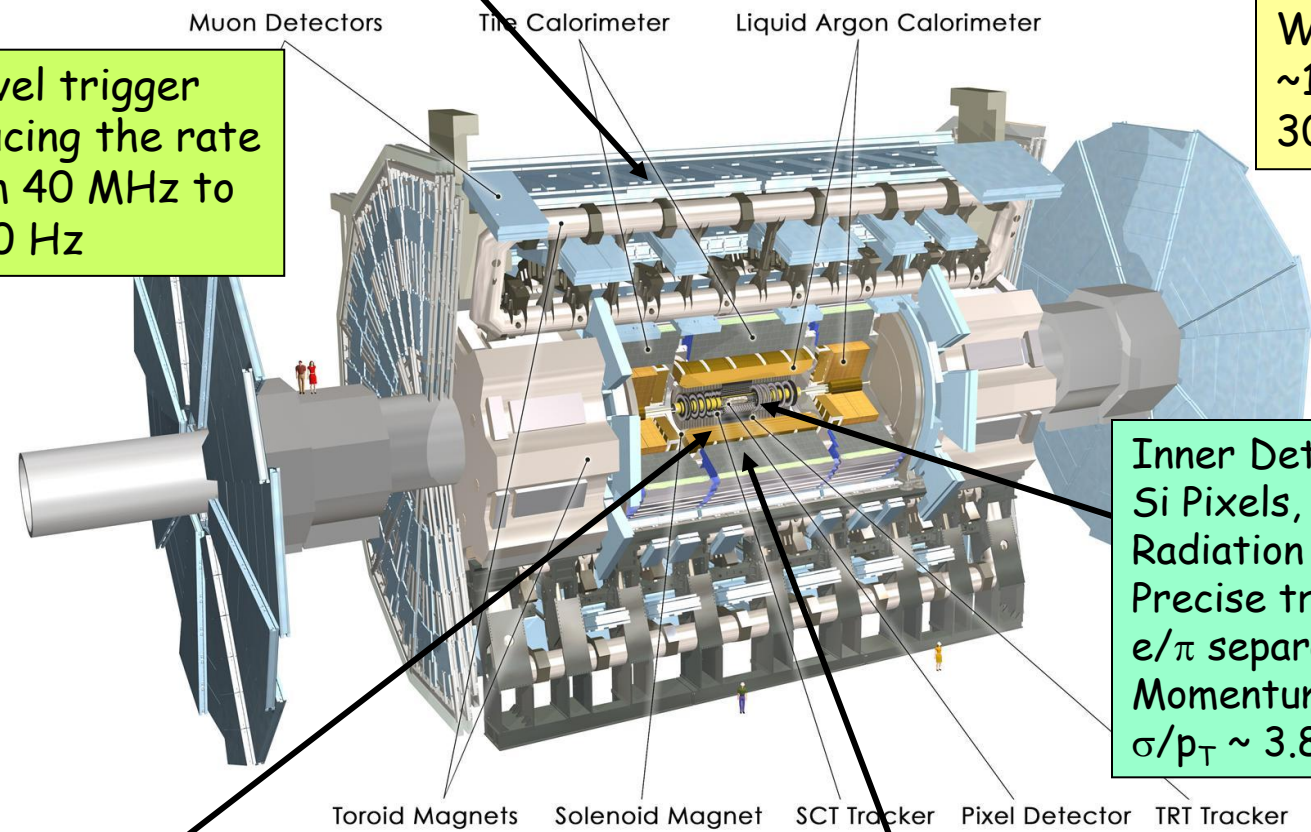
Inner Detector ($|\eta|$<2.5, B=2T):
Si Pixels, Si strips, Transition Radiation detector (straws)
Precise tracking and vertexing, e/π separation
Momentum resolution:
σ/p_T ~ 3.8×10^{-4} p_T (GeV) $\oplus$ 0.015

EM calorimeter: Pb-LAr Accordion
e/γ trigger, identification and measurement
E-resolution: σ/E ~ 10%/$\sqrt{E}$

HAD calorimetry ($|\eta|$<5): segmentation, hermeticity
Fe/scintillator Tiles (central), Cu/W-LAr (fwd)
Trigger and measurement of jets and missing E_T
E-resolution: σ/E ~ 50%/$\sqrt{E}$ $\oplus$ 0.03

Tracking Requirements

Precise and efficient tracking at LHC is needed to extract physics signals from competitive but reducible background signals:

- **Mass cut: precise invariant mass determination from precise momentum measurement of the decay products**

- **Isolation cut: high track reconstruction efficiency in dense environment (pile-up, jets…)**

- **Long-lifetime particles tagging: precise and efficient measurement of the track impact parameter and secondary vertices.**

The approach

❑ **Silicon microstrip detectors allow a very good point resolution (10-30 microns) that coupled to large lever arms in solenoidal field of 2-4T would allow an adequate momentum resolution, good impact parameter resolution for b-tagging and excellent measurement of the charge up to 1TeV and beyond.**

❑ **Single bunch crossing resolution is feasible in silicon (collection time <10ns) with fast read-out electronics.**

❑ **The real challenge is pattern recognition for track reconstruction: the high density of tracks typical of the inner regions of high luminosity hadronic colliders can be tackled with extreme segmentations both in r-phi and r-z : pixel detectors and silicon microstrip modules.**

❑ **Silicon detectors are well radiation resistant ($\Phi > 10^{14}$ n/cm^2) and can be produced in large scale at rather low cost.**

$\Rightarrow$**Pixel detector** (in the radial region 5cm<r<20cm: 10^{14}cm^{-2}<Φ<10^{15}cm^{-2})

$\Rightarrow$**Silicon microstrip** (in the radial region r>20cm: 10^{13}cm^{-2}<Φ<10^{14}cm^{-2})

Two different strategies

This approach has been followed very aggressively by **CMS** who decided to build the first full silicon tracker in HEP

- more challenge in terms of technology and costs
- higher performance particularly in pattern recognition

ATLAS has adopted a more traditional approach based on a hybrid tracker:
pixel and silicon microstrip detectors in the innermost part and a large gaseous detectors in the outer part (straw tubes).

Hadronic Calorimeter

<u>Fluctuations - Other methods to improve resolution</u>

Particle Flow Concept
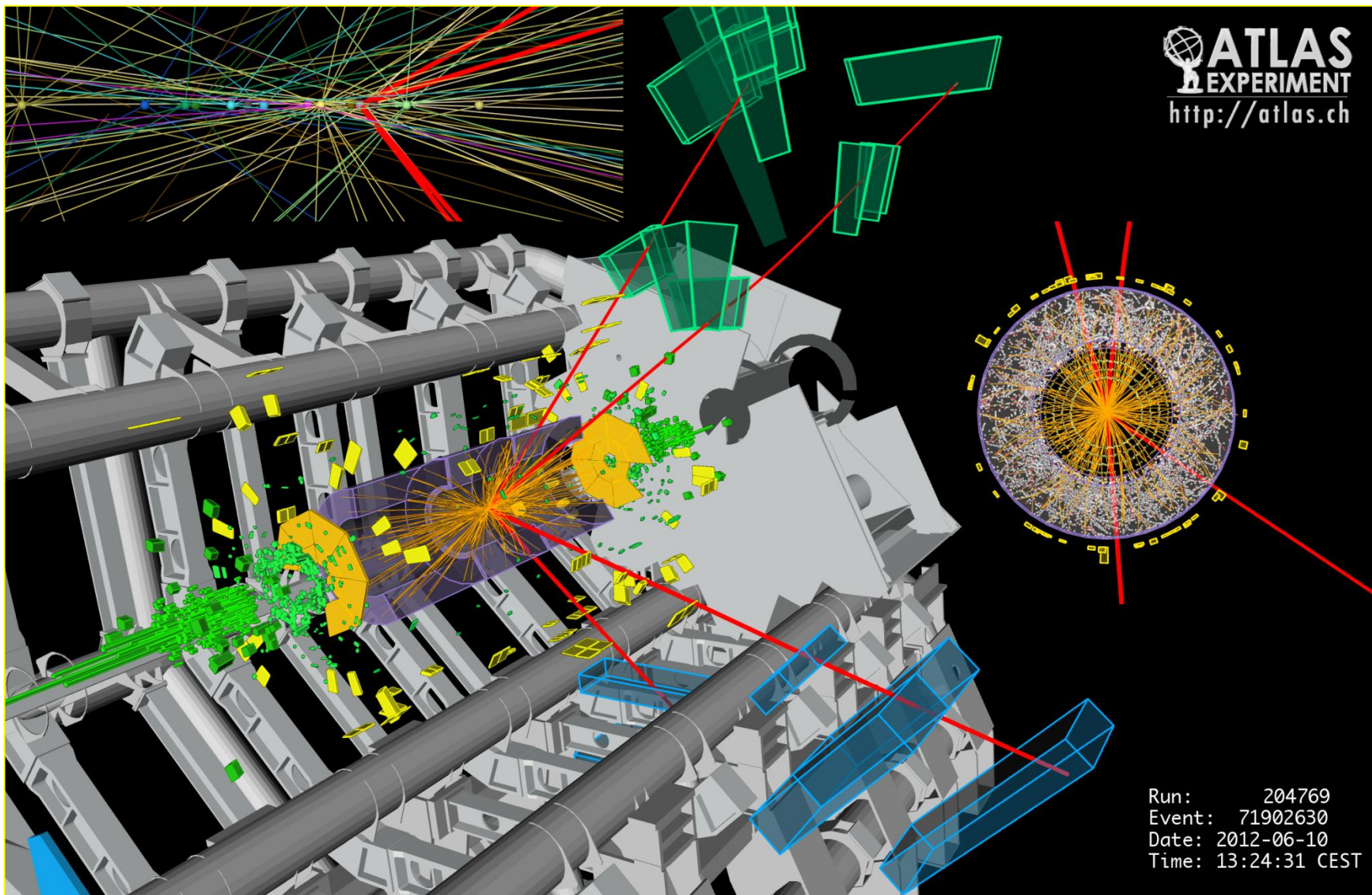
Particle flow scheme:
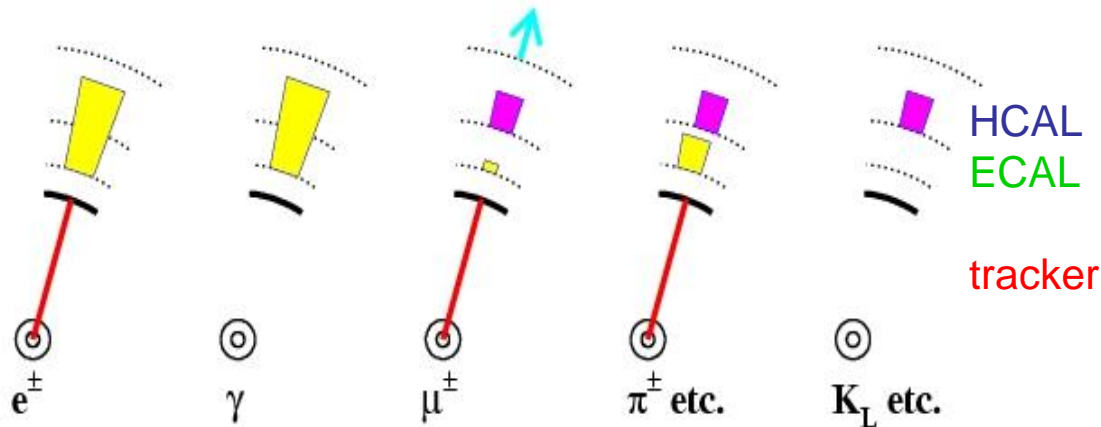
→ Tracker (tracking detector to reconstruct charge particles)   (<65%> of a jet)

→ ECAL for γ reconstruction (<25%>)

→ ECAL+HCAL for h^0 (π^0, etc) reconstruction (<10%>)

p_T (muons)= 36.1, 47.5, 26.4, 71 .7GeV m_{12}= 86.3 GeV, m_{34}= 31.6 GeV
15 reconstructed vertices

ATLAS
EXPERIMENT
http://atlas.ch

Run: 204769
Event: 71902630
Date: 2012-06-10
Time: 13:24:31 CEST

Unità di misura

○ **Energia**

$$1 \text{ eV}$$

$$(1.6 * 10^{-19} \text{ J})$$

(1.6 decimiliardesimi di miliardesimi di J)

1 Volt e^- $\vec{E}$

○ **Multipli di 1 eV** *keV, MeV, GeV, TeV*

$$(10^3, \quad 10^6, \quad 10^9, \quad 10^{12})$$

mille   milione   miliardo   mille-miliardi

○ **Energia di una particella**

▬ **Relatività** $E = mc^2 ; \ m = \gamma * m_0$

$$\gamma = 1/\sqrt{1 - \beta^2}; \quad \beta = v/c$$

▪ **Elettrone** $m_0 = 9.11 * 10^{-31} \text{ kg}; \quad 0.51 \text{ MeV}$

▬ **Protone** $m_0 = 1.67 * 10^{-27} \text{ kg}; \quad 0.94 \text{ GeV}$

Ordini di grandezza

1 eV è una piccola energia   . $1 \text{ eV} = 1.6 \cdot 10^{-19} \text{ J}$
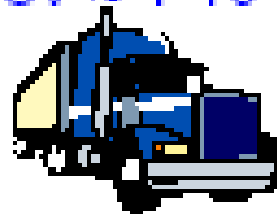
$m_{bee} = 2g = 3.6 \cdot 10^{32} \text{ eV}/c^2$

$v_{bee} = 1 m/s \rightarrow E_{bee} = 10^{-3} \text{ J} = 6.25 \cdot 10^{15} \text{ eV}$

$E_{LHC} = 14 \cdot 10^{12} \text{ eV}$

In LHC il singolo protone avrà un'energia mille volte inferiore alla energia cinetica della nostra ape; ma protoni con questa energia ce ne saranno ben 10^{14}, quindi l'energia immagazzinata nei fasci di LHC sarà:

$10^{14} \text{ protons} * 14 \cdot 10^{12} \text{ eV} \approx 1 \cdot 10^8 \text{ J}$

this corresponds to a

$m_{truck} = 100 \text{ T}$

$v_{truck} = 120 \text{ km/h}$

Una nuova tavola periodica

Total Energy in the Universe
(stars and planets are a very small part !)

Heavy Elements: 0.03%

Neutrinos: 0.3%

Stars: 0.5%

Free Hydrogen and Helium: 4%

Dark Matter: 25%

Dark Energy: 70%

Dark Energy

Dark Matter